

Towards an Optimized Laboratory Procedure for Accelerated Long-term Oxidative Aging of Asphalt Mix Specimens

by

Sarbjot Singh

A thesis
presented to the University of Waterloo
in fulfillment of the
thesis requirement for the degree of
Master of Applied Science
in
Civil Engineering

Waterloo, Ontario, Canada, 2018

© Sarbjot Singh 2018

AUTHOR'S DECLARATION

I hereby declare that I am the sole author of this thesis. This is a true copy of the thesis, including any required final revisions, as accepted by my examiners.

I understand that my thesis may be made electronically available to the public.

ABSTRACT

Pavement infrastructure forms one of the most important mode of passenger and freight transportation and trade between Canada and the United States, and plays an important role in national economy as a measure of Canada's global development index. For asphalt pavements, the durability of this infrastructure is highly dependent on the constituent asphalt binder, which even though comprises only 4-6 percent of the asphalt mixture, governs the behavior and has a great impact on its rheological characteristics.

Like most organic materials, asphalt binder evolves physically and chemically over time (referred to as aging or age hardening) owing to a number of aging mechanisms. Gradual oxidation resulting in formation of oxygen containing functional groups is one of the primary causes of asphalt binder hardening, however it is not the only mechanism attributed to aging. Other factors such as volatilization of lighter fractions, molecular reorientation, absorption of oily components by mineral aggregates, photo-oxidation and so forth could all lead to hardening of asphalt binder. From a design point of view, it is very important to understand these aging mechanisms and their subsequent effects on binder rheological properties to enhance pavement longevity and reduce the time period to rehabilitation and/or replacement.

Short-term aging is the term given to changes in binder properties during mixing at an asphalt plant and field compaction, and is mainly attributed to loss of volatiles or lighter oily fractions and high temperature oxidation. Long-term aging on the other hand, refers to rheological changes that occur during the pavement service life and is mainly attributed to oxidation at ambient temperatures. However, it must be noted that the rate of change, resulting chemical composition and rheological properties vary for different types of binder and even for same type of binder dependent on various environmental factors such as temperature, humidity, solar radiation (including ultraviolet and infrared) etc. as well as asphalt mixture properties such as air voids (distribution and interconnected voids), asphalt film thickness, type of aggregates, filler content and gradation.

Over the years, several laboratory procedures have been developed in a bid to accelerate the aging process while trying to accurately mimic the effects of construction and in-service conditions. For asphalt binder, the most commonly used methods are RTFOT (Rolling Thin Film Oven Test) and PAV (Pressure Aging Vessel), which simulate short-term and long-term aging respectively. For asphalt mix, SHRP methods are generally employed with STOA (loose-mix at 135°C for 4hrs) for short-term and LTOA (compacted samples at 85°C for 120hrs) for long-term aging. The acceleration in aging in these procedures is achieved by applying excessively high temperatures and/or pressures for extended periods of time. Previous studies have suggested that such extreme conditions (in comparison to actual service conditions) could alter the kinetics of oxidative aging in terms of the types and concentration of oxidation products formed, hence leading to different rheological and mechanical properties in comparison to those encountered after actual in-service pavement aging.

The main aim of this research project is to study the effects of less considered environmental degradation factors such as solar radiation (in particular UV) and rainfall on age hardening of asphalt binder, and hence optimize a laboratory accelerated aging procedure which provides a

better representation of actual conditions encountered by asphalt pavements in their service life. To this end, compacted asphalt mixture samples were subjected to three different types of conditioning procedures 1). Control conditioning procedure which is based on current widely used practices; and 2). and 3). Atlas Weatherometer and Bespoke Chamber conditioning procedures which are both based on limiting temperature conditioning and achieving acceleration in aging by applying cycles of water spray followed by drying under irradiation. The reason for choosing compacted mixture specimens was to avoid any issues related to compactability, and cohesion and adhesion for subsequent laboratory testing, which was carried out to characterize mixture rheological behavior (Complex Modulus) and to determine changes in fracture potential of aged mixtures (SCB). Another approach that was utilized was extraction and recovery of asphalt binder from aged mixtures, which was then subsequently subjected to rheological (Complex Modulus), chemical (FT-IR), and performance (LAS and MSCR) testing to understand the effects of age hardening.

The effect of oxidative aging for both asphalt binders and asphalt mixtures was characterized by a constant increase in modulus values ($|G^*|$ and $|E^*|$) and a decrease in phase angle values (δ). In terms of rheological behavior, this can be described as an increase in stiffness along with a greater proportion of elastic behavior, which lead to an increase in resistance against rutting but also a reduction in pavement durability associated with brittleness and reduced resistance against fatigue. A difference in kinetics of aging along with variations in rheological behavior were also noticed for control conditioning procedure where asphalt binder and mixture samples were subjected to comparatively high temperatures and/or pressures. The effect of water conditioning was also studied, indicating an accelerating effect on the photo-oxidation of asphalt mixtures. This can be attributed to the water solubility of the chemical products of photo-oxidation, which are washed away thus exposing further layers to oxidation.

Conclusions hence drawn based on comparative analysis of the results were then used to recommend Bespoke Chamber conditioning procedure (with repetitive cycles of UV and water conditioning), which was able to reproduce desirable levels of natural age hardening in compacted asphalt mixture samples while satisfying all of the requirements for an ideal conditioning procedure.

ACKNOWLEDGEMENTS

Firstly, I would like to express sincere gratitude to my supervisor, Professor Hassan Baaj, for giving me the opportunity to pursue graduate studies at the Center for Pavement and Transportation Technology (CPATT), and for his unwavering support and guidance throughout the course of my MAsc program. I would also like to thank Professor Liping Fu and Professor James R. Craig for serving as members of the review committee for my thesis.

Appreciation is extended to the Ministry of Transportation Ontario (MTO) for technical and financial support of this project. In particular, I would like to thank Mr. Imran Bashir, for his continued guidance and help with organizing Semi Circular Bending tests that were carried out at MTO laboratory. Appreciation is also extended to COCO Paving Ltd., especially Ms. Selena Lavorato, Mr. Steve Manolis, Mr. Porfirio Vela, and all laboratory technicians for their guidance and continued support with Atlas Weatherometer conditioning and FT-IR testing. I would also like to thank CPATT partner Steed and Evans Ltd., especially Mr. Richard Marco and Mr. Jim Karageorgos for their help with collection of plant mixed loose asphalt and virgin binder that was utilized in this research project.

My gratitude is also extended to a number of other individuals who helped me during the course of my research studies. The outstanding technical staff members at the Department of Civil and Environmental Engineering, Mr. Terry Ridgway, Mr. Christopher Peace, Mr. Richard Morrison, and Mr. Douglas Hirst, for their assistance and help with many of the laboratory tests detailed in this thesis. Special thanks is also extended to my colleague Mr. Yashar Azimi Alamdary for his continued help with many aspects of this research project, including but not limited to 2S2P1D rheological modelling of asphalt binders and mixtures.

I would also like to thank my other colleagues and friends at CPATT. Mr. Seyedata Nahidi, Mr. Taher Baghaee Moghaddam, Mr. Sergey Averyanov, Mr. Saeid Salehiashani, Mr. Drew Dutton, Mr. Eskedil Melese, Dr. Daniel Pickel, Mr. Shenglin Wang, Mr. Ali Qabur, Ms. Haya Almutairi, Ms. Hanna al-Bayati, Ms. Hawraa Kadhim, Dr. Peter Mikhailenko, Dr. Luke Zhao, and Mr. Rajandeep Chandpuri, who have helped me throughout the course of my studies, be it collection of materials, getting familiar with test procedures and equipment, or emotional support and encouragement. Thanks is also extended to CPATT undergraduate co-op students Dandi Zhao, Sona Khalifeh, Timothy Wang, Victoria Yang, and Azka Aqib for their capable assistance with laboratory tests at many points along the course of my research project.

DEDICATION

This thesis is dedicated to my family, my parents Jagir and Satwant, and my sisters Rupinder and Maninder, without whose love and support this would never have been possible.

TABLE OF CONTENTS

Author's Declaration.....	ii
Abstract.....	iii
Acknowledgements.....	v
Dedication.....	vi
List of Figures.....	ix
List of Tables.....	xii
CHAPTER 1 INTRODUCTION.....	1
1.1 Research Hypothesis.....	2
1.2 Scope and Objectives.....	2
1.3 Thesis Organization.....	2
CHAPTER 2 LITERATURE REVIEW.....	4
2.1 Introduction.....	4
2.2 Background on Asphalt.....	4
2.3 Asphalt Binder Grading.....	4
2.3.1 Penetration Grading.....	5
2.3.2 Viscosity Grading.....	5
2.3.3 SuperPave Performance Grading.....	5
2.4 Rheological Behavior of Asphalt Binder and Asphalt Mixture.....	8
2.4.1 Complex Modulus (G^* for binders / E^* for mixes) and Phase Shift Angle (δ).....	8
2.4.2 Rheological Modelling.....	9
2.5 Chemistry of Asphalt Binder.....	12
2.6 Characterization of Aging based on Chemical Composition.....	14
2.6.1 Corbett Analysis.....	15
2.6.2 High Performance Gel Permeation Chromatography (HP-GPC).....	15
2.6.3 Infrared Spectroscopy.....	16
2.7 Aging in Asphalt Pavements.....	17
2.7.1 Aging during Storage, Mixing and in Service life.....	17
2.7.2 Aging Mechanisms.....	19
2.8 Laboratory Accelerated Aging Methods.....	21
2.8.1 Accelerated Aging of Asphalt Binder.....	22
2.8.2 Accelerated Aging of Asphalt Mixtures.....	24

2.8.3	Photo Oxidation of Asphalt Binders and Mixtures	25
CHAPTER 3	RESEARCH METHODOLOGY	27
3.1	Introduction	27
3.2	Material Selection	29
3.3	Preparation of Laboratory Compacted Samples for Long-Term Conditioning	30
3.4	Laboratory Accelerated Conditioning Procedures	31
3.4.1	Control Conditioning Procedure	31
3.4.2	Atlas Weatherometer	32
3.4.3	Bespoke Chamber	33
3.5	Laboratory Testing	34
3.5.1	Asphalt Binder Tests	34
3.5.2	Asphalt Mixture Tests	37
CHAPTER 4	STATISTICAL ANALYSIS OF RESULTS AND DISCUSSIONS	40
4.1	Asphalt Binder	40
4.1.1	Rheological Analysis	40
4.1.2	Performance Analysis	50
4.1.3	Chemical Analysis	56
4.2	Asphalt Mixtures	58
4.2.1	Rheological Analysis	58
4.2.2	Performance Analysis	61
CHAPTER 5	CONCLUSIONS, RECOMMENDATIONS, AND FUTURE RESEARCH	63
5.1	Conclusions	63
5.2	Recommendations	65
5.3	Future Research Opportunities	65
REFERENCES	67
Appendix A:	Mix Design Sheets	70
Appendix B:	Apogee Sensor Data Sheets	82
Appendix C:	Rheological Analysis – Asphalt Cement	87
Appendix D:	MSCR Test Reports	105
Appendix E:	LAS Test Reports	157
Appendix F:	Rheological Analysis – Asphalt Mixture	192

LIST OF FIGURES

Figure 2-1 Graphical Representation of Viscoelastic Behavior [7].....	8
Figure 2-2 Vector diagram illustrating the relation between complex modulus (G^*/E^*), storage modulus(G'/E'), loss modulus (G''/E'') and phase shift angle (δ) [8].....	8
Figure 2-3 Representation of 2S2P1D rheological model [11]	10
Figure 2-4 Isothermal Mastercurve of Complex Modulus over a wide range of frequencies	10
Figure 2-5 Isothermal Mastercurve of Phase Angle over a wide range of frequencies	11
Figure 2-6 Isothermal Mastercurve of Storage & Loss Modulus over a wide range of frequencies	11
Figure 2-7 Black Space Diagram.....	11
Figure 2-8 Cole Cole Diagram.....	12
Figure 2-9 Separation of Asphalt Binder into four generic groups [12].....	13
Figure 2-10 Colloidal Structure of Asphalt Binder showing SARA fractions [3].....	14
Figure 2-11 Effect of vacuum reduction on composition of Asphalt Binder [12].....	15
Figure 2-12 Chromatograms of Virgin and Short Term aged Asphalt Binder [17].....	16
Figure 2-13 Typical FTIR spectra showing Carbonyl, CH ₂ , CH ₃ & Sulfoxide peaks	17
Figure 2-14 Aging during mixing, storage, transportation, and pavement service life [3].....	19
Figure 2-15 Atlas Weatherometer Suntest XXL [33].....	26
Figure 2-16 Inside view of APWS showing mixture sample under conditioning [35]	26
Figure 3-1 Research Plan Methodology	28
Figure 3-2 Loose Mix being sampled at Asphalt Plant.....	29
Figure 3-3 Compaction, Cutting & Coring at CPATT Laboratory.....	30
Figure 3-4 PAV residue, Degassing & AASHTO R30-02 Compacted Sample Conditioning.....	31
Figure 3-5 Atlas Weatherometer Ci35A showing external, and internal view with metal mesh platform for beam support	32
Figure 3-6 Bespoke Conditioning Chamber	33
Figure 3-7 Centrifuge Extractor, High-Speed Centrifuge and Rotavapor at CPATT lab.....	34
Figure 3-8 Linear Viscoelastic Region	34
Figure 3-9 Perkin Elmer Spectrum Two FT-IR Spectrometer.....	35
Figure 3-10 810 MTS Loading Frame and 651 MTS Environmental Chamber.....	37
Figure 3-11 Different Stages of SCB Test (Cutting & Notch Preparation, Drying followed by Temperature Conditioning, Testing using DTS-30 Frame, and Samples after Testing)	38

Figure 4-1 Predicted Complex Modulus Mastercurve along with Experimental Data Points.....	40
Figure 4-2 Predicted Phase Angle Mastercurve along with Experimental Data Points	40
Figure 4-3 Prediction for Loss & Storage Modulus along with Experimental Data Points	41
Figure 4-4 Complex Modulus VS Phase Angle (Predicted and Experimental).....	41
Figure 4-5 Disjointed Black Space curves as noted for Virgin (left) & Extracted & Recovered Virgin (right) binder samples.....	42
Figure 4-6 Effect of Aging on Complex Modulus Mastercurves	42
Figure 4-7 Effect of Aging on Phase Angle Mastercurves	43
Figure 4-8 Effect of Short-term Conditioning Procedures on Complex Modulus	43
Figure 4-9 Effect of Short-term Conditioning Procedures on Phase Angle Mastercurves.....	44
Figure 4-10 Effect of Long-term Conditioning Procedures on Complex Modulus.....	44
Figure 4-11 Effect of Long-term Conditioning Procedures on Phase Angle Mastercurves	45
Figure 4-12 Effect of Water Conditioning on BC5 & BC10 Samples – Complex Modulus	46
Figure 4-13 Effect of Water Conditioning on BC5 & BC10 Samples – Phase Angle	46
Figure 4-14 Effect of Water Conditioning on BC15 & BC20 Samples – Complex Modulus	47
Figure 4-15 Effect of Water Conditioning on BC15 & BC20 Samples – Phase Angle	47
Figure 4-16 Effect of Age Hardening on Black Space Curves.....	48
Figure 4-17 Shift Factor VS Temperature for Binders (Control & Atlas Procedure)	49
Figure 4-18 Shift Factor VS Temperature for Binders (Bespoke Chamber)	49
Figure 4-19 Comparison of Jnr for different Conditioning Procedures.....	51
Figure 4-20 Comparison of Jnr_diff for different Conditioning Procedures	51
Figure 4-21 Comparison of Nf (2.5% & 5% Strain) for different Conditioning Procedures	53
Figure 4-22 Fatigue Life for Control and Atlas Weatherometer Conditioning Procedures	54
Figure 4-23 Fatigue Life for Bespoke Chamber Conditioning Procedure.....	54
Figure 4-24 Amplitude Sweep for Control and Atlas Weatherometer Conditioning	55
Figure 4-25 Amplitude Sweep for Bespoke Chamber Conditioning Procedure.....	55
Figure 4-26 FT-IR Spectra for Binders subjected to different Conditioning Procedures.....	56
Figure 4-27 Comparison of Sulfoxide to Carbonyl Ratio.....	57
Figure 4-28 Comparison of Complex Modulus Mastercurves for Asphalt Mixtures.....	58
Figure 4-29 Comparison of Phase Angle Mastercurves for Asphalt Mixtures.....	59
Figure 4-30 Comparison of Black Space Diagrams for Asphalt Mixtures.....	59

Figure 4-31 Comparison of Cole-Cole Diagrams for Asphalt Mixtures	60
Figure 4-32 Shift Factor VS Temperature for Asphalt Mixtures.....	60
Figure 4-33 Load VS Displacement Curves for SCB Testing	62

LIST OF TABLES

Table 2-1 Tests used for Penetration, Viscosity and PG Grading of Asphalt Binder.....	6
Table 2-2 Asphalt Aging Mechanisms [3].....	20
Table 2-3 Accelerated Aging Methods for Asphalt Binders [29].....	23
Table 2-4 Accelerated Aging Methods for Asphalt Mixtures [29].....	24
Table 3-1 List of Asphalt Binder Samples subjected to Laboratory Testing.....	36
Table 3-2 List of Asphalt Mixture Samples subjected to Laboratory Testing.....	39
Table 4-1 Multiple Stress Creep Recovery Test results sorted by magnitude of Jnr (3.2kPa).....	50
Table 4-2 Nf values calculated for 2.5% and 5% Strain level	52
Table 4-3 FT-IR Functional Group Analysis sorted in order of Carbonyl Index values	57
Table 4-4 SCB Test Results for Unconditioned Samples	61
Table 4-5 SCB Test Results for AASHTO R30 Conditioned Samples	61
Table 4-6 SCB Test Results for Atlas Weatherometer Conditioned Samples.....	61

CHAPTER 1 INTRODUCTION

Canada's road and highway network comprises of more than one million kilometers of roads, 40 percent of which are paved. The transportation network forms one of the most important mode of passenger and freight transportation and trade between Canada and the United States, and plays an important role in national economy as a measure of Canada's global development index.

Records published by statistics Canada in 2009 shows that there was a 10 percent increase in the percentage of roads and highway investment budgets that have been spent on network rehabilitation as compared to network expansion. This trend has further exacerbated over the last 8 years, highlighting the need to better understand pavement aging and enhance durability [1].

Over 95 percent of Ontario's roads are paved with asphalt, an organic material that evolves physically and chemically over time owing to a number of aging mechanisms. Asphalt pavements are designed based on the rheological properties of asphalt binder, which even though comprises only around 4 – 6 percent of the asphalt mixture, has a great impact on durability and governs the behavior of the mixture. Thus it is very important to understand the various aging mechanisms and their subsequent effects on binder rheological properties, to enhance pavement longevity and reduce the time period to rehabilitation and/or replacement.

The change in binder properties during construction (short-term) and pavement service life (long-term) is referred to as asphalt aging or age hardening and is a measure of pavement durability. In general, asphalt aging tends to increase binder viscosity making it stiffer and brittle which would lead to an increase in resistance against rutting but would also lead to a reduction in pavement durability with reduced resistance against fatigue, low temperature distresses and stripping.

Generally, loss of volatiles or lighter oily fractions and high temperature oxidation are the two main factors associated with short-term aging, and oxidation at ambient temperatures is the main factor associated with long-term aging. However, the rate of change, resulting chemical composition and rheological properties vary for different types of binder and even for same type of binder dependent on various environmental factors such as temperature, humidity, solar radiation (including ultraviolet and infrared) etc. as well as asphalt mixture properties such as air voids (distribution and interconnected voids), asphalt film thickness, type of aggregates, filler content and gradation [2].

Several accelerated laboratory aging methods have been developed for both short-term and long-term aging for asphalt binder and asphalt concrete. These methods are used to age binder and mixture samples on which further performance and rheological tests are then carried out. For asphalt binder the most commonly used methods are RTFOT (Rolling Thin Film Oven Test) and PAV (Pressure Aging Vessel) which simulate short-term and long-term aging respectively. For asphalt mix, SHRP methods are generally employed with STOA (loose-mix at 135°C for 4hrs) for short-term and LTOA (compacted samples at 85°C for 120hrs) for long-term aging.

However, most of the current laboratory accelerated aging methods rely solely on high temperatures and air flow for accelerated oxidative aging and do not consider any environmental factors and other mix design parameters. This project aims at identifying the importance of these

less considered factors, and incorporate them into a new accelerated aging procedure which could be used to produce samples which are more representative of actual field aging. Further performance and rheological testing could then be utilized to identify any premature pavement distresses and enhance durability.

1.1 Research Hypothesis

The main hypotheses for this research project are briefly summarized as below:

1. Asphalt binder aging, a measure of pavement durability, leads to better rutting performance and reduced resistance against fatigue and low temperature distresses.
2. Current accelerated aging mechanisms rely mainly on high temperatures, pressure, and air flow for oxidative aging and hence do not accurately mimic field aging.
3. Performance and rheological test results carried out on current laboratory aged samples might not be able to fully explain pavement characteristics after aging.
4. Environmental factors viz. temperature, amount and intensity of solar radiation, humidity and rainfall, and other mix design parameters all have an effect on asphalt oxidative aging in terms of its kinetics, chemical path and subsequent performance and rheological test results.
5. Accelerated laboratory aging incorporating these less considered factors could be used to better understand pavement durability.

1.2 Scope and Objectives

The objective of this project is to optimize an accelerated laboratory aging method, capable of simulating long-term field aging by studying the combined effect of asphalt binder and mixture properties, and various environmental factors.

In order to achieve this objective samples will be aged using different conditioning procedures and then subjected to subsequent laboratory rheological, chemical and performance tests. The results would then be analyzed to evaluate the importance of different conditioning parameters, and hence identify an accelerated aging procedure which provides a more representative sample for further testing.

1.3 Thesis Organization

This thesis is organized into chapters with following contents:

Chapter 1: Introduction – The concept of oxidative aging along with its subsequent effects on pavement durability is introduced, followed by hypothesis and overall scope and objectives of this research project.

Chapter 2: Literature Review – A comprehensive review of current state of the art knowledge on Asphalt binder and mixture properties and life cycle, along with an insight into various aging mechanisms and concepts and approaches related to accelerated laboratory aging procedures.

Chapter 3: Research Methodology – Methodology employed to optimize a laboratory accelerated aging procedure which could be used to simulate real life aging conditions on asphalt mixture samples, thus providing a more accurate representation of changes in pavement rheological and mechanical behavior with time.

Chapter 4: Statistical Analysis of Results and Discussions - Laboratory test results for both asphalt binder and asphalt mixtures along with subsequent analysis and discussions are presented in this chapter.

Chapter 5: Conclusions, Recommendations and Future Research – Recommendations based on conclusions drawn from comparative analysis of the results are presented along with identification of possible areas for beneficial future research.

CHAPTER 2 LITERATURE REVIEW

2.1 Introduction

The purpose of this chapter is to provide current state of the art knowledge on Asphalt binder and mixture properties and life cycle along with an insight into various aging mechanisms and concepts and approaches related to accelerated laboratory aging procedures.

2.2 Background on Asphalt

Asphalt, also known as bitumen is a viscoelastic material formed of a mixture of different hydrocarbons of natural and/or pyrogenous origin, and is highly viscous, sticky, and black in appearance. Historically natural asphalt from lakes, rock formations, gilsonite and oil sands have been used for a diverse range of applications including but not limited to waterproofing, as a bonding agent, construction, paving, and so on. This natural material is often accompanied by mineral matter, the amount and nature of which is dependent on the source and extraction processes involved [3]. In Canada, large natural deposits of bituminous sands are found in the valley of Athabasca river, Alberta, and natural deposits of Albertite occur in the valley of Peticodiac river in Albert county, NB [4].

There are over 250 known applications of asphalt as a construction and engineering material with around 85% of the total production being used for the pavement industry. About 10% is used for roofing applications with the remaining part (approximately 5%) being used for a variety of other applications such as waterproofing, paints, sealing etc. [5].

Almost all of the asphalt used today for paving comes from petroleum crude oil, a complex mixture of hydrocarbons differing in molecular weight, viscosity and consequently in boiling range. Liquid asphalt, also referred to as straight-run asphalt binder is the heaviest part of the crude and residuum of the vacuum distillation tower after distillation of volatile, light fractions such as LPG, gasoline, diesel etc. These straight-run asphalts are generally soft, with their properties directly related to the constituent crude and often require further processing (air-rectification, mild oxidation, blending, additives such as polymers etc.) to produce penetration grade asphalt binders that are suitable for road construction.

2.3 Asphalt Binder Grading

Dependent on the type of processing involved there is great variance in the physical and chemical properties of asphalts making them difficult to use for road construction. With increasing technological advances asphalt specifications have evolved greatly over time to ensure consistency. Explained below are the different types of asphalt binder grading specifications.

2.3.1 Penetration Grading

This system was developed in the early 1900's to characterize the consistency of semi solid asphalts. The penetration depth of a 100gm needle in asphalt binder maintained at 25°C is measured after 5 seconds and used for specification. This penetration depth is a measure of asphalt binder viscosity or softness and is roughly related to its performance, i.e. a higher penetration asphalt (soft) would be better suited for use in colder climates as compared to a lower penetration asphalt (hard). There are five different penetration grades as specified in AASHTO M20 ranging from 40-50 (hardest grade) to 200-300 (softest grade) [6].

One of the main disadvantages of using Penetration Grading is that because the test is performed at a constant temperature (25°C), it does not provide any information about the temperature susceptibility and mixing/compaction temperatures for asphalt binder.

2.3.2 Viscosity Grading

Viscosity, the ratio between the applied shear stress and the rate of shear was introduced in the early 1960's as an improved system for asphalt grading. Viscosity tests are carried out at different temperatures (typically 60°C and 135°C) and are hence able to characterize the mixing/compaction temperatures and also provide an insight into the temperature susceptibility of asphalt binder.

Viscosity grading can be carried on original or neat asphalt binder (AC grading) as well as short-term aged binder (AR grading). AR grading takes into account the age hardening effects that happens during the production of hot mix asphalt (HMA) and are hence a better representative of actual pavement performance [6].




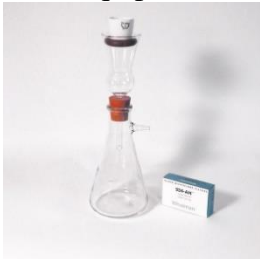

2.3.3 SuperPave Performance Grading

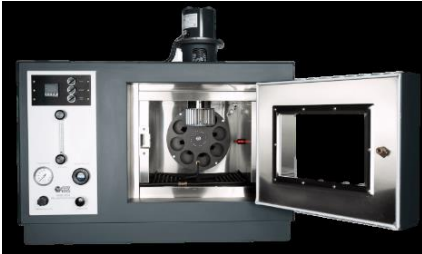

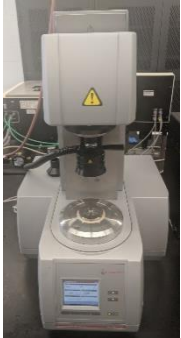


Superpave performance grading (PG) system is based on the climatic conditions under which an asphalt pavement is to be used, and utilizes tests that specifically address pavement performance parameters such as rutting, fatigue cracking and thermal cracking. These tests are carried out on neat, short-term aged and long-term aged binder samples at specific temperatures that are dependent upon the climatic conditions in the area of use.

PG grading is reported in two numbers (for e.g. PG 64-22), where the first and the second numbers are the average seven-day maximum and the minimum temperatures respectively that the pavement is likely to experience. Dependent on the type of crude used polymers and/or extenders are added to the binder to enhance the high temperature and low temperature performance respectively and as a general rule of thumb these additives are generally required if the temperature specification differs by 90°C or more.

Table 2-1 lists the different tests used for Penetration, Viscosity and PG Grading of Asphalt Binder, along with a brief description of their purpose and the laboratory equipment used.

Table 2-1 Tests used for Penetration, Viscosity and PG Grading of Asphalt Binder

Test	Purpose	Equipment
Penetration Test	To obtain penetration depth of a 100gm needle in asphalt binder maintained at 25°C (measured after 5 seconds). Considered an index for consistency of binder at intermediate temperatures.	Standard Penetrometer 
Flash Point Test	To determine the lowest liquid temperature at which application of test flames causes the vapors of the sample to ignite.	Anton Paar® Open Cup tester 
Ductility	To measure asphalt binder ductility by stretching a standard-sized briquette to its breaking point. Considered an index of flexibility at low temperatures (4°C) and compatibility at 25°C.	Ductilometer 
Solubility / Purity	To quantify any mineral impurities in asphalt binder by dissolving a sample in a suitable solvent (methylene chloride, trichloroethylene etc.) through a filter mat.	Solubility Test Equipment 
Rotational Viscosity (RV)	To measure dynamic viscosity of asphalt binder at different temperatures and hence provide information about binder's pumpability, mixability and workability.	Brookfield® RV 

<p>Short-term Aging</p>	<p>To simulate short-term age hardening effects that occurs during plant production of asphalt mixture.</p>	<p>Despatch® Rolling Thin Film Oven (RTFO)</p> 
<p>Long-term Aging</p>	<p>To simulate long-term age hardening effects that occurs during service life of a pavement.</p>	<p>Prentex® Pressure Aging Vessel (PAV) and Degassing Chamber</p> 
<p>Dynamic Shear Rheometer (DSR)</p>	<p>To characterize the viscous and elastic behavior of asphalt binders at medium to high temperatures ensuring adequate resistance against rutting and fatigue cracking.</p>	<p>Anton Paar® DSR</p> 
<p>Bending Beam Rheometer (BBR)</p>	<p>To measure low temperature stiffness and relaxation properties of asphalt binders giving an indication of its ability to resist low temperature cracking. Tests are carried out on small simply supported PAV aged binder beams.</p>	<p>Cannon® BBR</p> 
<p>Direct Tension Tester (DTT)</p>	<p>To measure low temperature failure stress and strain of PAV aged binder. DTT, along with BBR is used to determine low temp PG grading.</p>	<p>Interlaken® DTT</p> 

2.4 Rheological Behavior of Asphalt Binder and Asphalt Mixture

Asphalt binders and the subsequent flexible pavements display a viscoelastic behavior i.e. when subjected to shear loading they behave partly like an elastic solid (recoverable deformation) and partly like a viscous liquid (non-recoverable deformation). This behavior is also time and temperature dependent i.e. at higher temperatures and slower rate of loading a softer response is encountered as compared to lower temperatures and faster rate of loading. The rheological properties are a function of the internal forces between the intricate hydrocarbon structures which changes with the use of additives (polymers, extenders etc.) and age hardening (mainly due to oxidation) resulting in changes in mechanical properties of both asphalt binder and asphalt mixtures. Historically, empirical properties have been used to provide an indication of the rheological characteristics, which can now be determined much more accurately by carrying out tests at a range of frequencies and temperatures.

2.4.1 Complex Modulus (G^* for binders / E^* for mixes) and Phase Shift Angle (δ)

Under sinusoidal cyclic loading, the ratio between the amplitude of peak stresses and strains is calculated as the normal value of the Complex Modulus (a measure of total resistance to deformation under loading) and the time lag between the two is referred to as the Phase Shift Angle. Both of these parameters combined characterize the viscoelastic behavior and can be used to determine the Storage Modulus (elastic portion) and the Loss Modulus (viscous portion).

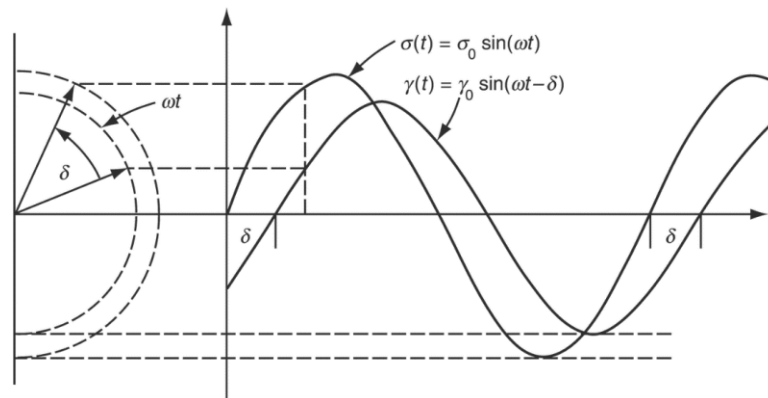


Figure 2-1 Graphical Representation of Viscoelastic Behavior [7]

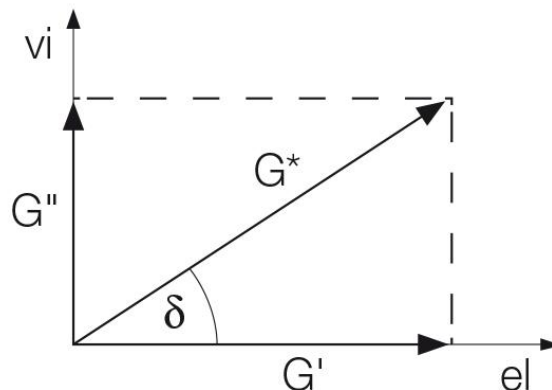


Figure 2-2 Vector diagram illustrating the relation between complex modulus (G^*/E^*), storage modulus (G'/E'), loss modulus (G''/E'') and phase shift angle (δ) [8]

2.4.2 Rheological Modelling

As mentioned before the behavior of asphalt binder and asphalt mixtures is time and temperature dependent i.e. with increasing temperature and decreasing frequency of loading, the complex modulus values would decrease, and the phase angle values would increase. In order to fully characterize the rheological behavior, frequency sweep tests are carried out at different temperatures. It is vital that these tests are carried out within the linear viscoelastic region (LVE), which is defined as a region where the relationship between stress and strain is influenced by temperature and time alone and not by the magnitude of the stress or strain [9].

The rheological data hence collected can be used for the construction of mastercurves characterizing the full rheological behavior of binders and mixtures, using the time temperature superposition principle (TTS) or the method of reduced variables. This principle is based on the interrelation between temperature and frequency (loading time), which through shift factors can be used to bring measurements done at different temperatures and frequencies to fit one overall continuous curve. Mastercurves can be generated in two different ways, Isothermal plots (where a reference temperature is first selected followed by shifting of rheological data at all other temperatures with respect to time or reduced frequencies) and Isochronal plots (where a reference frequency is first selected followed by shifting of rheological data at all other frequencies with respect to temperature) [10].

Many attempts have been made to use phenomenological and analogical models, defined by curve fitting of experimental data to describe the viscoelastic properties of asphalt binders and mixtures. These models are comprised of a combination of springs (elastic elements), linear dashpots (Newtonian viscous elements), and parabolic elements (parabolic creep function). Examples of some of these models are the Maxwell and Kelvin-Voigt model, CA (Christensen-Anderson) model, CAM (Christensen-Anderson-Marasteanu) model, Zeng model, Huet model, and the Huet-Sayegh model. The reader is directed to [11] for further information and mathematical representation of these models.

2.4.2.1 2S2P1D Rheological Model

F. Olard and H. Di Benedetto introduced the 2S2P1D (two springs, two parabolic elements, and one dashpot) model which is a generalization of the Huet-Sayegh model. This model is valid for both asphalt binders and asphalt mixtures, and at a given temperature has seven constants, each with a physical meaning and representation. Complex Modulus (E^*) for the 2S2P1D model given by the following expression (in complex form):

$$E^*(i\omega\tau) = E_0 + \frac{E_\infty - E_0}{1 + \delta(i\omega\tau)^{-k} + (i\omega\tau)^{-h} + (i\omega\beta\tau)^{-1}}$$

Eq. 2-1 [11]

where

E_0 = Static modulus (at very high temperature or very low frequency)

= 0 for binders (no aggregate skeleton effect)

E_∞ = Glassy modulus (at very low temperature or very high frequency)

- i = complex number defined by $i^2 = -1$
- ω = Angular frequency (2π *frequency), the solicitation pulsation
- τ = characteristic time with values varying only with temperature (accounts for TTS)
- k, h = parabolic creep element exponents such that $0 < k < h < 1$
- δ = dimensionless shape parameters
- β = Constant that depends on dashpot viscosity [Newtonian Viscosity (η) = $(E_\infty - E_0)\beta\tau$]

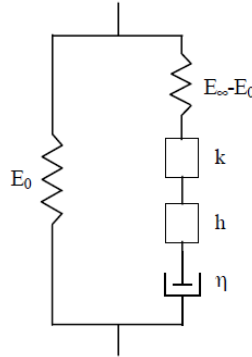


Figure 2-3 Representation of 2S2P1D rheological model [11]

In this research project, the 2S2P1D model has been used to analyze the rheological behavior of both asphalt binders and asphalt mixtures, given its ease of use with one equation for predicting both complex modulus and phase angle, and its ability to accurately model complex rheological behavior. Also (as mentioned before) the variables used in this model have a physical meaning representing actual rheological behavior rather than just curve fitting variables. Shown below are example analysis results for tests carried out on a typical asphalt mix sample. Figure 2-4, Figure 2-5, and Figure 2-6 shows the developed mastercurves for Complex Modulus, Phase Angle, and Storage and Loss Modulus respectively over a wide range of frequencies. Figure 2-7 and Figure 2-8 shows the Black Space diagram (plot of complex modulus against phase angle) and Cole Cole diagram (plot of loss modulus against storage modulus) respectively. Since both of these plots are not affected by the TTS manipulations, they serve as a useful tool to identify any inconsistencies in experimental rheological data.

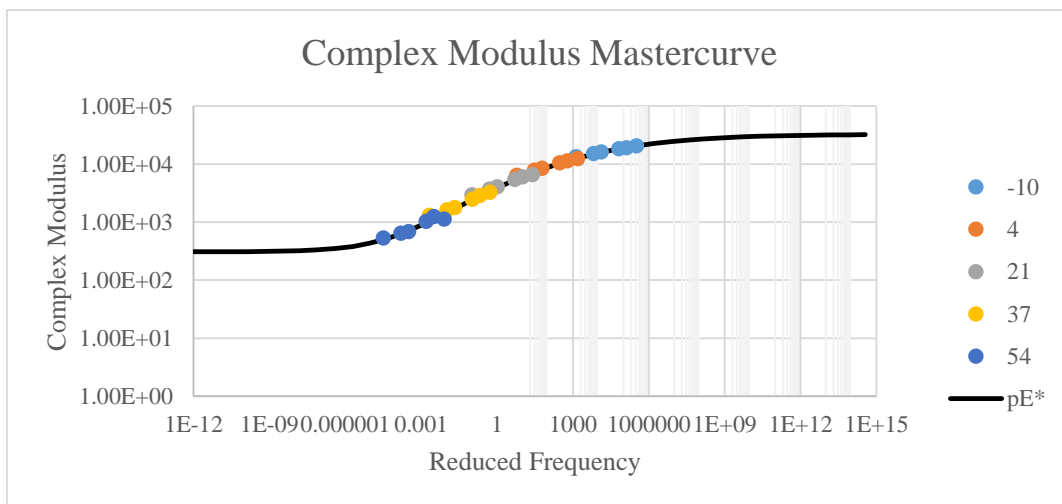


Figure 2-4 Isothermal Mastercurve of Complex Modulus over a wide range of frequencies

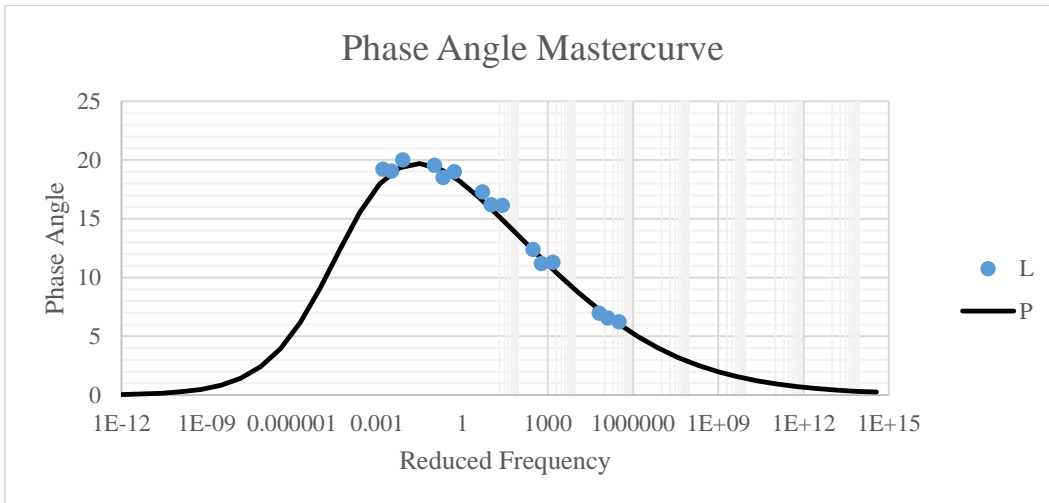


Figure 2-5 Isothermal Mastercurve of Phase Angle over a wide range of frequencies

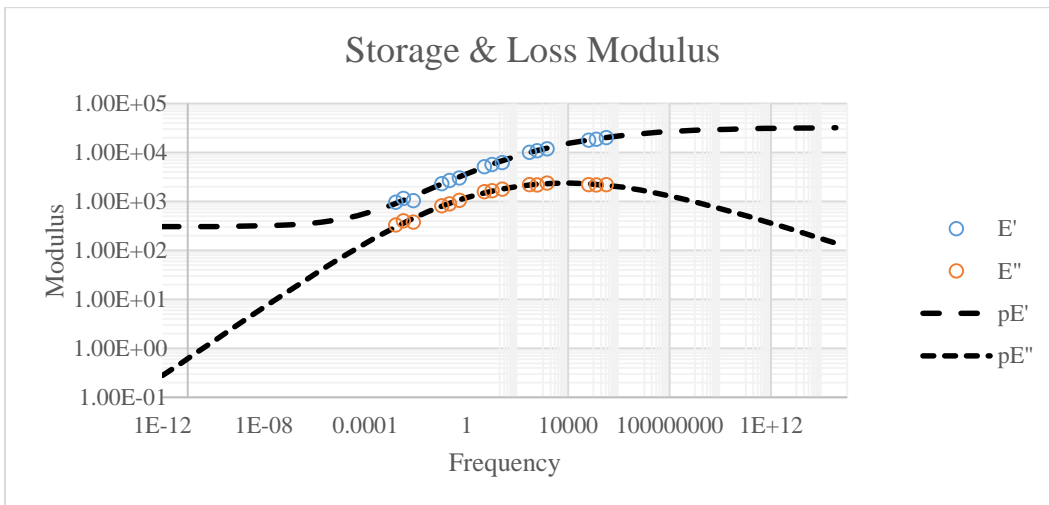


Figure 2-6 Isothermal Mastercurve of Storage & Loss Modulus over a wide range of frequencies

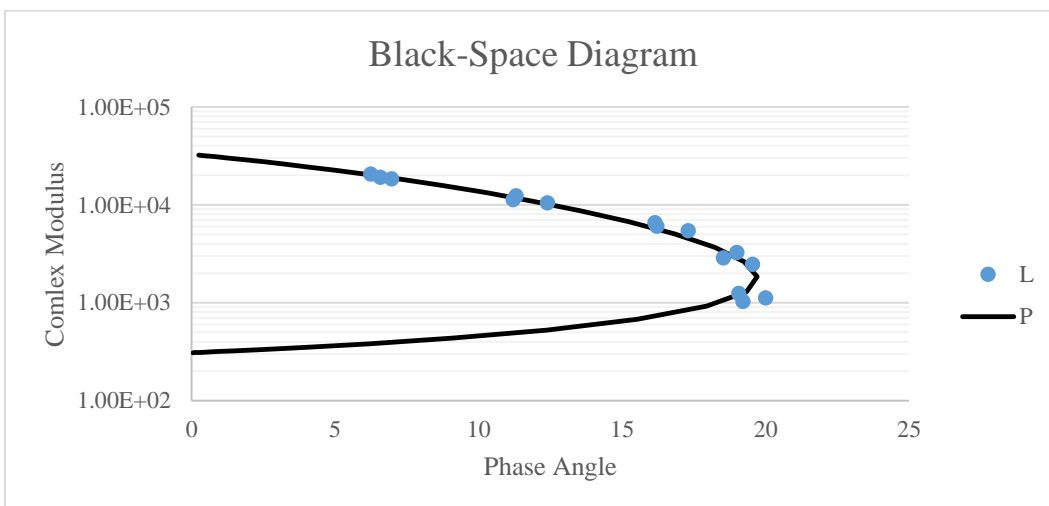


Figure 2-7 Black Space Diagram

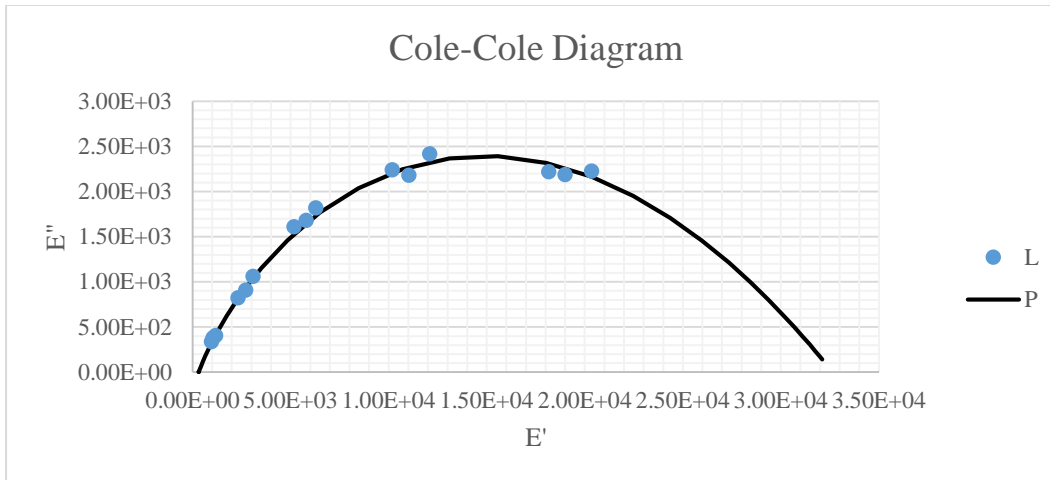


Figure 2-8 Cole Cole Diagram

Note that in all these diagrams the solid black line (annotated as P) represents the rheological behavior as predicted by the 2S2P1D model and dots represent the actual experimental test data. Also for this particular asphalt mixture sample, the root mean squared error over the interquartile range (RMSEIQR) has been calculated as 3.7% indicating that the 2S2P1D model was able to accurately characterize the rheological behavior.

2.4.2.2 Effect of Aging on Rheological Behavior

As mentioned before, asphalt binder is an organic material which is affected by oxidation, temperature, solar radiation, humidity etc. and hardens with aging with a subsequent increase in its viscosity. This results in a constant increase in complex modulus and decrease in phase angle i.e. an increase in stiffness and proportion of elastic behavior as compared to virgin binder.

2.5 Chemistry of Asphalt Binder

The chemical composition of asphalt binder is extremely complex, dependent on the source of crude oil used, and varying during its lifecycle (mainly due to oxidative aging). Asphalt binder is a mixture of different hydrocarbons (82-88% carbon and 8-11% hydrogen) along with a small amount of other functional groups containing sulphur, nitrogen and oxygen atoms. It may also contain a trace amount of metals such as vanadium, nickel, iron, magnesium and calcium [3]. This complex and diverse chemical composition makes complete chemical analysis of asphalt binder not only challenging but also impractical in terms of any meaningful correlation with its rheological properties.

As a result, researchers tried to separate asphalt binder into broader chemical fractions based on hydrocarbon properties such as molecular weight, particle size, polarity etc. Different techniques such as solvent extraction, filtration and chromatography have been utilized in the past to separate asphalt binder into fractions. Out of these, a method developed by Corbett in 1969 gained popularity given its ease of use and ability to fractionalize asphalt binder into four reasonably distinct hydrocarbon groups, also known as SARA fractions (Saturates, Aromatics, Resins and

Asphaltenes). This method utilizes solvent extraction followed by elution-adsorption chromatography (refer to Figure 2-9) [12].

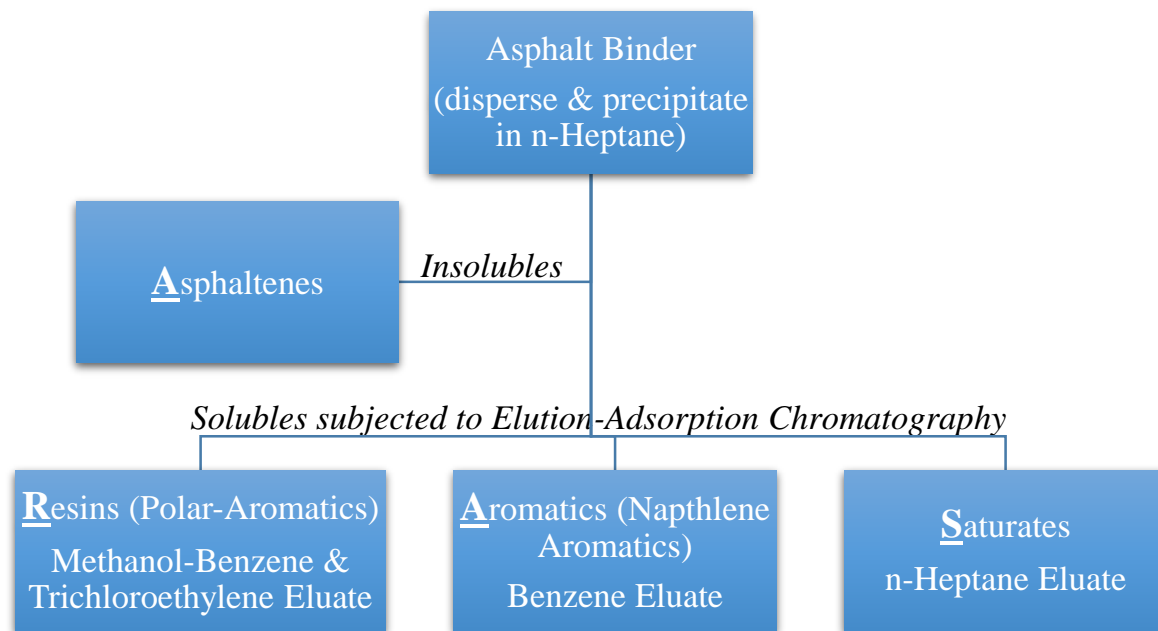


Figure 2-9 Separation of Asphalt Binder into four generic groups [12]

A brief description of the physical nature and properties of these groups is discussed below:

Asphaltenes: These are black or brown in color, highly polar, solid, aromatic hydrocarbons comprised mainly of carbon and hydrogen with small amounts of nitrogen, sulphur and oxygen. Asphaltenes are the biggest and the heaviest molecules among all other fractions with a molecular weight ranging between 1000 & 100,000 and a particle size of 5 to 30nm [3]. In terms of rheological characteristics, increasing the asphaltene content would lead to a subsequent increase in stiffness and binder viscosity.

Resins (Polar Aromatics): These are similar to asphaltenes in terms of their composition with a lower molecular weight (500 to 50,000) and particle size (1 - 5nm). They are in solid to semi-solid state with a dark brown color and polar nature. In asphalt binder structure, resins surround the asphaltenes acting as a stabilizing solvent layer (Figure 2-10).

Aromatics (Naphthalene Aromatics): These are non-polar carbon chains with a molecular weight of 300 to 2000. These are dark brown viscous liquids with a high dissolving ability and act as a medium in which resin coated asphaltenes are dispersed (Figure 2-10).

Saturates: These are white or straw colored non polar oils comprised of straight and branch chain hydrocarbons. Saturates can be both waxy and non-waxy with a similar molecular weight as aromatics and form a part of the dissolving medium in asphalt binder structure (Figure 2-10).

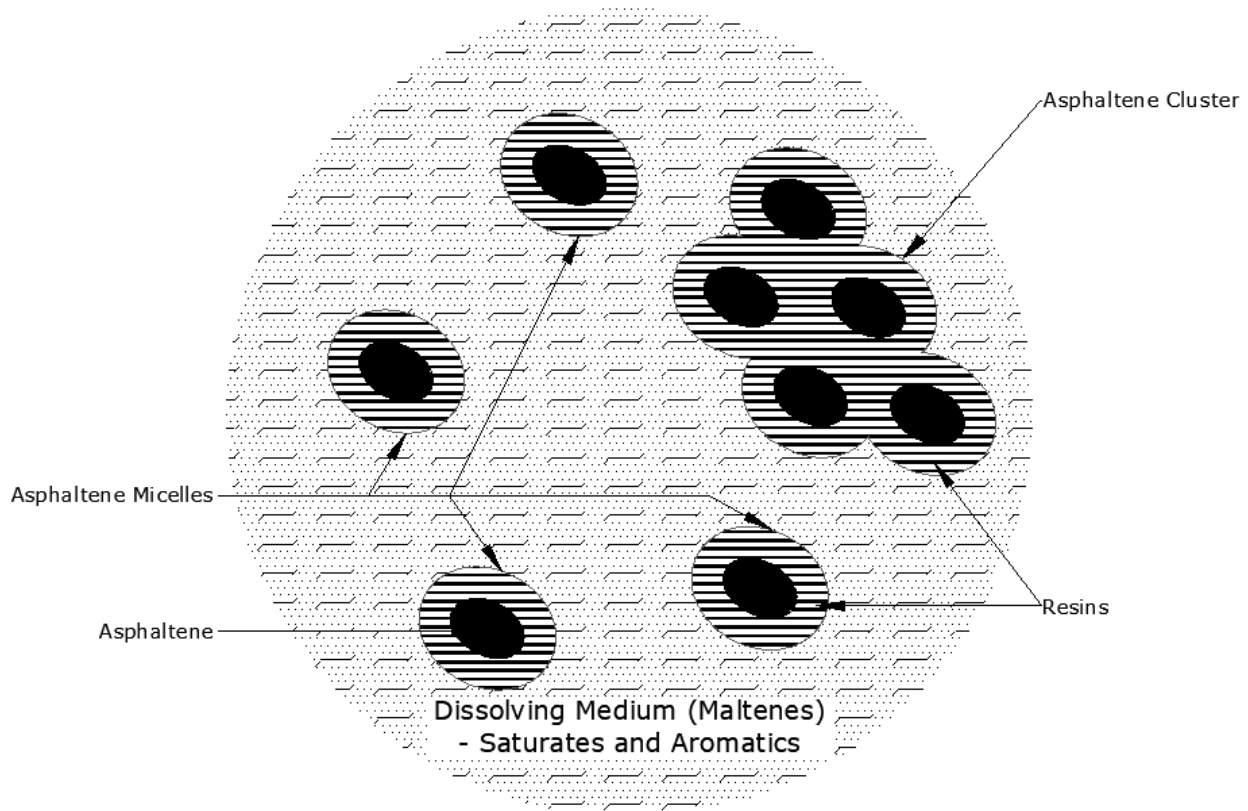


Figure 2-10 Colloidal Structure of Asphalt Binder showing SARA fractions [3]

2.6 Characterization of Aging based on Chemical Composition

One of the major causes of failure of asphalt pavements is aging, caused mainly due to oxidative aging of asphalt binder and resulting in an increase in its viscosity and brittleness, and generally speaking a subsequent increase in resistance against rutting but a reduction in fatigue life and thermal resistance properties.

Oxidative aging leads to a change in the colloidal structure and chemical composition of asphalt binder with formation of highly polar and strongly interacting functional groups containing oxygen [13]. Over the years, studies carried out on oxidative aging have almost uniformly concluded that age hardening of asphalt binder is marked by the formation of sulfoxides (by oxidation of sulphur) and ketones or carbonyl (by oxidation of carbon) [14]. These two major oxidation products (carbonyl and sulfoxide), also accompanied with some minor amounts of dicarboxylic anhydrides and carboxylic acids can be used as an index to quantify the rate and level of oxidative aging [15].

In terms of asphalt binder structural analysis, various methods such as Corbett analysis, gel permeation chromatography, x-ray diffraction and scattering, and electron microscopy can be used to study the molecular weights and fractions [13]. Out of these Corbett analysis and gel permeation chromatography are the most popular techniques given their simplicity, capability and rapidness. Both of these methods are discussed briefly in section 2.6.1 and section 2.6.2.

However, it must be noted that even though structural analysis provides a very good understanding of asphalt binder's chemistry it does not provide any meaningful measure of the kinetics and rate of aging which can be determined more accurately by studying the formation and reactivity of functional groups (carbonyl and sulfoxide). Many instrumental techniques such as x-ray diffraction, mass spectrometry, infrared spectrometry (IR), and nuclear magnetic resonance spectroscopy (NMR) can be used and among these, IR is the fastest and most sensitive technique that can be used for detection of asphalt binder functional groups [13]. This technique is subsequently described in section 2.6.3.

2.6.1 Corbett Analysis

Asphalt binder fractionalization was carried out on binders obtained from different stages in the vacuum reduction distillation process by Corbett [12]. The results show that as the distillation progresses (i.e. increasing level of aging), both of the lighter fractions (Saturates and Aromatics) decrease in concentration while the heavier fractions (Resins and Asphaltenes) increase in concentration (Figure 2-11).

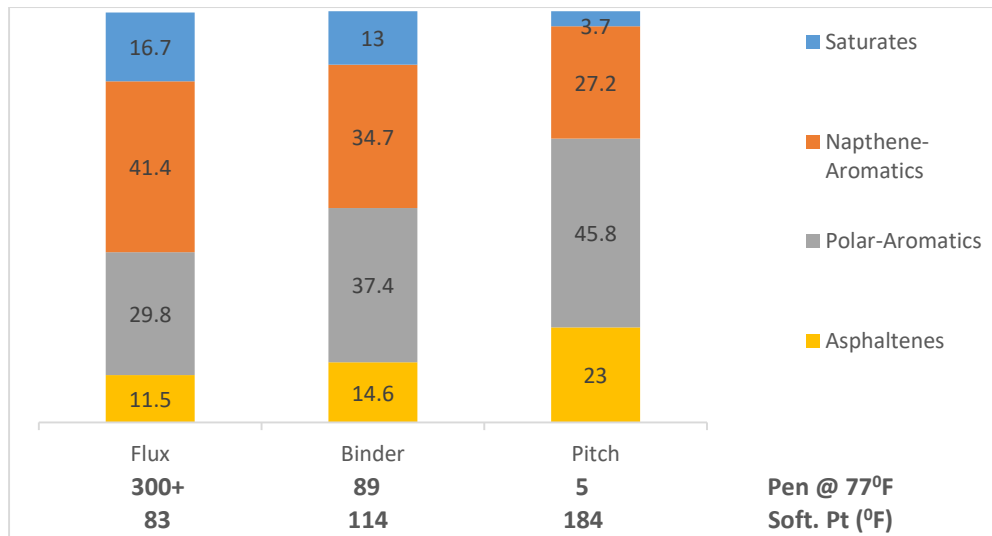


Figure 2-11 Effect of vacuum reduction on composition of Asphalt Binder [12]

2.6.2 High Performance Gel Permeation Chromatography (HP-GPC)

Similar to Corbett analysis (fractionalization of asphalt binder), another approach that can be used to separate asphalt binder based on the apparent molecular size distribution is High Performance Gel Permeation Chromatography (HP-GPC). This approach is analogous to sieve analysis and is based on the elution time of asphalt molecules through a column chromatograph packed with permeable gel, under high pressure. Using this approach asphalt binder can be divided into three regions namely Large Molecular Size (shortest elution time), Medium Molecular Size, and Small Molecular Size (longest elution time). In a previous study carried out by Jennings (1985), asphalt binder samples extracted from a wide variety of pavements in different stages of their lifecycle were subjected to HP-GPC analysis. Results indicate that an increase in concentration of LMS is associated with an increase in aging of asphalt binder and a subsequent increase in cracking of pavements. It was also concluded that asphalt binders with a higher concentration of LMS are comparatively better suited for colder climates [16].

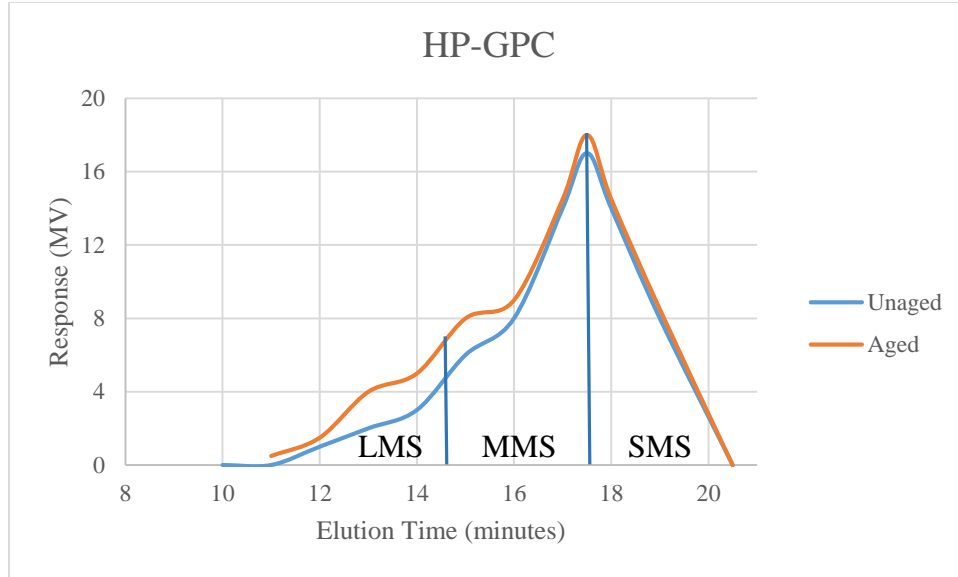


Figure 2-12 Chromatograms of Virgin and Short Term aged Asphalt Binder [17]

These results are in agreement with the Corbett analysis results shown in Figure 2-11, i.e. an increase in level of aging leads to an increase in concentration of large molecular size fractions (asphaltenes and resins).

2.6.3 Infrared Spectroscopy

Infrared spectroscopy (IR) can be used to measure functional groups by analyzing the interaction (absorption, emission and reflection) of infrared light with a molecule [18]. Fourier Transform Infrared Spectrometers (FTIR) allows for these spectral measurements to be taken quickly over a wide scan range and with high accuracy. For asphalt binder, the obtained spectrum can then be analyzed to quantitatively calculate structural indices for the two main functional groups formed during oxidative aging: carbonyl functional group (around 1700 cm^{-1}) and sulfoxide functional group (around 1030 cm^{-1}). These calculations are based on the assumption that the CH_2 ethylene groups (at 1460 cm^{-1}) and the CH_3 methyl groups (at 1375 cm^{-1}) are not significantly modified by oxidative aging [19]. Carbonyl index (I_c) and Sulfoxide index (I_s) can be calculated using the following formulas.

$$I_c (\text{Carbonyl Index}) = \frac{\int_{W=1680}^{W=1750} F(W)dW}{\int_{1400}^{1500} F(W)dW + \int_{1357}^{1390} F(W)dW} \quad \text{Eq. 2-2}$$

$$I_s (\text{Sulfoxide Index}) = \frac{\int_{W=980}^{W=1060} F(W)dW}{\int_{1400}^{1500} F(W)dW + \int_{1357}^{1390} F(W)dW} \quad \text{Eq. 2-3}$$

where

$F(W)$ represents the spectrum and W the wavenumber; and

$\int_{W=1680}^{W=1750} F(W)dW$ = Area under the Carbonyl peak.

$$\int_{W=980}^{W=1060} F(W)dW = \text{Area under the Sulfoxide peak.}$$

$$\int_{1400}^{1500} F(W)dW + \int_{1357}^{1390} F(W)dW = \text{Area under the CH}_2 \text{ \& CH}_3 \text{ peaks.}$$

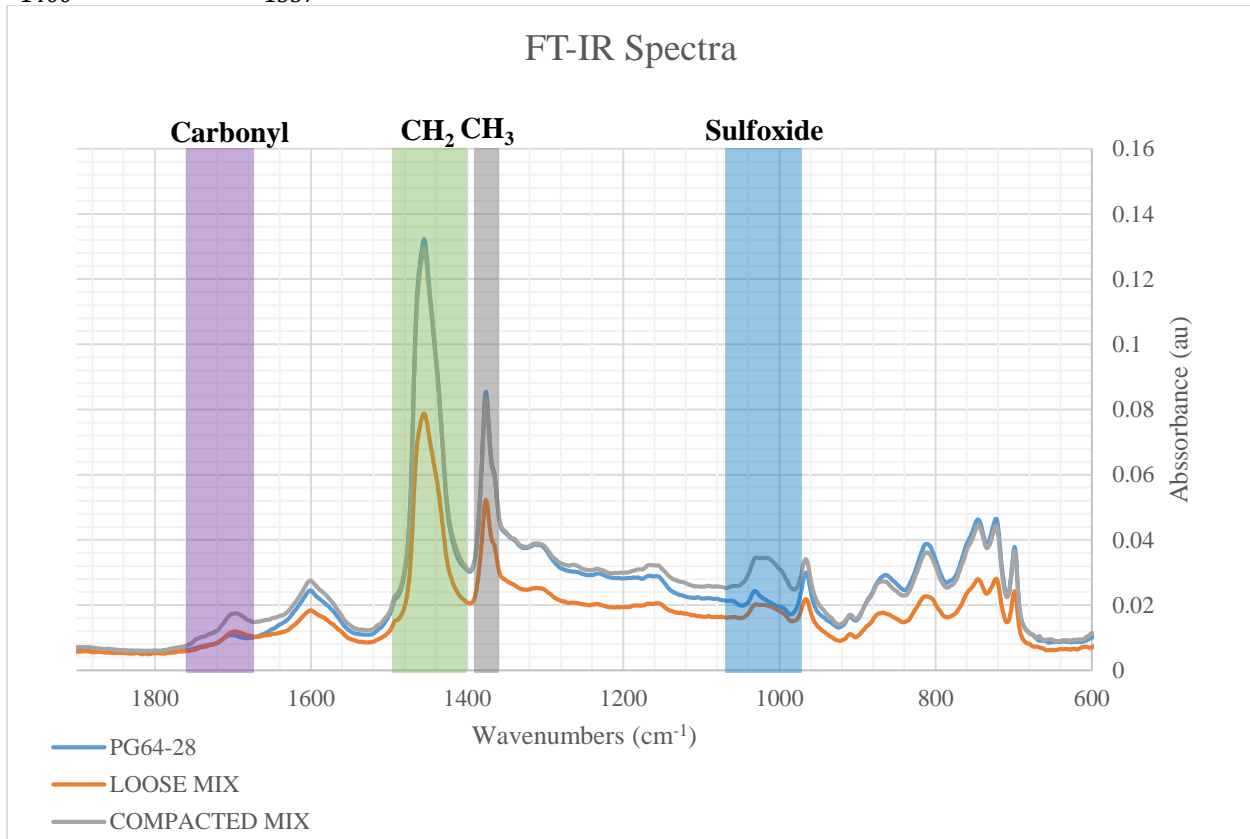


Figure 2-13 Typical FTIR spectra showing Carbonyl, CH₂, CH₃ & Sulfoxide peaks

2.7 Aging in Asphalt Pavements

In pavement industry, the lifecycle of asphalt binder constitutes of different stages, with each of them having a particular type of effect on its structure and chemical composition, leading to aging or age hardening. Like any other organic material, asphalt binder is affected by temperature, presence of oxygen, and environmental degradation caused by ultraviolet radiation, humidity and so on. The conditions that prevail in these different stages along with their effects on rheological and mechanical properties, and the various aging mechanisms as identified by the literature are subsequently discussed in the following subsections.

2.7.1 Aging during Storage, Mixing and in Service life

For an asphalt pavement to achieve its desired design life, it is imperative to inhibit excessive aging during production of asphalt binder, its storage and transportation, production and transportation of asphalt mix, and in pavement service life.

Manufacturing of asphalt binder: Following fractional distillation of crude oil, asphalt binder goes through various levels of air rectification/blowing process at very high temperatures and/or further modification (mainly by addition of polymers) to obtain the desired grading. During this

process oxidation, dehydrogenation, and polymerization takes place leading to an increase in overall molecular size and concentration of asphaltenes.

Aging during transportation and bulk storage of asphalt binder: In this stage asphalt binder can be reheated or kept at elevated temperatures for a considerable amount of time (days or even weeks). This can be carried out without adversely affecting the properties of asphalt binder by controlling a number of parameters such as temperature, oxygen access, surface area to volume ratio, and the duration of exposure. The design of storage tanks is also important and should avoid refilling via pouring from the top as this would lead to a sudden increase in surface area and subsequent aging [3].

Aging during mixing with aggregates: During the production of asphalt mixture hot aggregates and filler material are coated with a very thin layer of asphalt binder (5-15 μ m), thus creating a very large surface area which in turn leads to relatively excessive oxidation and loss of lighter volatile fractions (upto 30% loss in penetration grade). The level of aging is a function of a number of factors such as temperature, oxygen access, film thickness (with accelerated aging noted in samples less than 9-10 μ m) and type of mixer (with less than half reduction in penetration grade of drum mixed samples as compared to a conventional batch mixed samples) [3], [20].

Aging during storage, transportation and compaction of asphalt mix: The extent of aging in this stage is relatively lower because of the low surface area of asphalt mixture. The only source of oxygen is from the air entrapped within the mixture during transfer from mixer to silo storage, and from silo storage to a delivery truck. With regards to the free surface, oxidation of the top layer produces carbon dioxide which due to its higher density tends to blanket the surface thus protecting it from further oxidation. Aging that occurs during mixing, storage, transportation and compaction of asphalt mix is also referred to as short-term aging.

Aging during pavement service life: After construction, pavements are subjected to midrange temperatures along with exposure to environmental factors such as sunlight, latitude (affecting intensity of UV radiation), altitude (affecting partial pressure of oxygen), humidity and rainfall for a long period of time. Aging at this stage occurs at a much slower pace as compared to short term aging and is also referred to as long-term aging (Figure 2-14). The level of age hardening on the surface layer of asphalt pavements is much more as compared to the lower layers due to constant air supply, relatively higher temperatures and photo-oxidation caused due to ultraviolet radiation.

Asphalt mix properties such as percentage and distribution of air voids affecting oxygen access, aggregate gradation, and asphalt binder content also have a considerable effect on the level of aging. In terms of aggregate gradation, for the same air void content gap-graded mixtures are considered more durable than continuously-graded mixtures as they are less permeable to air with a lower level of interconnected voids. Asphalt binder content on the other hand also plays a very important role in durability as it affects the film thickness which delays oxygen diffusion and in turn age hardening [3], [20]. The presence of any polymer additives in asphalt binder may also have an effect on aging, particularly if they are susceptible to photo-oxidation.

With regards to asphalt pavement base layers, even though they are shielded from environmental effects, studies have shown that age hardening still occurs (at a slower rate). This is mainly attributed to reorientation of asphalt molecules and slow crystallization of waxes.

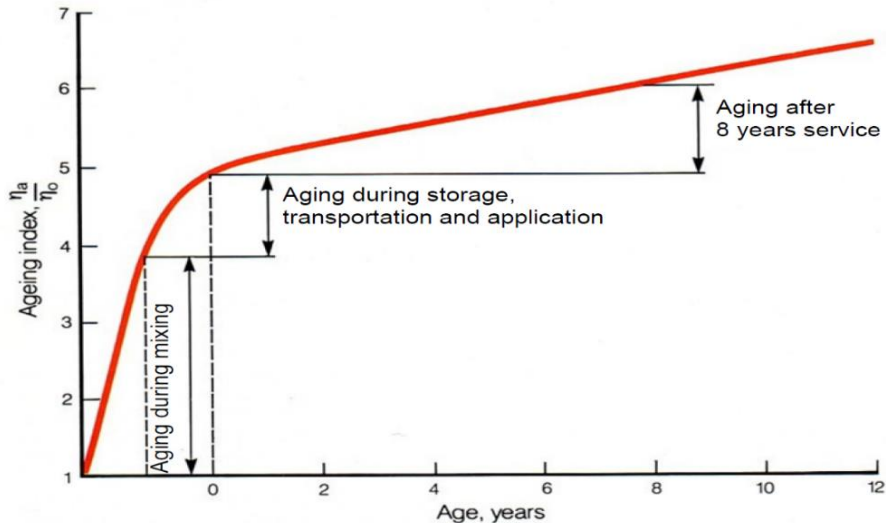


Figure 2-14 Aging during mixing, storage, transportation, and pavement service life [3]

2.7.2 Aging Mechanisms

The age hardening of asphalt binder is attributed to a number of different processes or mechanisms as highlighted in Table 2-2. The most important of these are briefly discussed below:

Oxidation: Oxidative aging, resulting in formation of oxygen containing functional groups is one of the primary causes of asphalt binder hardening. The resulting increase in stiffness and viscosity is attributed to both increase of molecular size and weight, and to the increased polarity of these functional groups [21]. The rate and kinetics of oxidation is highly dependent on temperature which has both a chemical effect (doubled chemical reactivity with almost every 10°C rise) and physiochemical effect (increased mobility of potentially reactive hydrocarbons) [22]. Studies have also shown that temperature levels decipher the polarity of the oxidation products, i.e. same levels of oxidation carried out at different temperatures could result in asphalt binders with varying mechanical and rheological properties [23].

Studies have also shown that certain minerals that exist naturally in aggregates can have a catalytic effect on the oxidation process (particularly for the non-polar fractions). An example of this is quartzite aggregates which can lead to accelerated oxidation of the saturates fraction. Hydrated lime (used in pavements to enhance resistance against moisture damage), on the other hand has a decelerating effect on oxidation attributed to its ability to absorb oxidation sensitive fractions in asphalt binder [22].

Certain metals such as vanadium (naturally occurring in asphalt binder), iron (through aggregate contamination), ferric chloride (used as a catalyst in refinery air blowing process) can also have a catalytic effect on the oxidation process [22]. Another example is addition of Recycled Engine Oil Bottom (REOB) which can be used as a modifier in asphalt binder to improve its low temperature

characteristics and may contain considerable amounts of catalytic metals accelerating the age hardening effects in asphalt binder [24].

Volatilization: The evaporation of volatile components (lower molecular weight fractions) is highly dependent on temperature and exposure conditions and is one of the main factors in short-term aging of asphalt binder.

Steric or physical hardening: Steric hardening refers to the reduction in binder viscosity over time and is mainly attributed to reorientation of molecules into a more closely packed state (greater thermodynamic stability) and slow crystallization of waxes. The effects of steric hardening can be easily reversed by simple reheating [25], [3].

Syneresis or Exudation: Exudative hardening refers to absorption of the oily components by mineral aggregates and is a function of both aggregate porosity and composition of asphalt binder.

Photo-oxidation: Photo-oxidation is induced by natural high energy ultraviolet light, which can result in instability of weaker hydrocarbon bonds (leading to formation of highly reactive free radicals) and an increased rate of oxidation [25]. It can penetrate up to 10 μ m in an asphalt film, and leads to the formation of a protective skin of oxidized materials (4 to 5 μ m thick), thus preventing further photo-oxidation. However, this protective skin is water soluble and can be washed away by rainwater, hence exposing further layers to oxidation [3]. Photo-oxidation can also lead to degradation of polymer additives in asphalt binder, resulting in loss of properties that they were originally designed for.

Table 2-2 Asphalt Aging Mechanisms [3]

Factors that influence aging:	Influenced by:					Occurring:	
	Time	Heat	Oxygen	Sunlight	Beta & Gamma rays	At the surface	Through out mixture
Oxidation (in dark)	✓	✓	✓			✓	
Photo-oxidation (direct light)	✓	✓	✓	✓		✓	
Volatilization	✓	✓				✓	✓
Photo-oxidation (reflected light)	✓	✓	✓	✓		✓	
Photo-chemical (direct light)	✓	✓		✓		✓	
Photo-chemical (reflected light)	✓	✓		✓		✓	✓
Polymerization	✓	✓				✓	✓
Steric or physical	✓					✓	✓
Exudation of Oils	✓	✓				✓	
Changes by nuclear energy	✓	✓			✓	✓	✓
Action by water	✓	✓	✓	✓		✓	
Absorption by solid	✓	✓				✓	✓
Absorption of components at a solid surface	✓	✓				✓	

2.8 Laboratory Accelerated Aging Methods

As discussed in previous sections, asphalt aging is one of the key factors that determines durability and service life of pavements. Different types of asphalt binders behave differently to conditions encountered at various stages of pavement lifecycle, and it is imperative to have reliable laboratory test methods that could quantitatively determine resistance against age hardening (mainly oxidation and volatilization).

Laboratory accelerated aging test methods are designed to condense many years of age hardening effects into few days or hours while maintaining reproducibility and providing an accurate representation of real field aging. There are four main techniques that can be utilized to accelerate a laboratory aging procedure [23]. These techniques along with their associated considerations for implementation in test development are briefly discussed below:

Temperature: The rate of oxidation is directly proportional to temperature and can be accelerated by using test temperatures that are higher than pavement service temperatures (doubled chemical reactivity with almost every 10°C rise). However, it must be noted that test temperatures significantly higher than pavement service temperatures would alter the kinetics of oxidative aging, and the resultant sample would not be an accurate representation of actual field aging. One of the main effects of temperature is on the molecular association of asphalt binder. At lower near pavement service temperatures, many of the inherently chemically reactive molecular species (polar aromatics and asphaltenes) are more tightly bound in asphalt microstructure and thus unavailable for oxidation [23]. Also in terms of the nature and concentration of oxidation products, temperature can have an effect on relative amounts (carbonyl to sulfoxide ratio) and polarity, due to decomposition of sulfoxides at higher temperatures into free radicals which can then initiate or intensify a subsequent oxidation reaction [22].

Pressure: Rate of oxidation can also be accelerated by carrying out aging tests at higher pressures as compared to atmospheric pressure, and by using highly oxidative gases (pure oxygen, ozone, nitric oxides etc.). Using this method however requires high pressure equipment which is not commonly available in most highway department laboratories, and also raises some safety concerns associated with their use.

Film Thickness: Reducing film thickness results in a higher relative surface area for oxygen diffusion thus increasing the rate of oxidation. One of the main concern for using this approach is small sample size, which often does not produce enough aged sample for subsequent testing.

Chemical Accelerants: Certain chemicals can have a catalytic effect on the rate of oxidation and can be used for accelerated aging, however these may also affect the mechanism and kinetics of oxidative aging resulting in samples that are not representative of actual field aging.

An ideal accelerated aging test must consider all these factors accordingly, highlight any potential detrimental effects, and employ tradeoffs as required. Over the years, several laboratory accelerated aging procedures have been developed, trying to simulate real life age hardening effects. These procedures or tests can be divided into two categories, based on the type of sample (Asphalt Binder or Asphalt Mixture) used for aging simulation. Furthermore, some of these tests

are designed particularly for short-term or long-term aging, while some try to simulate both in one procedure. The most important and accepted tests based on their ease of use and ability to simulate aging for both asphalt binder and asphalt mixture are discussed in the subsequent subsections.

2.8.1 Accelerated Aging of Asphalt Binder

Over the last seventy years a number of accelerated aging tests have been developed for asphalt binder (Table 2-3). Acceleration in these methods is mainly achieved by extended heating on a thin film of asphalt binder to exacerbate volatilization (at very high temperatures to simulate short-term aging) and oxidation (at high temperatures to simulate long-term aging). Out of these methods the most commonly used standardized tests are briefly discussed below:

Rolling Thin Film Oven Test (RTFOT): This test is a modified version of the thin film oven test (TFOT), and addresses the issue of limited diffusion and homogeneous hardening (due to skin formation). Aging in this test is carried out at 163°C for 75minutes on a relatively thin film of asphalt binder (1.25mm), which is continuously rotated and also periodically exposed to hot air flow set at a rate of 4000ml/min. This ensures homogeneous aging of asphalt binder, which is found comparable to the short-term age hardening effects experienced during full scale mixing in a conventional batch mixer [3].

Rutting is one of the major concerns during early and mid-life of asphalt pavements which is why superpave performance grading specifications requires testing of short-term aged RTFOT residue to determine its stiffness (resistance against loading) and elasticity (ability to dissipate energy by regaining shape after loading). This test is done using the dynamic shear rheometer (DSR) to calculate $G^*/\sin\delta$ at asphalt binder's high performance temperature, which is then compared against a minimum specification value of 2.2kPa [26].

Pressure Aging Vessel (PAV): This test was developed by the Strategic Highway Research Project (SHRP) team to simulate long-term in-service aging of asphalt binder. In this method further oxidative aging of RTFOT residue is carried out under a pressurized environment (2.10 MPa) for 20hrs at temperatures of 90°C, 100°C, or 110°C (dependent on in-service cold, moderate, or hot climatic conditions respectively). PAV residue may be used to estimate asphalt binder properties after 5 to 10yrs of in-service aging, however it must be noted that age hardening effects can vary significantly for different types of asphalt binders (especially polymer modified binders) [27]. Furthermore, the elevated temperatures and pressure used in PAV aging (to accelerate the process) can have a significant effect on the functional groups formed, resulting in deviation of oxidative aging kinetics when compared to natural in-service aging [28].

Fatigue and low temperature cracking are the major concerns during the late service life of asphalt pavements. In order to inhibit fatigue cracking, superpave performance grading specifications requires DSR tests to be carried out at medium service temperatures on PAV aged residue to calculate $G^*\sin\delta$ (a measure of elasticity and stiffness), which should be limited to a maximum specification value of 5000kPa [26]. In terms of low temperature performance, PAV aged binder is tested for compliance using bending beam rheometry and direct tension testing.

Table 2-3 Accelerated Aging Methods for Asphalt Binders [29]

Test Method	Temperature (°C)	Duration	Film Thickness
Thin film oven test (TFOT) (Lewis and Welborn, 1940)	163	5hr	3.2mm
Modified thin film oven test (MTFOT) (Edler et al., 1985)	163	24hr	100µm
Rolling thin film oven test (RTFOT) (Hveem et al., 1963)	163	75min	1.25mm
Extended rolling thin film oven test (ERTFOT) (Edler et al., 1985)	163	8hr	1.25mm
Nitrogen rolling thin film oven test (NRTFOT) (Parmeggiani, 2000)	163	75min	1.25mm
Rotating Flask Test (RFT) DIN 52016, EN12607-3	165	150min	-
Shell microfilm test (Griffin et al., 1955)	107	2hr	5µm
Modified Shell microfilm test (Hveem et al., 1963)	99	24hr	20µm
Modified Shell microfilm test (Traxler, 1961; Halstead and Zenewitz, 1961)	107	2hr	15µm
Rolling microfilm oven test (RMFOT) (Schmidt and Santucci, 1969)	99	24hr	20µm
Modified RMFOT (Schmidt, 1973)	99	48hr	20µm
Tilt-oven durability test (TODT) (Kemp and Prodoehl, 1981)	113	168hr	1.25mm
Alternative TODT (McHattie, 1983)	115	100hr	1.25mm
Thin film accelerated ageing test (TFAAT) (Petersen, 1989)	130 or 113	24 or 72hr	160µm
Modified rolling thin film oven test (RTFOTM) (Bahia et al., 1998)	163	75min	1.25mm
Iowa durability test (IDT) (Lee, 1973)	65	1000hr	3.2mm
Pressure oxidation bomb (POB) (Edler et al., 1985)	65	96hr	30µm
Accelerated ageing test device/Rotating cylinder ageing test (RCAT) (Verhasselt and Choquet, 1991)	70-110	144hr	2µm
Pressure ageing vessel (PAV) (Christensen and Anderson, 1992)	90-110	20hr	3.2µm
High pressure ageing test (HiPAT) (Hayton et al., 1999)	85	65hr	3.2µm

2.8.2 Accelerated Aging of Asphalt Mixtures

Laboratory accelerated aging procedures on asphalt mixture samples (both loose and compacted) are required to better understand the durability of pavements in their service life. As discussed before, fatigue and low temperature performance are the major concerns later in the service life of a pavement, and carrying out accelerated laboratory aging on asphalt mixtures allow for these properties to be determined directly by use of performance tests (such as Complex Modulus, 4-Point Flexural Bending-fatigue, and Thermal Stress Restrained Specimen Test-TSRST). Another approach that can be utilized is to characterize the rheological, mechanical, and chemical behavior of asphalt binder, which is extracted and recovered from aged mixtures. Understandably, the accuracy of these tests rely on accurate methods minimizing any differential disruption of asphalt binder microstructure by the solvent used.

Over the years a number of laboratory accelerated aging procedures have been developed for asphalt mixtures (Table 2-4). The acceleration in these methods is achieved by extended heating, high pressure oxidation, or by use of highly oxidant gas. Short-term accelerated aging is usually carried out on loose mixtures and compacted samples are generally used for long-term accelerated aging. Performance testing on samples compacted after aging may not provide representative results given the effects of aging on compactability, and cohesion and adhesion of compacted mix samples [28].

Table 2-4 Accelerated Aging Methods for Asphalt Mixtures [29]

Test Method	Temperature (°C)	Duration	Sample	Extra Features
Production ageing (Von Quintas, 1988)	135	8, 16, 24, 36hr	Loose	-
SHRP short-term oven ageing (STOA)	135	4hr	Loose	-
Bitutest protocol (Scholz, 1995)	135	2hr	Loose	-
Ottawa sand mixtures (Pauls and Welborn, 1952)	163	Various periods	Compacted	-
Plancher et al. (1976)	150	5hr	Compacted	-
Ottawa sand mixtures (Kemp and Prodoehl, 1981)	60	1200hr	-	-
Hugo and Kennedy (1985)	100	4 or 7days	-	80% relative humidity
Long-term ageing (Von Quintas, 1988)	60 and 107	2 and 3days	Compacted	-
SHRP long-term oven ageing (LTOA)	85	5days	Compacted	-
Bitutest protocol (Scholz, 1995)	85	5days	Compacted	-
Kumar and Goetz (1977)	60	1 to 10days	Compacted	Air at 0.5mm of water
Long-term ageing (Von Quintas, 1988)	60	5 to 10days	Compacted	0.7MPa Air
Oregon mixtures (Kim et al., 1986)	60	1 to 5days	Compacted	0.7MPa Air
SHRP low pressure oxidation (LPO)	60 or 85	5days	Compacted	1.9l/min Oxygen
Khalid and Walsh (2000)	60	Upto 25days	Compacted	3l/min Air
PAV mixtures (Korsgaard, 1996)	100	72hr	Compacted	2.07MPa Air

The most commonly used accelerated aging procedures for asphalt mixtures were developed under the SHRP-A-003A project and are briefly discussed below:

SHRP Short-Term Oven Aging (STOA): The STOA method is based on work done by Von Quintas (1988) and requires loose mixtures to be aged in a forced draft oven [29]. AASHTO R30-02 adopted and standardized this procedure for two types of conditioning (1) For volumetric mix design which requires 2hr conditioning at mixture's specified compaction temperature to allow for binder absorption during mix design; (2) For mixture mechanical property testing which requires

4hr conditioning at 135°C to simulate the aging effects of mixing and construction on asphalt mixtures [30].

SHRP Long-Term Oven Aging (LTOA): Following the STOA procedure, this method simulates the long-term in-service aging, by conditioning a compacted mixture of asphalt binder and aggregates in a forced draft oven at 85°C for 120hrs. This conditioning procedure is designed to simulate roughly 7-10yrs of in-service aging and is adopted by AASHTO R30-02 specification for mechanical property testing of compacted mixtures [30].

SHRP Low Pressure Oxidation (LPO): Similar to LTOA, this procedure is also designed to simulate long-term aging effects and requires compacted samples to be placed in a triaxial cell to apply confining pressure. Oxygen flow is then started through the cell and it is placed in a preheated water bath at 60 or 85°C for 5 days. After this procedure the sample is allowed to cool to room temperature and then stand for another 24hrs prior to any mechanical testing [31].

Viennese Aging Procedure (VAPro): This is a recently developed modified version of the SHRP LPO procedure, and aims to better represent the kinetics of in-service oxidative aging. A highly oxidant gas enriched with ozone and nitric oxides is used to accelerate the rate of oxidation, hence allowing for a moderate conditioning temperature of 60°C. The procedure is carried out for four days at a constant air flow rate of 1litres/min. Preliminary test results have showed that asphalt binder extracted from samples aged using this procedure have a similar viscoelastic behavior as encountered after RTFOT + PAV aging [28].

2.8.3 Photo Oxidation of Asphalt Binders and Mixtures

Solar radiation that reaches the earth's surface can be broadly divided into three electromagnetic spectrums, approximately 7% Ultraviolet (UVC band at 240-280nm, UVB band at 280-315nm, and UVA band at 315-400nm), 42% visible band (400-800nm), and infrared radiation (800-3000nm). Out of these the shorter wavelength UV bands are the most destructive and have been studied over the last 60 years in terms of their effects on asphalt aging, showing clear evidence of volatilization, polymerization, and oxidation (particularly for thin film thickness i.e. <3µm). Also photochemical treatment produced significantly different aging kinetics which may not be necessarily reproduced by thermal oxidative aging alone (e.g. RTFOT, PAV and AASHTO R30), indicating the need to incorporate these techniques into a long-term aging procedure [29]. To this end some of the laboratory test equipment capable of inducing accelerated aging by combined effects of solar radiation, humidity and rainwater are briefly discussed below:

Atlas Weatherometer: Over the last 100 years, Atlas has developed a range of different laboratory weathering instruments which are capable of accelerating the effects of environmental degradation. These are mainly used for quality control and research purposes by a number of industries such as roofing materials, paints and coatings, automobiles, plastics and additives, photovoltaics etc. [32].

One of such equipment is the Atlas Weatherometer Suntest XXL (Figure 2-15), which is capable of combining the effects of sunlight, temperature, humidity and water on 3-D specimens. Kane et al (2013) calibrated the weatherometer based on local weather conditions in Nantes, France, and

subsequently subjected asphalt mixture samples to 500 cycles of 2hrs each (2 minutes of watering followed by 118 minutes of drying under irradiation), representing one-year of natural outdoor aging. Comparison of carbonyl index measurements taken on samples aged naturally and in the weathering chamber showed that aging was accelerated by a factor of 10, or in other words 3 days of accelerated aging corresponded to roughly a month of natural aging [19].



Figure 2-15 Atlas Weatherometer Suntest XXL [33]

Accelerated Pavement Weathering System (APWS): APWS (Figure 2-16) was designed by PRI Asphalt technologies and similar to Atlas weatherometer is capable of accelerating the effects of environmental degradation of asphalt mixture samples. In a study carried out by Grzybowski et al (2011), asphalt mixtures were subjected to 3000 cycles of 1hr each (51 minutes drying followed by 9 minutes of watering) at 60°C in the APWS. Preliminary results from tests carried out on asphalt binder extracted from the aged mixes, show that accelerated aging was achieved, however further testing and comparison with real world data is required for correlation and to better understand the kinetics of aging [34].



Figure 2-16 Inside view of APWS showing mixture sample under conditioning [35]

CHAPTER 3 RESEARCH METHODOLOGY

3.1 Introduction

The main purpose of this research project is to optimize a laboratory accelerated aging procedure, which could be used to simulate real life aging conditions on asphalt mixture samples, thus providing a more accurate representation of changes in pavement rheological and mechanical behavior with time.

As discussed in literature, aging in asphalt pavements is dependent on a number of factors such as solar radiation, temperature, oxygen access, humidity and rainwater, aggregate gradation and so on. However, most of the commonly used laboratory accelerated aging procedures rely mainly on extended heating at excessively high temperatures, which could significantly alter the kinetics of oxidative aging.

To develop an efficient laboratory accelerated aging procedure, the following issues must be considered:

1. Conditioning should be carried out on compacted asphalt mixture samples in order to avoid any issues related to compactability and the quality of cohesion and adhesion, which could affect the results of any subsequent laboratory tests.
2. Excessively high temperatures, which can have an effect on molecular association and the nature and concentration of resultant oxidation products should be avoided. Chemical analysis using the FT-IR technique could be used to calculate the carbonyl and sulfoxide indices and identify any abrupt changes in these oxidation products.
3. It is understood that the chemical products of photo oxidation which form a protective layer inhibiting further oxidation are water soluble. In order to simulate real in-service conditions cycles involving sunlight simulation and rainfall should be considered.
4. Solvent extraction of asphalt binder from conditioned mixture samples, followed by subsequent removal of solvent, should be carried out accurately using the same solvent and laboratory procedures, in order to avoid any differential disruption of asphalt binder microstructure.
5. Consideration must also be given to ease of use and safety aspects of the accelerated conditioning procedures.

In order to achieve the overall objectives, research plan as shown in Figure 3-1 was developed to systematically evaluate the effects of different conditioning procedures on chemical, rheological, and mechanical properties of asphalt mixtures.

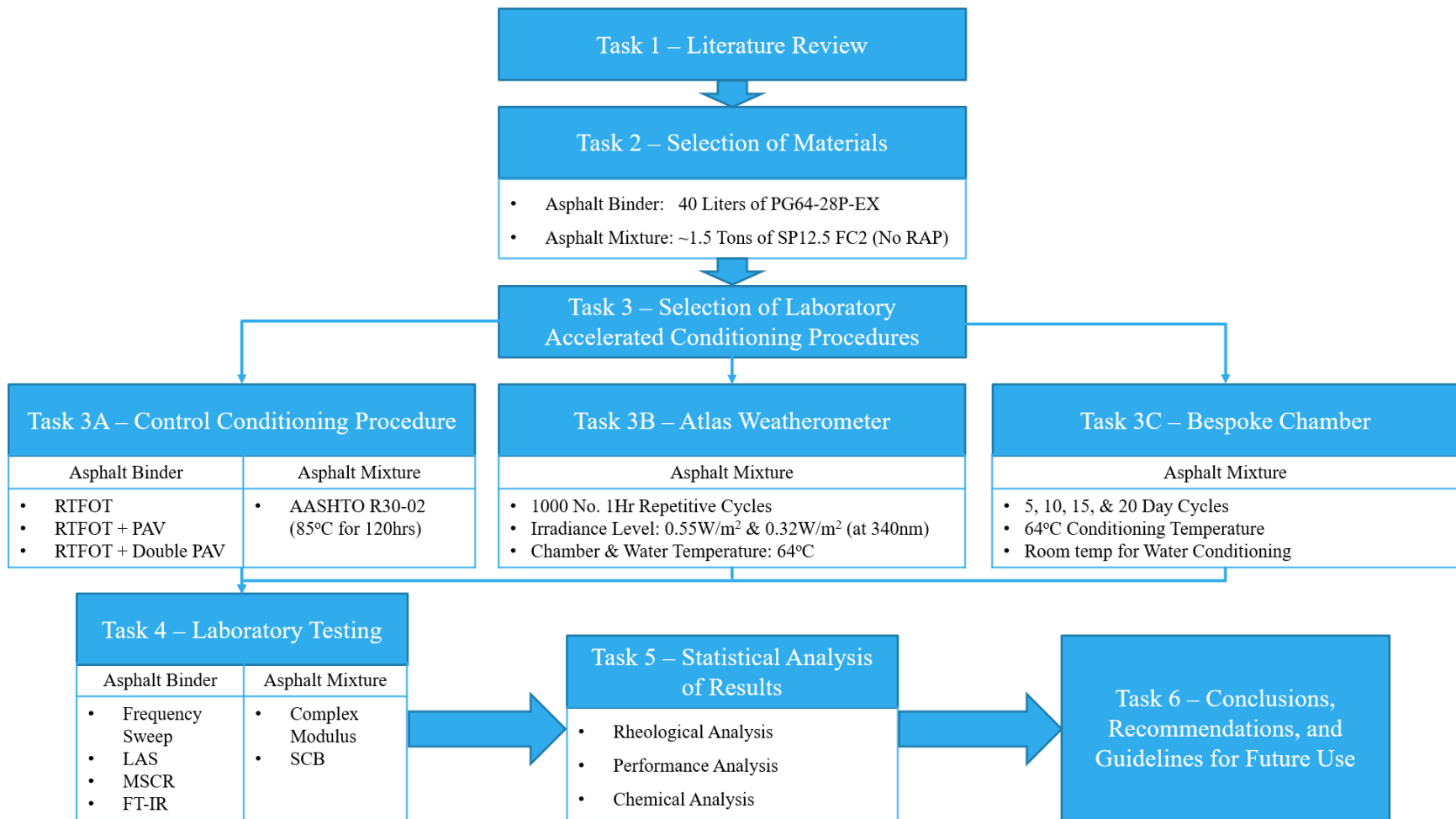


Figure 3-1 Research Plan Methodology

3.2 Material Selection

The level of aging in an asphalt pavement is a function of its depth, with reduced levels encountered for lower layers due to the enclosure provided by the pavement structure. For this reason, preference was given to a plant produced surface course which would also account for the short-term aging effects, hence allowing further long-term conditioning procedures to be carried out. Preference was also given for the constituent asphalt binder to be polymer modified, which could be tested to identify any effects of polymer degradation due to UV exposure. Also in order to allow for future correlation and calibration with natural field aging, preference was given to a Ministry of Transportation, Ontario (MTO) project from where field cores could be collected at a later date. All of these material selection considerations were accounted for in this research project and details of the collected materials are given below.

Project: MTO 2017-3006
Location: Highway 8 - Between Franklin Overpass & Grandriver Bridge, Kitchener
Paver: Steed & Evans
AC: McAsphalt PG64-28P-EX
Mix Design: SP12.5 FC2 (No RAP)
Material Collected: ~1.5 tons of Loose Mix Asphalt and 40 liters of Virgin Binder



Figure 3-2 Loose Mix being sampled at Asphalt Plant

3.3 Preparation of Laboratory Compacted Samples for Long-Term Conditioning

The temperature viscosity chart for PG64-28P-EX, prepared by McAsphalt (refer to appendix A) was used to identify the compaction temperature (138°C) for the collected mix. Since this mix was produced at an asphalt plant, the 4hr short –term conditioning at 135°C as per AASHTO R30-02 was not required.

Laboratory compaction was carried out at CPATT (Centre for Pavement and Transportation Technology) laboratory using the Superpave Gyrotory Compactor (SGC), in accordance with AASHTO PP60-13, “Standard Practice for Preparation of Cylindrical Performance Test Specimens Using the Superpave Gyrotory Compactor (SGC)”. A uniform level of compaction with targeted air void content of $7\pm 1\%$ was required in order to minimize any deviation in test results. For this reason, all of the samples produced for long-term conditioning were fabricated from 7kg of loose mix, compacted under 30No gyrations at 600kPa ram pressure. The resulting cylindrical samples were then cored and cut into desired dimensions as required for Complex Modulus and Semi-Circular Bend (SCB) Geometry testing.

For asphalt mixture beams, compaction was carried out using the Asphalt Shear Box compactor. The maximum density from the mix design sheets was entered into the software and target 7.3% air voids were chosen for all beam compactations (from 20kg loose mix). These asphalt beams were then cut to produce samples in accordance with dimension requirements for 4-Point Flexural Bending (fatigue), and Thermal Stress Restrained Specimen Test (TSRST).



Figure 3-3 Compaction, Cutting & Coring at CPATT Laboratory

3.4 Laboratory Accelerated Conditioning Procedures

Three different conditioning procedures were selected to simulate the long-term aging in compacted asphalt samples. The first procedure is based on the current widely used practices, acting as a control procedure, and the other two were carefully designed, based on the guidelines extracted from the literature review to incorporate the effects of solar radiation, humidity and water. A brief description of these conditioning procedures is given in the following subsections.

3.4.1 Control Conditioning Procedure

This conditioning procedure was carried out both for asphalt binder and asphalt mixtures, and is based on the current methods widely used by asphalt laboratories across North America. A summary of the laboratory test procedures carried out are shown in Figure 3-4.

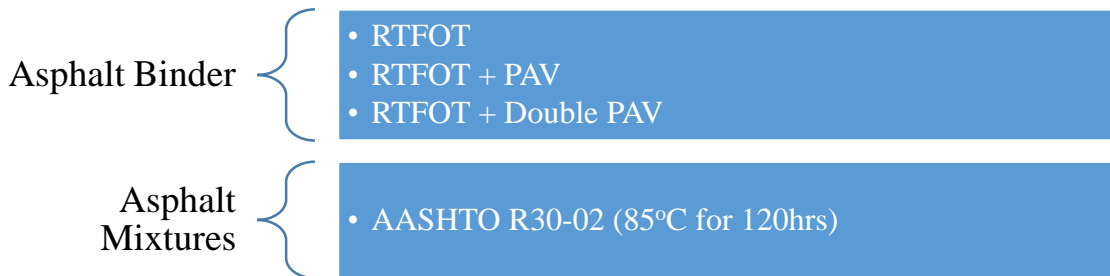


Figure 3-4 PAV residue, Degassing & AASHTO R30-02 Compacted Sample Conditioning

3.4.2 Atlas Weatherometer

This conditioning procedure utilized an Atlas Weatherometer Ci35A (courtesy of COCO Paving), to simulate long term aging on compacted asphalt mixture samples. Ci35A was originally designed for paints/coatings with a rotating frame to ensure uniform exposure, and allows for repetitive conditioning cycles to be programmed for a selected set of parameters. Conditioning cycles that were selected for this project to incorporate UV, reduced temperature, humidity and water spray are shown below.

Irradiance Level: 0.55W/m^2 & 0.32W/m^2 (at 340nm)

Chamber and Water Temperature: 64°C

Cycles: 1hr (51minutes light; 9minutes light and specimen spray)

As identified in literature, in order to induce a measurable amount of aging, it was decided to apply 1000 repetitive cycles with the above selected parameters. These were divided into four batches of 250 cycles each, while rotating the samples to ensure even aging. This long-term conditioning was carried out successfully for Dynamic Modulus and SCB samples with irradiance of 0.55W/m^2 . With regards to fatigue and TSRST beams, initially they were hung from the sides of the rotating frame which lead to their collapse. A metal mesh platform was then installed within the chamber for additional support, however it didn't serve the purpose and the beams cracked again. Finally, a lower irradiance level of 0.32W/m^2 was selected for the aging of these samples.



Figure 3-5 Atlas Weatherometer Ci35A showing external, and internal view with metal mesh platform for beam support

3.4.3 Bespoke Chamber

This chamber was fabricated at the CPATT test track facility to allow for better control over the aging parameters. It was equipped with 3No. full spectrum lamps, with a combined power output of approximately 1800 Watts to simulate solar radiation, and for heating. Internally the chamber was lined with a reflective coating, allowing for most of the radiation to bounce back and to be absorbed by the black asphalt samples. 2No. fans were then used for cooling and to calibrate sample temperature.

An automated data collection unit (referred to as a “data logger”) was used to collect data every five minutes for sample temperature (dummy sample with a thermocouple installed at mid-depth), box temperature, incoming solar radiation (using an Apogee SP-110-SS silicon-cell pyranometer with a spectral range of 360nm to 1120nm), and incoming UV radiation (using an Apogee SU-100-SS UV sensor with a spectral range of 250nm to 400nm). Sensor data sheets indicating the calibration factor used have been appended in Appendix B.

Data logger readings were averaged over the conditioning period and recorded as Sample Temperature: 63°C – 68°C, Incoming Solar: 2.22W/m², Incoming UV: 0.0035W/m².

In terms of sample conditioning 5, 10, 15, and 20 days (or cycles) were selected (as multiples of the currently used AASTO R30-02 long term aging procedure), with each cycle representing 23hrs of drying under irradiation followed by 1hr for specimen spray. This conditioning procedure was carried out for compacted Complex Modulus specimens. 6No. samples were selected for each of the four conditioning periods (referred to as BC5, BC10, BC15, and BC20), with three of them being subjected to the full cycle (with water conditioning), while the other three were only conditioned under irradiation and temperature. The reason for this was to predict or identify any differences in long-term aging with water conditioning.

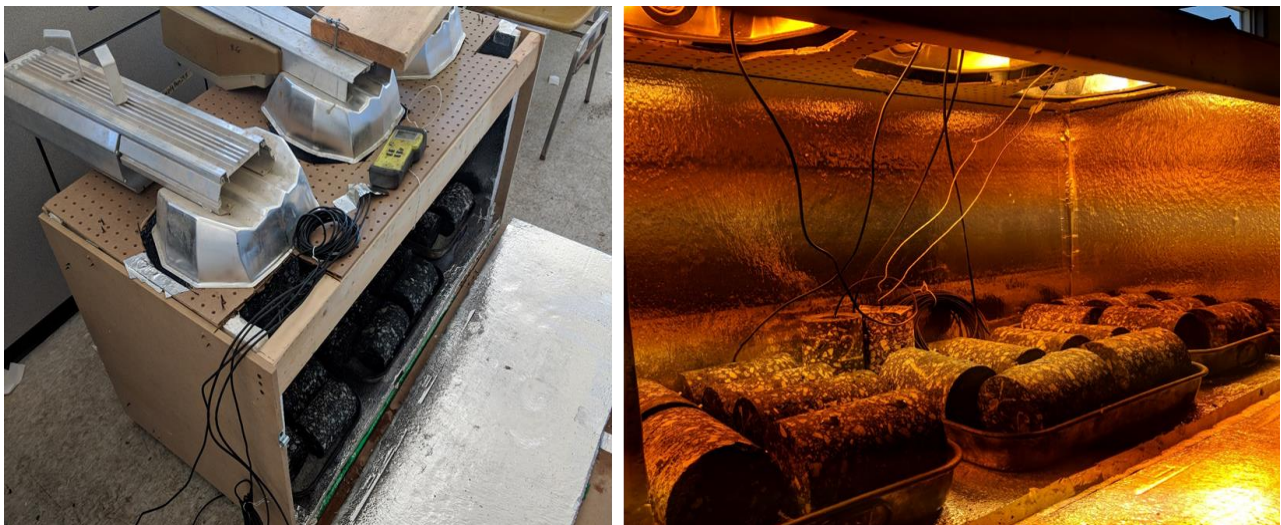


Figure 3-6 Bespoke Conditioning Chamber

3.5 Laboratory Testing

In this step, a number of laboratory tests both for asphalt binder and compacted mixture samples were selected based on their relevance as identified by the literature. These are briefly discussed in the following subsections and have been summarized in Table 3-1 and Table 3-2.

3.5.1 Asphalt Binder Tests

Asphalt binder tests were carried out on binders aged directly (RTFOT and PAV procedures), and on binders that were extracted and recovered from aged samples conditioned using the other procedures as discussed in section 3.4. As discussed before, in order to avoid any differential disruption of asphalt binder microstructure, the extraction and recovery procedures were carried out very carefully using the same solvent (methylene chloride) and in accordance with the MTO laboratory testing manuals (LS).



Figure 3-7 Centrifuge Extractor, High-Speed Centrifuge and Rotavapor at CPATT lab

Rheological Testing: A Dynamic Shear Rheometer (DSR) was used to analyze the rheological behavior of asphalt binder. Asphalt binders were tested at sixteen different loading frequencies (ranging from 0.1 to 100 rad/s) and nine different temperatures (2, 5, 15, 25, 35, 40, 50, 60, and 70°C) to fully characterize their viscoelastic behavior. These tests were carried out in a strain controlled mode, with very low strain levels (0.1% for 2°C-35°C and 0.5% for 40°C-70°C) in order to ensure that they are within the linear viscoelastic region (LVE), which was determined separately (Figure 3-8). The results were then analyzed using the 2S2P1D rheological modelling.

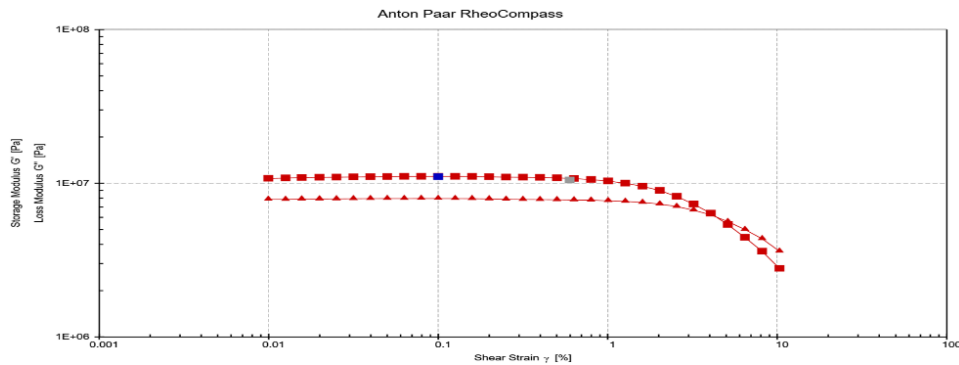


Figure 3-8 Linear Viscoelastic Region

Performance Testing: In order to characterize asphalt binder's high temperature (rutting) and medium temperature (fatigue) performance, Multiple Stress Creep Recovery (MSCR) and Linear Amplitude Sweep (LAS) tests were carried out respectively using the dynamic shear rheometer.

In terms of fatigue characterization, the PG test parameter $G^*\sin\delta$ is based only on small strain rheology and does not consider any damage resistance. For this reason, LAS test was introduced under AASHTO TP101-14, as a performance based assessment of asphalt binder fatigue resistance. This test is carried out at PG intermediate temperature (22°C for PG64-28), by applying cyclic loadings with an increasing amplitude to accelerate damage. Fatigue performance is then predicted using Viscoelastic Continuum Damage (VECD) analysis [36], [37].

Similar to fatigue, the PG test parameter $G^*/\sin\delta$ is also based on small strain rheology and does not correlate well with field rutting measurements. This is particularly the case for polymer modified asphalt binders, as the polymer network is never really activated at very low levels of stress and strain. The MSCR test was hence introduced under AASHTO TP70 and AASHTO MP19, as a new high temperature specification. This test is carried out at PG high temperature (64°C for PG64-28) and repetitive cycles of creep load (1 second) and recovery period (9 seconds) are applied at varying stress levels (typically 0.1 & 3.2kPa), to measure non-recoverable creep compliance (J_{nr}) and percent recovery (R). Findings from a previous study at the Federal Highway Administration's (FHWA) Accelerated Loading Facility (ALF) indicated that J_{nr} provides a significantly better correlation to rutting as compared to $G^*/\sin\delta$ [38].

Chemical Testing: As identified in the literature, Fourier Transform Infrared Spectroscopy (FTIR), which quantitatively calculates structural indices for the carbonyl and sulfoxide functional groups, can be used as an effective tool to characterize the level and kinetics of oxidative aging. In this research project Perkin Elmer Spectrum Two FT-IR Spectrometer at COCO Paving Asphalt Laboratory, Toronto was used.



Figure 3-9 Perkin Elmer Spectrum Two FT-IR Spectrometer

Table 3-1 List of Asphalt Binder Samples subjected to Laboratory Testing

Asphalt Binder Tests (Frequency Sweep, LAS, MSCR, and FT-IR)	
Sample	Conditioning Procedure Used
Virgin 64-28P-EX	-
RTFOT	Short-term aging
RTFOT & PAV	Long-term aging
RTFOT & Double PAV	Extended long-term aging
Virgin 64-28P-EX*	To evaluate effects of extraction and recovery
Loose Mix*	Short-term aging at Asphalt Plant
After Compaction*	Evaluate effects of laboratory compaction on aging
AASHTO R30*	Long-term aging at extended temperatures
Atlas Weatherometer*	Long-term aging cycles
BC5-H ₂ O* (Water Conditioning)	Long-term aging cycles
BC5-NoH ₂ O*	Long-term aging cycles
BC10-H ₂ O*	Long-term aging cycles
BC10-NoH ₂ O*	Long-term aging cycles
BC15-H ₂ O*	Long-term aging cycles
BC15-NoH ₂ O*	Long-term aging cycles
BC20-H ₂ O*	Long-term aging cycles
BC20-NoH ₂ O*	Long-term aging cycles

*Indicates binder samples that were obtained by Extraction and Recovery Procedures

3.5.2 Asphalt Mixture Tests

In addition to asphalt binder tests which provides a useful insight into overall pavement behavior, laboratory tests on asphalt mixtures are also required to evaluate binder performance in the mixture. As identified in literature, aging or age hardening of asphalt leads to an increase in stiffness and brittle behavior, subsequently leading to an increase in rutting resistance but a reduction in durability with reduced resistance against fatigue and low temperature distresses. For this reason, laboratory tests for this research project mainly focus on characterization of rheological behavior and mechanical behavior in terms of fatigue and low temperature cracking. A brief description of the tests that were carried out on compacted asphalt mixture samples is given below.

Rheological Testing: Complex Modulus tests on cylindrical samples (length 150mm, diameter 100mm), were carried out in accordance with AASHTO T342-11. These tests were carried out using the Material Testing System (MTS) loading frame and environmental chamber at CPATT laboratory. Sample response, when subjected to cyclic compressive and sinusoidal loading was measured using three extensometers attached at 120° intervals. In order to fully characterize the rheological behavior these tests were carried out at five different temperatures (-10, 4, 21, 37, and 54°C) and six different loading frequencies (25, 10, 5, 1, 0.5, and 0.1Hz) [39]. The test results were then analyzed using the 2S2PID rheological modelling as discussed in Section 2.4.2.



Figure 3-10 810 MTS Loading Frame and 651 MTS Environmental Chamber

Performance Testing: The Semicircular Bend Geometry (SCB) test at intermediate test temperature (25°C), was used in this research project to determine fracture energy (G_f -J/m²) and Flexibility Index (FI). Fracture energy provides an insight into asphalt mixture's overall capacity to resist cracking related damage, with a higher value related to higher damage resistance indicating the ability to cope with greater stresses. Flexibility index on the other hand, provides a mean to quantify asphalt mixture's brittleness with a lower value related to premature cracking [40]. This test requires a constant loading rate of 50mm/min to be applied on half discs (50mm thick, 150mm diameter) that have been notched (1.5mm wide, 15mm deep) parallel to the loading axis. The test procedure and subsequent calculation of parameters have been carried out in accordance with AASHTO TP 124-16, utilizing the I-FIT (Illinois Flexibility Index Test) software developed by The Illinois Center for Transportation (ICT). These tests were carried out at MTO Asphalt Laboratory using 30kN – Dynamic Testing System (DTS) frame.



Figure 3-11 Different Stages of SCB Test (Cutting & Notch Preparation, Drying followed by Temperature Conditioning, Testing using DTS-30 Frame, and Samples after Testing)

Table 3-2 List of Asphalt Mixture Samples subjected to Laboratory Testing

Asphalt Mixture Tests			
Sample	Conditioning Procedure Used	No. of Samples	
		Dynamic Modulus	SCB
Unconditioned	-	6	4
AASHTO R30	Long-term aging	3	6
Atlas Weatherometer	Long-term aging	3	6

CHAPTER 4 STATISTICAL ANALYSIS OF RESULTS AND DISCUSSIONS

Laboratory test results for both asphalt binder and asphalt mixtures, along with subsequent analysis and discussions are presented in this chapter.

4.1 Asphalt Binder

4.1.1 Rheological Analysis

Rheological analysis for asphalt binder samples have been carried out using the 2S2P1D model. Plots for isothermal mastercurves (at 15°C for 1. Complex Modulus, 2. Phase Angle, and 3. Loss and Storage Modulus) and Black Space diagrams were prepared for each type of asphalt binder tested and have been attached in Appendix C. Plots that were prepared for Atlas Weatherometer conditioning procedure have been presented below for reference purposes.

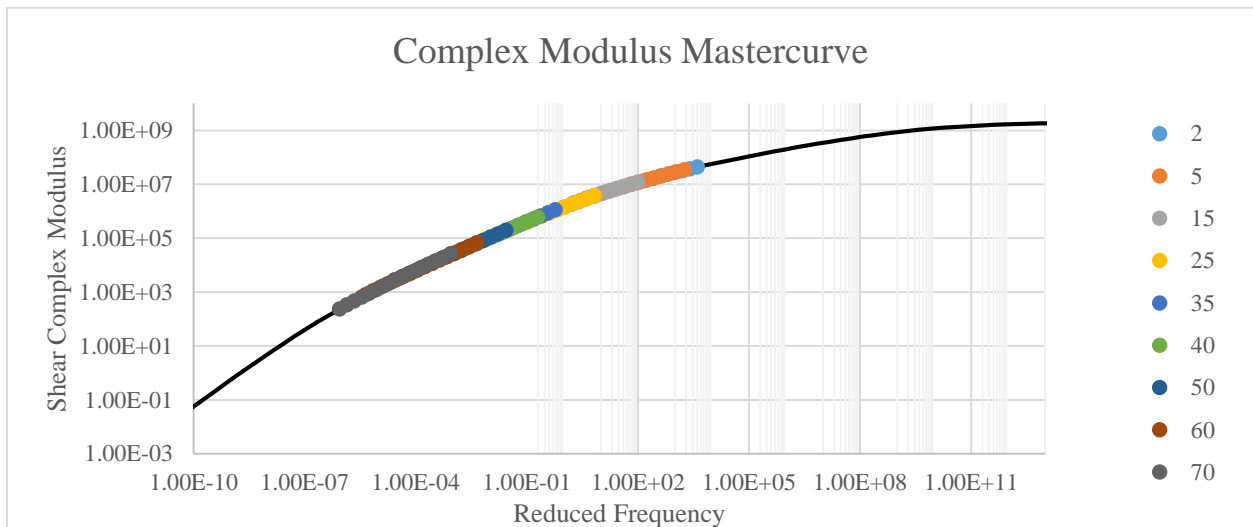


Figure 4-1 Predicted Complex Modulus Mastercurve along with Experimental Data Points

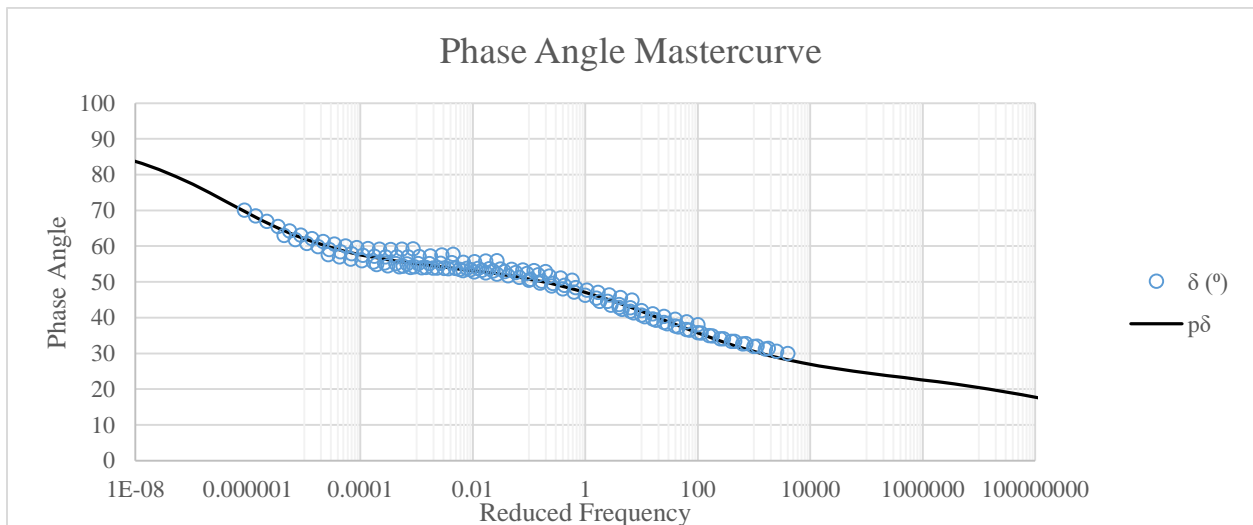


Figure 4-2 Predicted Phase Angle Mastercurve along with Experimental Data Points

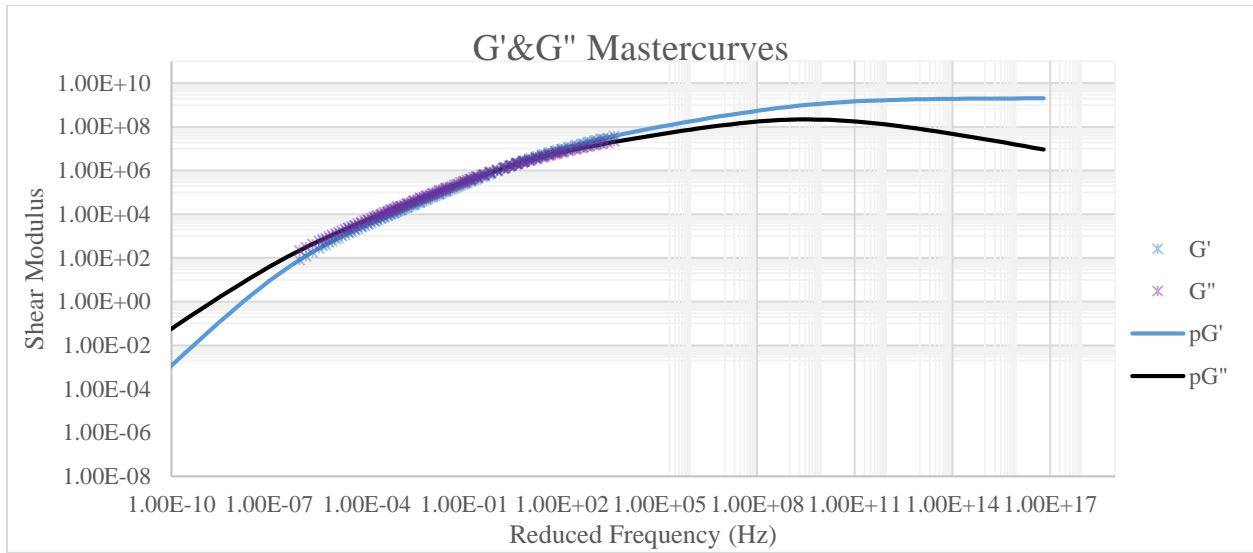


Figure 4-3 Prediction for Loss & Storage Modulus along with Experimental Data Points

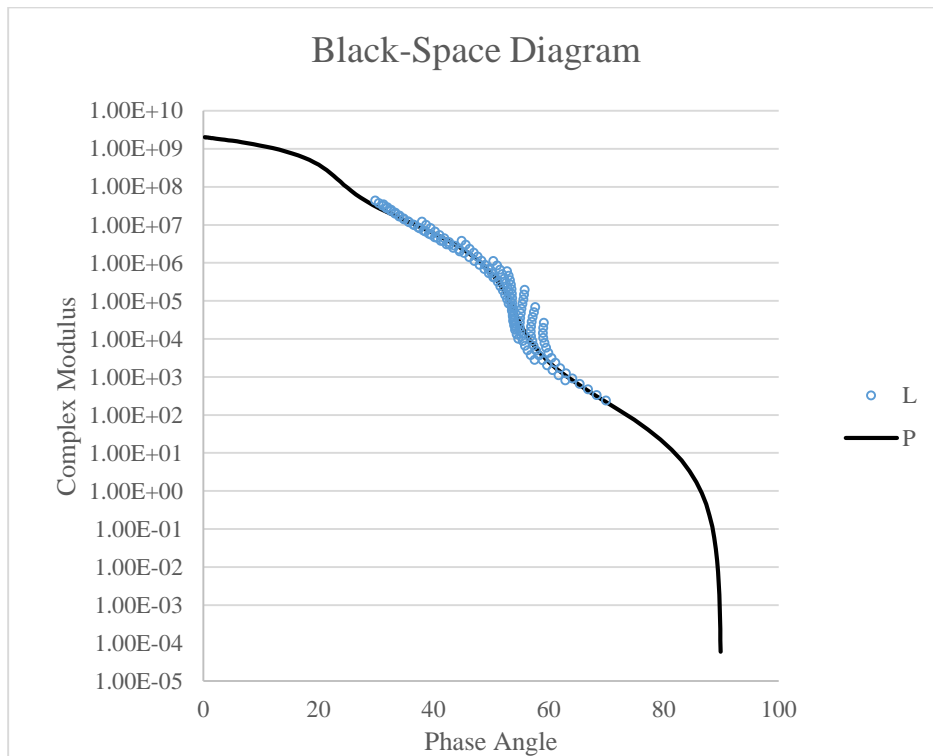


Figure 4-4 Complex Modulus VS Phase Angle (Predicted and Experimental)

Black space diagram is a plot of norm of complex modulus ($|G^*|$) versus the phase angle (δ), and as identified in literature, they can be used as a means to identify time temperature equivalency of an asphalt binder sample [10]. This is because frequency and temperature parameters are eliminated from the plot. It was noted that both for virgin binder (PG64-28P-EX) and virgin binder that was subjected to extraction and recovery procedures only, a disjointed black space curve was obtained (refer to Figure 4-5). This can be attributed to the high polymer content in these binder samples. Smoother curves were obtained for aged or conditioned asphalt binder samples which can be attributed to the thermo-oxidative degradation of the polymer.

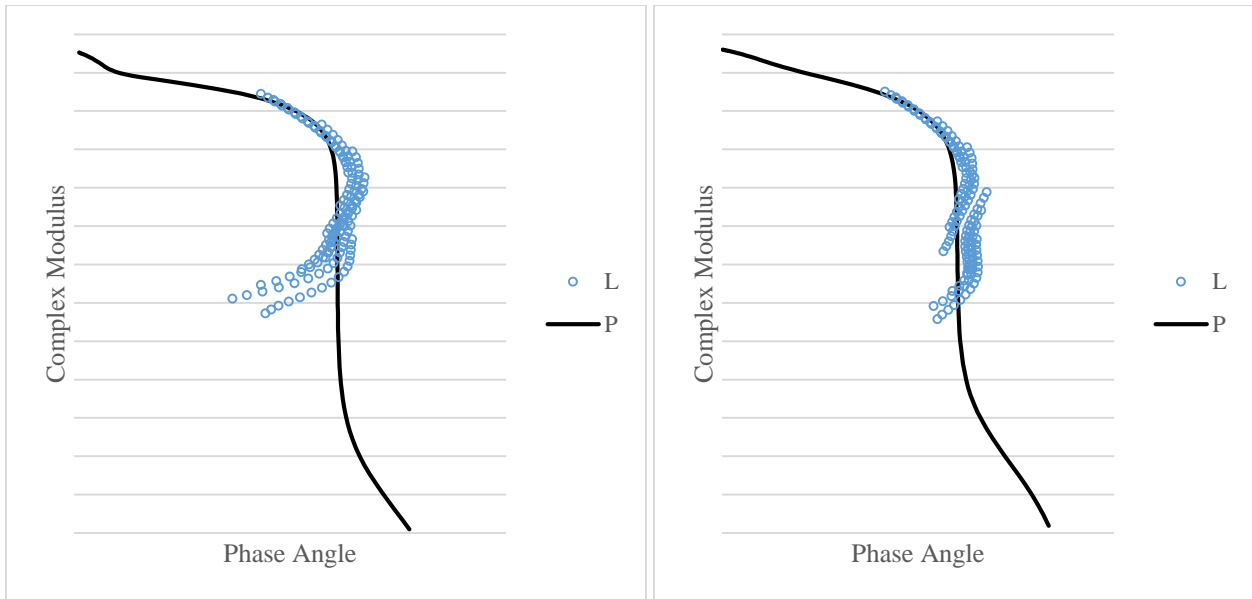


Figure 4-5 Disjointed Black Space curves as noted for Virgin (left) & Extracted & Recovered Virgin (right) binder samples

Effect of Aging on Complex Modulus and Phase Angle: Generally speaking, it was noticed that oxidative aging of asphalt binder is characterized by a constant increase in $|G^*|$ and a reduction in δ (Figure 4-6 and Figure 4-7). In terms of rheological behavior, this can be described as an increase in stiffness along with a greater proportion of elastic behavior when compared to virgin binder.

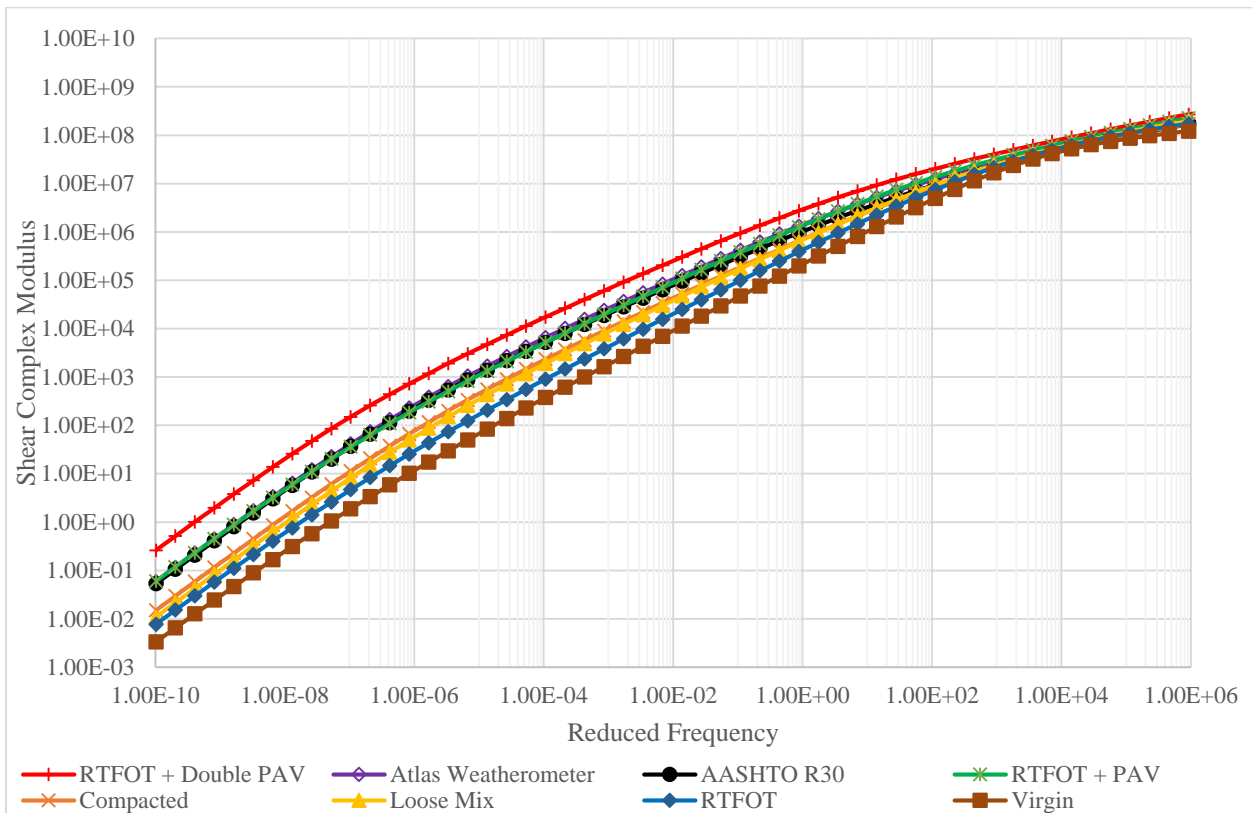


Figure 4-6 Effect of Aging on Complex Modulus Mastercurves

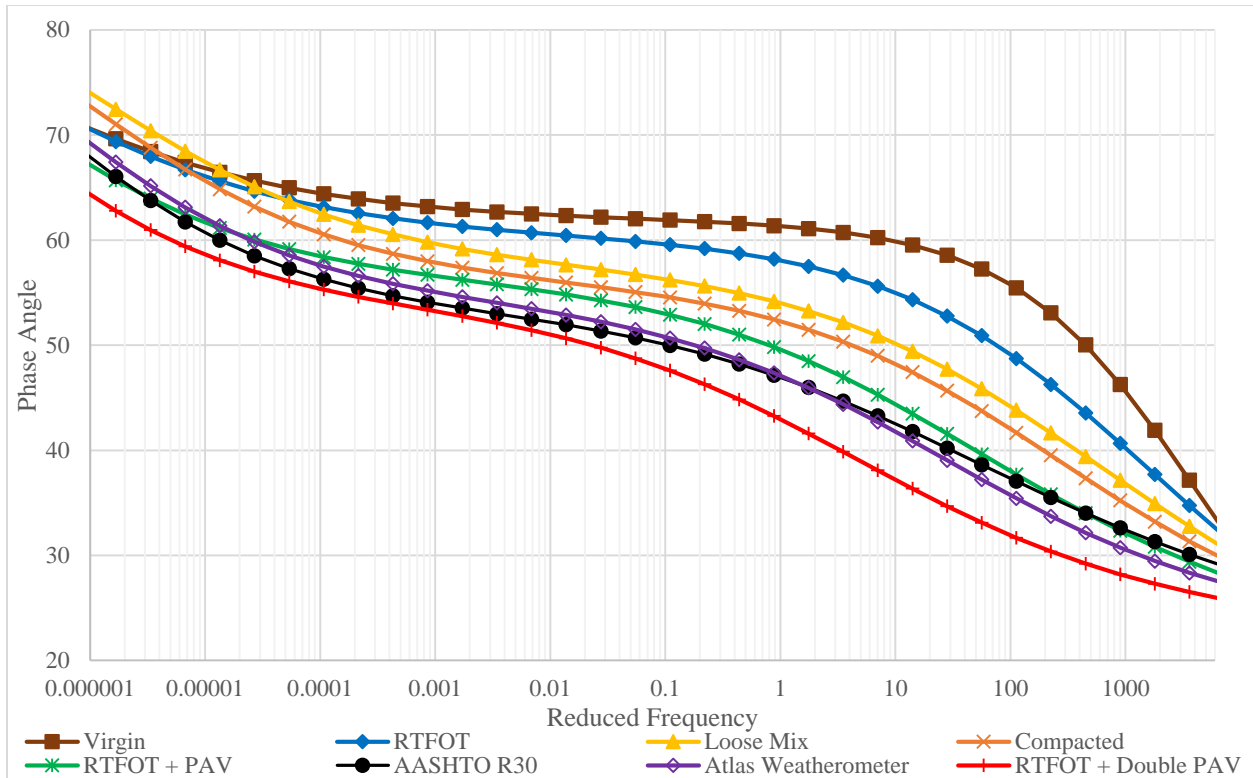


Figure 4-7 Effect of Aging on Phase Angle Mastercurves

Comparison of Control and Atlas Weatherometer Conditioned Samples: As expected, virgin binder exhibits the lowest $|G^*|$ and highest δ . In terms of short-term age conditioning, it was noted that asphalt binder samples extracted and recovered from plant loose mix, and after laboratory compaction exhibited similar rheological parameters. However, when compared to control laboratory accelerated aging procedure for short-term field aging (RTFOT), it was noted that both of these samples showed higher levels of age hardening effects (Figure 4-8 and Figure 4-9).

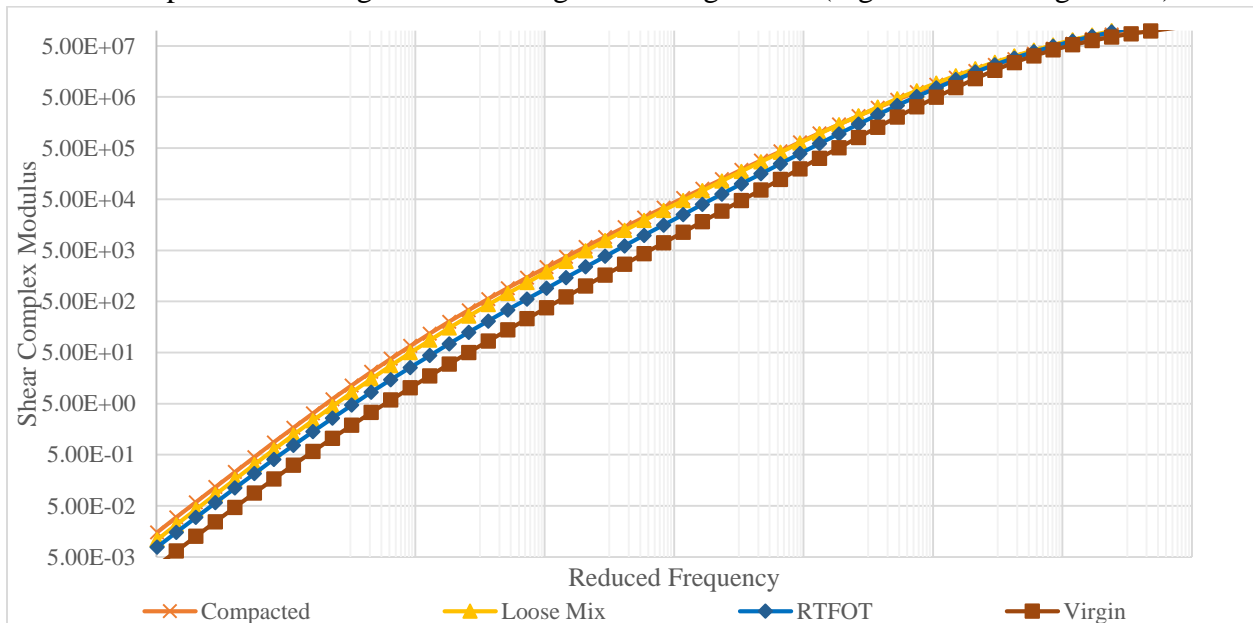


Figure 4-8 Effect of Short-term Conditioning Procedures on Complex Modulus

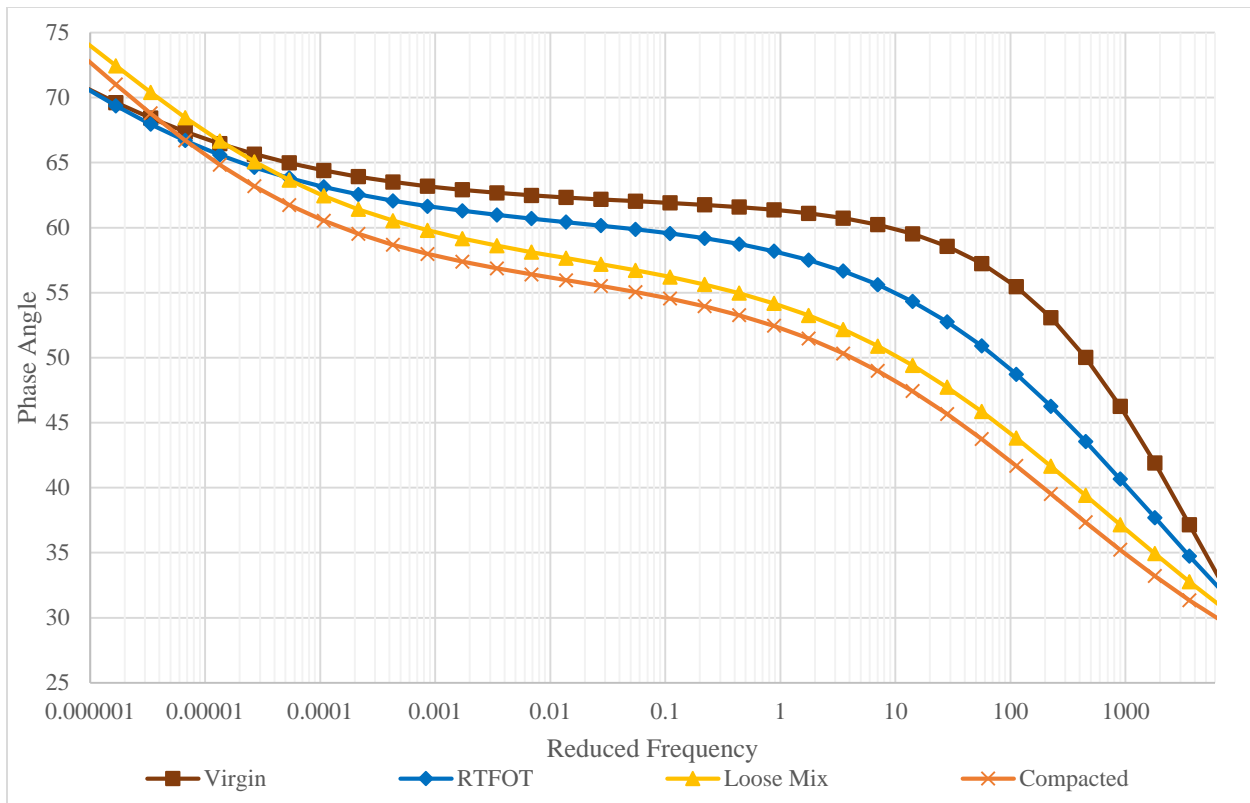


Figure 4-9 Effect of Short-term Conditioning Procedures on Phase Angle Mastercurves

In terms of long-term age hardening effects, it was noted that control laboratory conditioning procedures for asphalt binder (RTFOT + PAV) and for asphalt mixtures (AASHTO R30) produced similar results in terms of rheological parameters ($|G^*|$ & δ).

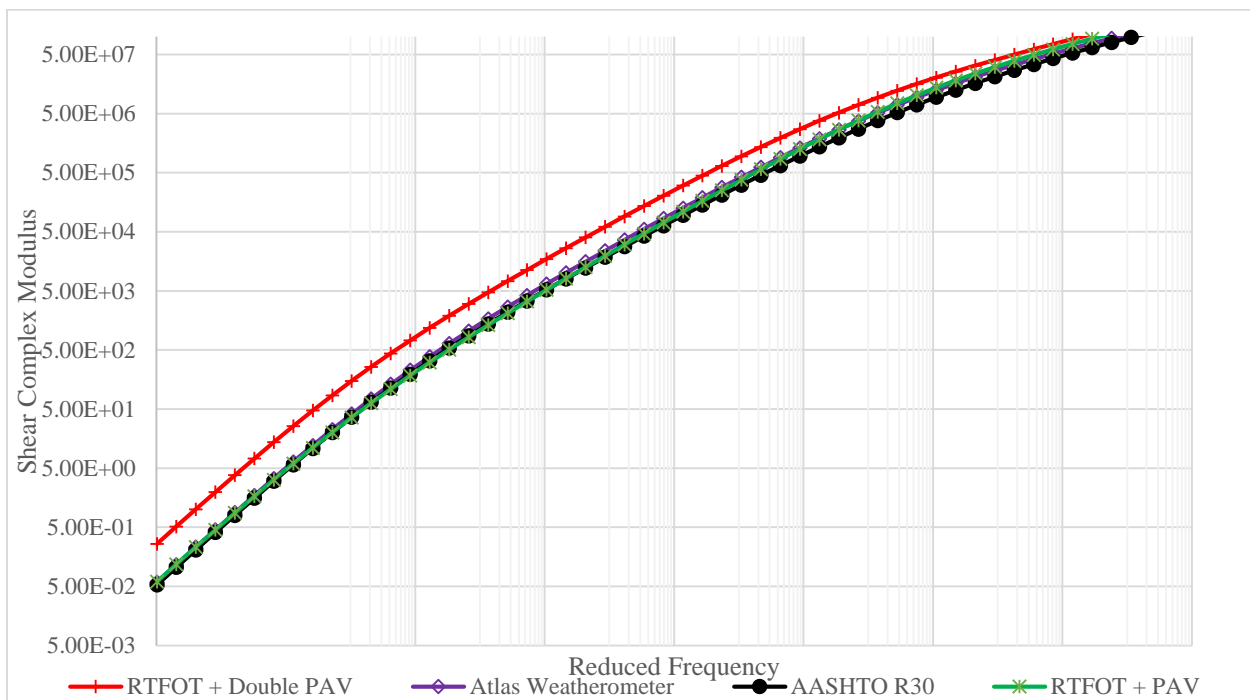


Figure 4-10 Effect of Long-term Conditioning Procedures on Complex Modulus

Age hardening effects of Atlas Weatherometer conditioning were slightly more when compared to both AASHTO R30 and RTFOT + PAV, which can be attributed to the prolonged exposure time and environmental exposure (UV and water). The prolonged PAV exposure (RTFOT + double PAV), however produced very severe age hardening effects when compared to either of the above mentioned procedures (Figure 4-10 and Figure 4-11).

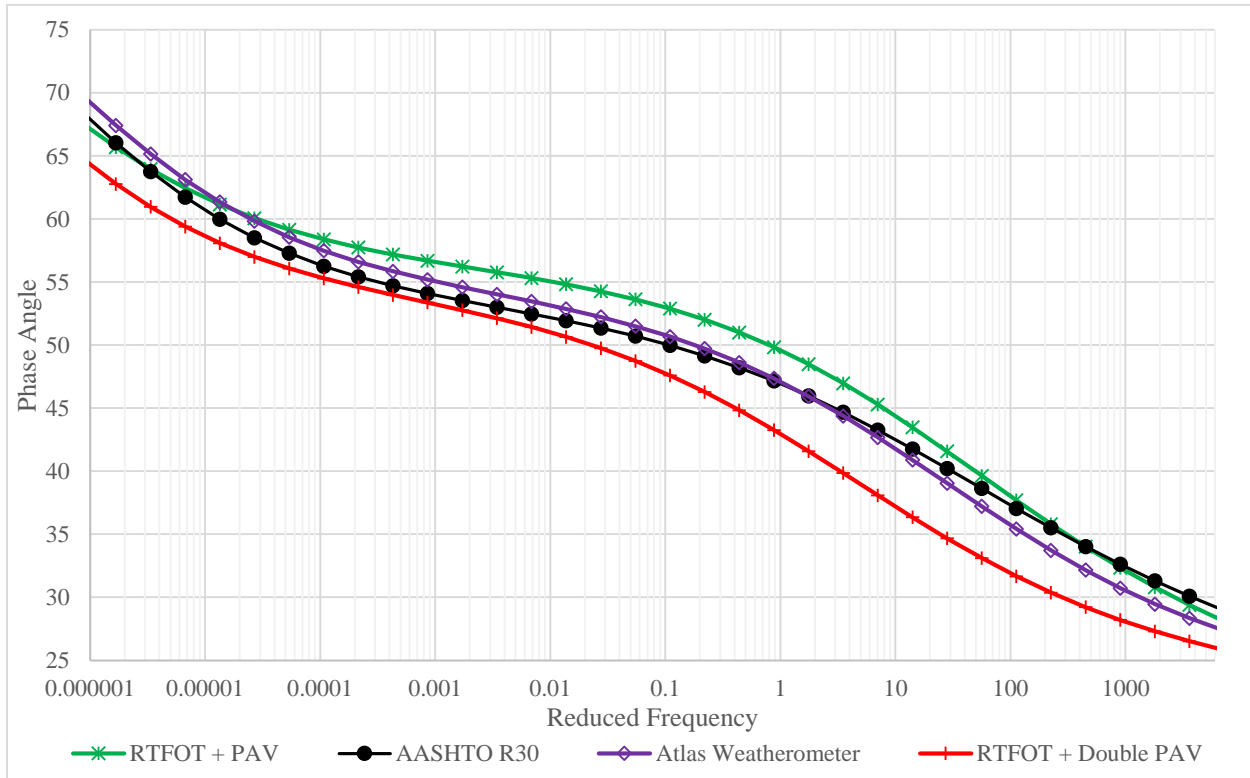


Figure 4-11 Effect of Long-term Conditioning Procedures on Phase Angle Mastercurves

Comparison of Bespoke Chamber Conditioned Samples: In terms of the samples aged using the bespoke chamber conditioning procedure it was found that there was a subsequent increase in stiffness and reduction in phase angle with increasing number of cycles.

Water conditioning however seemed to have a varying effect on rheological parameters with increasing number of cycles. For BC5 samples, it was found that water conditioning lead to comparatively lower stiffness and higher phase angles (Figure 4-12 and Figure 4-13). This can be attributed to the thermal shock effect, as conditioning water at room temperature was used. However, this gap closed with slightly reversed effects encountered with increasing conditioning time for BC10, BC15 and BC20 samples (Figure 4-14 and Figure 4-15).

When compared with other long-term conditioning procedures, it was found that rheological parameters for BC5-NoH₂O, and BC10-H₂O and NoH₂O samples were comparable to those for AASHTO R30, RTFOT + PAV, and Atlas Weatherometer while BC15 and BC20 samples exhibited a higher level of aging. The level of age hardening encountered in bespoke chamber conditioned samples was higher than all other short-term conditioning procedures but still lower than the long-term extended PAV conditioning procedure.

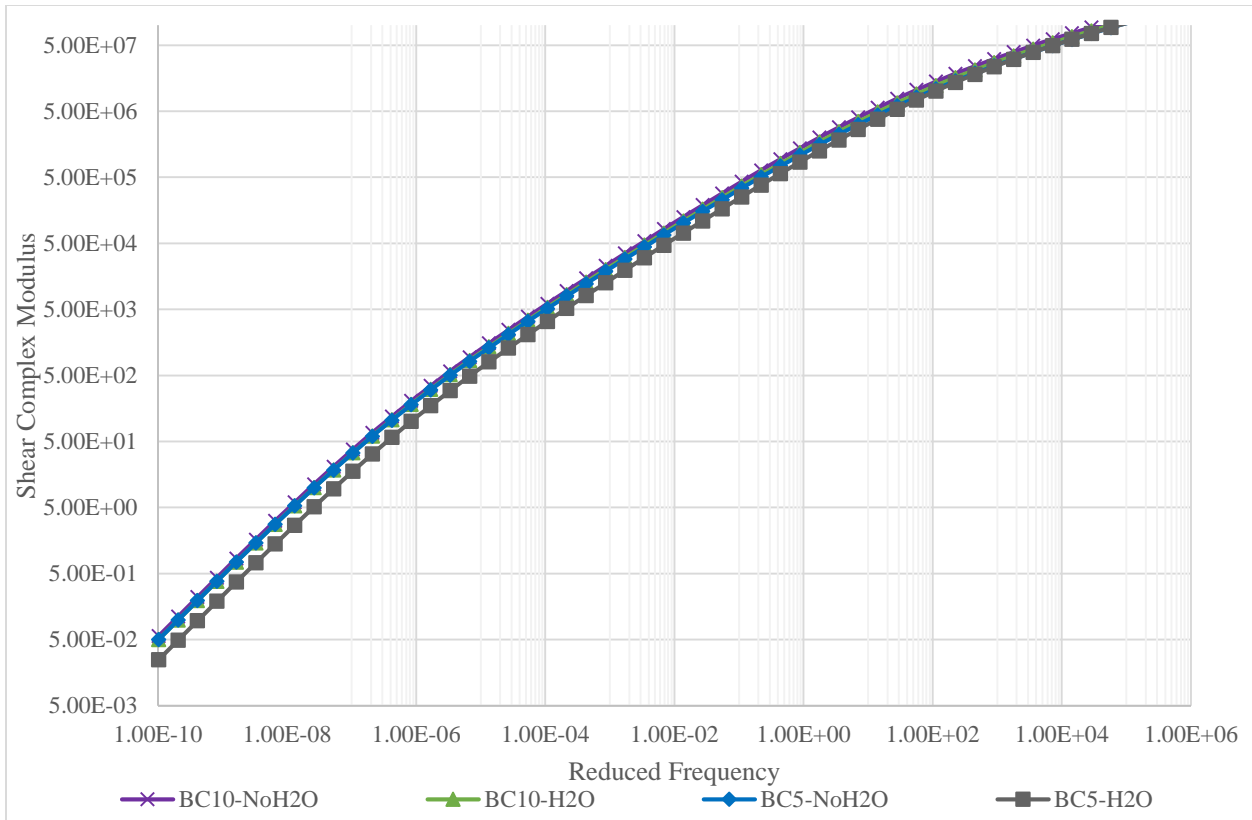


Figure 4-12 Effect of Water Conditioning on BC5 & BC10 Samples – Complex Modulus

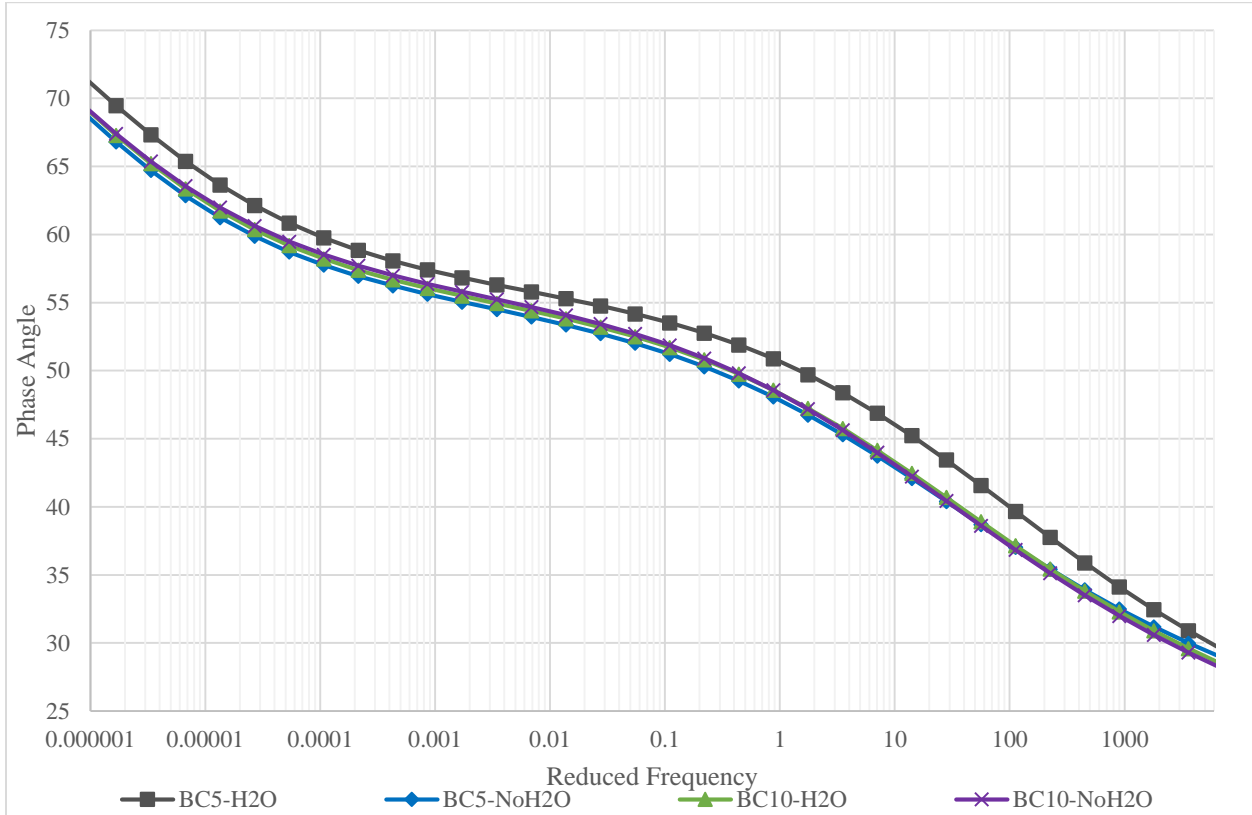


Figure 4-13 Effect of Water Conditioning on BC5 & BC10 Samples – Phase Angle

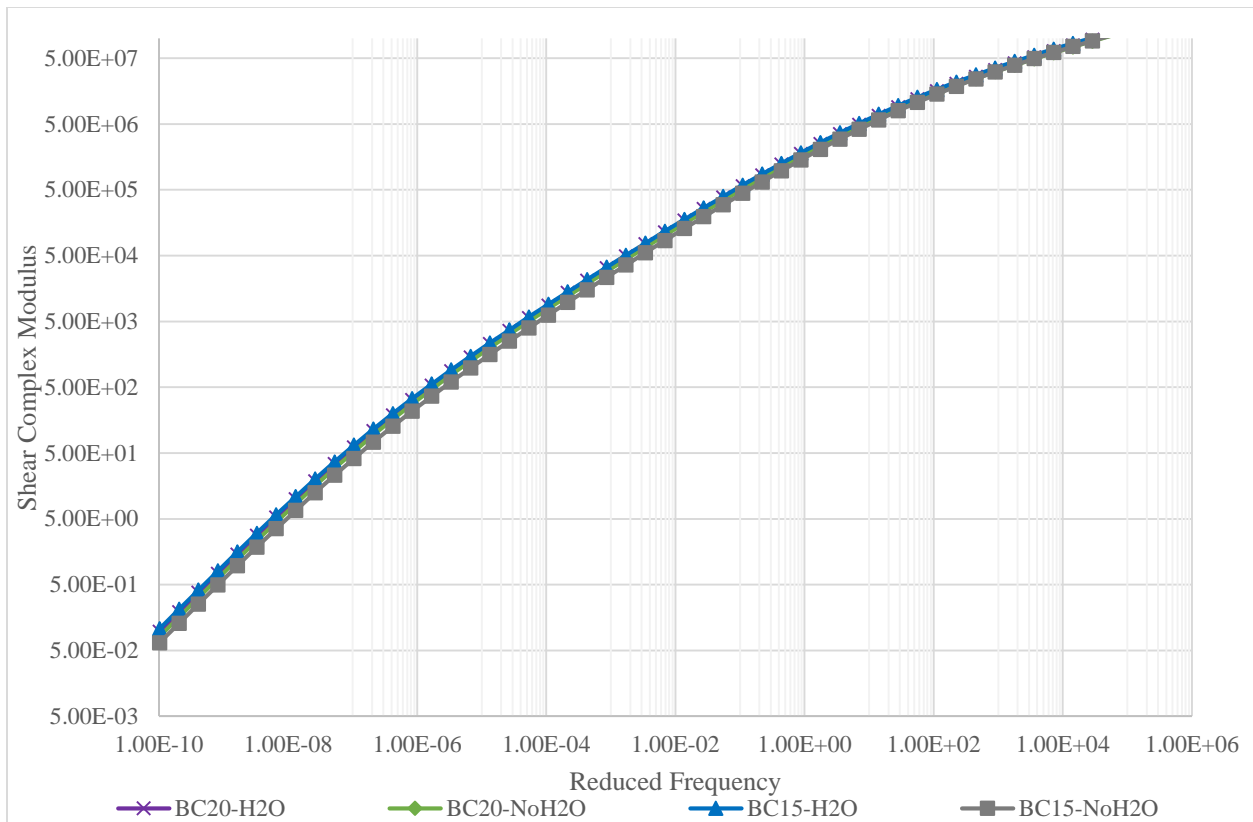


Figure 4-14 Effect of Water Conditioning on BC15 & BC20 Samples – Complex Modulus

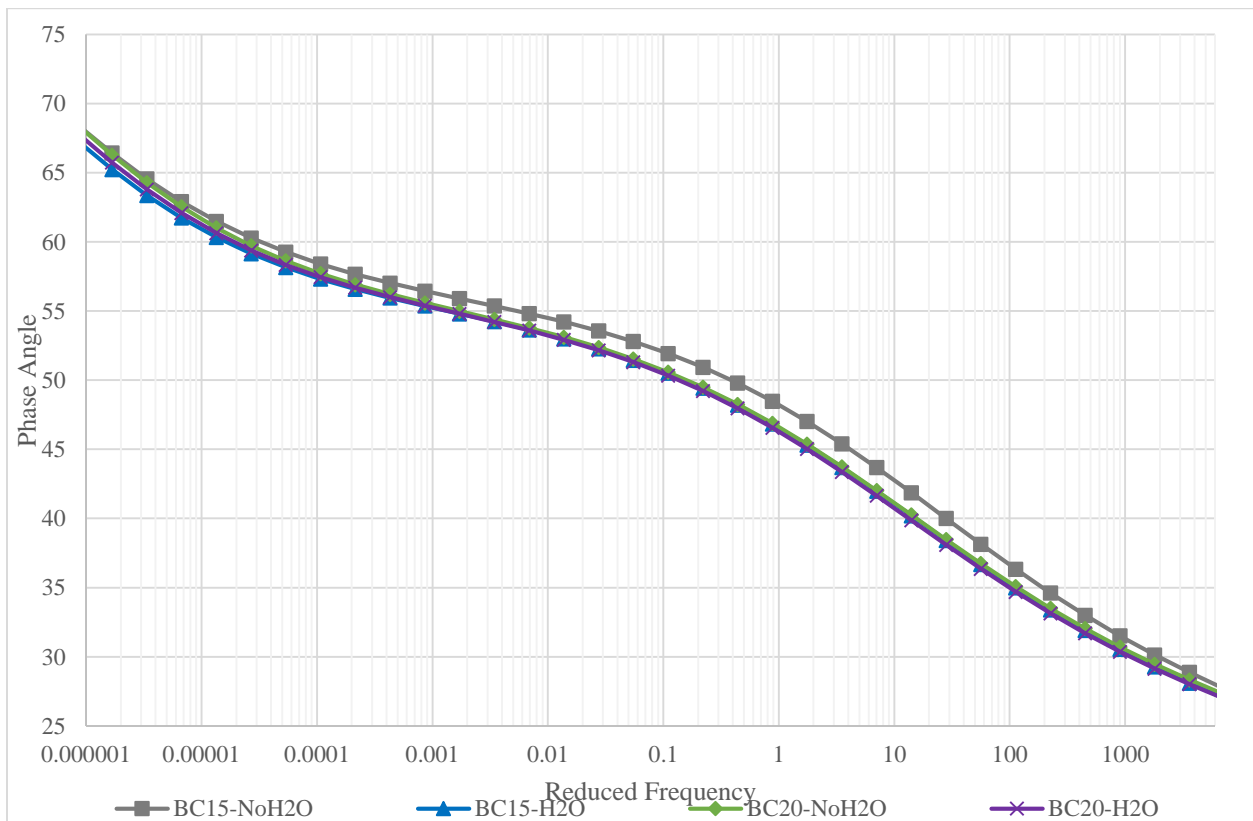


Figure 4-15 Effect of Water Conditioning on BC15 & BC20 Samples – Phase Angle

Comparison of Black Space Curves: The comparison of black space curves shows similar results as encountered for complex modulus and phase angle, with age hardening leading to an increase in stiffness and elastic behavior (Figure 4-16). AASHTO R30 results are however contrary to the ones from the mastercurves showing highest elastic behavior (lowest δ) as compared to all other conditioning procedures.

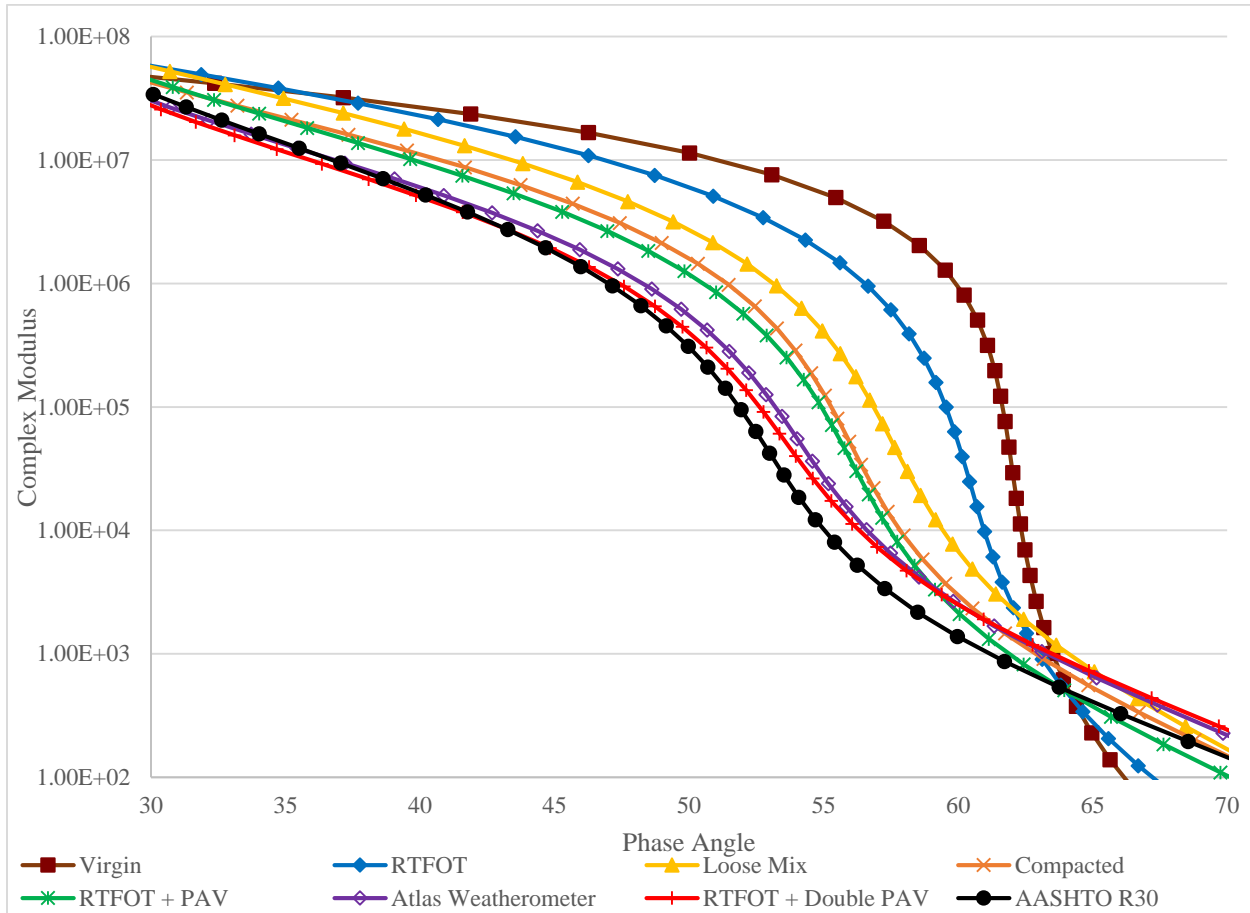


Figure 4-16 Effect of Age Hardening on Black Space Curves

Effect of Aging on Temperature Sensitivity: Shift factor $a(T)$, is a measure of the amount of shifting required at each temperature in order to form a smooth continuous mastercurve. A plot of shift factor versus temperature can be used as an indication of viscosity changes with temperature [10]. Since age hardening of asphalt binder has an effect on binder stiffness and viscosity, noting the changes in these shift factors with respect to temperature can give an idea of how aging affects the viscoelastic behavior.

Similar to the mastercurves, a reference temperature of 15°C was chosen for the preparation of these plots. As expected these plots show that there is a general increase in binder viscosity with aging. Again as noted in black space curves, AASHTO R30 shows contrary behavior with lower viscosity or temperature sensitivity as compared to both plant short-term aged loose mix and after laboratory compaction, and just slightly higher viscosity than the laboratory short-term aging procedure of RTFOT (Figure 4-17).

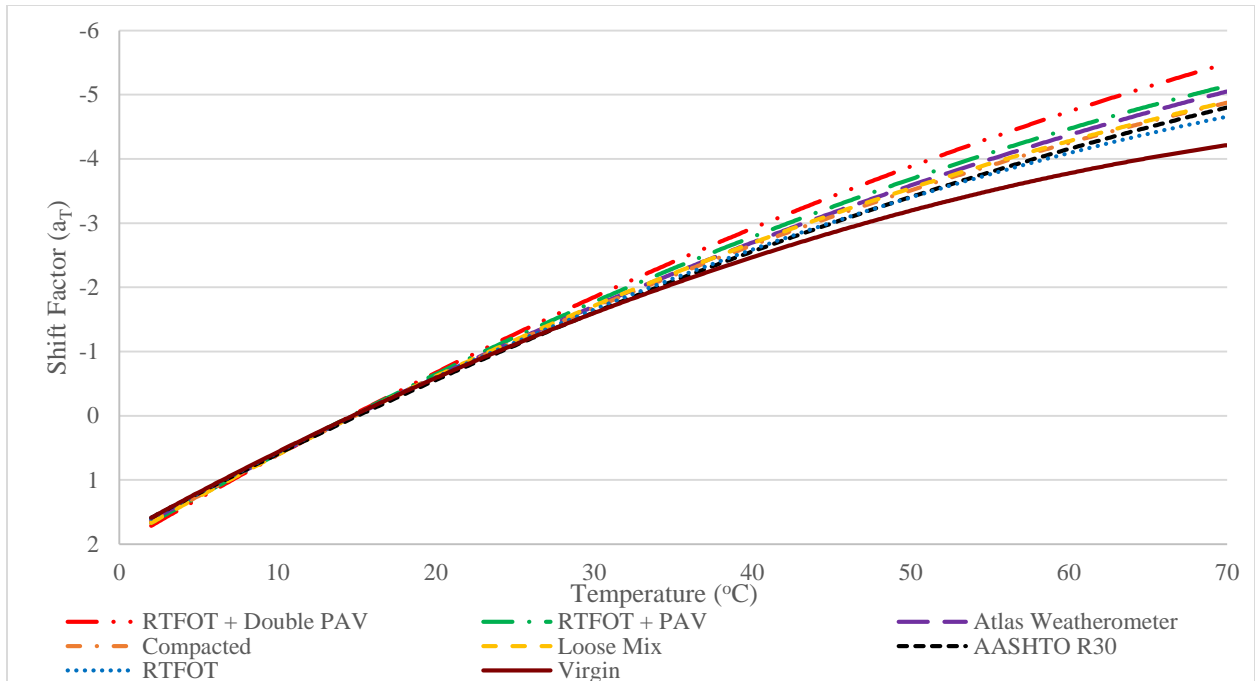


Figure 4-17 Shift Factor VS Temperature for Binders (Control & Atlas Procedure)

With regards to the bespoke chamber conditioning procedure, similar aging trend as noticed with the mastercurves was obtained. BC5-H₂O showed lowest viscosity which was still higher than the short term aging procedures of RTFOT, plant loose mix, and laboratory compacted samples. All of the other BC samples showed a subsequent increase in viscosity surpassing Atlas Weatherometer and RTFOT + PAV conditioning, but still lower than the extended PAV conditioning (Figure 4-18).

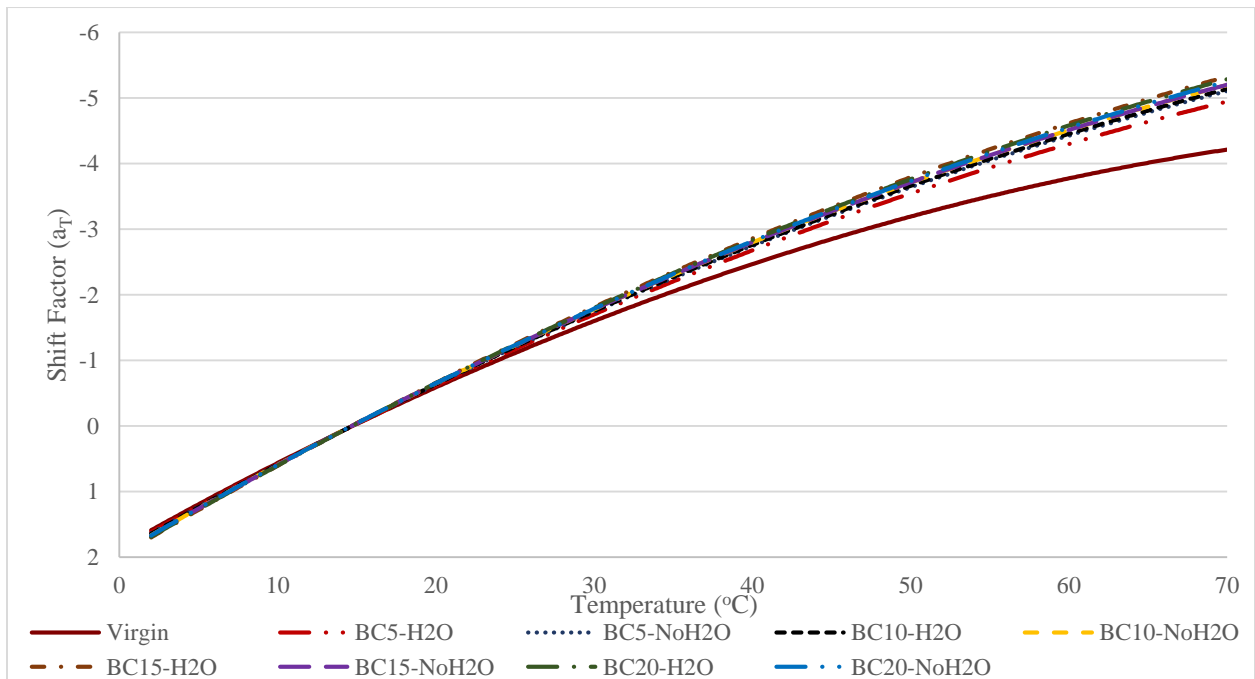


Figure 4-18 Shift Factor VS Temperature for Binders (Bespoke Chamber)

4.1.2 Performance Analysis

Rutting: Multiple Stress Creep Recovery (MSCR) tests as described in section 3.5.1, were carried out in accordance with AASHTO T350-14. A copy of the test reports (produced using Anton Parr software RheoCompass™) for each of these samples are attached in Appendix D and have also been summarized in Table 4-1. Asphalt binder grading in accordance with AASHTO M322-14, indicating traffic grades at 64°C are also included in these reports. As expected, the non-recoverable creep compliance (J_{nr}) versus percent recovery plot for all of these samples, indicate that the asphalt binder is modified using an acceptable elastomeric polymer.

Table 4-1 Multiple Stress Creep Recovery Test results sorted by magnitude of J_{nr} (3.2kPa)

Sample	Load Level				R_diff - % diff of recovery (0.1 & 3.2 kPa)	J _{nr} _diff - % diff of non-recoverable creep compliance (0.1 & 3.2 kPa)
	0.1kPa		3.2kPa			
	J _{nr}	% Recovery	J _{nr}	% Recovery		
<i>Virgin</i>	0.3995	89.97	3.725	27.27	69.69	832.49
<i>RTFOT</i>	0.4059	79.45	0.8465	58.98	25.77	108.54
<i>Loose Mix</i>	0.4658	66.82	0.8345	43.61	34.73	79.15
<i>Extracted Virgin</i>	0.0826	97.22	0.8284	70.77	27.21	903.27
<i>Compacted</i>	0.3382	69.17	0.5814	48.19	30.33	71.92
<i>BC5-H₂O</i>	0.206	74.68	0.3366	58.29	21.94	63.39
<i>RTFOT + PAV</i>	0.1539	77.45	0.2253	67.14	13.31	46.33
<i>BC10-H₂O</i>	0.1395	77.33	0.2135	64.29	16.87	53.01
<i>AASHTO R30</i>	0.1446	74.25	0.2109	60.63	18.34	45.85
<i>Atlas Weatherometer</i>	0.1411	74.56	0.2053	61.36	17.71	45.49
<i>BC5-NoH₂O</i>	0.1278	78.72	0.2048	64.54	18.01	60.21
<i>BC15-NoH₂O</i>	0.137	77.08	0.2041	65.51	15.01	48.97
<i>BC10-NoH₂O</i>	0.1338	77.42	0.1981	65.08	15.94	48.09
<i>BC20-NoH₂O</i>	0.1134	77.06	0.1603	66.24	14.05	41.39
<i>BC15-H₂O</i>	0.1024	78.33	0.1411	68.94	11.98	37.75
<i>BC20-H₂O</i>	0.1012	78.16	0.1383	68.83	11.94	36.74
<i>RTFOT + Double PAV</i>	0.0618	79.09	0.08	72.37	8.5	29.47

As identified in literature, the non-recoverable creep compliance (J_{nr}) provides a good correlation to rutting, and results show that with increasing levels of aging there is a reduction in J_{nr} , and hence a subsequent reduction in rutting potential. RTFOT aged binder results are very similar to those for plant short-term aged binder, and RTFOT + Double PAV aged binder has the lowest J_{nr} values indicating highest increase in stiffness ($|G^*|$). The aging trend obtained by this test correlates very

well with the aging trend obtained from rheological analysis or by comparing the increase in $|G^*|$ (Figure 4-19).

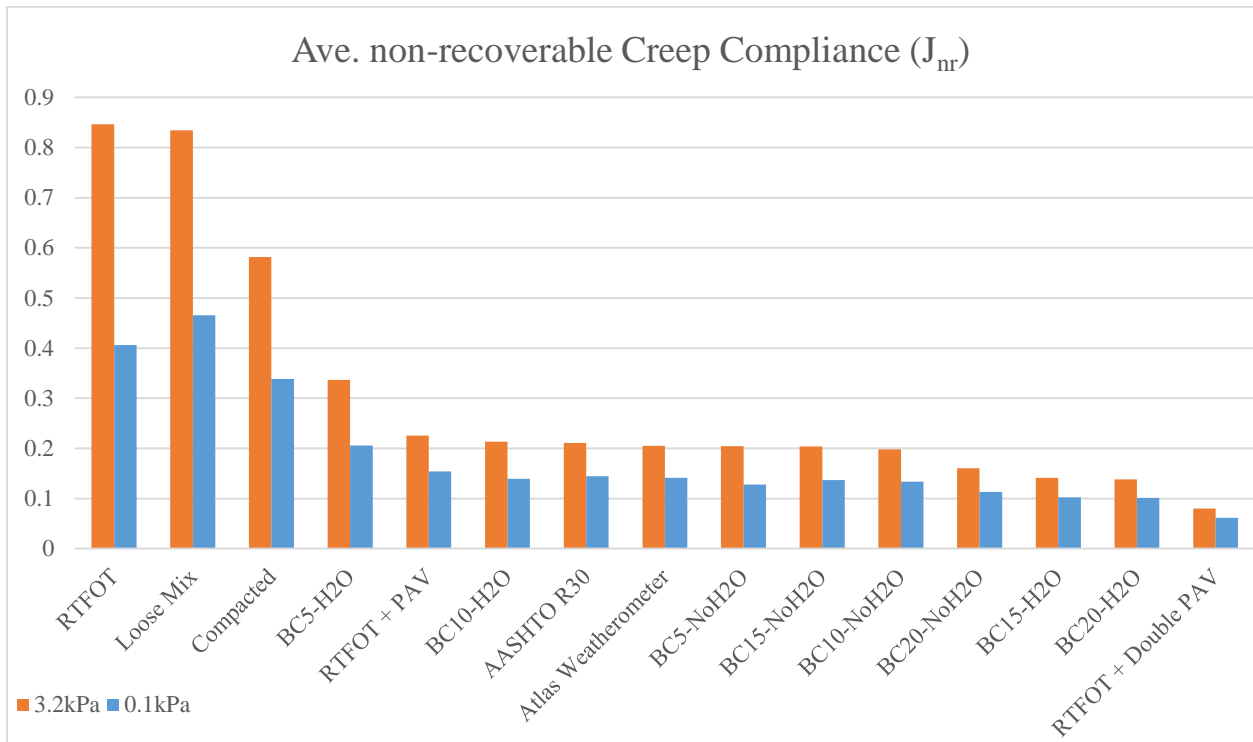


Figure 4-19 Comparison of J_{nr} for different Conditioning Procedures

Figure 4-20 shows a plot of percentage difference of non-recoverable creep compliance (J_{nr_diff}) for load levels of 0.1 & 3.2kPa indicating that age hardening of asphalt binder leads to a better rutting performance at higher stress levels.

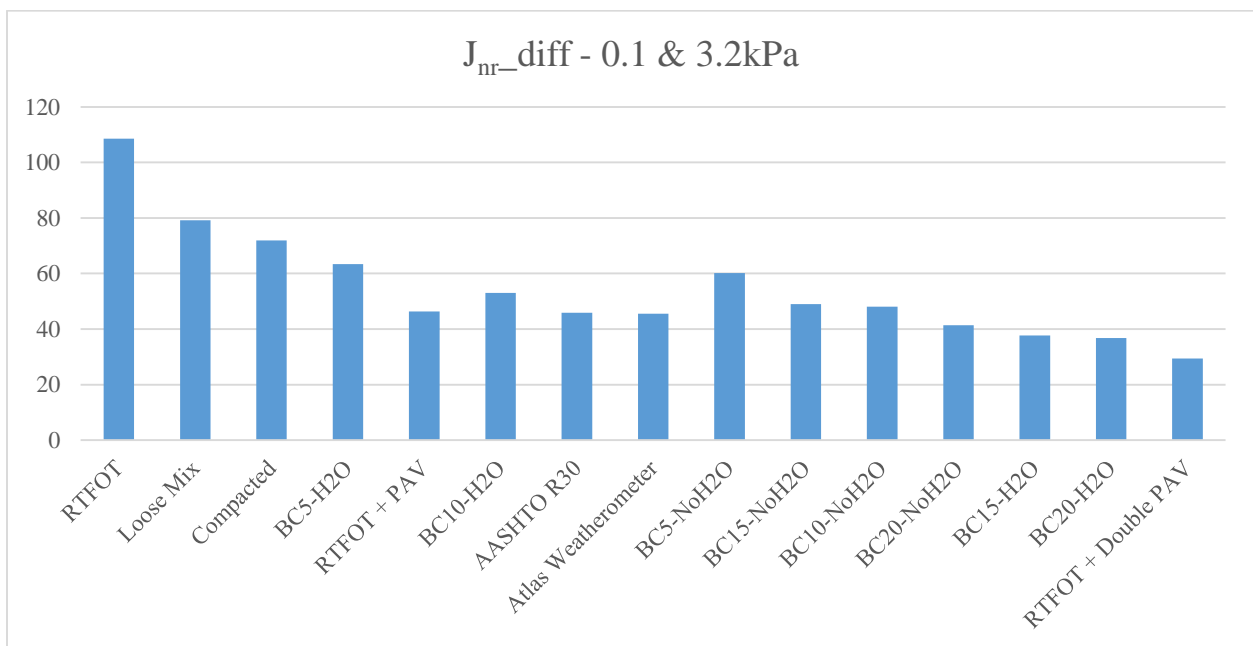


Figure 4-20 Comparison of J_{nr_diff} for different Conditioning Procedures

NOTE: Spikes were noted in J_{nr} (0.1 & 3.2kPa) values for both virgin binder and extracted and recovered virgin binder. As discussed previously, this can be attributed to the high polymer content in these binders. As such these results have been omitted from Figure 4-19 and Figure 4-20 for comparison purposes.

Fatigue: Test reports generated by Anton Parr software RheoCompass™ for Linear Amplitude Sweep (LAS) tests, carried out in accordance with AASHTO TP101-14 have been attached in Appendix E. Viscoelastic Continuum Damage (VECD) analysis was then carried out using the Frequency Sweep and Amplitude Sweep data from these reports to calculate parameters A and B such that [41]:

$$N_f = A(\gamma_0)^B$$

Eq. 4-1

where

N_f = Number of cycles to failure based on 35% reduction in initial modulus.

γ_0 = Applied Strain (%).

N_f values hence calculated for 2.5% and 5% strain levels are tabulated in Table 4-2, and have also been plotted in Figure 4-21. The chosen strain levels correspond to approximate strain induced in binder (~50 times pavement strain) for a typical “strong” pavement (assumed 500 μ strain) and “weak” pavement (assumed 1000 μ strain) [36].

Table 4-2 N_f values calculated for 2.5% and 5% Strain level

Sample	Number of cycles to failure	
	N_f (2.5% Strain)	N_f (5% Strain)
<i>Extracted Virgin</i>	35040.75992	4796.9977
<i>Virgin</i>	25436.50933	3900.852075
<i>RTFOT</i>	17036.60334	2241.511418
<i>Loose Mix</i>	11581.15477	1300.917752
<i>Compacted</i>	11407.41463	1170.893201
<i>BC5-H2O</i>	11007.76357	1010.43421
<i>BC10-H2O</i>	8817.591814	704.1621023
<i>BC5-NoH2O</i>	8522.810937	666.0297624
<i>RTFOT + PAV</i>	7087.49083	645.9828347
<i>AASHTO R30</i>	8024.711803	625.6227299
<i>BC10-NoH2O</i>	7686.9039	613.2478169
<i>BC15-NoH2O</i>	6836.469495	551.8240103
<i>Atlas Weatherometer</i>	6254.914637	474.3008793
<i>BC20-NoH2O</i>	6474.87023	470.8295443
<i>BC15-H2O</i>	6346.218014	464.6302313
<i>BC20-H2O</i>	6060.818537	463.7114458
<i>RTFOT + Double PAV</i>	4639.438105	282.0991894

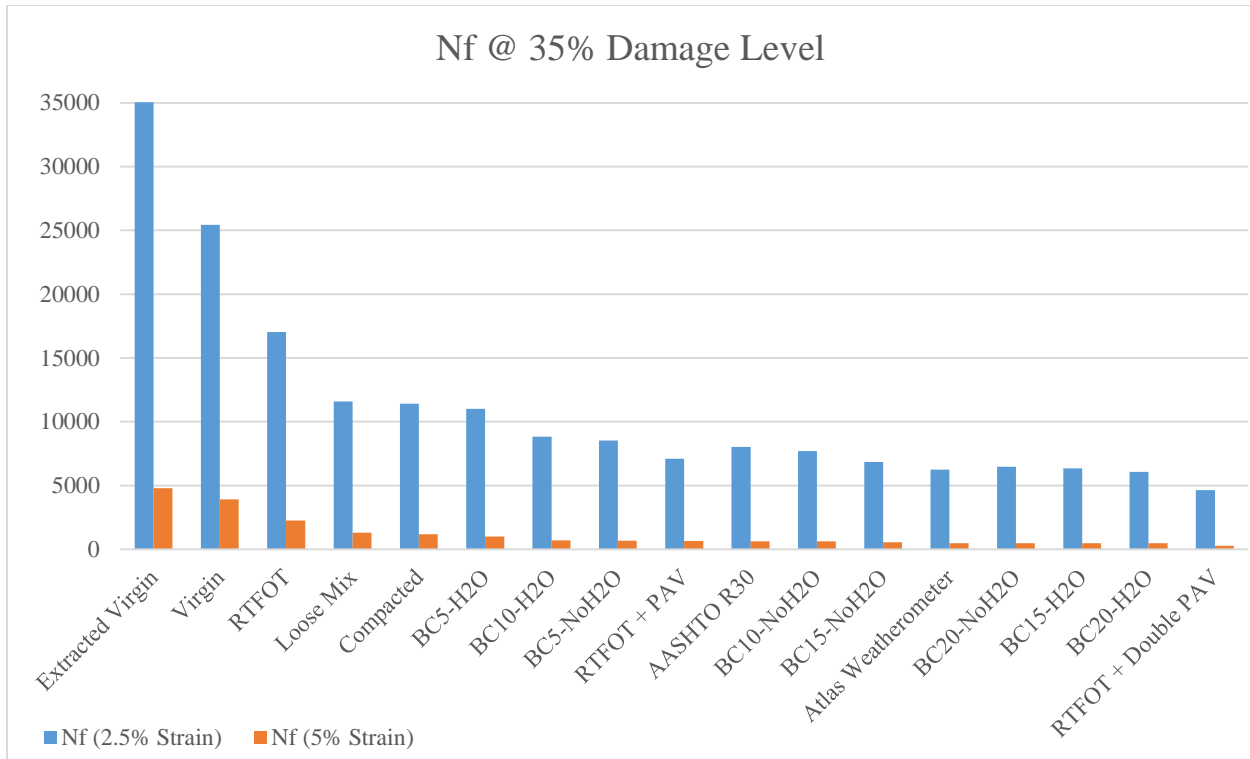


Figure 4-21 Comparison of Nf (2.5% & 5% Strain) for different Conditioning Procedures

As identified in literature, this data suggests that age hardening of asphalt binder leads to a reduction in durability with reduced resistance against rutting. The aging trend obtained from Figure 4-21 can also be reasonably compared to the aging trend obtained from MSCR and rheological analysis.

In order to further understand the effects of aging on fatigue life, N_f was plotted against varying strain levels (Figure 4-22 and Figure 4-23). Generally, it was noticed that increasing levels of aging leads to an increase in parameter A (y-intercept), and a subsequent decrease in parameter B (higher slope) indicating brittle behavior. The effect of extraction and recovery procedures on virgin binder was noted as a slight increase in the number of cycles at low strain levels, however at higher strain levels similar fatigue performance was noted (higher slope). The effect of laboratory compaction was noted as a slight decrease in fatigue life in comparison to the plant produced loose mix, however both of these samples showed a lower fatigue life in comparison to the control laboratory short-term conditioning procedure of RTFOT.

With regards to the long-term conditioning procedures, AASHTO R30 exhibited slightly lower fatigue life in comparison to RTFOT + PAV, while both of these still performed better than Atlas Weatherometer conditioning procedure. The effect of water conditioning on bespoke chamber samples was similar to the one noted in rheological analysis, with a slight increase in fatigue life for BC5 samples while a slight reduction was noted for BC10, BC15, and BC20 samples. A progressive decrease was noted in the fatigue life with increasing conditioning time for the bespoke chamber samples, with BC20 samples showing a slightly lower fatigue when compared to Atlas Weatherometer conditioned samples. Fatigue life for all of these samples was still considerably higher than the extended PAV procedure.

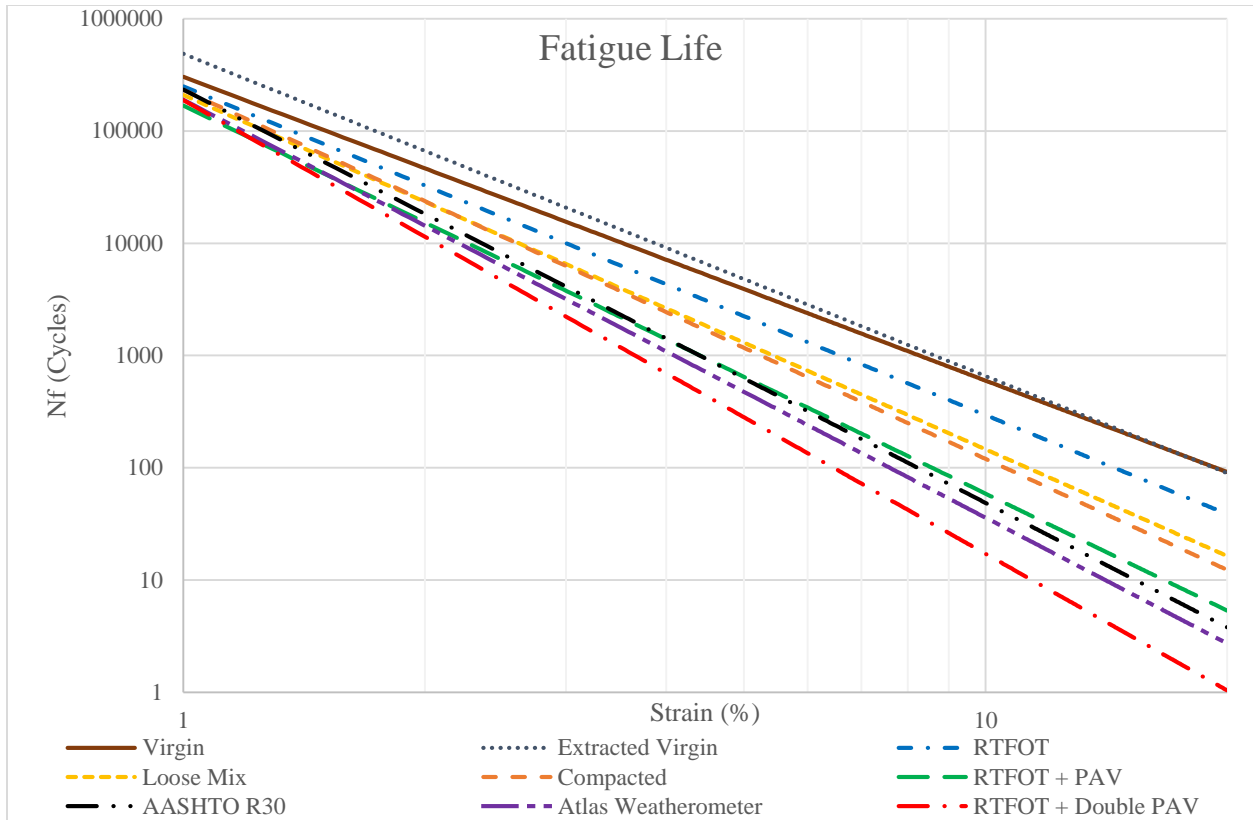


Figure 4-22 Fatigue Life for Control and Atlas Weatherometer Conditioning Procedures

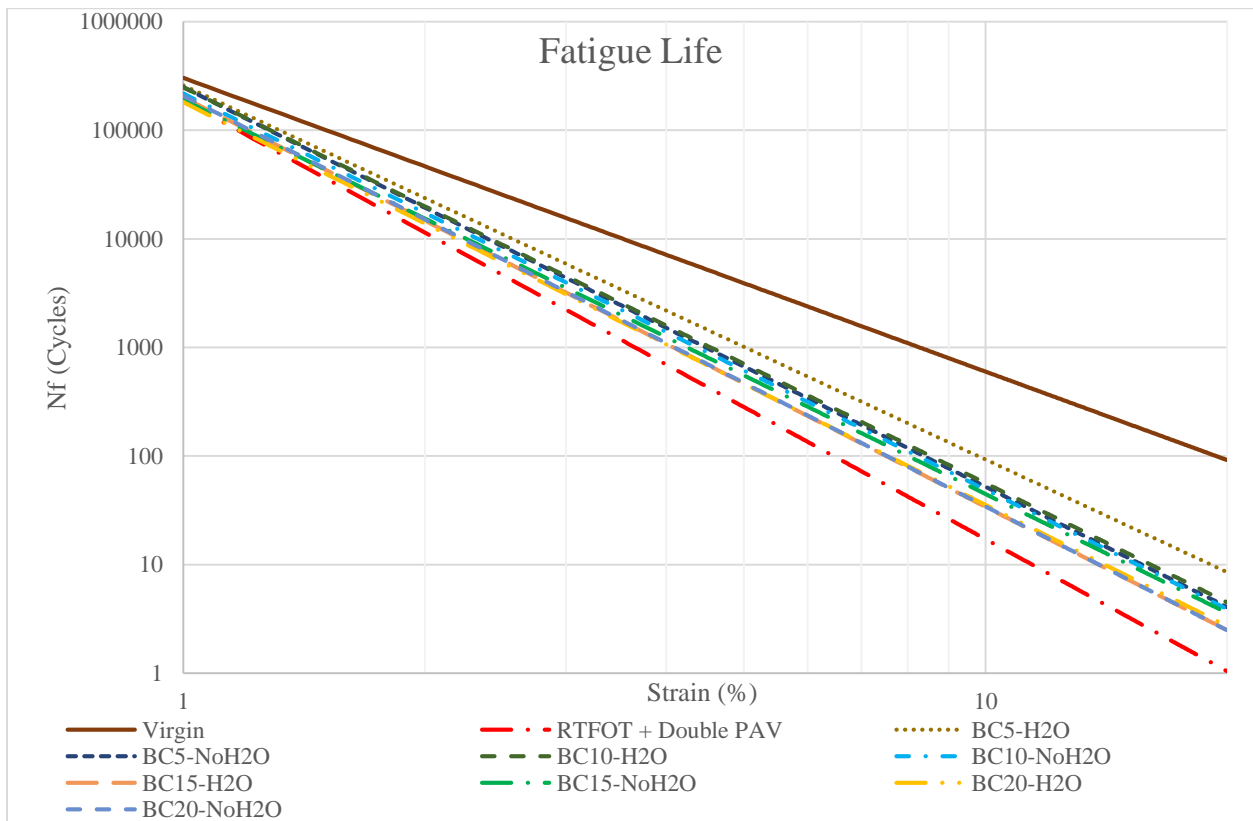


Figure 4-23 Fatigue Life for Bespoke Chamber Conditioning Procedure

Amplitude Sweep data from LAS tests was also used to plot stress-strain curves for asphalt binder samples subjected to different conditioning procedures (Figure 4-24 and Figure 4-25). Results are in agreement with observations noted from other tests indicating that increasing levels of aging lead to an increase in elastic behavior with higher levels of stored energy.

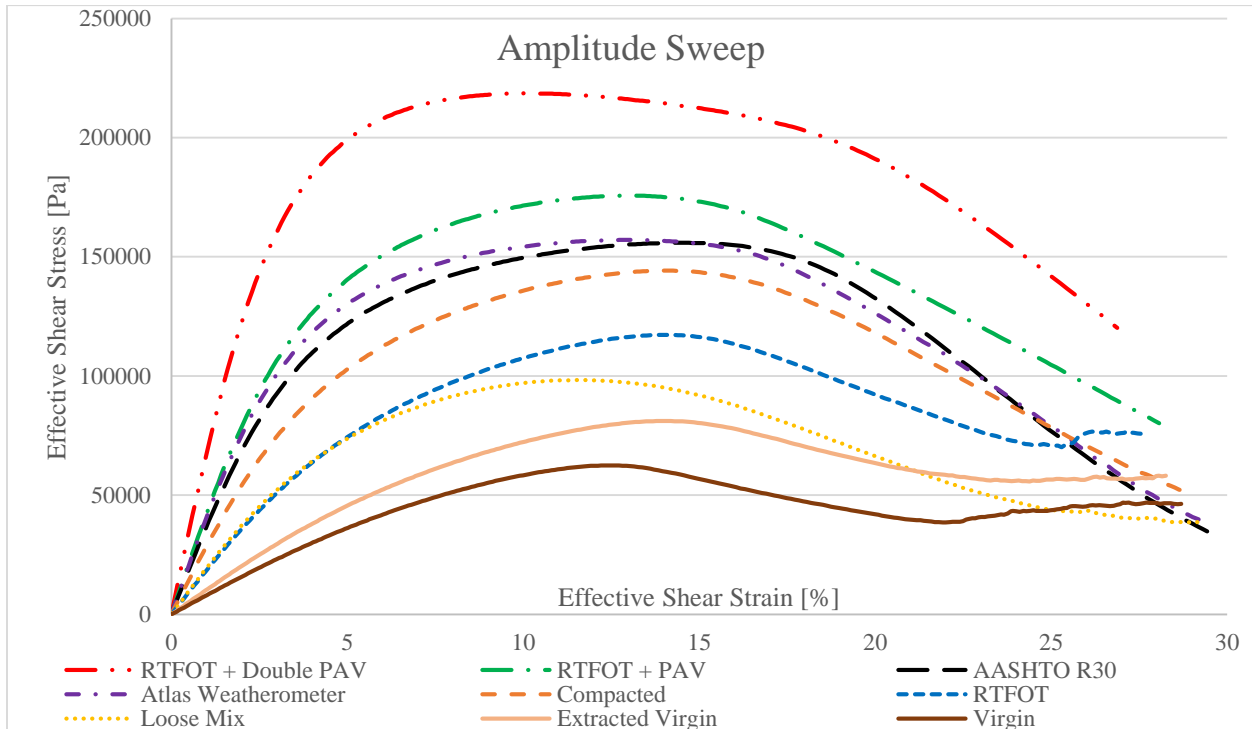


Figure 4-24 Amplitude Sweep for Control and Atlas Weatherometer Conditioning

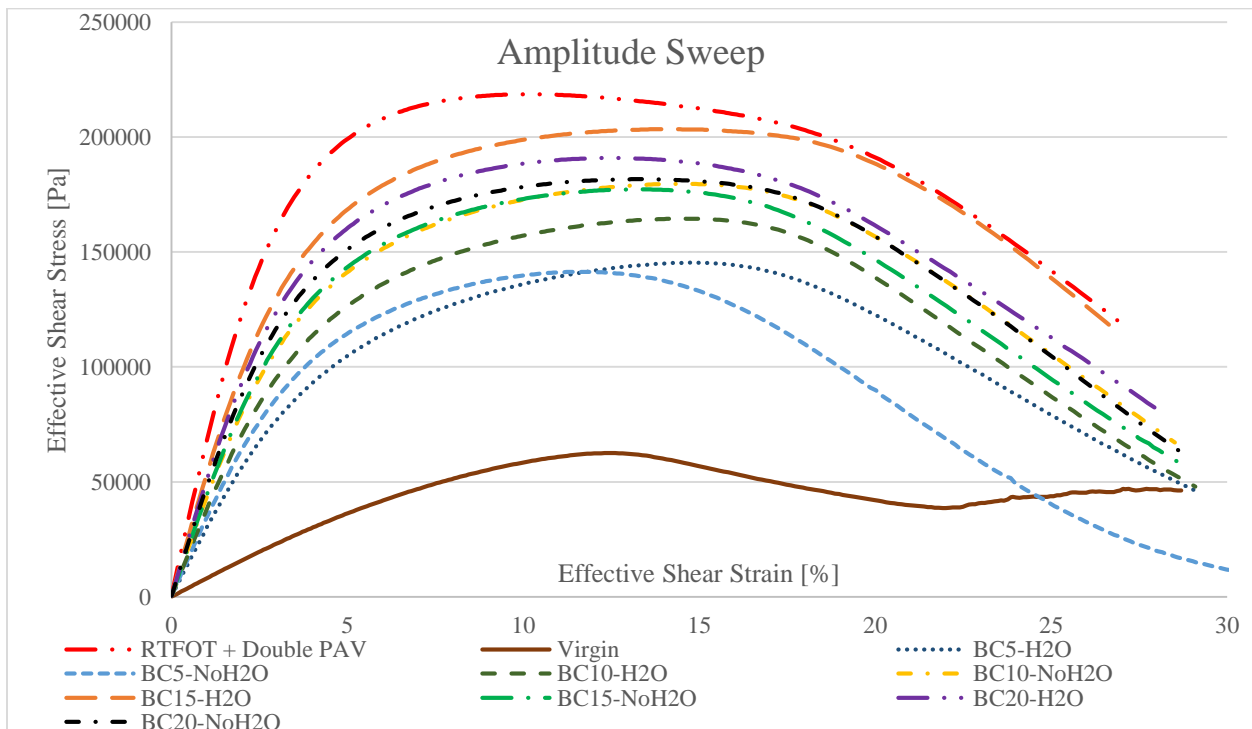


Figure 4-25 Amplitude Sweep for Bespoke Chamber Conditioning Procedure

4.1.3 Chemical Analysis

The chemical modifications in asphalt binder with respect to aging have been characterized using the FT-IR test. Obtained spectrum for all of the tested samples has been plotted in Figure 4-26. The two main functional groups formed during oxidative aging: Carbonyl and Sulfoxide functional groups were then quantitatively calculated using Equation 2-2 and Equation 2-3. These have been tabulated in increasing order of Carbonyl Index in Table 4-3. Similar trend, in terms of the level of aging is noticed, however a good correlation cannot be obtained when comparing these results with rheological and performance analysis results. Note that spikes were noted in obtained spectra for BC5-NoH₂O samples, which have subsequently been removed from the dataset.

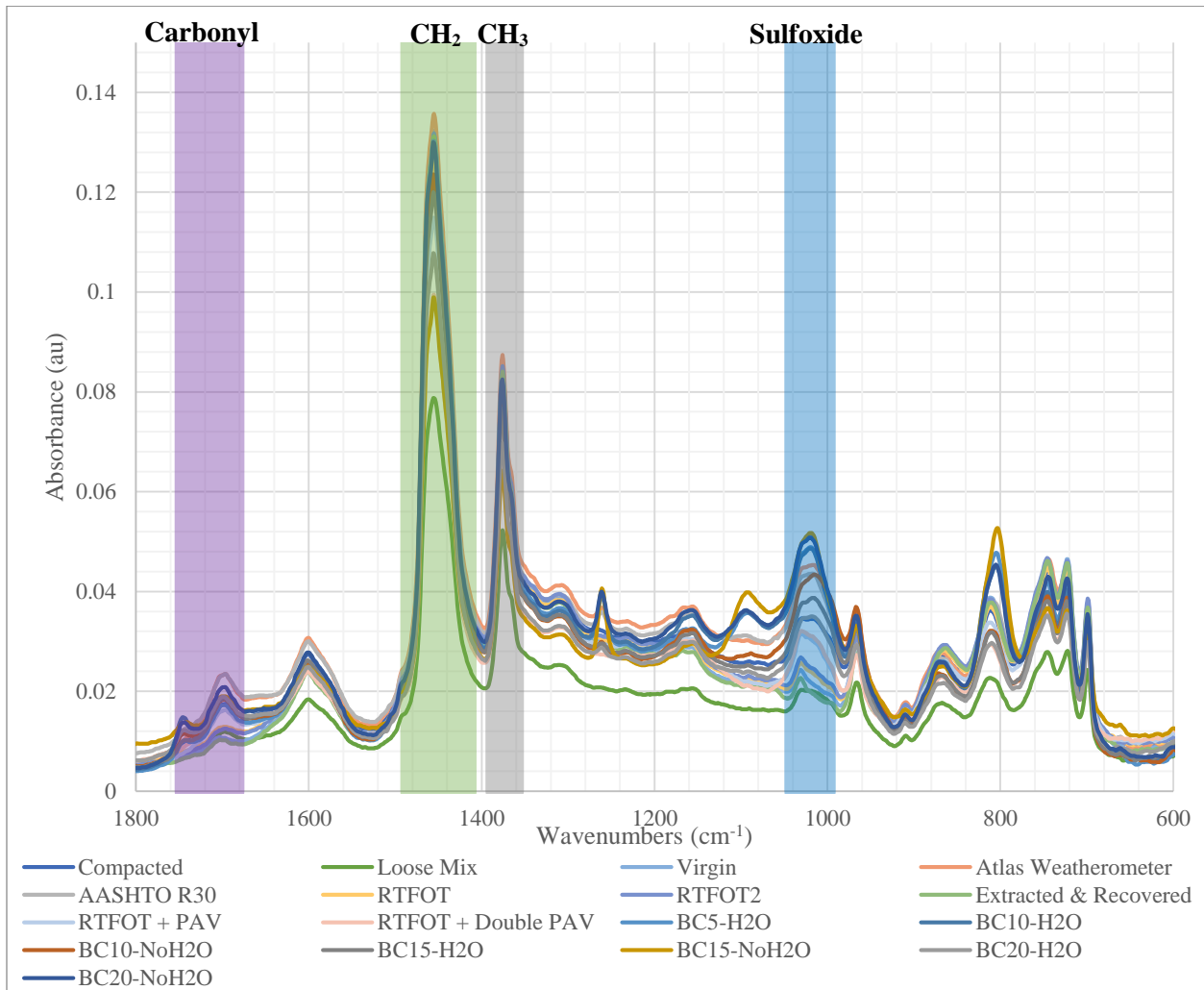


Figure 4-26 FT-IR Spectra for Binders subjected to different Conditioning Procedures

As mentioned in literature review, high conditioning temperatures could lead to a lower rate of sulfoxide formation in comparison to ketones (carbonyl group), given their thermal instability, and dissociation of carbon-containing aromatic molecules which are otherwise locked up into molecular agglomerates at lower temperatures [22]. For this reason, Sulfoxide to Carbonyl ratio was calculated and compared (Figure 4-27). Results are in agreement with this statement showing very low ratio for the high temperature RTFOT procedure (163°C). An increase in this ratio is then

noted for comparatively lower temperature PAV procedures (100°C), with a further increase noted for AASHTO R30 (85°C) and finally the bespoke chamber conditioning procedures (lowest temperature range).

Table 4-3 FT-IR Functional Group Analysis sorted in order of Carbonyl Index values

Sample	Carbonyl Index	Sulfoxide Index	Sulfoxide/Carbonyl
<i>Extracted & Recovered</i>	0.011326	0.007992	0.7056604
<i>Virgin</i>	0.01225	0.0168279	1.3737024
<i>RTFOT</i>	0.014044	0.0340229	2.4233657
<i>BC10-H2O</i>	0.01527	0.1766814	11.57079
<i>BC5-NoH2O</i>	0.019789	0.5292722	26.746082
<i>Loose Mix</i>	0.023301	0.0657688	2.82263
<i>BC15-NoH2O</i>	0.024264	0.2328684	9.5973236
<i>BC10-NoH2O</i>	0.025022	0.1450568	5.7971275
<i>BC5-H2O</i>	0.025162	0.1635499	6.5
<i>Compacted</i>	0.025171	0.0901375	3.5809769
<i>BC20-NoH2O</i>	0.026443	0.1800899	6.8104575
<i>BC20-H2O</i>	0.030763	0.1394964	4.5345858
<i>RTFOT + PAV</i>	0.031093	0.1063087	3.4190476
<i>BC15-H2O</i>	0.031811	0.1395305	4.3861968
<i>AASHTO R30</i>	0.037859	0.145582	3.8453427
<i>Atlas Weatherometer</i>	0.041758	0.147961	3.5433267
<i>RTFOT + Double PAV</i>	0.047391	0.143157	3.0207697

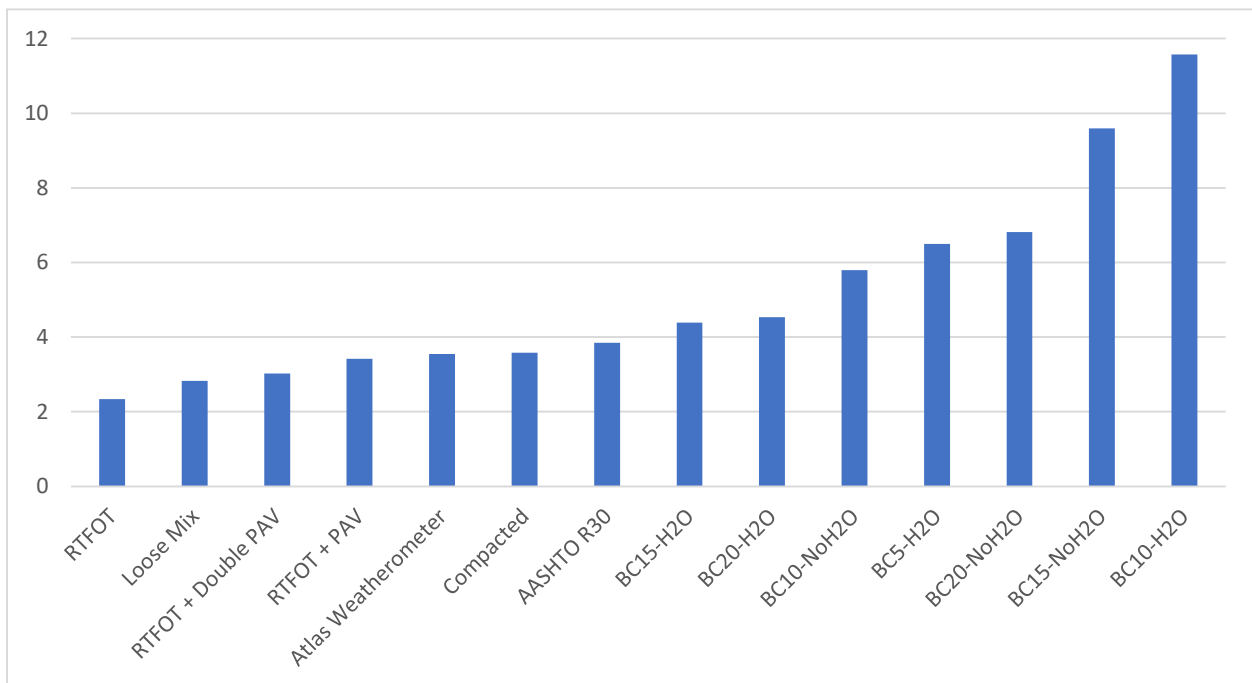


Figure 4-27 Comparison of Sulfoxide to Carbonyl Ratio

4.2 Asphalt Mixtures

4.2.1 Rheological Analysis

Similar to asphalt binders, rheological analysis for compacted asphalt mixture samples have been carried out using the 2S2P1D model. Rheological data for each type of conditioning procedure was averaged (6No. samples for Unconditioned, and 3No. each for AASHTO R30 and Atlas Weatherometer), to prepare plots for isothermal mastercurves (at 21°C for 1. Complex Modulus, and 2. Phase Angle), Black Space diagrams ($|E^*|$ vs δ), and Cole-Cole diagrams (E'' vs E'). A copy of these plots have been attached in Appendix F.

Effect of Aging on Rheological Behavior: Comparative plots for Complex Modulus mastercurve (Figure 4-28), Phase Angle mastercurve (Figure 4-29), Black Space diagram (Figure 4-30), Cole-Cole diagram (Figure 4-31), and Shift Factor versus Temperature at 21°C (Figure 4-32), were prepared for Unconditioned, AASHTO R30 and Atlas Weatherometer aged samples to understand the effect of aging on mixture rheological behavior.

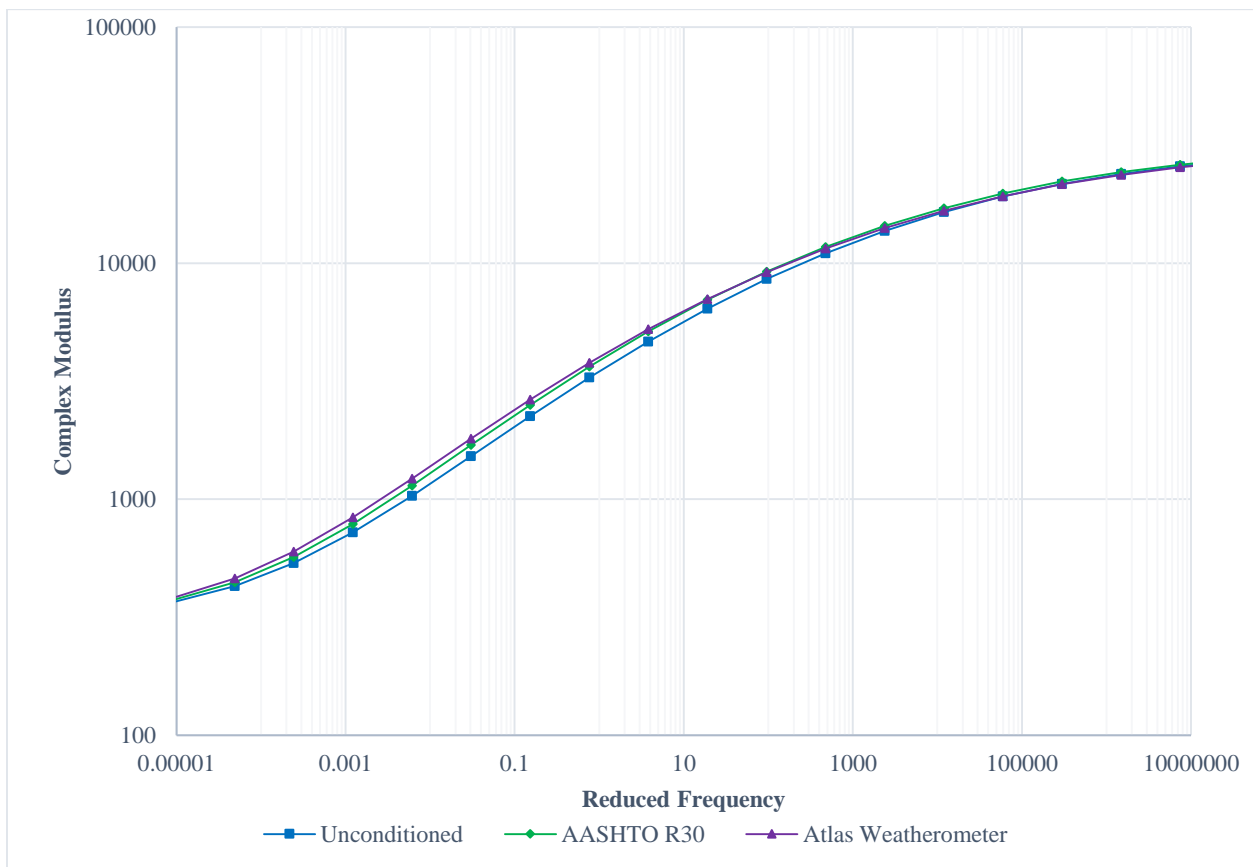


Figure 4-28 Comparison of Complex Modulus Mastercurves for Asphalt Mixtures

Asphalt mixtures exhibit a higher elastic behavior ($\delta \rightarrow 0$) at extreme loading conditions viz. low frequencies/high temperatures and high frequencies/low temperature. At low frequencies or high temperatures, this behavior is attributed to the elastic aggregate interlock structure and at high frequencies or low temperatures, this behavior is strongly influenced by the elastic behavior of asphalt binder.

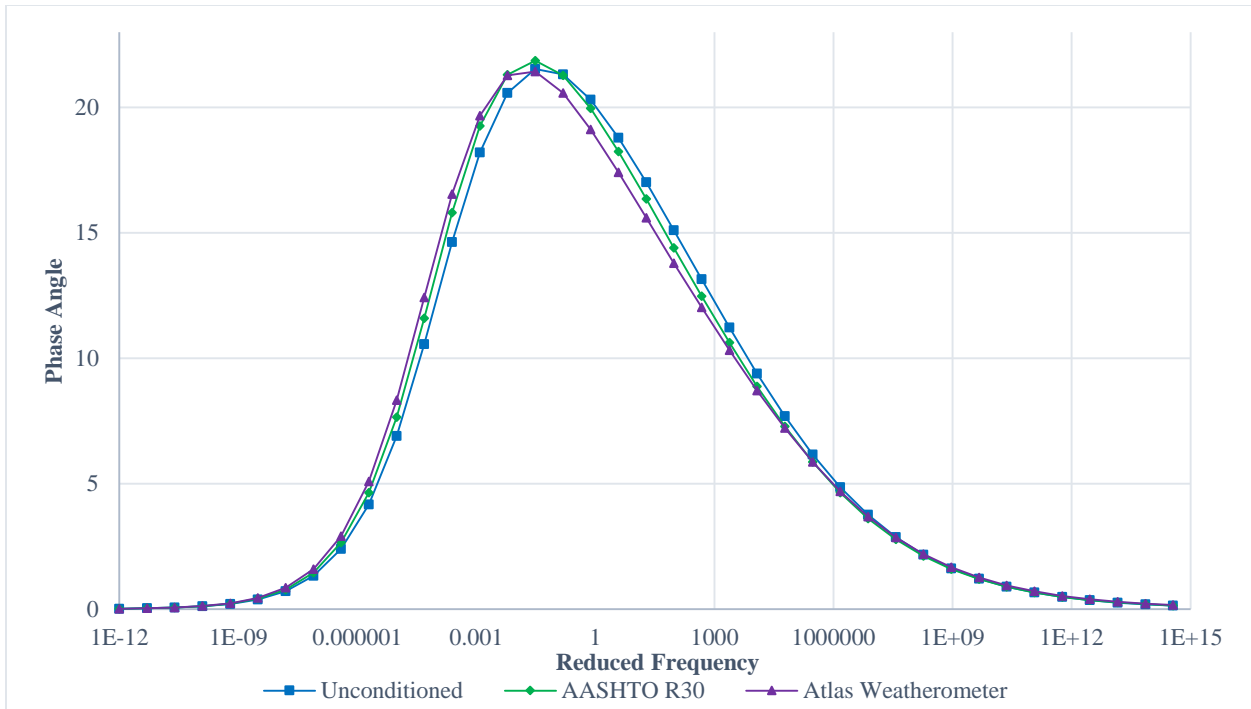


Figure 4-29 Comparison of Phase Angle Mastercurves for Asphalt Mixtures

A gradual increase in modulus values along with an associated decrease in phase angle values is noted with increasing level of asphalt binder aging, with Atlas Weatherometer aged mixtures presenting the highest modulus values followed by AASHTO R30 and Unconditioned mixture samples. This can be described as an increase in stiffness along with a greater proportion of elastic behavior with respect to aging.

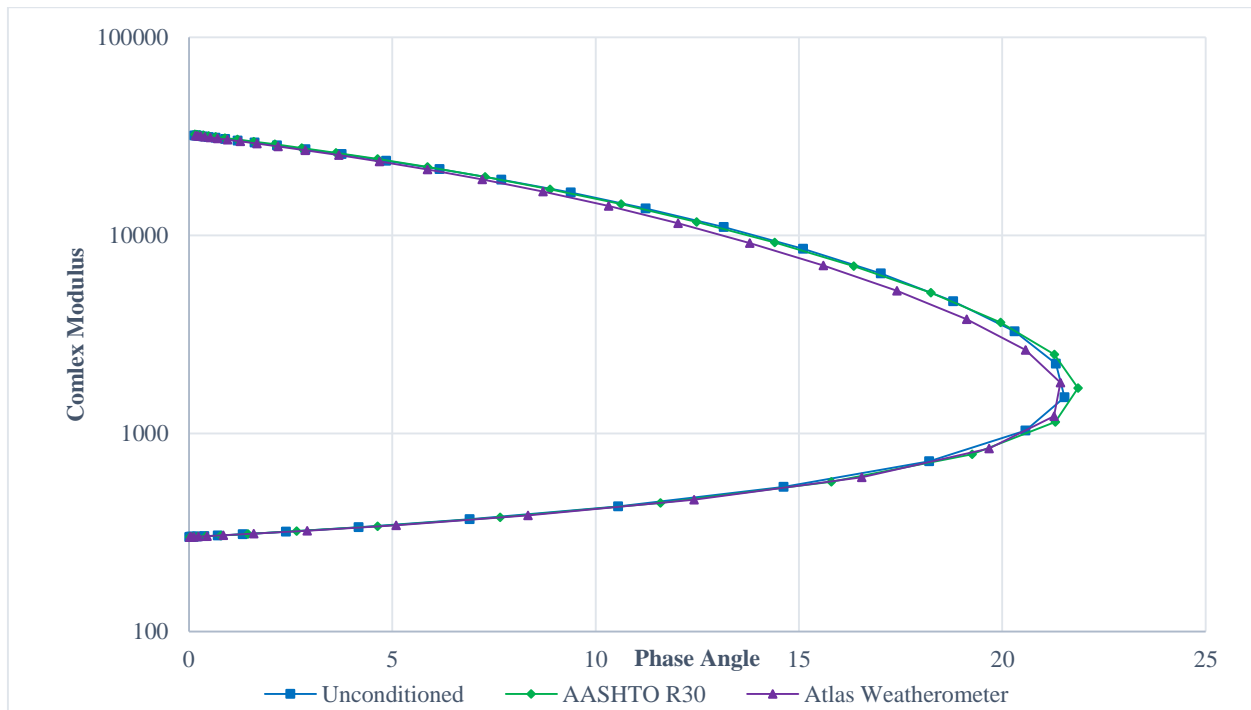


Figure 4-30 Comparison of Black Space Diagrams for Asphalt Mixtures

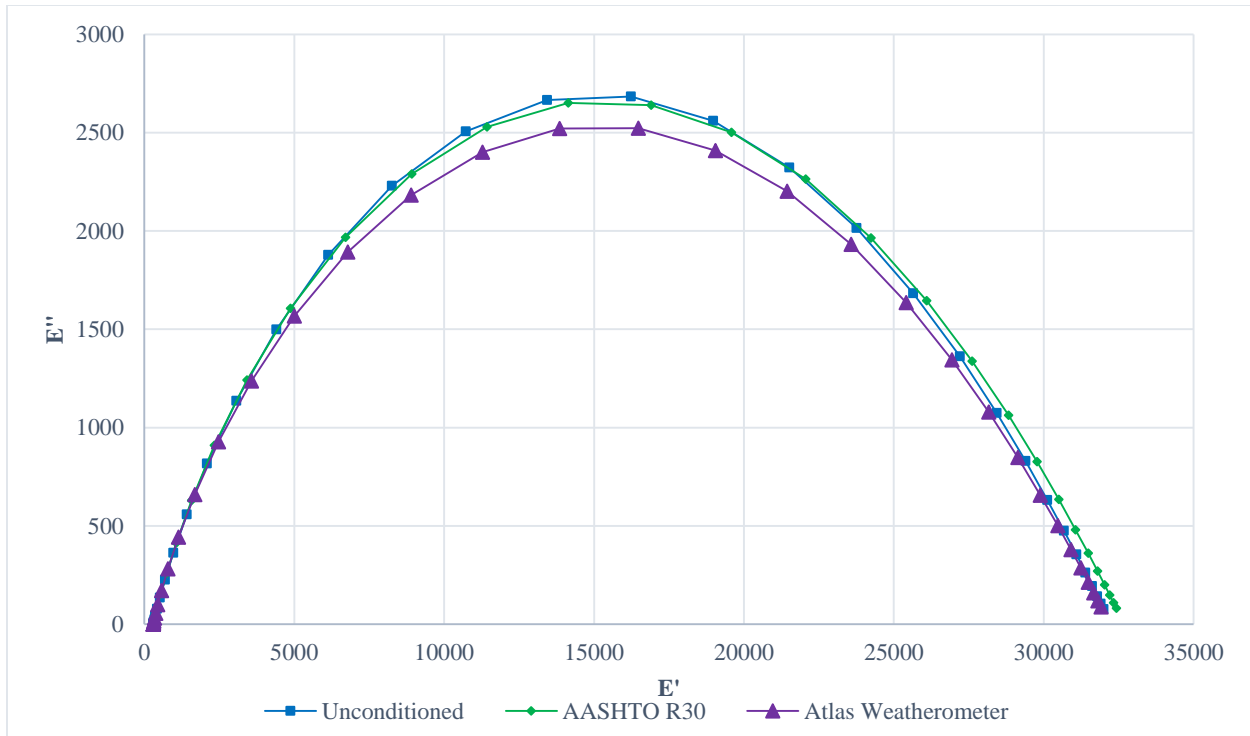


Figure 4-31 Comparison of Cole-Cole Diagrams for Asphalt Mixtures

The Black Space and Cole-Cole diagrams also show similar behavior, with Atlas Weatherometer conditioned mixtures showing lower maximum values for viscous modulus (E'') and phase angle (δ), hence indicating a comparatively smaller viscous tendency. Comparison of Shift Factor versus Temperature plot indicates slightly contrary behavior of AASHTO R30 conditioned mixes, which required a higher amount of shifting of rheological data at high temperatures.

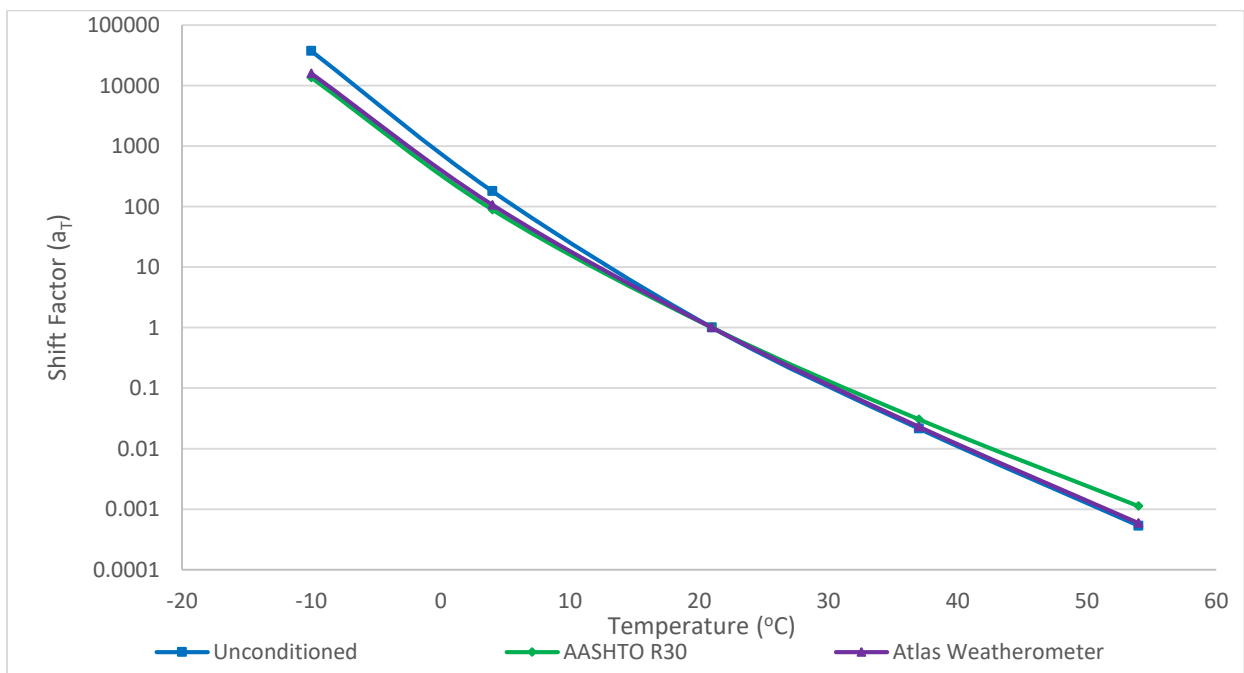


Figure 4-32 Shift Factor VS Temperature for Asphalt Mixtures

4.2.2 Performance Analysis

Semicircular Bend Geometry (SCB) test was carried out in accordance with AASHTO TP 124-16, for Unconditioned (4No. samples), AASHTO R30 conditioned (6No. samples), and Atlas Weatherometer conditioned samples (6No. samples). Since this test is carried out on notched samples, the accuracy of test results and subsequently calculated parameters (Fracture Energy and Flexibility Index) is highly dependent on the accuracy of sample and notch dimensions. For this reason, 3No. samples each with lowest variability in dimensions were selected for reporting.

Table 4-4 SCB Test Results for Unconditioned Samples

Specimen ID:	Fracture Energy (J/m²):	Strength (psi):	Slope:	Flexibility Index:	Max Load (kN):
Unconditioned#2	989.31	31.12	1.31	7.55	1.64
Unconditioned#3	965.46	31.56	1.32	7.31	1.73
Unconditioned#4	1236.29	33.11	1.14	10.84	1.76
Average	1063.69	31.93	1.26	8.57	1.71
<i>St Dev</i>	<i>149.95</i>	<i>1.05</i>	<i>0.10</i>	<i>1.97</i>	<i>0.07</i>
CV	14.10	3.27	8.05	23.02	3.85

Table 4-5 SCB Test Results for AASHTO R30 Conditioned Samples

Specimen ID:	Fracture Energy (J/m²):	Strength (psi):	Slope:	Flexibility Index:	Max Load (kN):
AASHTO R30#1	1085.19	40.68	1.75	6.20	2.13
AASHTO R30#4	1211.69	42.30	1.88	6.45	2.26
AASHTO R30#5	1097.91	37.69	1.67	6.57	1.98
Average	1131.60	40.22	1.77	6.41	2.12
<i>St Dev</i>	<i>69.65</i>	<i>2.34</i>	<i>0.11</i>	<i>0.19</i>	<i>0.14</i>
CV	6.16	5.81	6.00	2.95	6.58

Table 4-6 SCB Test Results for Atlas Weatherometer Conditioned Samples

Specimen ID:	Fracture Energy (J/m²):	Strength (psi):	Slope:	Flexibility Index:	Max Load (kN):
Atlas Weatherometer#4	1215.13	47.57	2.38	5.11	2.58
Atlas Weatherometer#5	1097.95	43.49	2.14	5.13	2.28
Atlas Weatherometer#6	1092.43	42.63	2.01	5.43	2.26
Average	1135.17	44.56	2.18	5.22	2.37
<i>St Dev</i>	<i>69.30</i>	<i>2.64</i>	<i>0.19</i>	<i>0.18</i>	<i>0.18</i>
CV	6.11	5.92	8.62	3.43	7.58

The calculated parameters are tabulated in Table 4-4, Table 4-5, and Table 4-6 for Unconditioned, AASHTO R30 conditioned, and Atlas Weatherometer conditioned samples respectively. The coefficient of variation (CV) for each of these conditioning procedures was also calculated and has been added to the tables.

As identified in these data tables, age hardening of asphalt mixtures lead to a gradual increase in Fracture Energy, indicating a stiffer response, along with a subsequent reduction in Flexibility Index, indicating brittle behavior which in turn can be related to a higher susceptibility to premature cracking.

Load versus Displacement curves for each type of conditioning procedure were prepared to better understand the effect of aging. A progressive increase in peak load is noted with increasing levels of age hardening indicating stiffer response, however by analyzing the post peak curve we can see that there is a subsequent increase in slope as well, indicating a higher rate of crack propagation and loss of ductility (Figure 4-33).

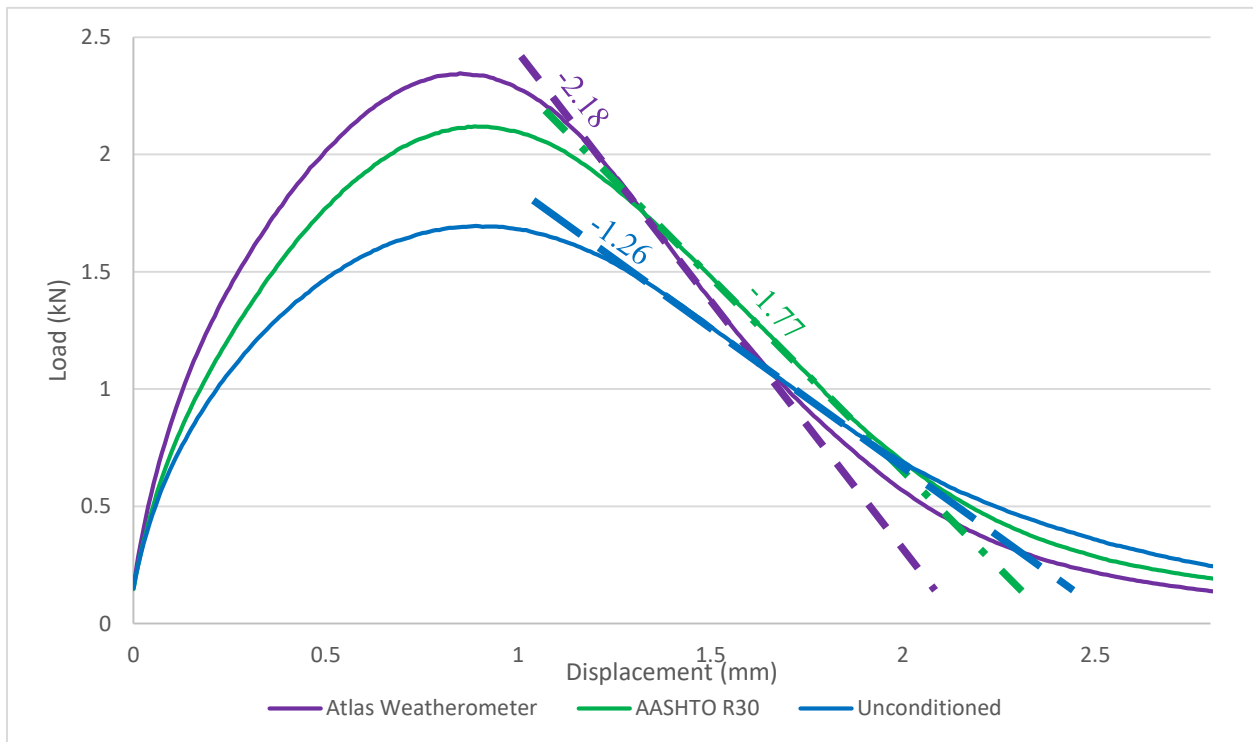


Figure 4-33 Load VS Displacement Curves for SCB Testing

The trend obtained is similar to rheological analysis, with Atlas Weatherometer conditioned mixtures showing highest stiffness and brittle behavior followed by AASHTO R30 conditioned mixtures and finally unconditioned mixtures.

CHAPTER 5 CONCLUSIONS, RECOMMENDATIONS, AND FUTURE RESEARCH

5.1 Conclusions

This research project was directed towards the optimization of a laboratory procedure for long-term oxidative aging of asphalt mix specimens. Based on literature review, it was found that the current widely used laboratory procedures rely solely on conditioning at extended temperatures and/or pressure to accelerate the aging process, while mostly neglecting environmental degradation factors such as solar radiation, humidity and rainwater. Such a large deviation from actual in-service pavement environment could have an effect on asphalt binder molecular association leading to a variation in the concentration of oxidation products formed, and hence in turn leading to entirely different aging kinetics and rheological properties.

It was hypothesized that a better representation of real in-service pavement aging could be achieved by using a balanced compromise between the various factors involved (UV, water, and temperature). To this end, asphalt binder and mixture samples were conditioned using different accelerated aging procedures and subsequently tested to identify any differences in rheological, chemical and mechanical behavior. General trends and conclusions drawn from comparative analysis are listed below:

- High levels of polymer modification could lead to an interference in test results as the polymer network is never really activated at very low strain levels, and there is a subsequent partial breakdown of time temperature superposition (TTS) principle. It was noted that this interference disappeared with age hardening, which can be attributed to the thermo-oxidative degradation of the polymer.
 - This was noted in virgin binder (64-28P-EX), and virgin binder subjected to extraction and recovery procedure by comparing Black Space curves (Figure 4-5), which provide a convenient means for identifying any inconsistencies in rheological data.
 - Similar effects of polymer modification were also noted for MSCR test results, where J_{nr_diff} (percentage difference of non-recoverable creep compliance for load levels of 0.1 & 3.2kPa) was considerably higher for virgin and extracted virgin asphalt binder samples (Table 4-1).
 - With regards to asphalt mixtures, polymer modification effect was noted as an increase in CV (Table 4-4) for Unconditioned mixtures in comparison to AASHTO R30 and Atlas Weatherometer conditioned mixtures.
- The effect of oxidative aging for both asphalt binders and asphalt mixtures is characterized by a constant increase in modulus values ($|G^*|$ and $|E^*|$), and a decrease in phase angle values (δ). In terms of rheological behavior, this can be described as an increase in stiffness along with a greater proportion of elastic behavior.
 - For asphalt binders, the increase in stiffness and viscosity was noted in Complex Modulus mastercurves (Figure 4-6), and Temperature Sensitivity curves (Figure 4-17 and Figure 4-18) respectively. The subsequent increase in proportion of elastic

behavior was noted in Phase Angle mastercurves (Figure 4-7), and Black Space curves (Figure 4-16).

- For asphalt mixtures, the increase in stiffness was noted in Complex modulus mastercurves (Figure 4-28), and the subsequent reduction in viscous behavior was noted in Phase Angle mastercurves (Figure 4-29), Black Space diagram (Figure 4-30), and Cole-Cole diagram (Figure 4-31).
- With aging, the increase in stiffness and greater proportion of elastic behavior would lead to an increase in resistance against rutting, but would also lead to a reduction in pavement durability associated with brittleness and reduced resistance against fatigue.
 - For asphalt binders, increasing levels of oxidative aging lead to an increase in resistance against rutting along with an associated decrease in fatigue life as noted in MSCR test results (Table 4-1 and Figure 4-19) and LAS test results (Table 4-2 and Figure 4-21) respectively.
 - For asphalt mixtures, SCB test results indicated a similar behavior with increase in brittleness and higher rate of crack propagation noted for aged samples (Figure 4-33).
- Water conditioning is considered to have an accelerating effect on the photo-oxidation of asphalt mixtures. This is because the water soluble chemical products of photo-oxidation are washed away, hence exposing further layers to oxidation.
 - This effect was noted for BC10, BC15, and BC20 samples (Figure 4-14 and Figure 4-15).
 - However, a contradictory effect (reduction in $|G^*|$ and increase in δ) was noted for BC5 samples (Figure 4-12 and Figure 4-13). This can be attributed to the thermal shock effect as conditioning water at room temperature was used.
- High conditioning temperatures could lead to a lower rate of sulfoxide formation in comparison to ketones (carbonyl group), given their thermal instability, and dissociation of carbon-containing aromatic molecules which are otherwise locked up into molecular agglomerates at lower temperatures.
 - FT-IR results showed a subsequent increase in Sulfoxide to Carbonyl ratio with decreasing conditioning temperatures (Figure 4-27).
- The aforementioned effect of high conditioning temperatures on chemical composition of asphalt binder could in turn have an effect on its rheological characteristics.
 - For asphalt binders, this effect was noted for binder samples extracted and recovered from AASHTO R30 aged mixtures, which showed similar rheological parameters $|G^*|$ and δ (Figure 4-10 and Figure 4-11), however contrary trends were noted in Black Space diagram (Figure 4-16) and Temperature Sensitivity diagram (Figure 4-17).
 - For asphalt mixtures, this behavior was again noted in Temperature Sensitivity diagram for AASHTO R30 conditioned mixtures, which required a higher amount of shifting of rheological data (for construction of mastercurves) at high temperatures (Figure 4-32).

5.2 Recommendations

Based on the conclusions drawn from this study, the following factors should be considered towards the optimization of an accelerated long-term age hardening laboratory procedure for asphalt mixtures:

- The procedure should be carried out on compacted asphalt mixture samples in order to avoid any issues related to compactability and the quality of cohesion and adhesion, for subsequent performance testing.
- Along with temperature, environmental degradation factors such as solar radiation (in particular UV) and rainfall must be considered in the design.
- The procedure should be tailored for each project by limiting temperature conditioning, which should be based on high temperature performance grading of the constituent asphalt binder.
- For effective photo-oxidation to occur, cycles of water spray or rainfall along with drying under irradiation should be considered.

Considering the aforementioned points would allow for production of laboratory aged samples which provide a better representation of real in-service aging of asphalt pavements. Performance and rheological test data from these samples could then be used by engineers to understand the changes in these properties over the pavement service life, hence providing them with better design tools.

From comparison of rheological and performance test data collected in this research project, it is considered that both Atlas Weatherometer and Bespoke Chamber conditioning procedures (with water), were able to reproduce desirable levels of natural age hardening in compacted asphalt mixture samples while satisfying all of the requirements for an ideal conditioning procedure. A better level of acceleration was however achieved with Bespoke Chamber conditioning with 15 and 20 days aged samples exhibiting a higher level of aging in comparison to samples aged for 41.6 days (1000hrs) in Atlas Weatherometer. It is considered that BC10-H₂O conditioning procedure provides the best compromise among all others, and should be selected for future research efforts.

5.3 Future Research Opportunities

Based on the work presented in this thesis, the following can be considered as possible areas for beneficial future research:

- The MTO project from where asphalt binder and loose mixture was collected, was carefully selected to allow for possible collection of field cores at a later date. Rheological, chemical and performance tests on these field cores could be used for calibration of laboratory aging procedure and to obtain the level of acceleration achieved.
- Consideration should be given to use of Environmental Scanning Electron Microscope (ESEM) for morphological analysis of asphalt binder. The images thus produced could be used to understand the effect of oxidative aging on binder microstructure and to possibly

identify any changes due to the use of excessively high temperatures in conditioning procedures. These images would also provide for a means to identify polymer modification and track its thermo-oxidative degradation with aging.

- Complex modulus tests on asphalt mixture samples aged using Bespoke Chamber conditioning procedure should be carried out to further understand changes in rheological parameters with aging.
- The effect of aging on low temperature performance of both asphalt binders and mixtures should be evaluated via bending beam rheometry and Thermal Stress Restrained Specimen Test (TSRST) respectively.
- High Performance Gel Permeation Chromatography (HP-GPC) could be used as a tool to identify changes in molecular size structure of asphalt binder with oxidative aging. The chromatograms thus obtained could also be used to evaluate the effects of high temperatures and pressures on asphalt binder composition.

REFERENCES

- [1] G. of C. T. C. P. Group, "Road Transportation," 10-Jul-2012. [Online]. Available: <https://www.tc.gc.ca/eng/policy/anre-menu-3021.htm>. [Accessed: 10-Apr-2018].
- [2] P. Kandhal and S. Chakraborty, "Effect of Asphalt Film Thickness on Short- and Long-Term Aging of Asphalt Paving Mixtures," *Transportation Research Record: Journal of the Transportation Research Board*, no. 1535, pp. 83–90, 1996.
- [3] J. Read and D. Whiteoak, *The Shell Bitumen Handbook*, Fifth Edition. Thomas Telford, 2003.
- [4] J. Murali Krishnan and K. Rajagopal, "Review of the uses and modeling of bitumen from ancient to modern times," *Appl. Mech. Rev.*, vol. 56, no. 2, pp. 149–214, Mar. 2003.
- [5] Asphalt Institute and European Bitumen Association, *The bitumen industry: a global perspective: production, chemistry use, specification and occupational exposure.*, Third Edition. 2015.
- [6] F. L. Roberts, P. S. Kandhal, E. R. Brown, D. Y. Lee, and T. W. Kennedy, *Hot Mix Asphalt Materials, Mixture Design, and Construction*. National Asphalt Pavement Association Education Foundation. Lanham, MD, 1996.
- [7] A. S. Argon, "Linear viscoelasticity of polymers," *The Physics of Deformation and Fracture of Polymers*, Mar-2013. [Online]. Available: [/core/books/physics-of-deformation-and-fracture-of-polymers/linear-viscoelasticity-of-polymers/E211A38328363E6390D8F63149607B0E](#). [Accessed: 11-Jul-2018].
- [8] T. G. Mezger, *Applied Rheology*, Second Edition. Austria: Anton Paar GmbH, 2015.
- [9] G. Airey, B. Rahimzadeh, and A. Collop, "Linear viscoelastic limits of bituminous binders," *Journal of the Association of Asphalt Paving Technologists*, p. 27.
- [10] G. D. Airey, "Use of Black Diagrams to Identify Inconsistencies in Rheological Data," *Road Materials and Pavement Design*, vol. 3, no. 4, pp. 403–424, Jan. 2002.
- [11] F. Olard and H. Di Benedetto, "General '2S2P1D' Model and Relation Between the Linear Viscoelastic Behaviours of Bituminous Binders and Mixes," *Road Materials and Pavement Design*, vol. 4, no. 2, pp. 185–224, Jan. 2003.
- [12] L. W. Corbett, "Composition of asphalt based on generic fractionation, using solvent deasphalting, elution-adsorption chromatography, and densimetric characterization," *Analytical Chemistry*, vol. 41, no. 4, pp. 576–579, Apr. 1969.
- [13] A. M. Usmani, Ed., *Asphalt Science and Technology*. Marcel Dekker Inc., 1997.
- [14] T. Mill, D. S. Tse, B. Loo, C. C. D. Yao, and E. Canavesi, "Oxidation Pathways for Asphalt," *ASC Division of Fuel Chemistry*, vol. 37, pp. 1367–1375, 1992.
- [15] J. C. Petersen, P. M. Harnsberger, and R. E. Robertson, "Factors Affecting the Kinetics and Mechanisms of Asphalt Oxidation and the Relative Effects of Oxidation Products on Age Hardening," *Preprints of Papers, American Chemical Society, Division of Fuel Chemistry*, vol. 41, no. 4, Dec. 1996.
- [16] P. W. Jennings and J. A. S. Pribanic, *The Expanded Montana asphalt quality study using high pressure liquid chromatography*. Bozeman, Montana : Montana State University, Dept. of Chemistry, 1985.
- [17] S.-J. Lee, S. N. Amirkhani, K. Shatanawi, and K. W. Kim, "Short-Term Aging Characterization of Asphalt Binders Using Gel Permeation Chromatography and Selected Superpave Binder Tests," *Construction and Building Materials*, vol. 22, no. 11, pp. 2220–2227, Nov. 2008.

- [18] “Infrared Spectroscopy,” *Chemistry LibreTexts*, 02-Oct-2013. [Online]. Available: [https://chem.libretexts.org/Textbook_Maps/Physical_and_Theoretical_Chemistry_Textbook_Maps/Supplemental_Modules_\(Physical_and_Theoretical_Chemistry\)/Spectroscopy/Vibrational_Spectroscopy/Infrared_Spectroscopy](https://chem.libretexts.org/Textbook_Maps/Physical_and_Theoretical_Chemistry_Textbook_Maps/Supplemental_Modules_(Physical_and_Theoretical_Chemistry)/Spectroscopy/Vibrational_Spectroscopy/Infrared_Spectroscopy). [Accessed: 18-Jul-2018].
- [19] M. Kane, D. Zhao, E. Chailleux, F. Delarrard, and M. Do, “Development of an accelerated pavement test reproducing the effect of natural ageing on skid resistance,” *Road Materials and Pavement Design*, vol. 14, no. 1, pp. 126–140, Mar. 2013.
- [20] P. Kandhal and S. Chakraborty, “Effect of Asphalt Film Thickness on Short- and Long-Term Aging of Asphalt Paving Mixtures,” *Transportation Research Record: Journal of the Transportation Research Board*, no. 1535, pp. 83–90, 1996.
- [21] J. C. Petersen, J. F. Branthaver, R. E. Robertson, P. M. Harnsberger, J. J. Duvall, and E. K. Ensley, “Effects of Physicochemical Factors on Asphalt Oxidation Kinetics,” *Transportation Research Record 1391*, p. 10.
- [22] J. G. Beckett, P. H. Bingham, C. J. Burbank, J. M. Crites, and L. Depue, “Transportation Research Board 2009–2010 Technical Activities Council,” p. 78.
- [23] Strategic Highway Research Program (U.S.), *Binder characterization and evaluation. Volume 2*. Washington, D.C.: Strategic Highway Research Program, National Research Council, 1993.
- [24] T. Bennert, C. Ericson, D. Pezeshki, E. Haas, R. Shamborovskyy, and R. Corun, “Laboratory Performance of Re-Refined Engine Oil Bottoms (REOB) Modified Asphalt,” in *Journal of the Association of Asphalt Paving Technologists*, 2016.
- [25] J. O’Connell and W. Steyn, “An Overview of the Ageing of Bituminous Binders,” *36th Southern African Transport Conference (SATC 2017)*, pp. 308–324.
- [26] American Association of State and Highway Transportation Officials (AASHTO), “T 315-12 Standard Method of Test for Determining the Rheological Properties of Asphalt Binder Using a Dynamic Shear Rheometer (DSR).” Aug-2016.
- [27] American Association of State and Highway Transportation Officials (AASHTO), “R 28-12 Standard Practice for Accelerated Aging of Asphalt Binder Using a Pressurized Aging Vessel (PAV).” Aug-2016.
- [28] D. Steiner *et al.*, “Towards an optimised lab procedure for long-term oxidative ageing of asphalt mix specimen,” *International Journal of Pavement Engineering*, vol. 17, no. 6, pp. 471–477, Jul. 2016.
- [29] G. D. Airey, “State of the Art Report on Ageing Test Methods for Bituminous Pavement Materials,” *International Journal of Pavement Engineering*, vol. 4, no. 3, pp. 165–176, Sep. 2003.
- [30] American Association of State and Highway Transportation Officials (AASHTO), “R30-02 Standard Practice for Mixture Conditioning of Hot Mix Asphalt (HMA).” 2015.
- [31] C. A. Bell and D. Sosnovske, *Aging: Binder Validation*. Washington, D.C.: Strategic Highway Research Program, National Research Council, 1994.
- [32] “ATLAS | Weathering Testing Solutions.” [Online]. Available: <https://www.atlas-mts.com/>. [Accessed: 29-Jul-2018].
- [33] “SUNTEST XXL+ Weathering Instruments | Atlas.” [Online]. Available: <https://www.atlas-mts.com/products/standard-instruments/xenon-weathering/suntest/xxl>. [Accessed: 29-Jul-2018].
- [34] K. Grzybowski, G. M. Rowe, and S. Prince, “Development of an Accelerated Weathering and Reflective Crack Propagation Test Methodology,” in *7th RILEM International Conference*

- on Cracking in Pavements*, A. Scarpas, N. Kringos, I. Al-Qadi, and L. A., Eds. Dordrecht: Springer Netherlands, 2012, pp. 125–135.
- [35] K. Grzybowski, “Accelerated Pavement Weathering System,” *2013 Petersen Asphalt Research Conference and P3Symposium July 18, 2013, Laramie, Wyoming*.
- [36] P. Teymourpour and H. Bahia, “Linear Amplitude Sweep Test: Binder Grading Specification and Field Evaluation,” *Modified Asphalt Research Center, University of Wisconsin*, p. 36, Sep. 2014.
- [37] American Association of State and Highway Transportation Officials (AASHTO), “TP101-14 Estimating Damage Tolerance of Asphalt Binders Using the Linear Amplitude Sweep.” Washington, D.C.
- [38] Federal Highway Administration, U.S. Department of Transportation, “The Multiple Stress Creep Recovery (MSCR) Procedure.” Apr-2011.
- [39] American Association of State and Highway Transportation Officials (AASHTO), “T342-11 Standard Method of Test for Determining Dynamic Modulus of Hot Mix Asphalt (HMA).” 2015.
- [40] American Association of State and Highway Transportation Officials (AASHTO), “TP 124-16 Standard Method of Test for Determining the Fracture Potential of Asphalt Mixtures Using Semicircular Bend Geometry (SCB) at Intermediate Temperature.” Aug-2016.
- [41] H. Bahia, “Linear Amplitude Sweep Analysis Template (AASHTO TP-101-12-Modified) Version 1.52.” Modified Asphalt Research Center, University of Wisconsin, 04-Apr-2013.

APPENDIX A: MIX DESIGN SHEETS

SUPERPAVE MIX DESIGN REPORT

PRODUCT NO.:	2017-17141E-SP 12.5FC2-CA#E-PG 64-28P-EX	HOT MIX TYPE / USE:	SP 12.5FC2	ITEM NO.:	
PROJECT:	Various		LOCATION:	Various	
TESTING LAB.:	Engtec Consulting Inc.		PROJECT NO.:	ET17-1019C	
LAB MIX NO.:	17141E		DATE SAMPLES RECD.:	July 1, 2017	
MIX SUPPLIER:	Cambridge Asphalt Supply		PLANT LOCATION:	Cambridge	
TEST DATA CERTIFIED BY:			DATE COMPLETED:	July 20, 2017	
ANDREW PAHALAN, C.Tech.					

JOB MIX FORMULA --- GRADATION PERCENT PASSING

% A.C / Sieve Sizes (mm)	% A.C	50.0	37.5	25.0	19.0	12.5	9.5	4.75	2.36	1.18	0.600	0.300	0.150	0.075
Job Mix Formula (JMF)	5.0				100.0	95.9	82.2	54.8	41.2	32.0	23.4	13.7	6.2	3.0

Superpave Volumetrics		REQUIRED	SELECTED	% CA #1	43.5	% RAP	--	
N_{des} (% Gmm)		96.0	96.0	% CA #2	--	%A.C RAP	--	
N_{tol} (% Gmm)		<=89	88.3	% CA #3	--	G_{mb}	2.479	
N_{max} (% Gmm)		<=98	97.4	% FA #1	46.5			
Air Voids (%) @ N_{des}		4.0	4.0	% FA #2	10.0	G_{mm}	2.583	
VMA (%)		14.0	14.8	% FA #3	--			
VFA (%)	Minimum	65.0	73.1	Composite G_{ab}				2.765
	Maximum	75.0		ASPHALT CEMENT				
Dust Proportion	Minimum	0.6	0.68	SUPPLIER				AC GRADE
	Maximum	1.2		McAsphalt				PG 64-28P-EX
Tensile Strength Ratio, %		80% Minimum	86.0	ADDITIVE				
Asphalt Film Thickness		--	10.1	SUPPLIER		TYPE		AS % OF AC
Traffic Category		E	E	--		--		--

AGGREGATE TYPE	AGGREGATE SOURCE / INVENTORY NUMBER	AGGREGATE TYPE	AGGREGATE SOURCE / INVENTORY NUMBER
CA No. 1	HL1 Stone - Fowler Rosewame B17-013-02	FA No. 2	Unwashed Sand - Fowler Rosewame B17-013-02
CA No. 2	--	FA No. 3	--
CA No. 3	--	RAP	--
FA No. 1	Washed Sand - Fowler Rosewame B17-013-02		

AGG.	Blended G_{ab} and Absorption	AGGREGATE GRADATION (Sieve Sizes in mm) --- PERCENT PASSING													
		50.0	37.5	25.0	19.0	12.5	9.5	4.75	2.36	1.18	0.600	0.300	0.150	0.075	
CA #1	$G_{sb} = 2.765$				100.0	90.5	58.8	7.4	2.5	1.5	1.3	1.2	1.0	0.9	
CA #2	$G_{sa} = 2.821$														
CA #3	Abs (%) = 0.715														
FA #1	$G_{sb} = 2.765$							100.0	89.3	67.6	51.8	36.5	19.3	6.3	1.5
FA #2	$G_{sa} = 2.821$							100.0	97.5	82.1	67.9	52.8	35.1	21.3	12.1
FA #3	Abs (%) = 0.718														
RAP	CA - G_{ab} , Abs = 2.667, 1.10% FA - G_{ab} , Abs = 2.693, 1.28%														

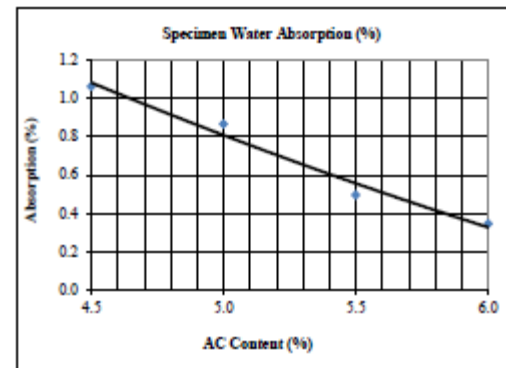
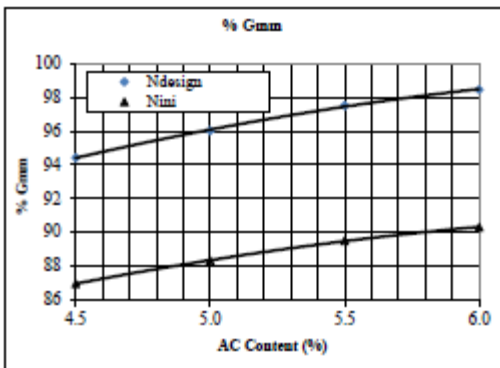
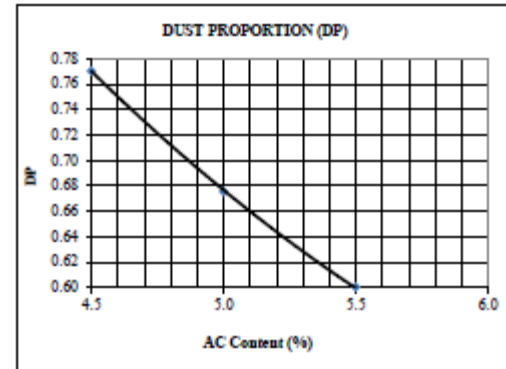
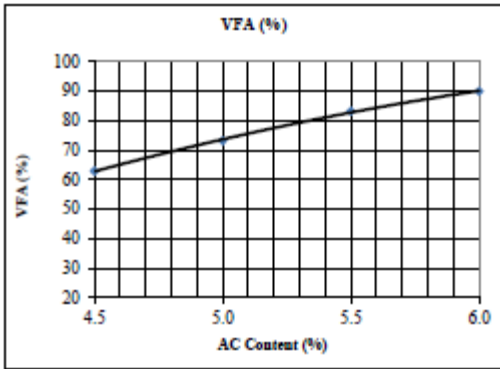
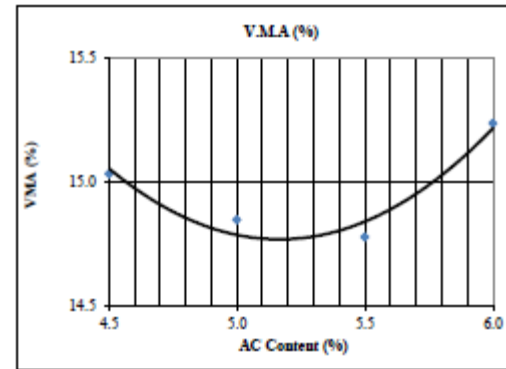
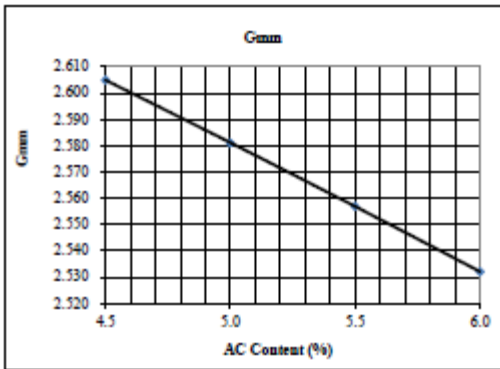
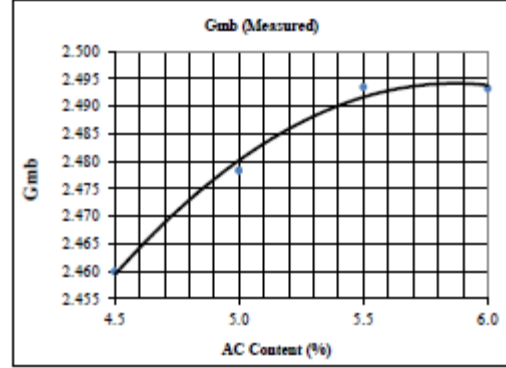
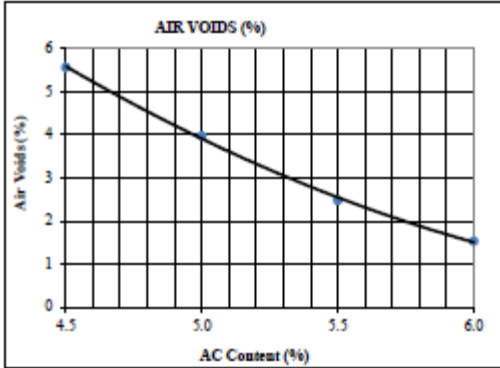
FINES RETURNED TO MIX: 0.75%

REMARKS:	1	Compaction Temperature = Recompaction Temperature = 138°C, Mixing Temperature = 161°C.	Consensus Properties
	2	Determination of aggregate densities as per L8 804/805 Rev. 28.	
	3	Weight required for 115 +/- 6mm Height of 3GC Specimen = 4882g.	
	4	The absorption of water at design point <0.83%; hence, no sealing of specimens is required.	
	5	Premium Aggregates are Pre-Limed (Hydrated Lime - 1% by Aggregate Mass)	
6	Virgin PGAC added to the Mix = 5.0%	% Crushed CA (1F/2F)	100/100
		% Flat and Elongated	1.8
		FA Angularity	48.9
		Sand Equivalent	91.3

REVIEWED BY: DATE: July 20, 2017

MIX PROPERTY CURVES

Project No.: ET17-1019C	Date: July 20, 2017
Supplier: Cambridge Asphalt Supply	Contract No.: Various
Mix No.: 17141E	Mix Type: SP 12.5FC2 Cat E



MIX VOLUMETRICS

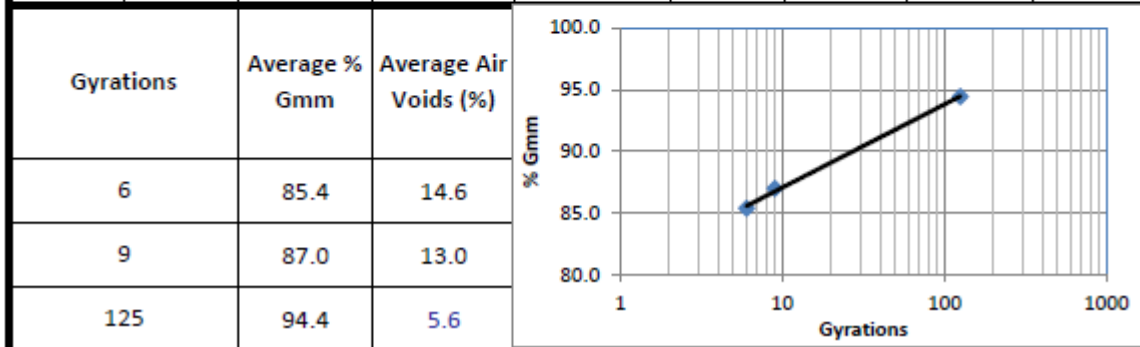
Property		1	2	3	4	Design
Percent PGAC	Pb	4.5	5.0	5.5	6.0	5.0
Blend Bulk Specific Gravity	Gb	2.765	2.765	2.765	2.765	2.765
% Gmm @ Nini	Nini	87.0	88.3	89.5	90.3	88.3
% Gmm @ Ndes	Ndes	94.4	96.0	97.5	98.5	96.0
Air Voids (%)	%	5.6	4.0	2.5	1.5	4.0
Water Absorption (%)	%	1.07	0.87	0.50	0.35	0.83
Voids in Mineral Aggregate	VMA	15.0	14.8	14.8	15.2	14.8
Voids Filled With Asphalt	VFA	63.0	73.2	83.2	90.0	73.1
Effective Specific Gravity	Gse	2.808	2.804	2.800	2.793	2.805
Maximum Specific Gravity	Gmm	2.605	2.581	2.557	2.532	2.583
Bulk Specific Gravity	Gmb	2.460	2.478	2.494	2.493	2.479
Dust Ratio	DP	0.77	0.68	0.60	0.54	0.68
Effective Asphalt Cement	Pbe	3.93	4.48	5.04	5.62	4.44
Percent Aggregates	Ps	0.955	0.950	0.945	0.940	0.950

Superpave BITUMINOUS LABORATORY WORKSHEET

PROJECT NO.:	ET17-1019C			DATE:	July 20, 2017		
SUPPLIER	Cambridge Asphalt Supply			MIX NO.	17141E		
% PASS PCS:	54.8	Gsb:	2.765	% AC:	4.5	SP 12.5FC2 Cat E	

PARAMETER	SPECIMEN 1	SPECIMEN 2
A1: MASS OF COMPACTED SPECIMEN IN AIR	4958.4	4968.9
A2: S.D.MASS IN AIR AFTER IMMERSION IN H ₂ O	4977.4	4992.9
B1: MASS OF COMPACTED SPECIMEN IN WATER	2960.3	2974.4
B2: VOLUME (= A2-B1)	2017.0	2018.5
C: BULK REL. DENSITY (= A1/B2), Gmb Measured	2.458	2.462
D: MAX. THEORITICAL DENSITY, Gmm	2.605	

Superpave GYRATORY DENSIFICATION DATA								
Mold Diameter, mm		150						
GYRATIONS	SPECIMEN 1				SPECIMEN 2			
	HEIGHT (mm)	Gmb - Estimated	Gmb - Corrected	% Gmm	HEIGHT (mm)	Gmb - Estimated	Gmb - Corrected	% Gmm
6	128.7	2.180	2.223	85.3	129.1	2.178	2.225	85.4
9	126.4	2.220	2.264	86.9	126.7	2.219	2.267	87.0
125	116.4	2.410	2.458	94.4	116.7	2.409	2.462	94.5



Superpave BITUMINOUS LABORATORY WORKSHEET

PROJECT NO.:	ET17-1019C			DATE:	July 20, 2017	
SUPPLIER	Cambridge Asphalt Supply			MIX NO.	17141E	
% PASS PCS:	54.8	Gsb:	2.765	% AC:	5.0	SP 12.5FC2 Cat E

PARAMETER	SPECIMEN 1	SPECIMEN 2
A1: MASS OF COMPACTED SPECIMEN IN AIR	4984.5	4995.0
A2: S.D.MASS IN AIR AFTER IMMERSION IN H ₂ O	5002.5	5012.0
B1: MASS OF COMPACTED SPECIMEN IN WATER	2989.4	2998.4
B2: VOLUME (= A2-B1)	2013.0	2013.6
C: BULK REL. DENSITY (= A1/B2), Gmb Measured	2.476	2.481
D: MAX. THEORITICAL DENSITY, Gmm	2.581	

Superpave GYRATORY DENSIFICATION DATA									
Mold Diameter, mm		150							
GYRATIONS	SPECIMEN 1				SPECIMEN 2				
	HEIGHT (mm)	Gmb - Estimated	Gmb - Corrected	% Gmm	HEIGHT (mm)	Gmb - Estimated	Gmb - Corrected	% Gmm	
6	126.8	2.224	2.236	86.6	127.3	2.220	2.241	86.8	
9	124.5	2.265	2.277	88.2	125.0	2.261	2.282	88.4	
125	114.5	2.463	2.476	95.9	115.0	2.458	2.481	96.1	
Gyrations	Average % Gmm	Average Air Voids (%)							
6	86.7	13.3							
9	88.3	11.7							
125	96.0	4.0							

Superpave BITUMINOUS LABORATORY WORKSHEET

PROJECT NO.:	ET17-1019C			DATE:	July 20, 2017		
SUPPLIER	Cambridge Asphalt Supply			MIX NO.	17141E		
% PASS PCS:	54.8	Gsb:	2.765	% AC:	5.5	SP 12.5FC2 Cat E	

PARAMETER	SPECIMEN 1	SPECIMEN 2
A1: MASS OF COMPACTED SPECIMEN IN AIR	5010.8	5021.4
A2: S.D.MASS IN AIR AFTER IMMERSION IN H ₂ O	5020.8	5031.4
B1: MASS OF COMPACTED SPECIMEN IN WATER	3009.4	3019.5
B2: VOLUME (= A2-B1)	2011.5	2011.9
C: BULK REL. DENSITY (= A1/B2), Gmb Measured	2.491	2.496
D: MAX. THEORITICAL DENSITY, Gmm	2.557	

Superpave GYRATORY DENSIFICATION DATA									
Mold Diameter, mm		150							
GYRATIONS	SPECIMEN 1				SPECIMEN 2				
	HEIGHT (mm)	Gmb - Estimated	Gmb - Corrected	% Gmm	HEIGHT (mm)	Gmb - Estimated	Gmb - Corrected	% Gmm	
6	125.1	2.266	2.246	87.8	125.5	2.264	2.249	88.0	
9	122.8	2.309	2.288	89.5	123.3	2.304	2.289	89.5	
125	112.8	2.513	2.491	97.4	113.1	2.512	2.496	97.6	
Gyrations	Average % Gmm	Average Air Voids (%)							
6	87.9	12.1							
9	89.5	10.5							
125	97.5	2.5							

Superpave BITUMINOUS LABORATORY WORKSHEET

PROJECT NO.:	ET17-1019C			DATE:	July 20, 2017		
SUPPLIER	Cambridge Asphalt Supply			MIX NO.	17141E		
% PASS PCS:	54.8	Gsb:	2.765	% AC:	6.0	SP 12.5FC2 Cat E	

PARAMETER	SPECIMEN 1	SPECIMEN 2
A1: MASS OF COMPACTED SPECIMEN IN AIR	5037.5	5048.0
A2: S.D.MASS IN AIR AFTER IMMERSION IN H ₂ O	5043.5	5056.0
B1: MASS OF COMPACTED SPECIMEN IN WATER	3024.0	3030.3
B2: VOLUME (= A2-B1)	2019.5	2025.7
C: BULK REL. DENSITY (= A1/B2), Gmb Measured	2.494	2.492
D: MAX. THEORITICAL DENSITY, Gmm	2.532	

Superpave GYRATORY DENSIFICATION DATA									
Mold Diameter, mm		150							
GYRATIONS	SPECIMEN 1				SPECIMEN 2				
	HEIGHT (mm)	Gmb - Estimated	Gmb - Corrected	% Gmm	HEIGHT (mm)	Gmb - Estimated	Gmb - Corrected	% Gmm	
6	123.5	2.308	2.246	88.7	124.1	2.302	2.241	88.5	
9	121.2	2.352	2.289	90.4	121.7	2.347	2.285	90.3	
125	111.2	2.563	2.494	98.5	111.6	2.559	2.492	98.4	
Gyrations	Average % Gmm	Average Air Voids (%)							
6	88.6	11.4							
9	90.3	9.7							
125	98.5	1.5							

Superpave BITUMINOUS LABORATORY WORKSHEET - Nmax

PROJECT NO.:	ET17-1019C			DATE:	July 20, 2017	
SUPPLIER	Cambridge Asphalt Supply			MIX NO.	17141E	
% PASS PCS:	54.8	Gsb:	2.765	% AC:	5.0	SP 12.5FC2 Cat E

PARAMETER	SPECIMEN 1	SPECIMEN 2
A1: MASS OF COMPACTED SPECIMEN IN AIR	4982.9	4993.5
A2: S.D.MASS IN AIR AFTER IMMERSION IN H ₂ O	4998.9	5010.5
B1: MASS OF COMPACTED SPECIMEN IN WATER	3016.0	3024.0
B2: VOLUME (= A2-B1)	1983.0	1986.5
C: BULK REL. DENSITY (= A1/B2), Gmb Measured	2.513	2.514
D: MAX. THEORITICAL DENSITY, Gmm	2.580	

Superpave GYRATORY DENSIFICATION DATA								
Mold Diameter, mm		150						
GYRATIONS	SPECIMEN 1				SPECIMEN 2			
	HEIGHT (mm)	Gmb - Estimated	Gmb - Corrected	% Gmm	HEIGHT (mm)	Gmb - Estimated	Gmb - Corrected	% Gmm
6	126.6	2.227	2.237	86.7	127.1	2.223	2.233	86.5
9	124.3	2.268	2.278	88.3	124.6	2.268	2.278	88.3
125	114.3	2.467	2.478	96.0	114.5	2.468	2.479	96.1
205	112.7	2.502	2.513	97.4	112.9	2.503	2.514	97.4
Gyrations	Average % Gmm	Average Air Voids (%)						
6	86.6	13.4						
9	88.3	11.7						
125	96.1	3.9						
205	97.4	2.6						

Moisture Sensitivity Data							
Product No	2017-17141E-SP 12.5FC2-CatE-PG 64-28P-EX						
Project No	ET17-1019C						
Date	July 20, 2017						
Sample		1	2	3	4	5	6
Diameter,mm	D	150	150	150	150	150	150
Thickness,mm	t	95.0	95.0	95.0	95.0	95.0	95.0
Dry mass,g	A	3956.1	3958.7	3959.4	3961.5	3958.2	3953.4
SSD mass, g	B	3973.0	3975.0	3975.0	3976.3	3974.7	3972.8
Mass in water,g	C	2321.3	2319.5	2324.0	2319.2	2322.5	2319.2
Volume, cc (B-C)	E	1651.7	1655.4	1651.0	1657.1	1652.2	1653.6
Bulk Sp Gravity (A/E)	F	2.395	2.391	2.398	2.391	2.396	2.391
Max Sp Gravity	G	2.583	2.583	2.583	2.583	2.583	2.583
% Air Voids (100(G-F)/G)	H	7.3	7.4	7.1	7.4	7.2	7.4
Vol Air Voids (HE/100)	I	119.9	122.6	117.9	123.2	119.5	122.8
Load,N	P	15454	15784	14924	17531	17588	18551
SSD mass, g	B ^l	4040.5327	4045.446	4045.3			
Vol Abs Water, cc (B ^l -A)	J ^l	84.434681	86.725235	85.892813			
% Saturation (100J ^l /I)		70.4	70.8	72.9			
Conditioned							
Thickness,mm	t ^{ll}	95.0	95.0	95.0	95.0	95.0	95.0
Dry Str. (2000P/(tDp))	Std				783.2	785.7	828.8
Wet Str. (2000P ^{ll} /(t ^{ll} Dp))	Stm	690.4	705.2	666.7			
Average Dry Strength (kPa)		799.2	Visual Moisture Damage (0 to 5 Rating)				1
Average Wet Strength (kPa)		687.4	Cracked/Broken Aggregates				< 5%
TSR,%		86.0					



**AGGREGATE TEST DATA - HOT MIX ASPHALT
Superpave - Consensus Properties (SSP110S12)**

Ministry of
Transportation

Contract No.: 2017-17141E-SP 12.5FC2-CatE-PG 6		Contractor: Cambridge Asphalt Supply		Contract Location: 2017-17141E-SP 12.5FC2-CatE-PG 64-28P-EX	
Testing Laboratory: Engtec Consulting Inc.			Telephone No.: (905) 793-9800		Fax No.: (905) 793-0641
Sampled By (Print Name): Cambridge Asphalt Supply			Date Sampled: (YY/MM/DD) 17-06-28		
Mix Type: SP 12.5FC2		Lot No.:		Quantity (tonnes):	

FINE AGGREGATE(S)						
Source Name & Location:	Washed Sand - Fowler Rosewame - Fowler Rosewam	Aggregate Inventory Number (AIN):	B17-013-02	Pit(P) or Quarry (Q):	-	% of Mtr: 46.5
Source Name & Location:	Unwashed Sand - Fowler Rosewame - Fowler Rosewam	Aggregate Inventory Number (AIN):	B17-013-02	Pit(P) or Quarry (Q):	-	% of Mtr: 10
Source Name & Location:	-----	Aggregate Inventory Number (AIN):	--	Pit(P) or Quarry (Q):	-	% of Mtr: --
Source Name & Location:	-----	Aggregate Inventory Number (AIN):	--	Pit(P) or Quarry (Q):	-	% of Mtr: --

Laboratory Test and Test Number	Requirement	Traffic Level Category					Test Result	
		A	B	C	D	E	Sample	Meets Requirement (Y/N)
		LS-629 Uncompacted Voids, % minimum	≤100 mm (Note 1)	--	40	45 (Note 3)		
	≥100 mm (Note 1)	--	40	40	40	45 (Note 3)	--	--
AAASHTO T176 Sand Equivalent Method 1, % minimum (Notes 2)		40	40	45	45	50	91.3	Y

COARSE AGGREGATE						
Source Name & Location:	HL1 Stone - Fowler Rosewame - Fowler Rosewam	Aggregate Inventory Number (AIN):	B17-013-02	Pit(P) or Quarry (Q):	Q	% of Mtr: 43.5
Source Name & Location:	-----	Aggregate Inventory Number (AIN):	B17-013-02	Pit(P) or Quarry (Q):	-	% of Mtr: --
Source Name & Location:	-----	Aggregate Inventory Number (AIN):	--	Pit(P) or Quarry (Q):	-	% of Mtr: --

Laboratory Test and Test Number	Requirement	Traffic Level Category					Test Result	
		A	B	C	D	E	Sample	Meets Requirement (Y/N)
		ASTM D5821 Fractured Particles in Coarse Aggregates, % minimum, (Note 4)	≤100 mm (Note 1)	55/-	75/-	85/80		
	≥100 mm (Note 1)	--	50/-	60/-	80/75	100/100	--	--
ASTM D4791 Flat and Elongated Particles (5:1), % maximum		--		10			1.80	Y

Notes

- Denotes the depth of the top of lift below final pavement surface. If less than 25% of a layer is within 100 mm of the surface, the layer may be considered to be below 100 mm.
- This requirement is waived for total fine aggregate containing RAP.
- A minimum uncompacted void content of 43% is acceptable provided that the selected mix satisfies the mix volumetrics specified elsewhere in the Contract Documents.
- 85/80 denotes that 85% of the coarse aggregate has one fractured face and 80% has two or more fractured faces.

Issued by (Testing Laboratory Representative):		
Salman Bhutta, Ph.D., P.Eng.		July 20, 2017
PRINT NAME	SIGNATURE	DATE
Received by (Contract Administrative Representative):		
PRINT NAME	SIGNATURE	DATE

Copies to: Contract Administrator Contractor Regional Quality Regional Geotechnical MERO (Soils and Aggregate)

PH-CO-449c Apr-10

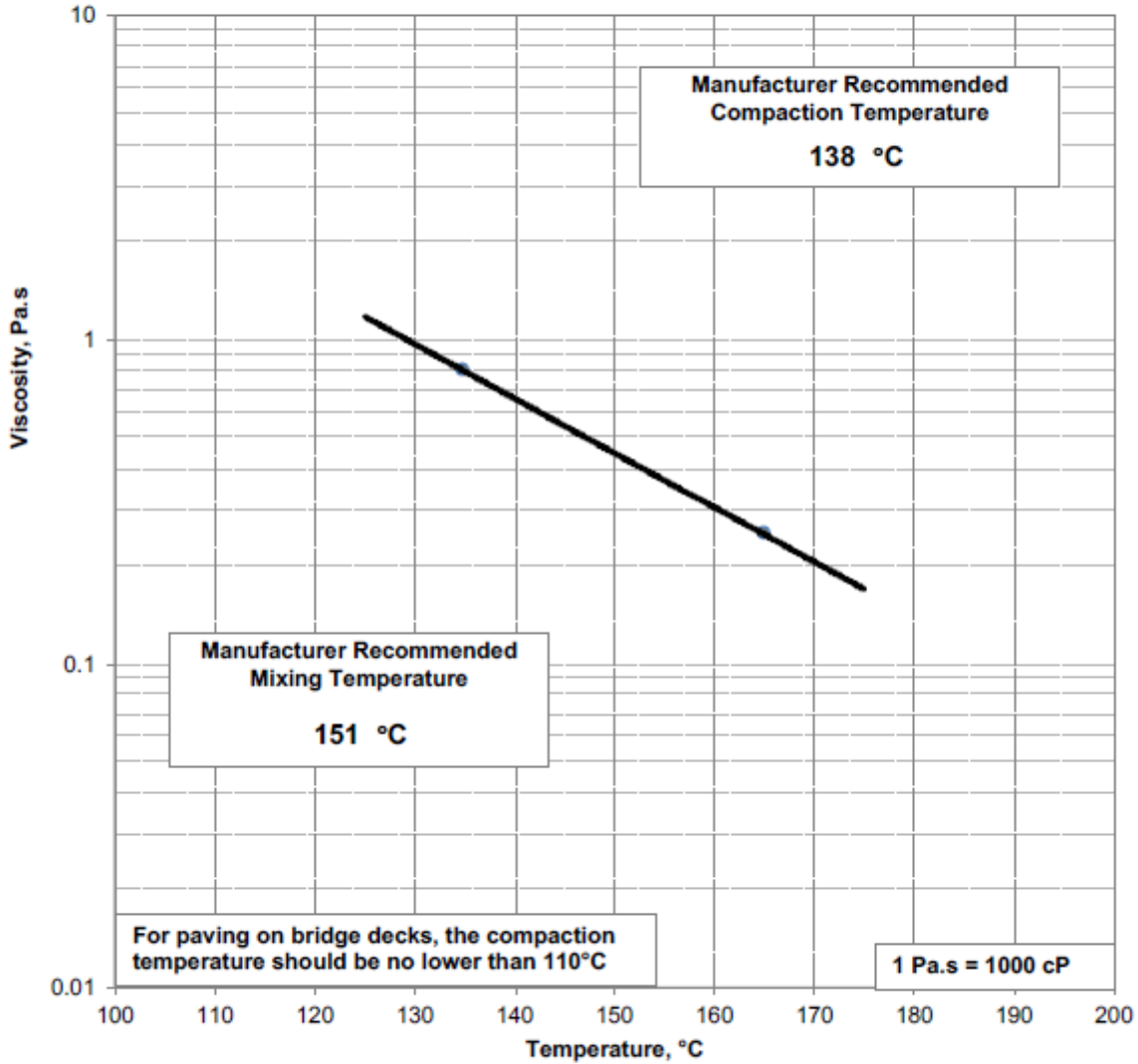
Lab No.



TEMPERATURE-VISCOSITY CHART

PG 64-28P-EX ASPHALT

TERMINALS	HAMILTON, OSHAWA & VALLEYFIELD
METHOD	Mixing and compaction temperatures determined by the Steady Shear Flow (SSF) method
PROJECT	All projects, unless otherwise specified
ISSUE DATE	January 13, 2017



WL6057 REV 2



McASPHALT INDUSTRIES LIMITED

8800 Sheppard Avenue East T 416.281.8181 TF 1.800.268.4238
Toronto, ON M1B 5R4 F 416.281.8842 E info@mcasphalt.com

mcasphalt.com
ISO 9001/14001

APPENDIX B: APOGEE SENSOR DATA SHEETS



SILICON-CELL PYRANOMETERS | SP-100 & SP-200 Series

Features

Output Options

- 0 to 350 mV
- 0 to 2.5 V
- 0 to 5 V
- 4 to 20 mA
- USB
- SDI-12

Stable Measurements

Long-term non-stability determined from multiple replicate pyranometers in accelerated aging tests and field conditions is less than 2 % per year.

Unique Design

An accurate, cosine-corrected patented design sheds water and dirt for a self-cleaning performance. A heated option is available with a 0.2 W heater to minimize errors caused by dew, frost, or snow.

Typical Measurement Applications

- Solar panel arrays
- Agricultural, ecological, and hydrological weather networks

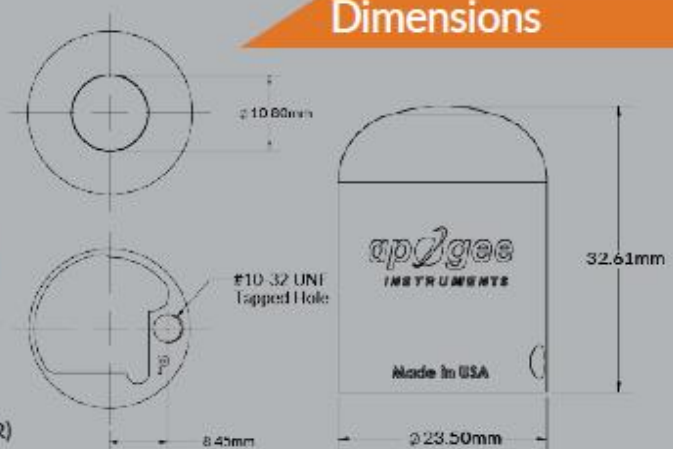
Calibration Traceability

Apogee SP sensors are calibrated through side-by-side comparison to the mean of (4) Apogee SP-110 transfer standard sensors under high intensity discharge metal halide lamps. The transfer standard sensors are calibrated through side-by-side comparison to the mean of at least (2) ISO-classified reference pyranometers under sunlight in Logan, UT. Each of (4) ISO-classified reference sensors are recalibrated on an alternating year schedule at the National Renewable Energy Laboratory (NREL) in Golden, Colorado. NREL reference standards are calibrated to the World Radiometric Reference (WRR) in Davos, Switzerland.

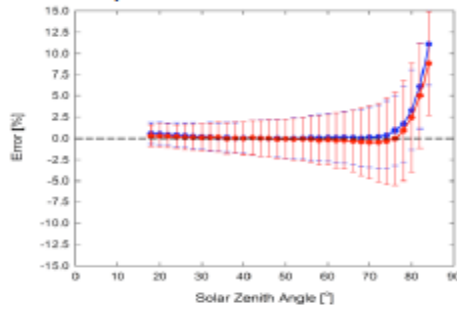
Accurate and stable global shortwave (solar) radiation measurement



Dimensions



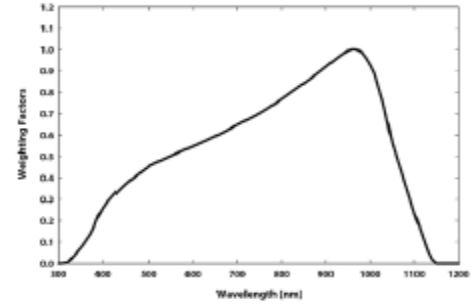
Cosine Response



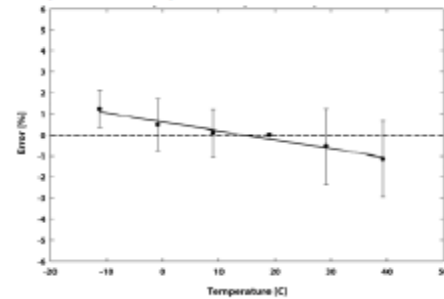
Mean **cosine response** of eleven Apogee silicon-cell pyranometers (error bars represent two standard deviations above and below mean). Cosine response measurements were made during broadband outdoor radiometer calibration (BORCAL) performed during two different years at the National Renewable Energy Laboratory (NREL) in Golden, Colorado. Cosine response was calculated as the relative difference of pyranometer sensitivity at each solar zenith angle to sensitivity at 45° solar zenith angle. The blue symbols are AM measurements; the red symbols are PM measurements.

Spectral response estimate of Apogee silicon-cell pyranometers. Spectral response was estimated by multiplying the spectral response of the photodiode, diffuser, and adhesive. Spectral response measurements of diffuser and adhesive were made with a spectrometer, and spectral response data for the photodiode were obtained from the manufacturer.

Spectral Response



Temperature Response



Mean **temperature response** of ten Apogee silicon-cell pyranometers (error bars represent two standard deviations above and below mean). Temperature response measurements were made at 10 C intervals across a temperature range of approximately -10 to 40 C in a temperature controlled chamber under a fixed, broad spectrum, electric lamp. At each temperature set point, a spectroradiometer was used to measure light intensity from the lamp and all pyranometers were compared to the spectroradiometer. The spectroradiometer was mounted external to the temperature control chamber and remained at room temperature during the experiment.

Product Specifications

	SP-110-SS	SP-212-SS	SP-214-SS	SP-215-SS	SP-230-SS
Power Supply	Self-powered	3.3 to 24 V DC; current draw 300 μ A	7 to 24 V DC, maximum current draw of 22 mA (2 mA quiescent current draw)	5.5 to 24 V DC; current draw 300 μ A	12 V DC for heater with a current draw of 15.4 mA
Output (sensitivity)	0.2 mV per $W m^{-2}$	2 mV per $W m^{-2}$	0.008 mA per $W m^{-2}$	4 mV per $W m^{-2}$	0.2 mV per $W m^{-2}$
Calibration Factor (reciprocal of output)	5 $W m^{-2}$ per mV	0.5 $W m^{-2}$ per mV	125 $W m^{-2}$ per mA, 4 mA offset	0.25 $W m^{-2}$ per mV	5 $W m^{-2}$ per mV
Calibration Uncertainty	$\pm 5\%$				
Measurement Repeatability	Less than 1%				
Long-term Drift	Less than 2% per year				
Non-linearity	Less than 1% up to 2000 $W m^{-2}$	Less than 1% up to 1250 $W m^{-2}$	Less than 1% up to 2000 $W m^{-2}$	Less than 1% up to 1250 $W m^{-2}$	Less than 1% up to 1750 $W m^{-2}$
Response Time	Less than 1 ms				
Field of View	180°				
Spectral Range	360 to 1120 nm				
Directional (Cosine) Response	$\pm 5\%$ at 75° zenith angle				
Temperature Response	0.04 \pm 0.04 % per C				
Operating Environment	-40 to 70 C; 0 to 100% relative humidity; can be submerged in water up to depths of 30 m				
Dimensions	24 mm diameter, 28 mm height				
Mass (with 5 m of cable)	90 g				
Cable	5 m of shielded, twisted-pair wire; additional cable available in multiples of 5 m; TPR jacket (high water resistance, high UV stability, flexibility in cold conditions); pigtail lead wires				
Warranty	4 years against defects in materials and workmanship				

www.apogeeinstruments.com | 435.792.4700 | Logan, UT



APOGEE ULTRA VIOLET SENSOR | SU-100-SS

Measure total radiation from 250 to 400 nm

Features

Wide Range

Sensitive from 250 to 400 nm, spanning the solar UV and range of electric lamps.

Measurement Units

Calibration factors for photon flux density units [$\mu\text{mol m}^{-2} \text{s}^{-1}$] and energy flux density [W m^{-2}] are provided with each sensor allowing for rapid unit conversions.

Rugged, Self-cleaning Housing

The patented dome-shaped sensor head facilitates runoff of dew and rain, helping to keep the detector clean and minimizing errors caused by dust blocking the radiation path. Sensors are housed in a rugged anodized aluminum body and electronics are fully-potted.

Output Options

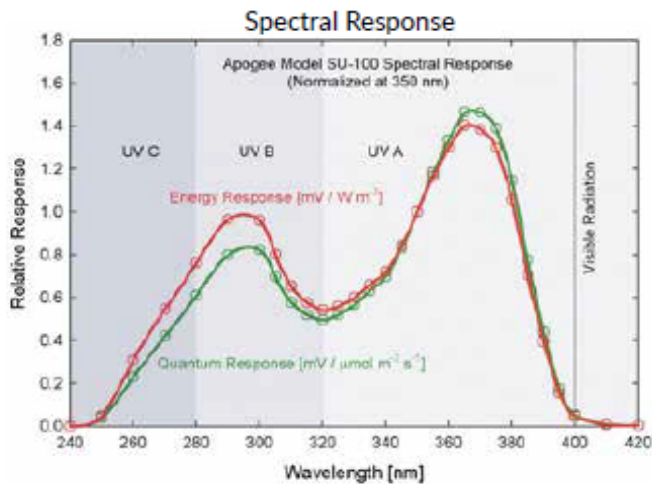
Analog and digital output options are available. Analog version is an unamplified voltage output. Sensor is available attached to a hand-held meter with digital readout.

Typical Applications

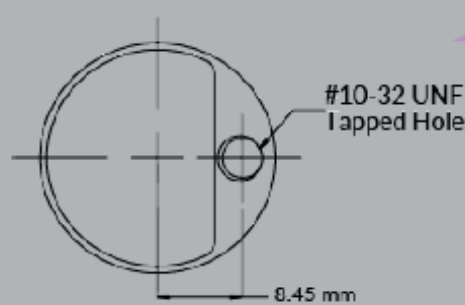
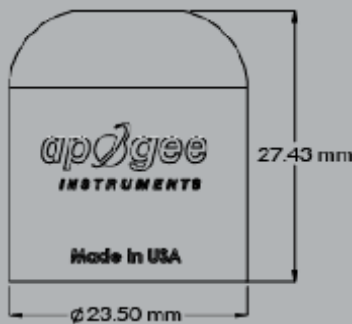
Applications include: UV radiation measurement in outdoor environments (sensor is not recommended for long-term continuous outdoor deployment), laboratory use with artificial light sources (e.g., germicidal lamps), and monitoring the filtering ability and stability of various materials.

Product Specifications

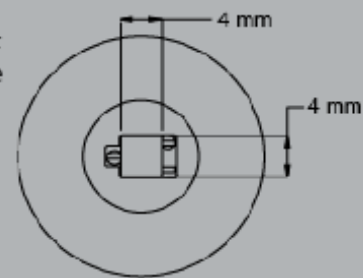
	SU-100-SS
Output (sensitivity)	0.2 mV per $\mu\text{mol m}^{-2} \text{s}^{-1}$; 0.61 mV per W m^{-2}
Calibration Factor (reciprocal of output)	5 $\mu\text{mol m}^{-2} \text{s}^{-1}$ per mV; 1.65 W m^{-2} per mV
Calibration Uncertainty	$\pm 10\%$
Measurement Repeatability	Less than 1 %
Long-term Drift (non-stability)	Less than 3 % per year
Non-linearity	Less than 1 % (up to 300 $\mu\text{mol m}^{-2} \text{s}^{-1}$)
Response Time	Less than 1 ms
Spectral Range	250 nm to 400 nm
Field of View	180°
Directional (Cosine) Response	$\pm 10\%$ at 75° zenith angle
Temperature Response	Approximately 0.1 % per C
Operating Environment	-40 to 70 C, 0 to 100 % relative humidity
Dimensions	24 mm diameter, 28 mm height
Mass	75 g (with 5 m of cable)
Cable	5 m of shielded, twisted-pair wire; TPR jacket (high water resistance, high UV stability, flexibility in cold conditions); pigtail lead wires stainless steel connector
Warranty	4 years against defects in materials and workmanship



Spectral response estimate of Apogee SU-100 UV sensors. Spectral response measurements were made at 10 nm increments across a wavelength range of 200 to 450 nm in a monochromator with an attached electric light source. Measured spectral data were normalized at 350 nm.



Dimensions



Radiation Source (Error Calculated Relative to sun, Clear Sky)	Error [%]
Sun (Clear Sky)	0.0
Sun (Cloudy Sky)	< 0.5
Reflected from Grass Canopy	< 0.5
Reflected from Deciduous Canopy	< 0.5
Reflected from Conifer Canopy	< 0.5
Reflected from Agricultural Soil	< 0.5
Reflected from Forest Soil	< 0.5
Reflected from Desert Soil	< 0.5
Reflected from Water	< 0.5
Reflected from Ice	< 0.5
Reflected from Snow	< 0.5
Cool White Fluorescent (T5)	9.0
Metal Halide	2.8
High Pressure Sodium	-1.7
Incandescent	-3.3
Mercury Arc	17.8

Spectral Errors

Spectral Error

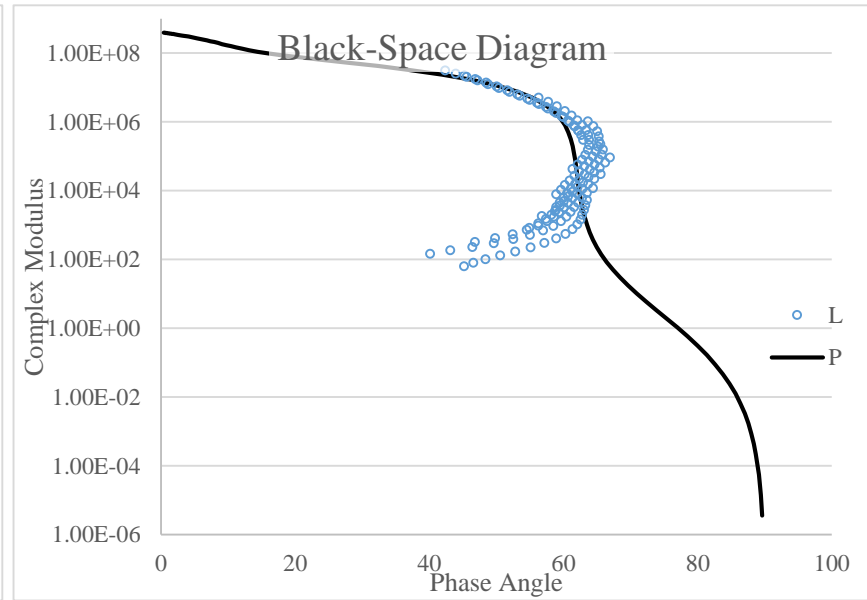
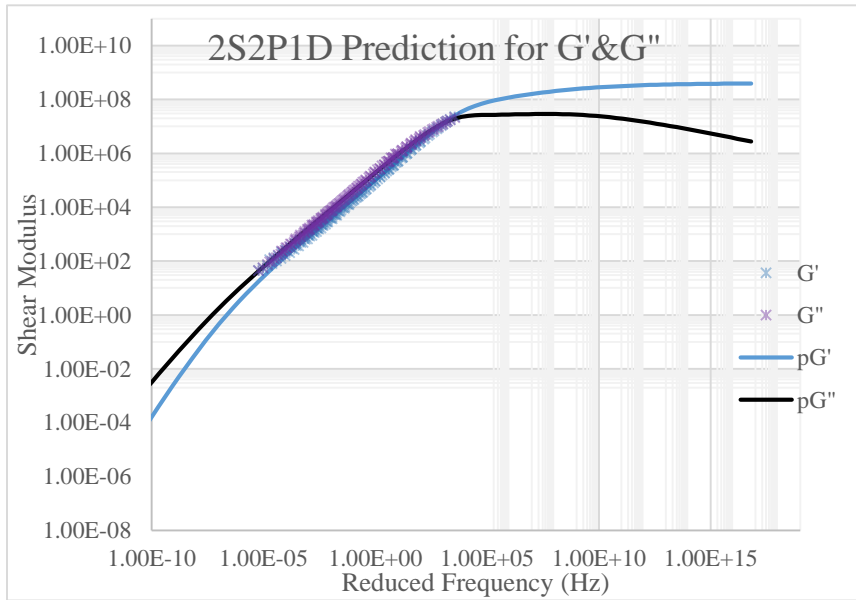
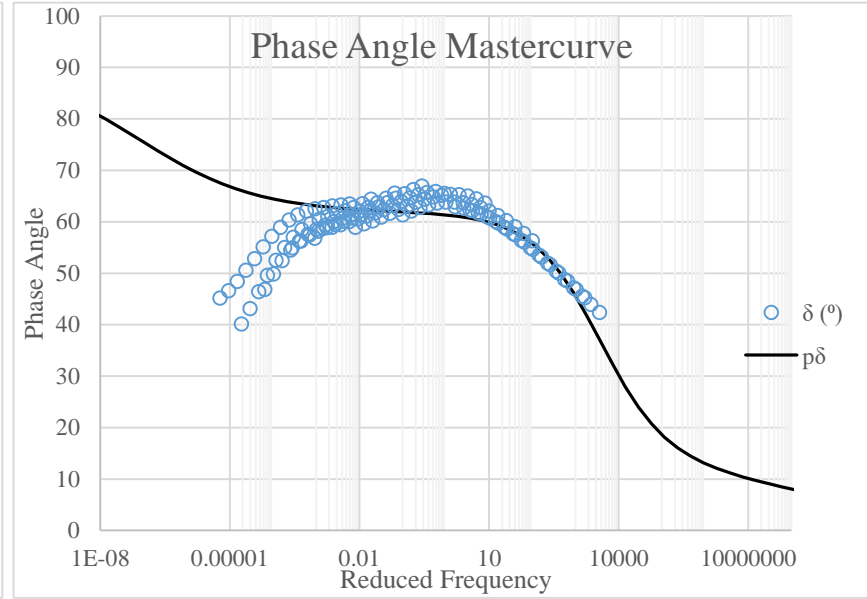
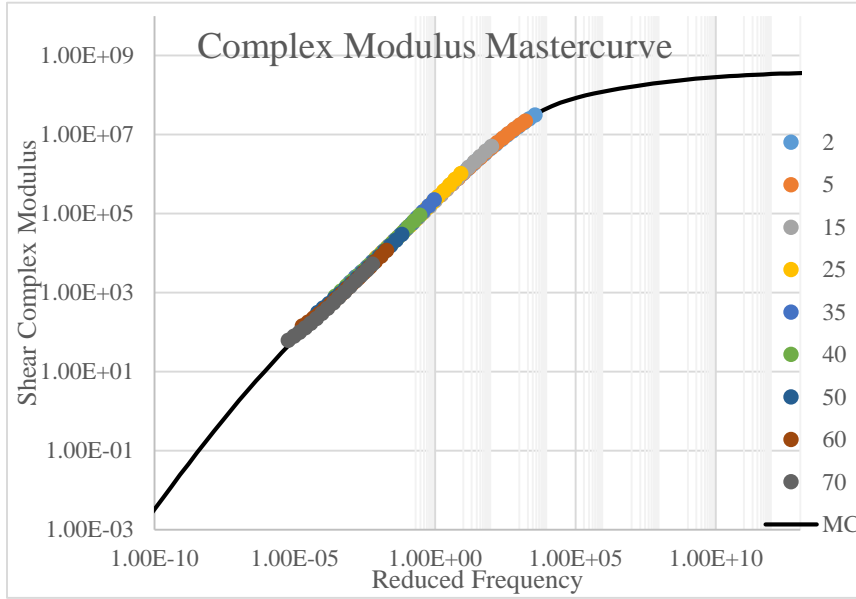
Although the relative wavelengths of UV radiation differ among sunlight and electric lights, the error estimates shown in the table below indicate that the SU-100 provides reasonable estimates of UV radiation coming from electric lamps.

Calibration Traceability

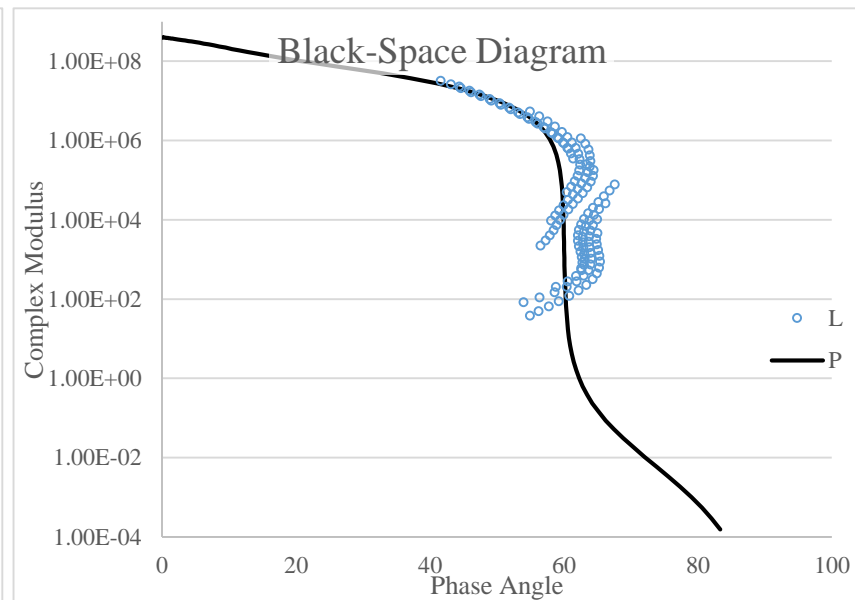
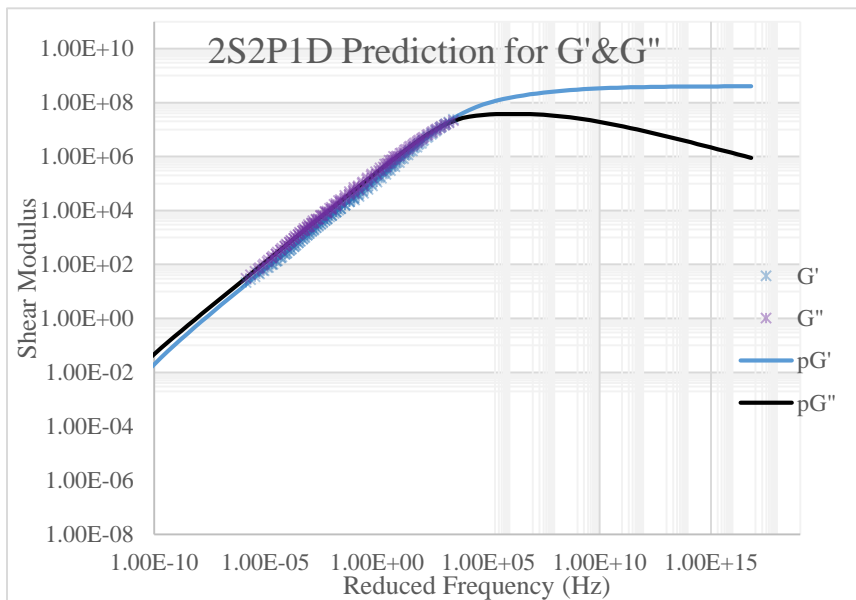
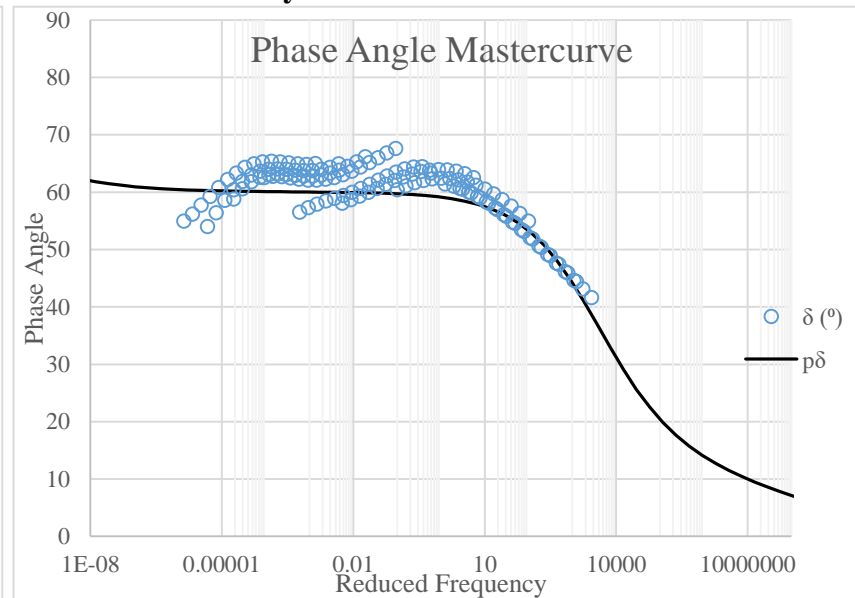
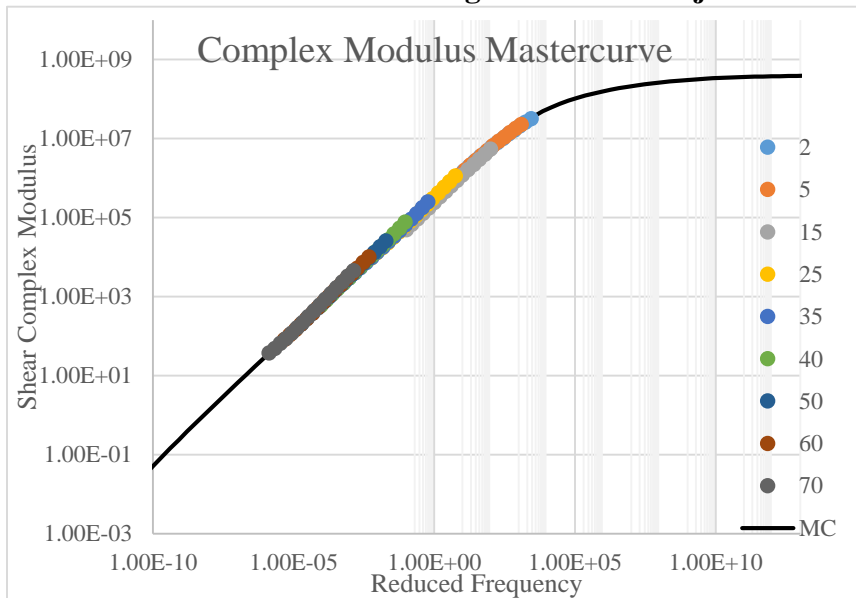
Apogee SU-100 UV sensors are calibrated through side-by-side comparison to the mean of four Apogee model SU-100 transfer standard UV sensors under high intensity discharge metal halide lamps. The transfer standard UV sensors are calibrated through side-by-side comparison to an Apogee model PS-200 spectroradiometer under sunlight in Logan, Utah. The PS-200 is calibrated with a LI-COR model 1800-02 Optical Radiation Calibrator using a 200 W quartz halogen lamp. The 1800-02 and quartz halogen lamp are traceable to the National Institute of Standards and Technology (NIST).

**APPENDIX C: RHEOLOGICAL ANALYSIS – ASPHALT
CEMENT**

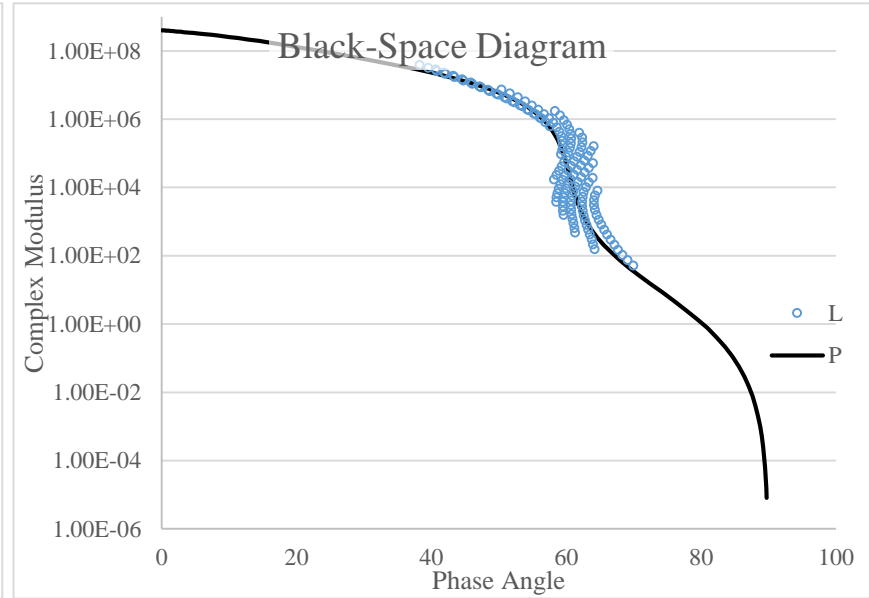
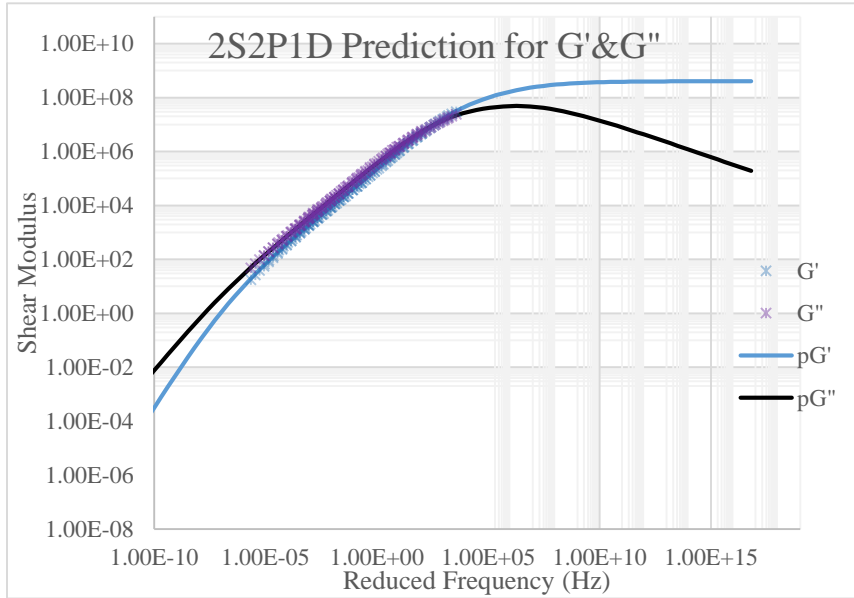
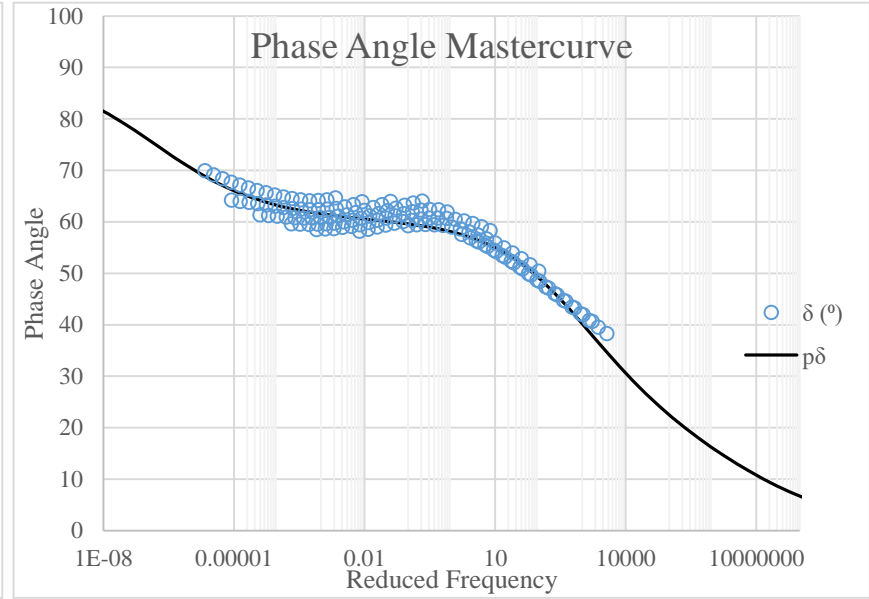
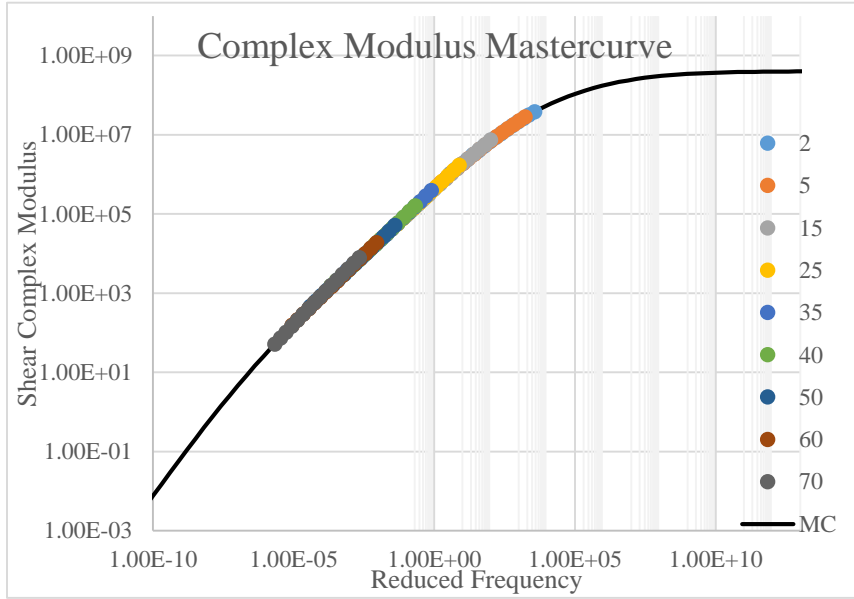
Virgin Binder – 64-28P-EX



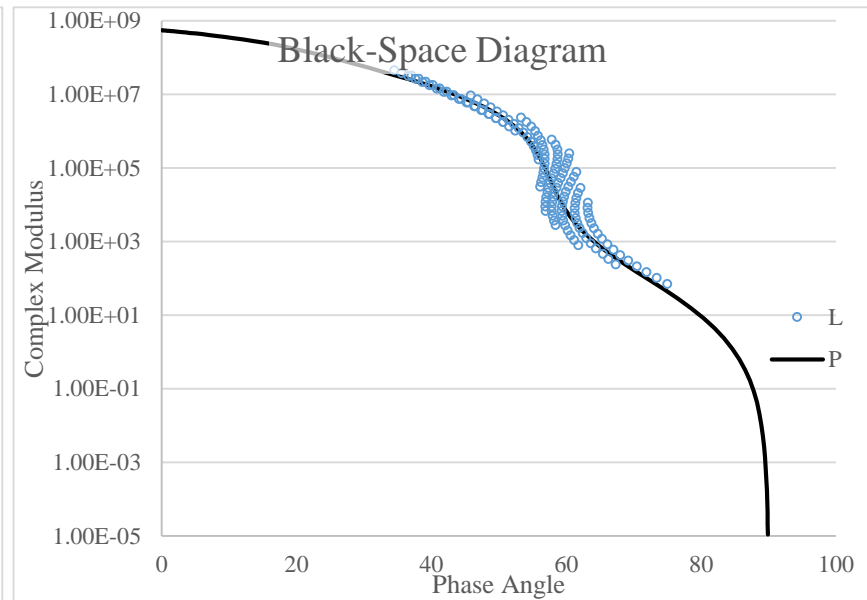
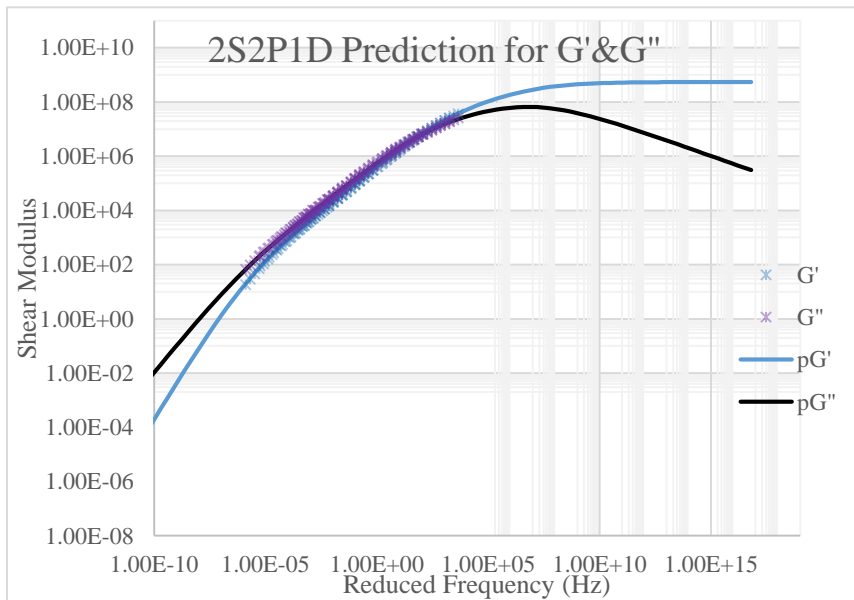
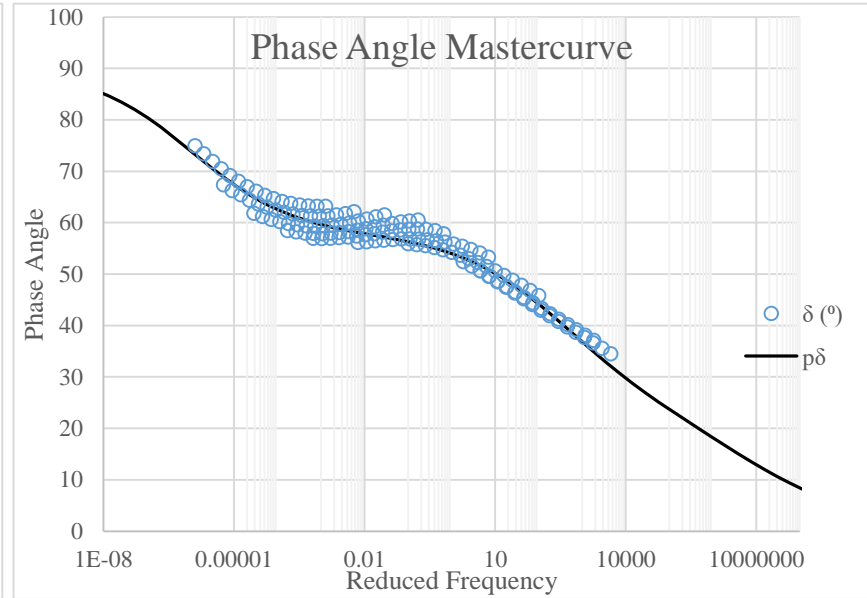
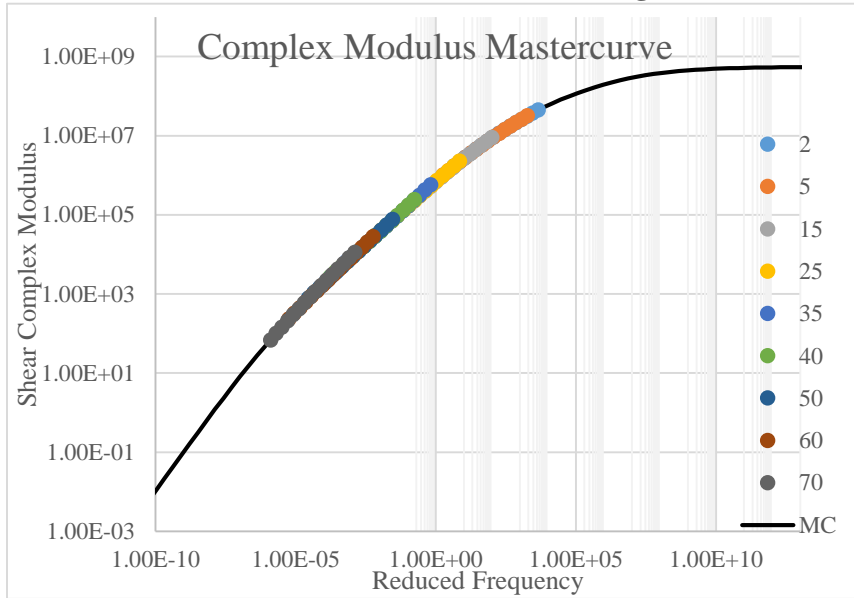
Virgin Binder – Subjected to Extraction and Recovery Procedures



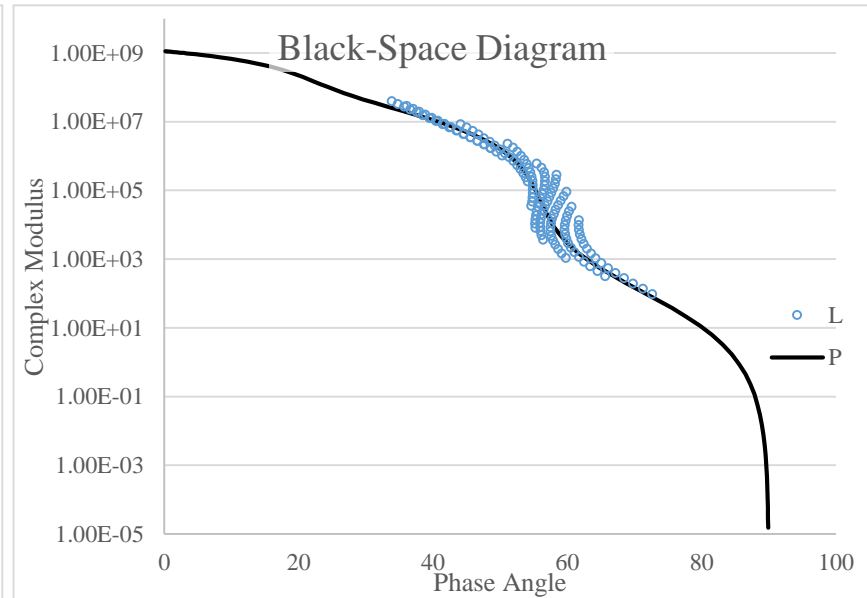
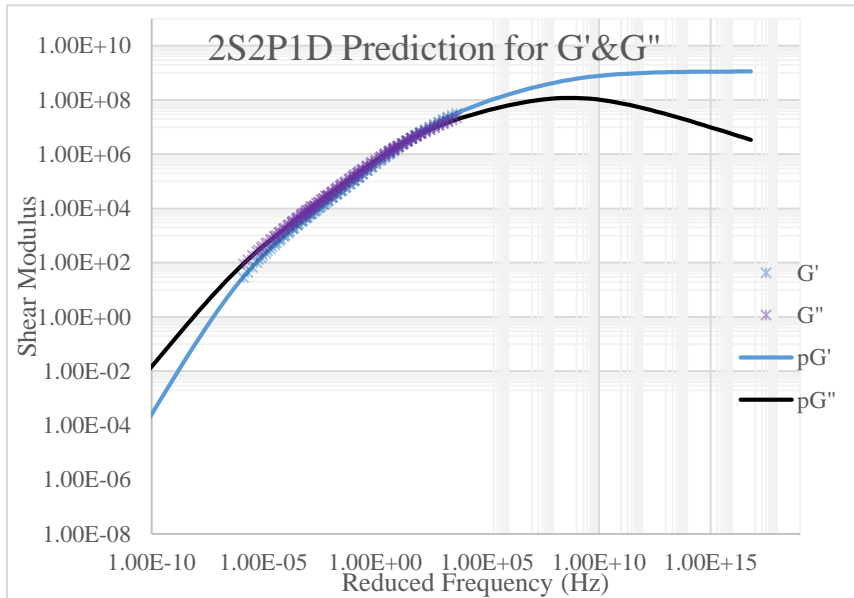
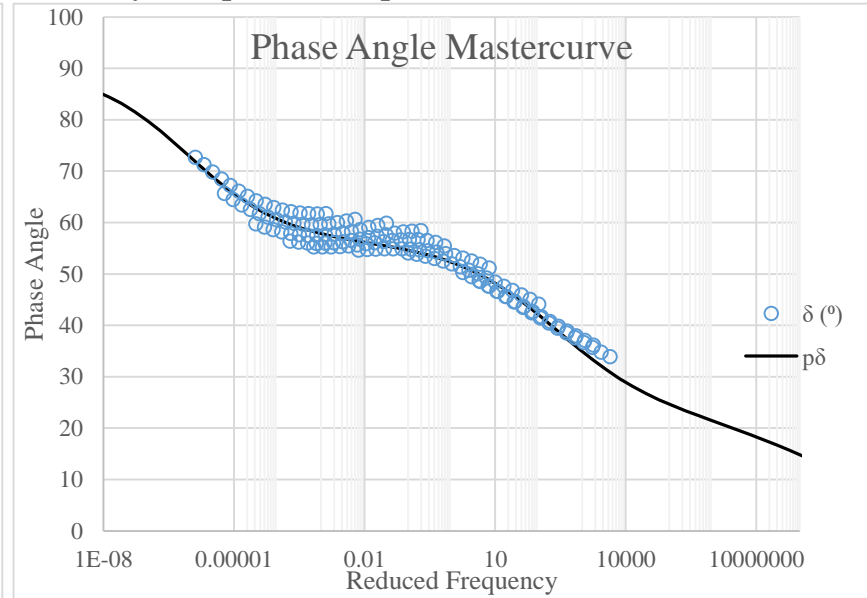
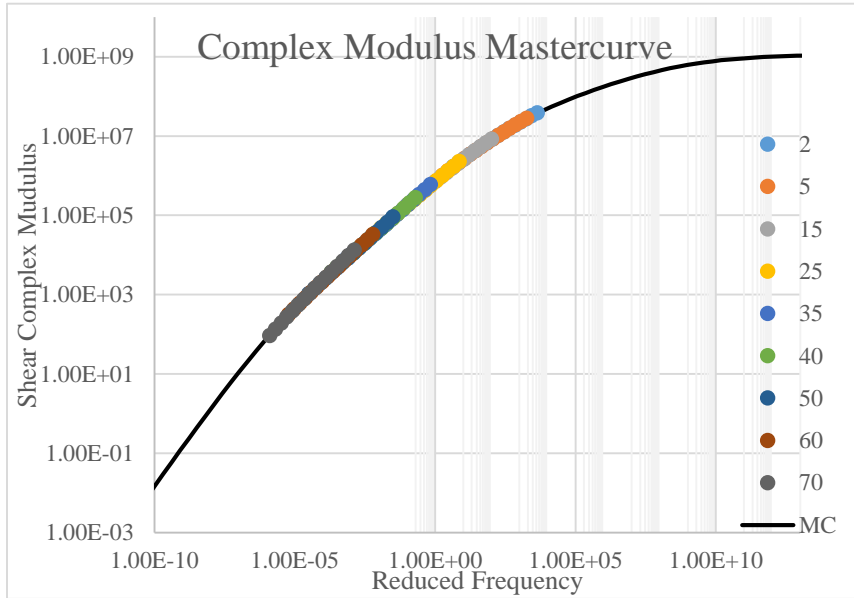
Laboratory Short-Term Aged Binder - RTFOT



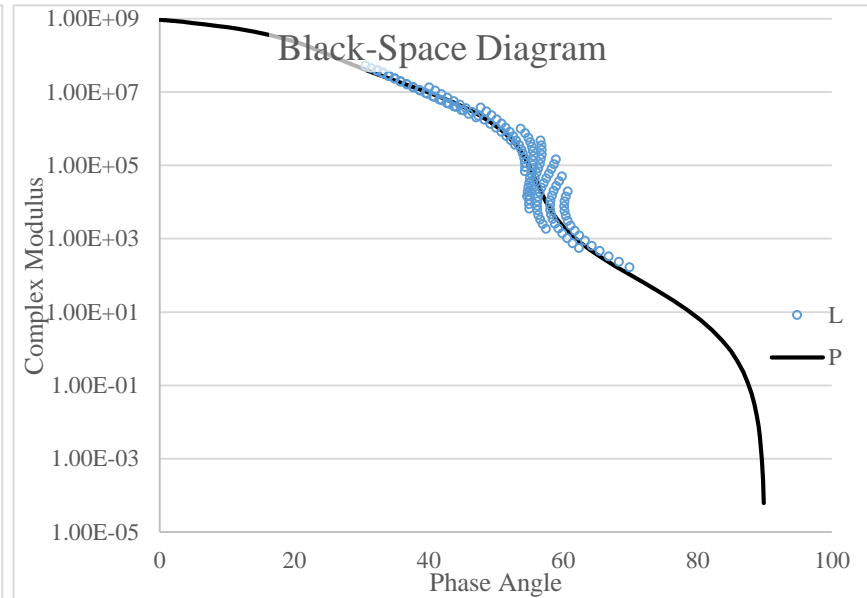
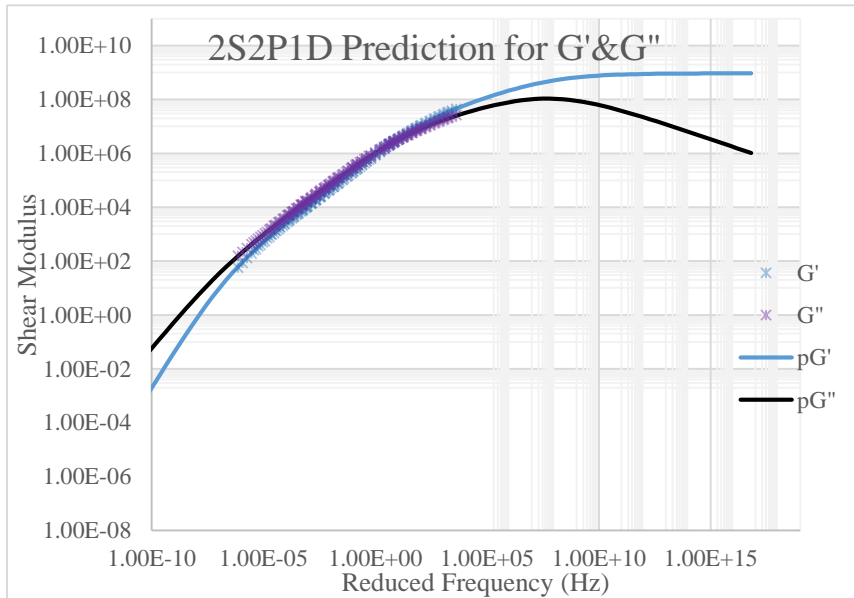
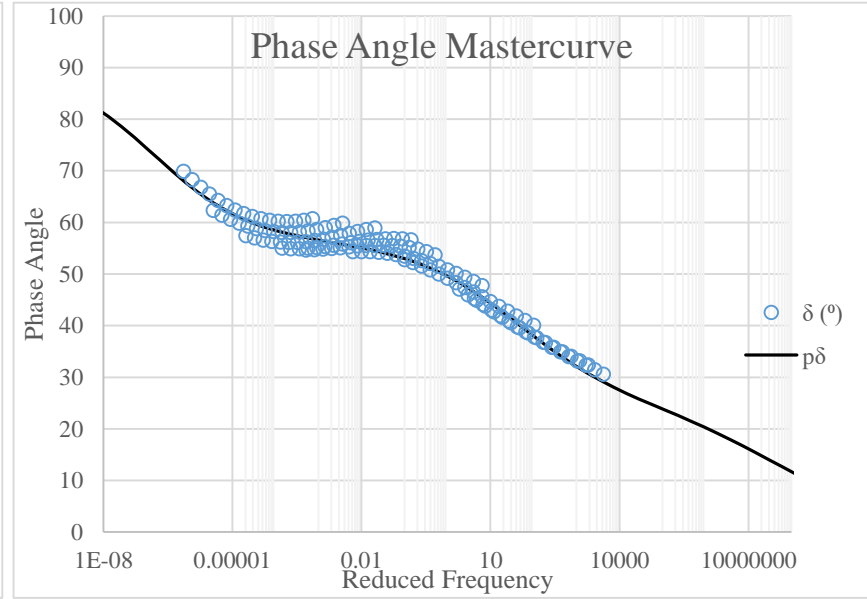
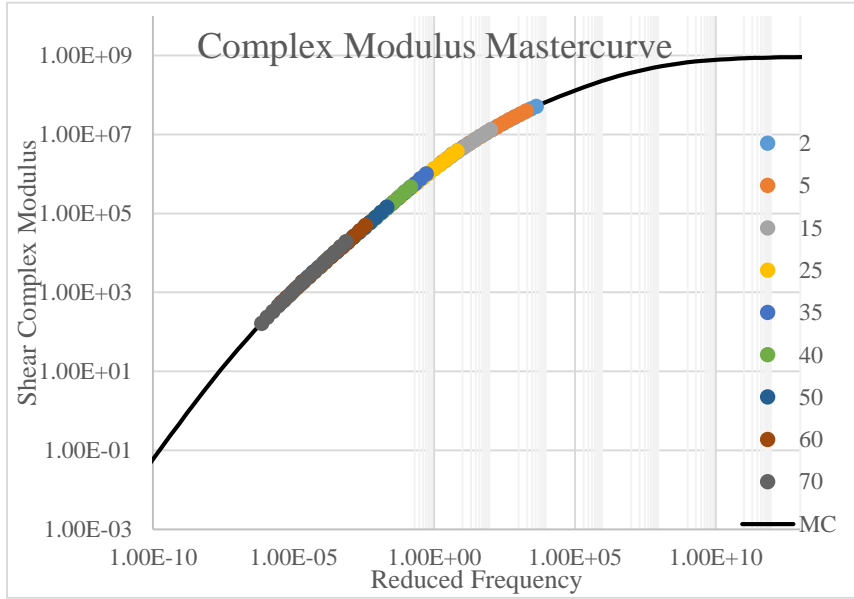
Plant Short-Term Aged Mixture – Extracted & Recovered from Loose Mix



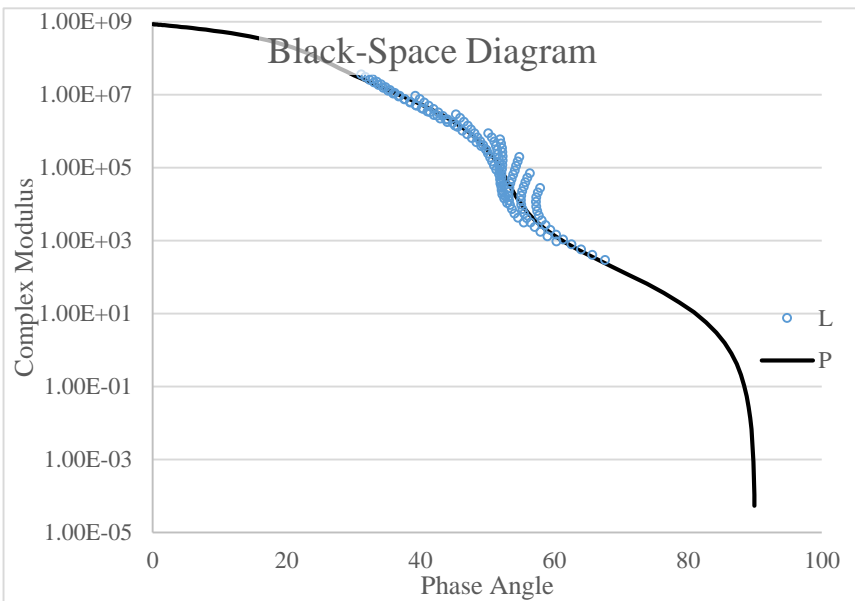
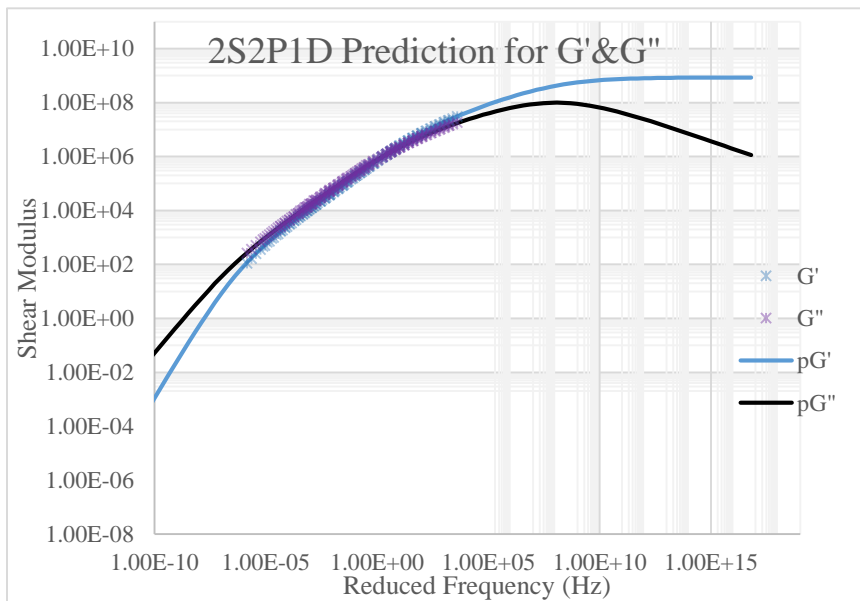
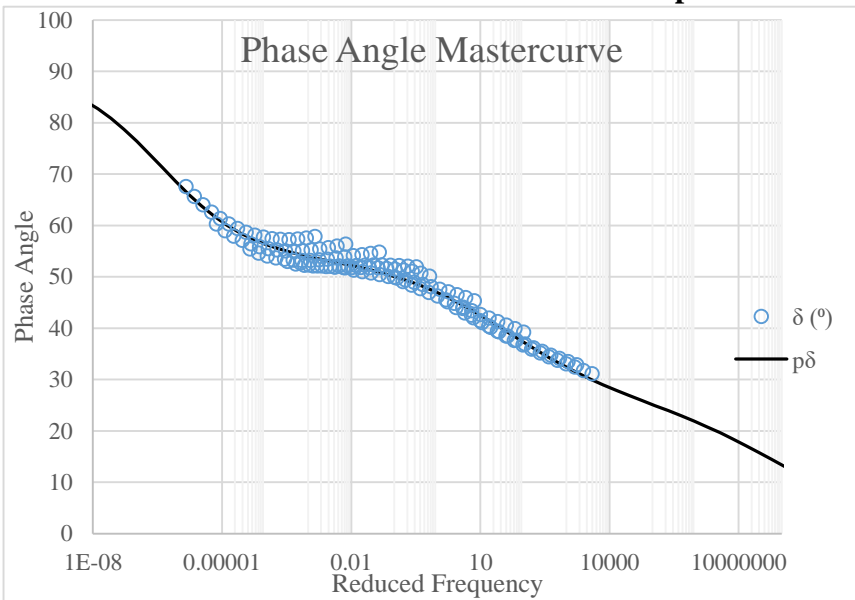
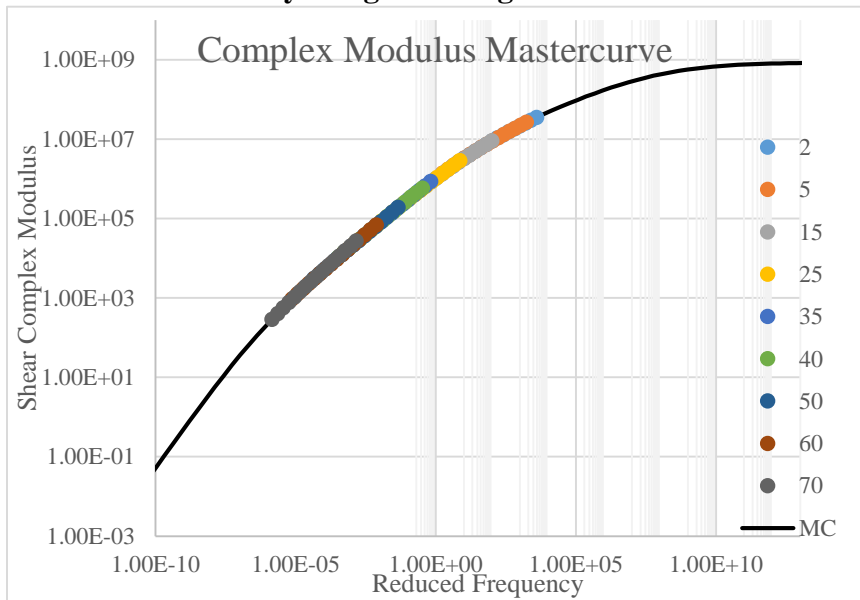
Extracted & Recovered from Laboratory Compacted Samples



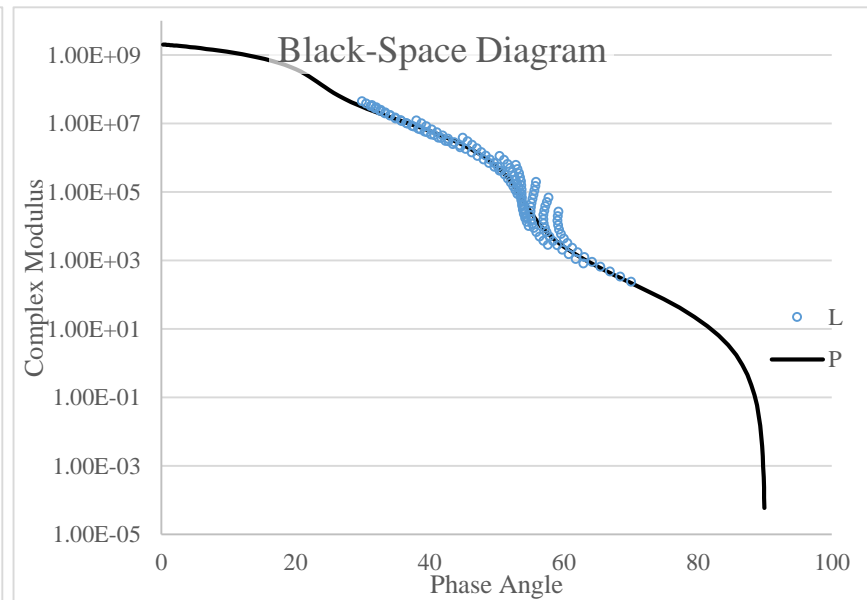
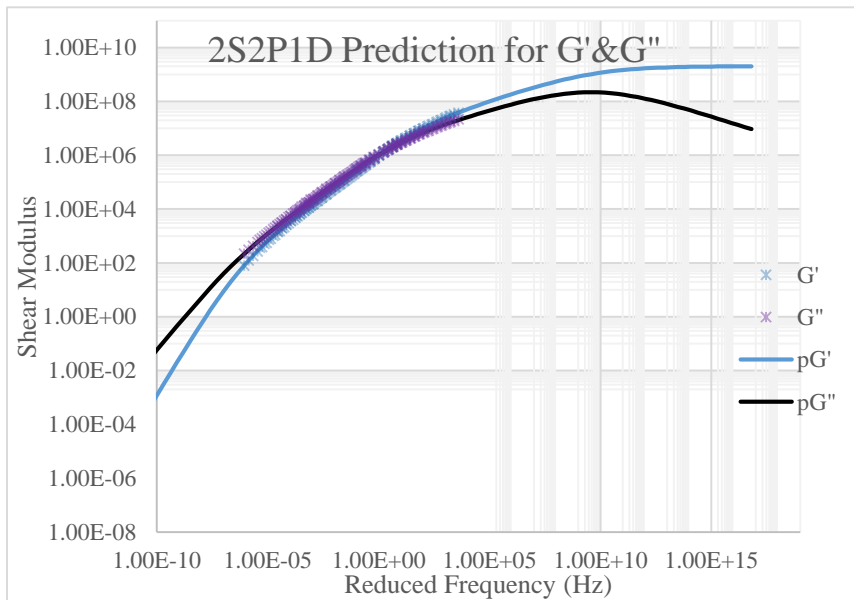
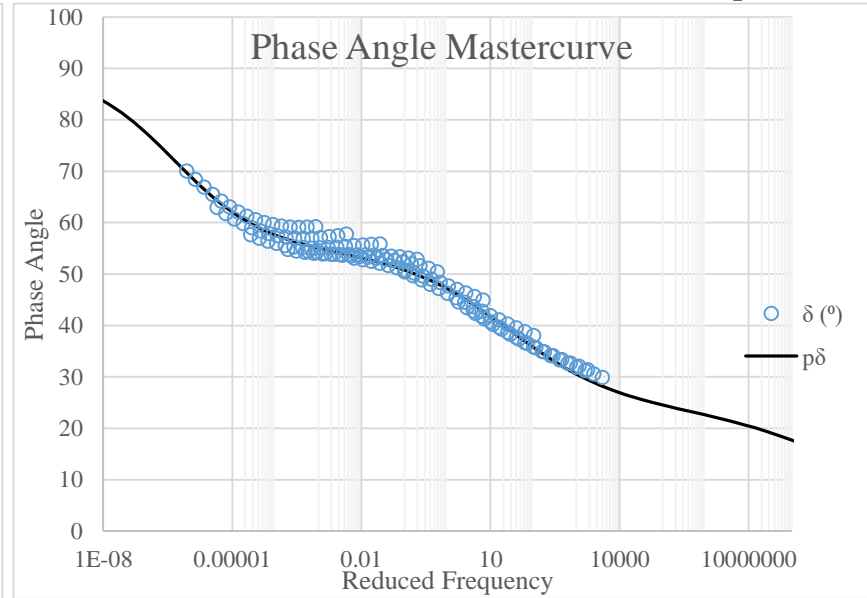
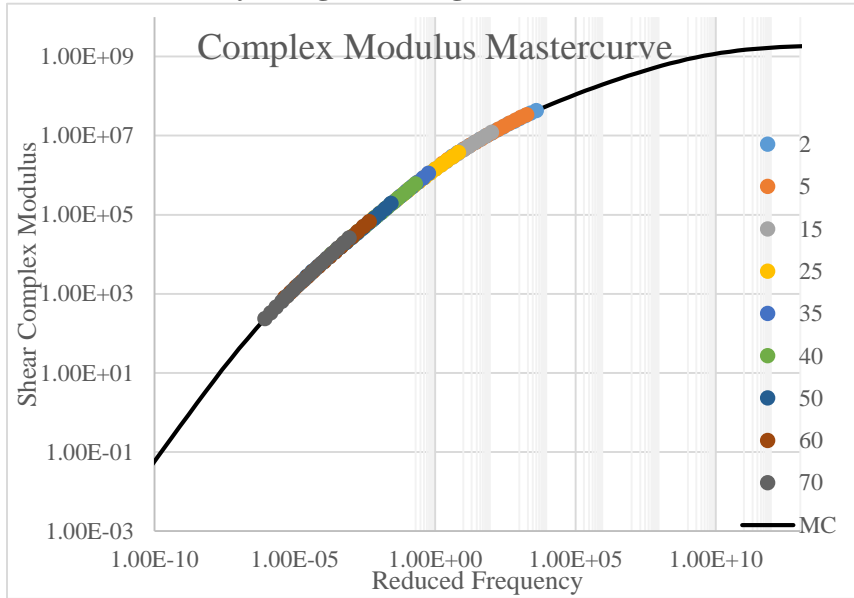
Laboratory Long-Term Aged Binder – RTFOT + PAV



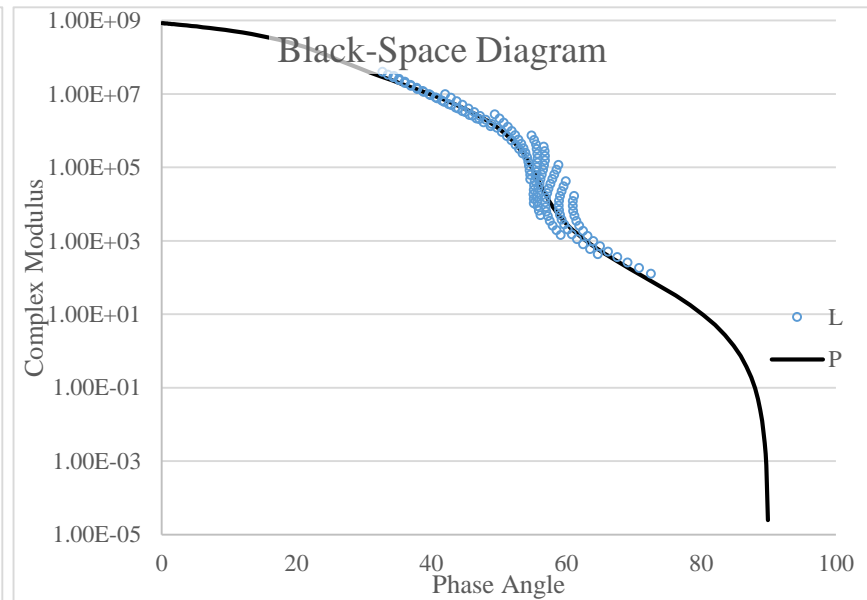
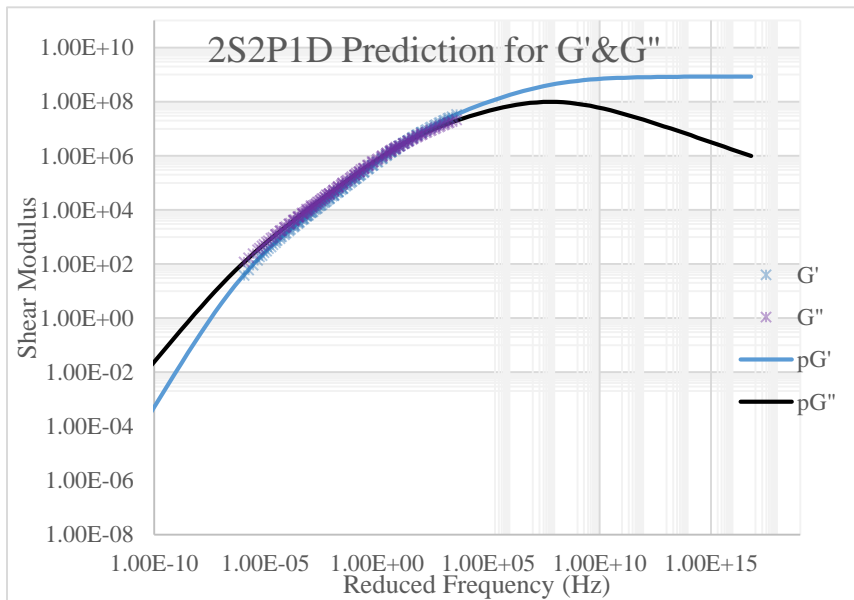
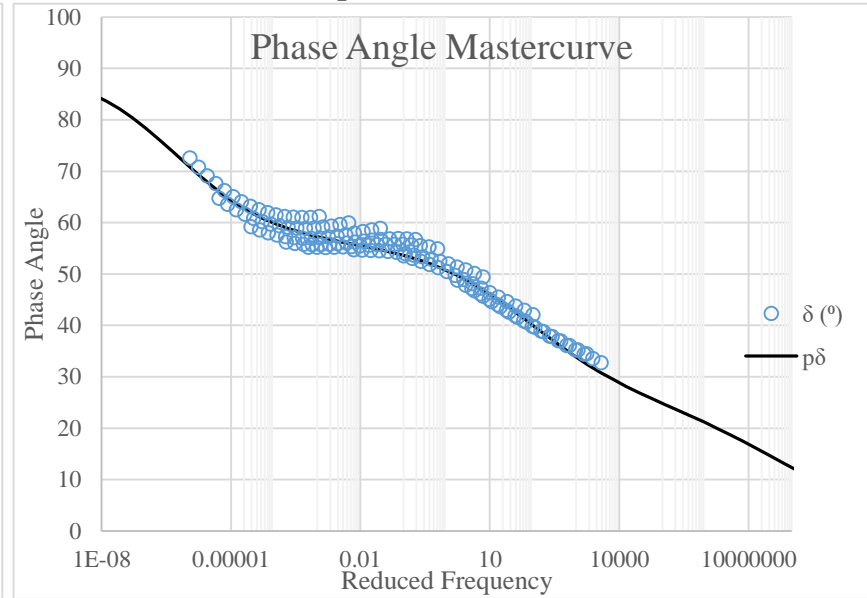
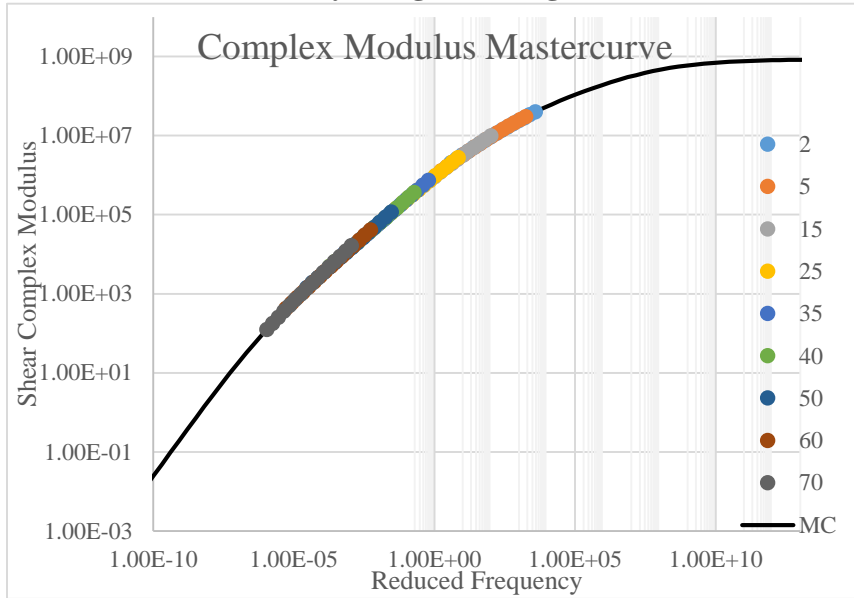
Laboratory Long-Term Aged Mixture – Extracted & Recovered from AASHTO R30 Conditioned Samples



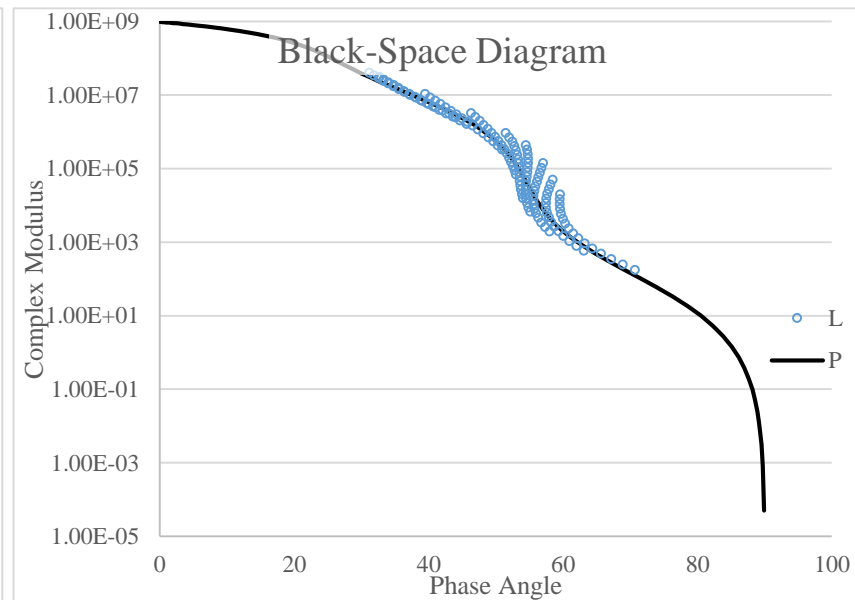
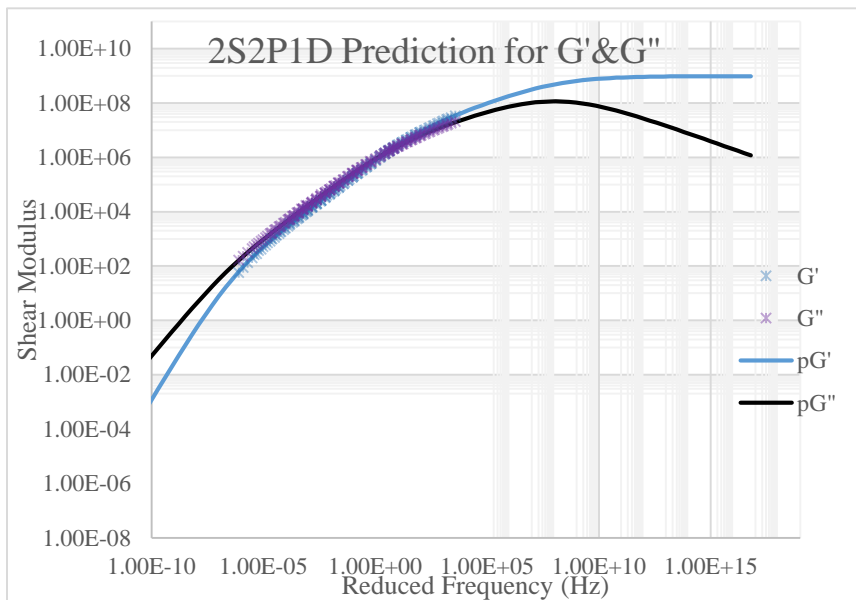
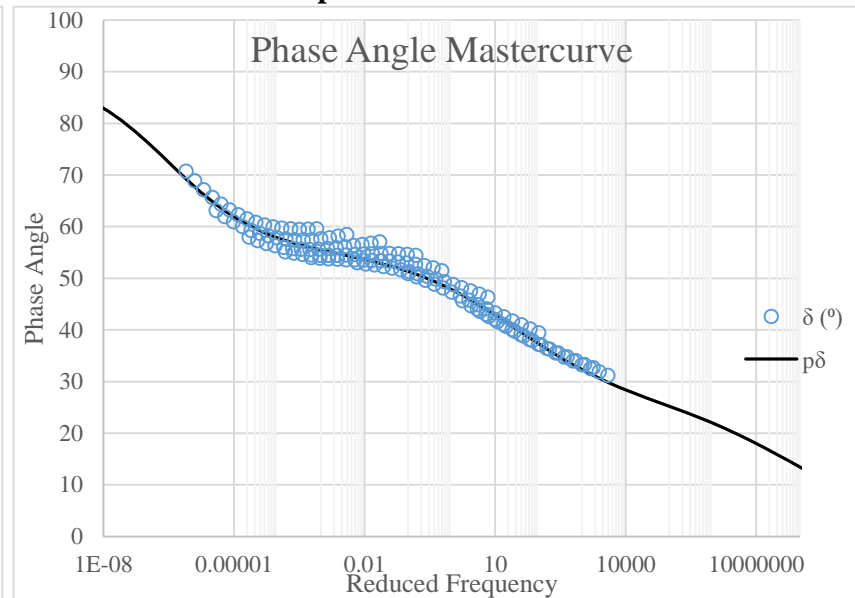
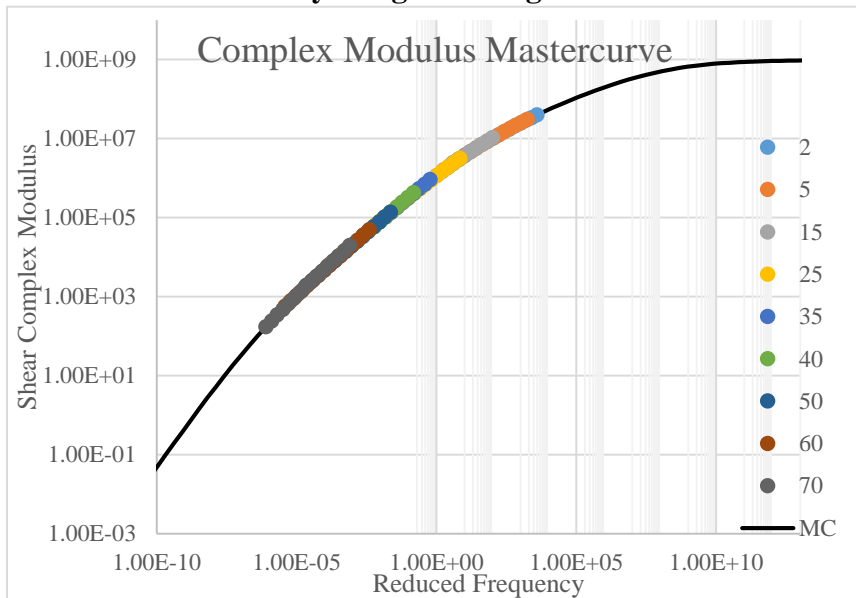
Laboratory Long-Term Aged Mixture – Extracted & Recovered from Atlas Weatherometer Conditioned Samples



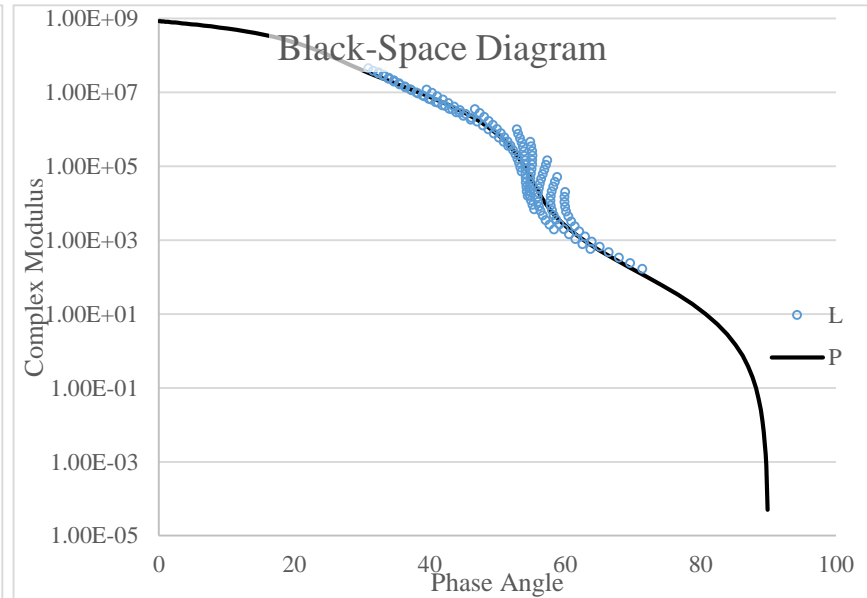
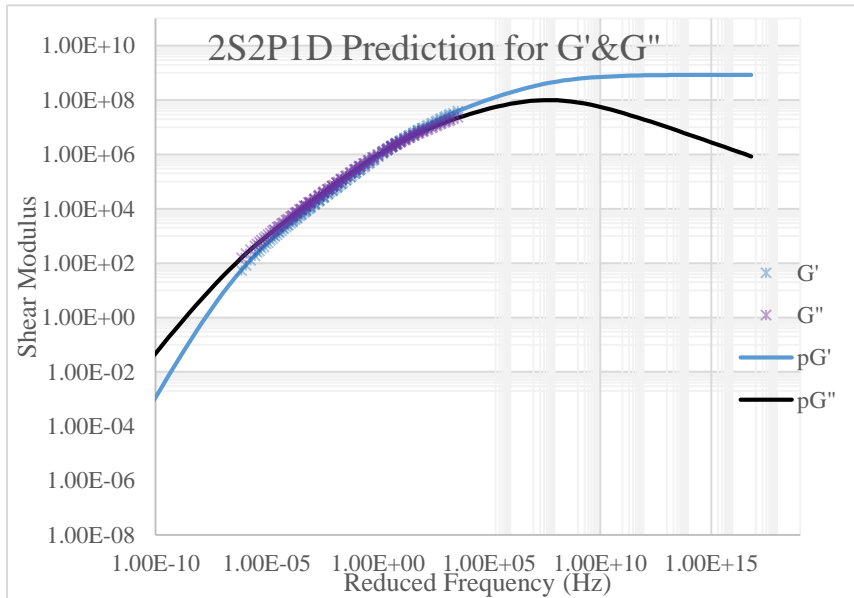
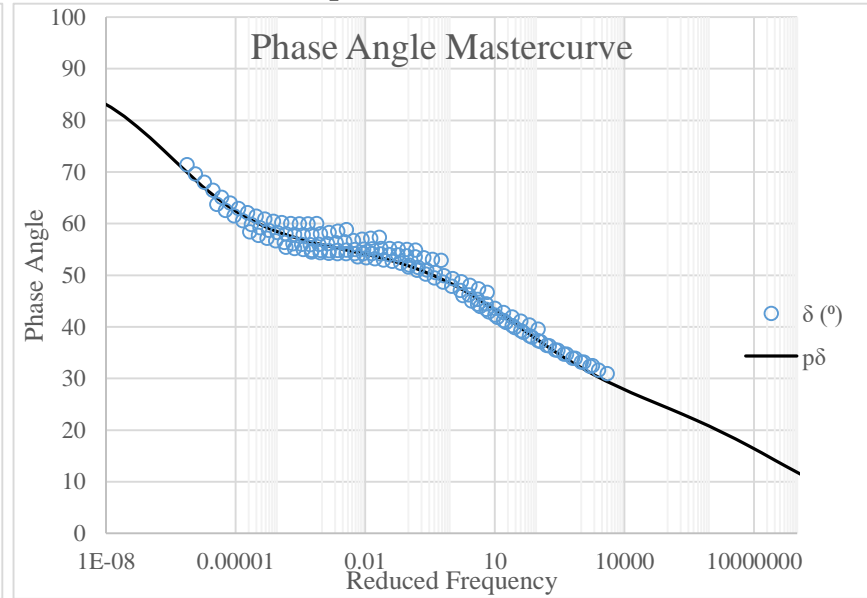
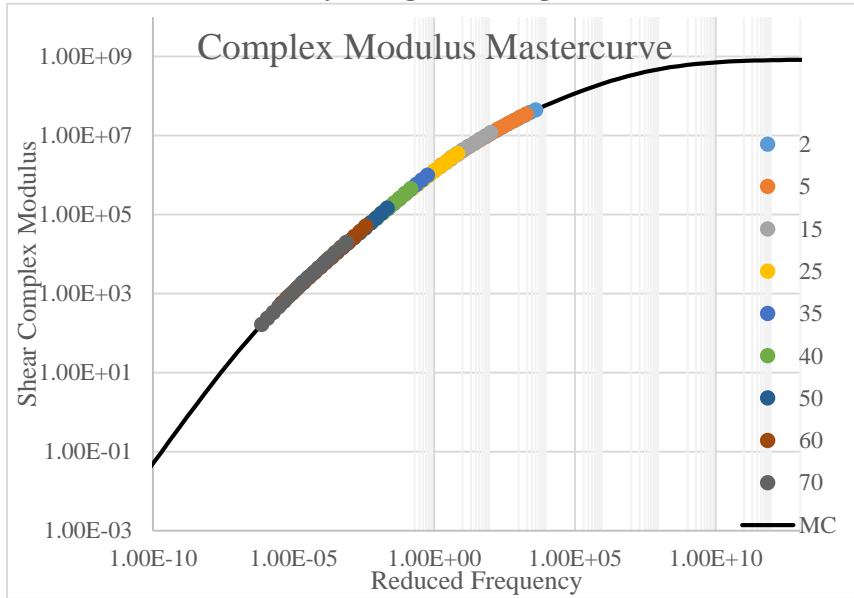
Laboratory Long-Term Aged Mixture – Extracted & Recovered from Bespoke Chamber: BC5-H₂O



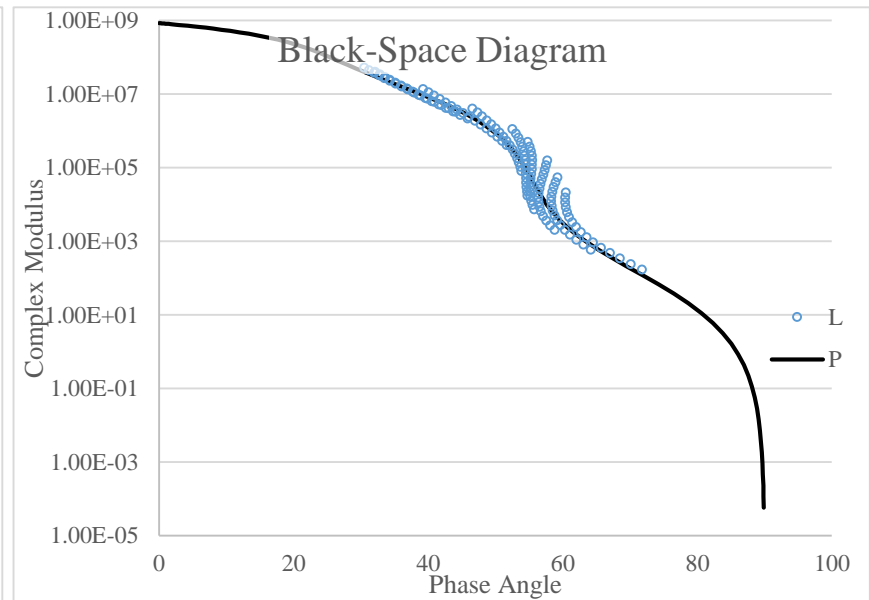
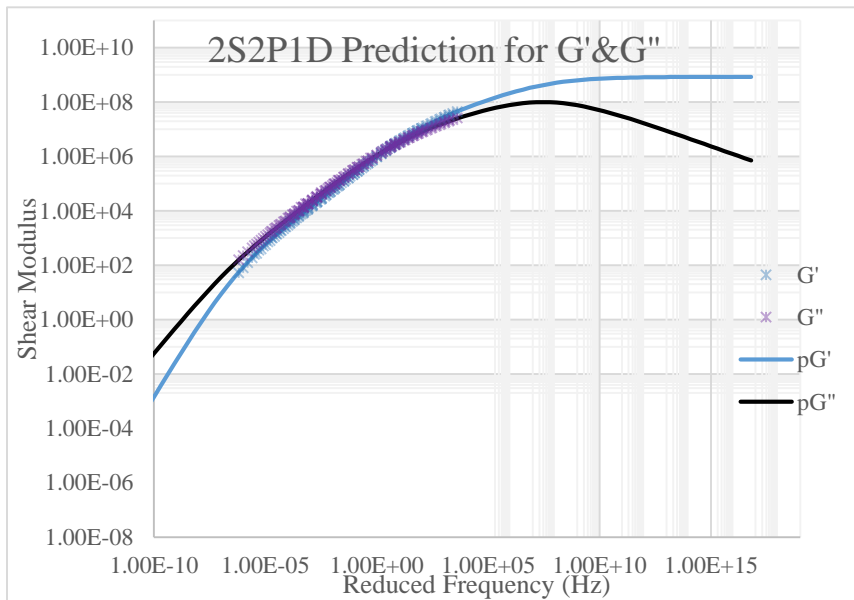
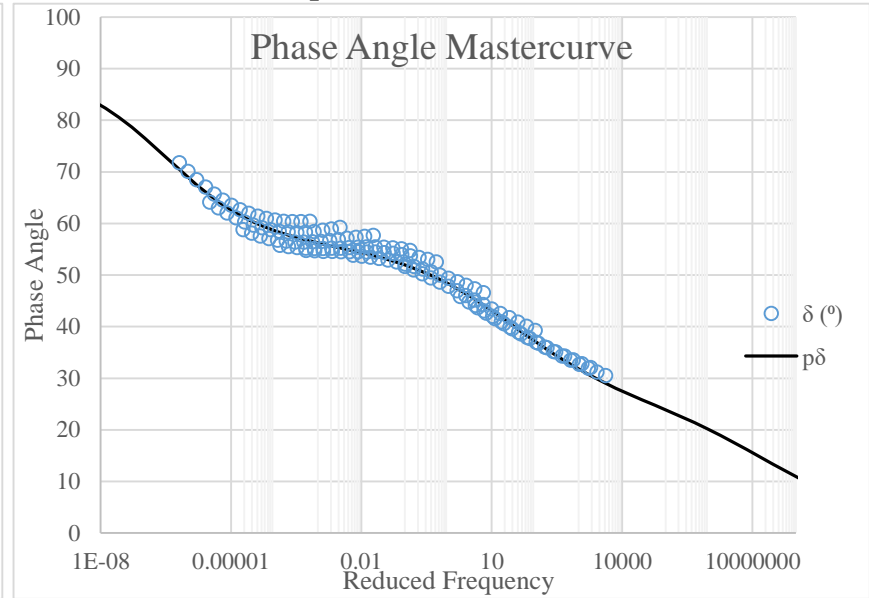
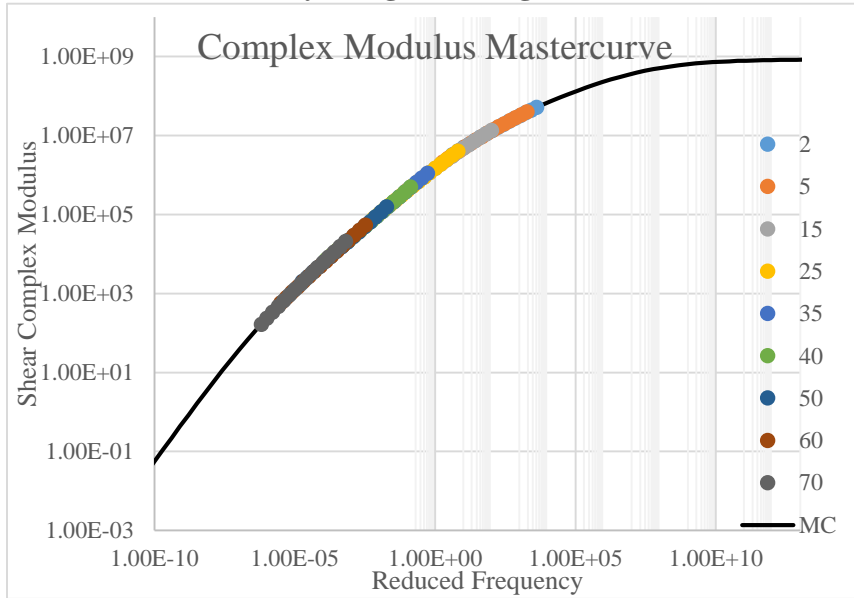
Laboratory Long-Term Aged Mixture – Extracted & Recovered from Bespoke Chamber: BC5-NoH₂O



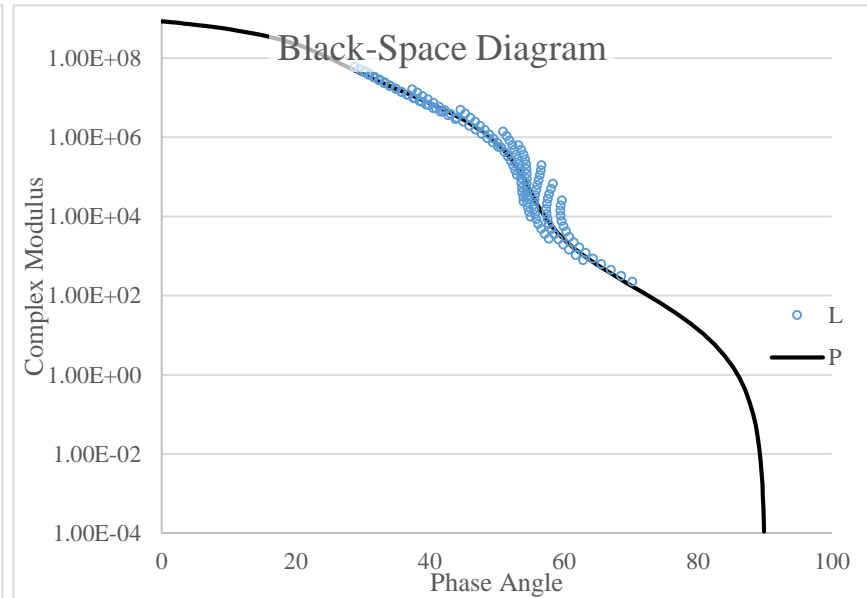
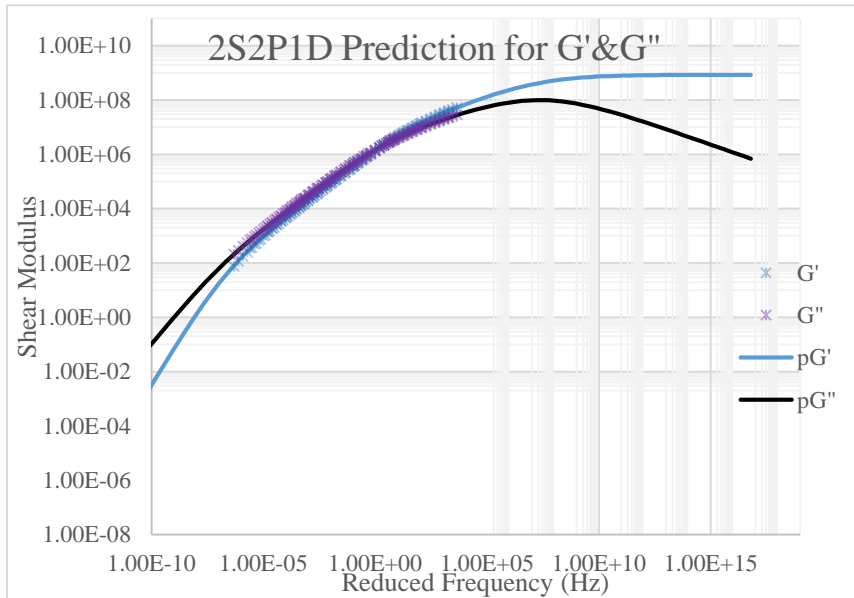
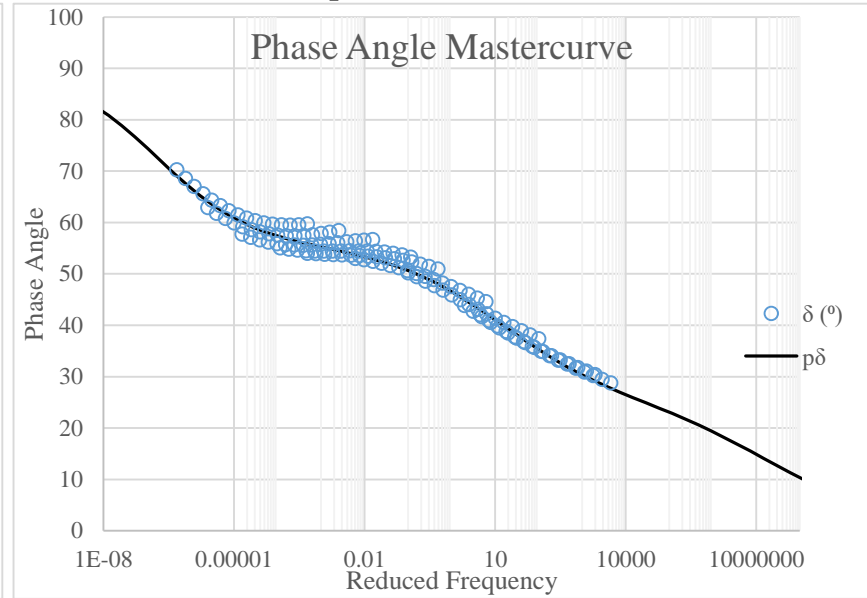
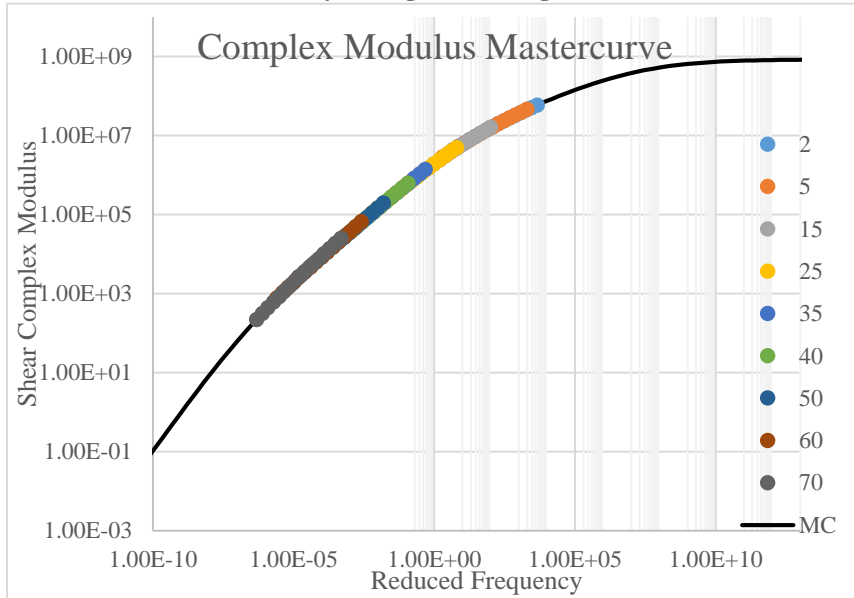
Laboratory Long-Term Aged Mixture – Extracted & Recovered from Bespoke Chamber: BC10-H₂O



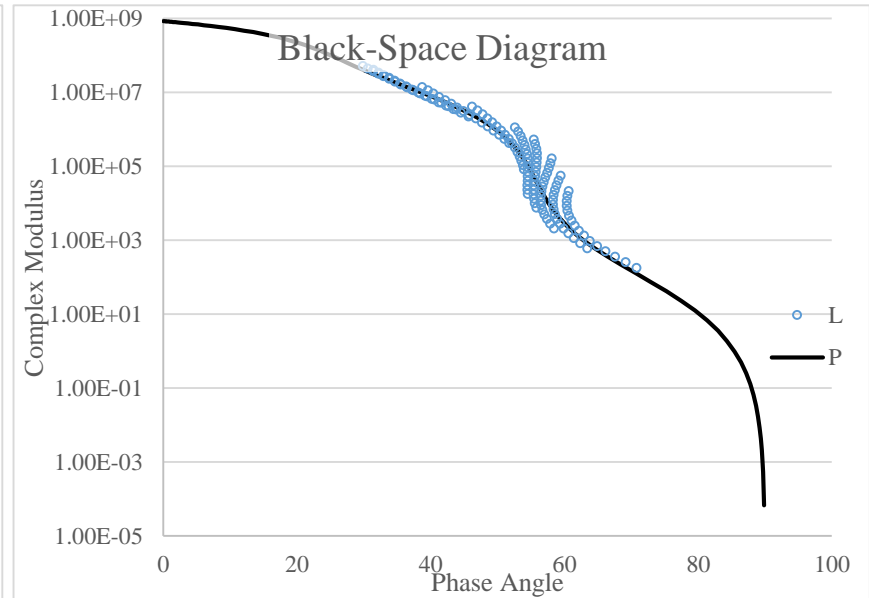
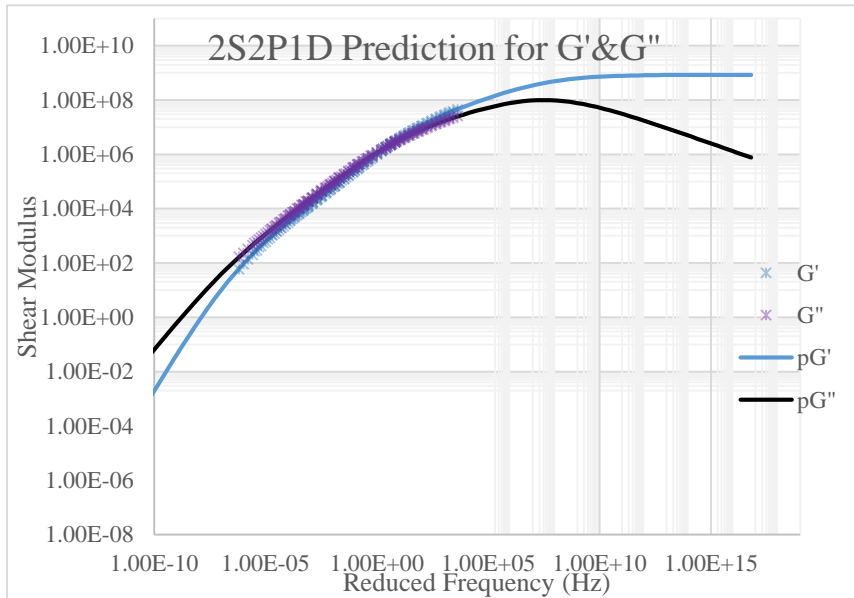
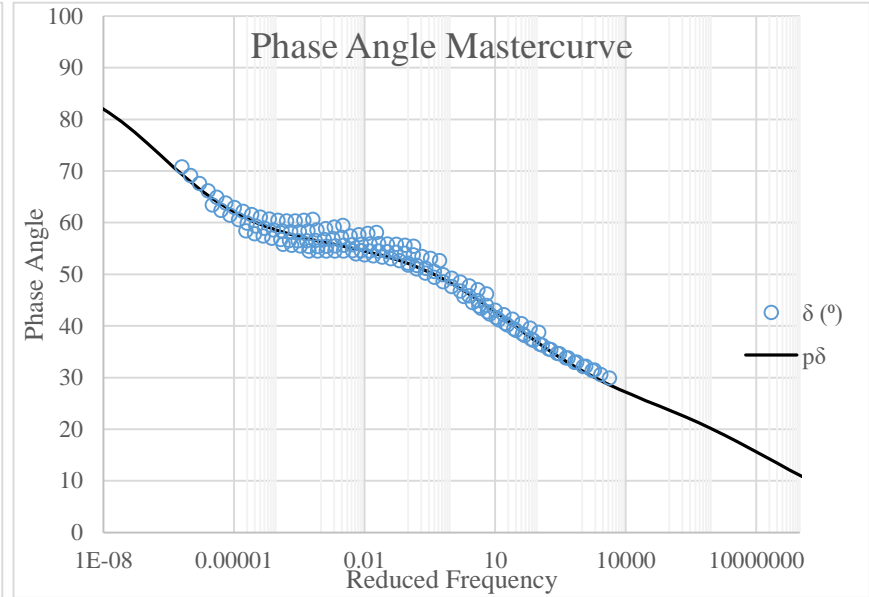
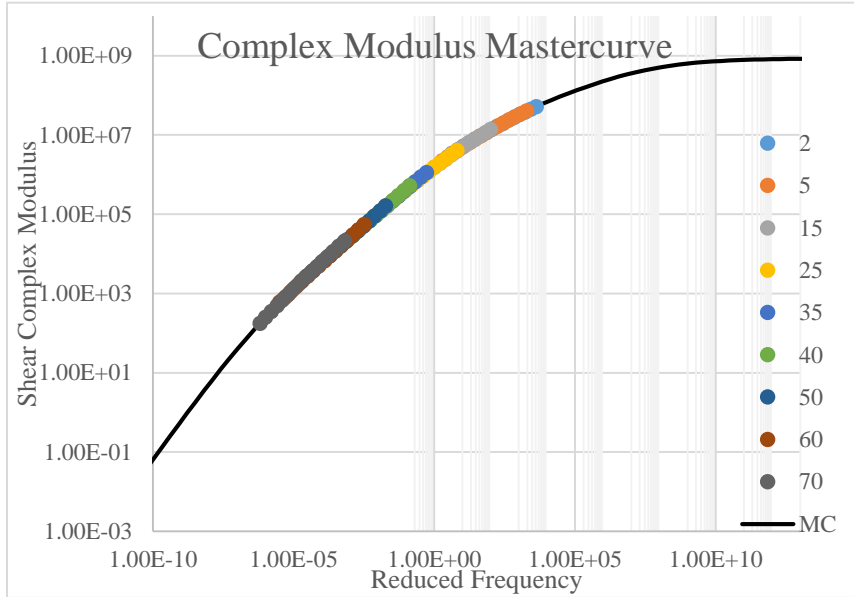
Laboratory Long-Term Aged Mixture – Extracted & Recovered from Bespoke Chamber: BC10-NoH₂O



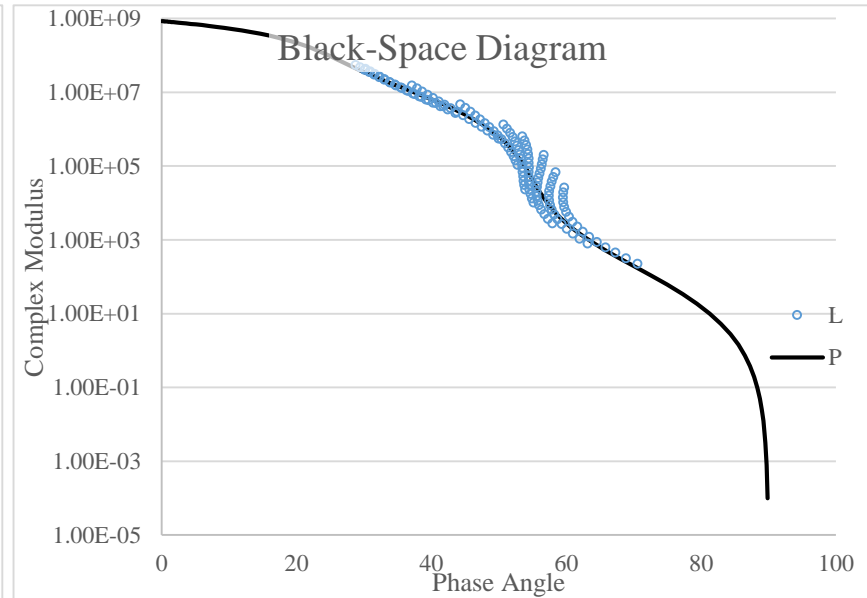
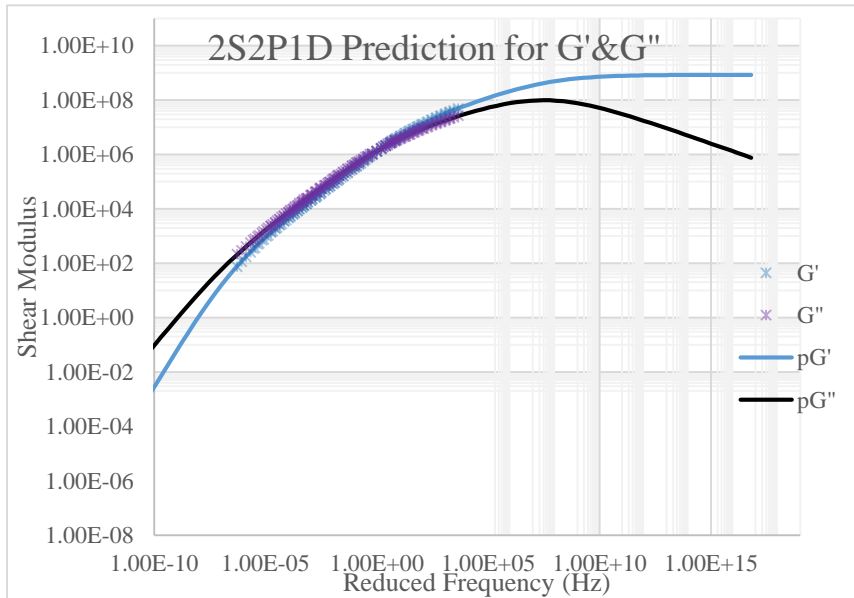
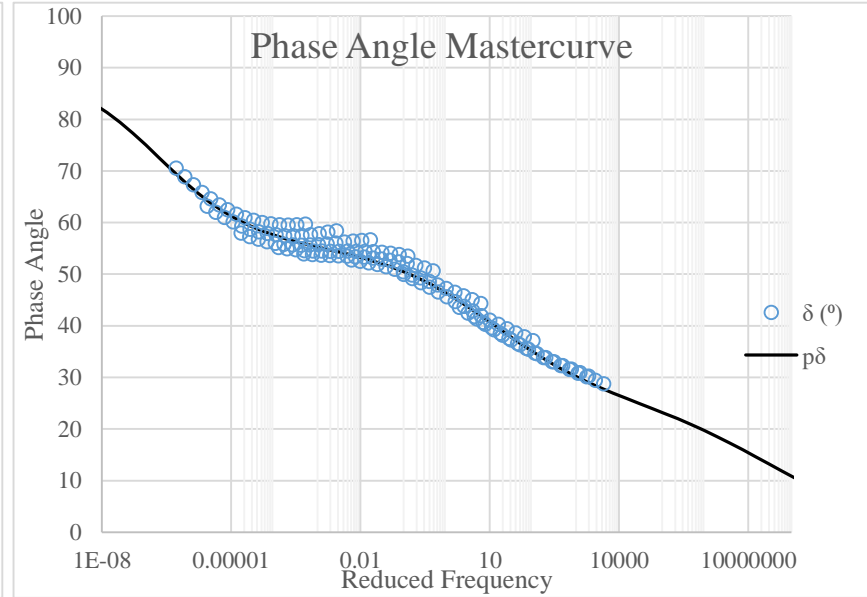
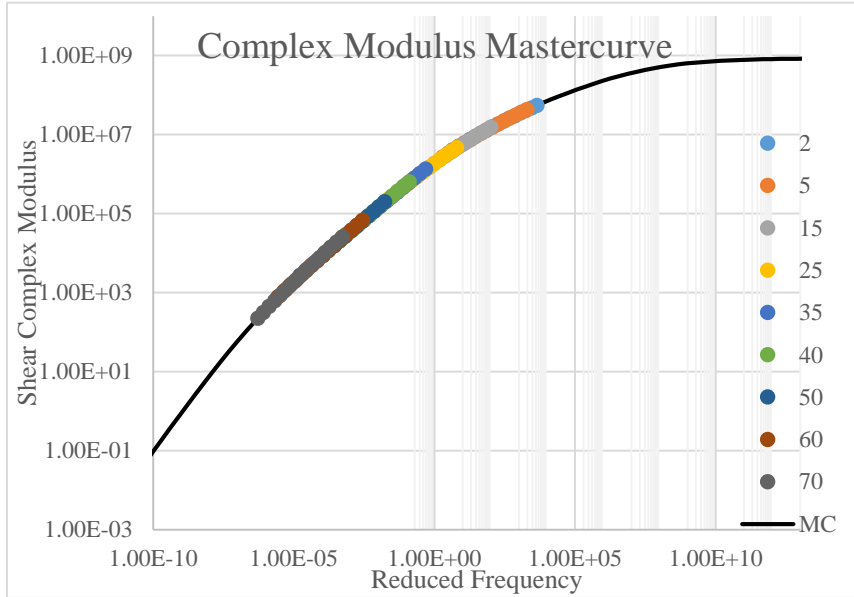
Laboratory Long-Term Aged Mixture – Extracted & Recovered from Bespoke Chamber: BC15-H₂O



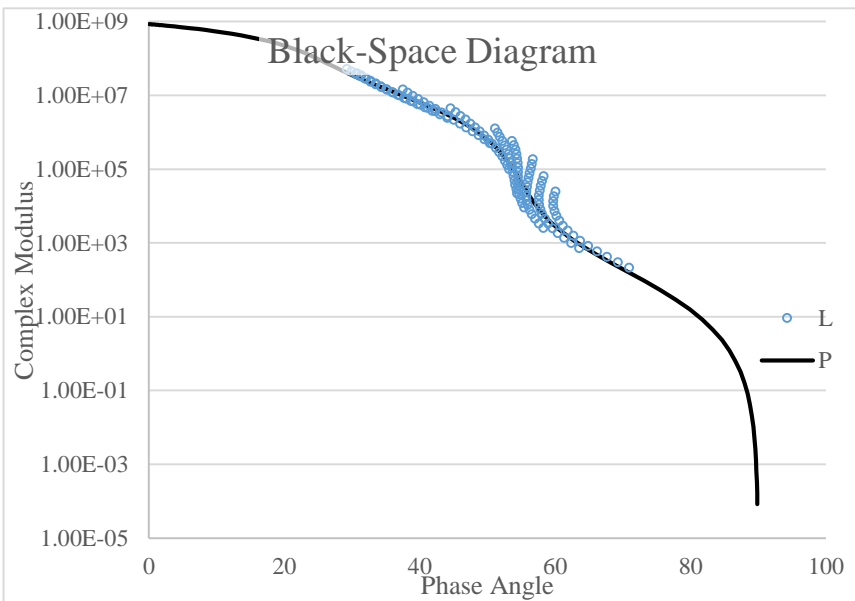
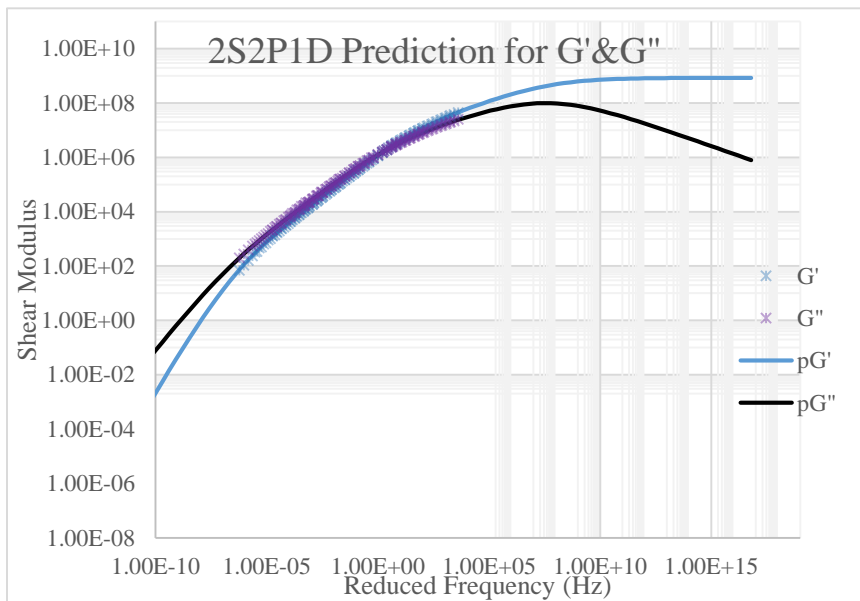
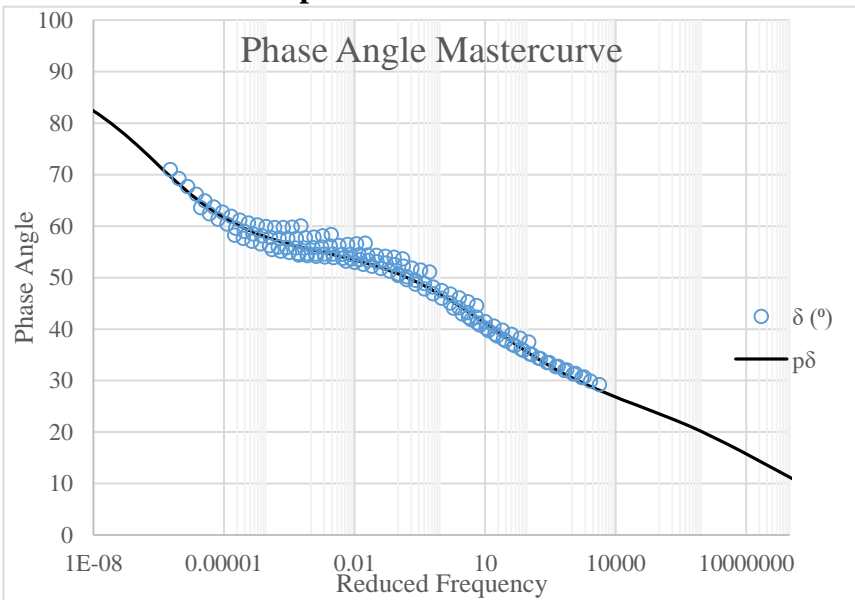
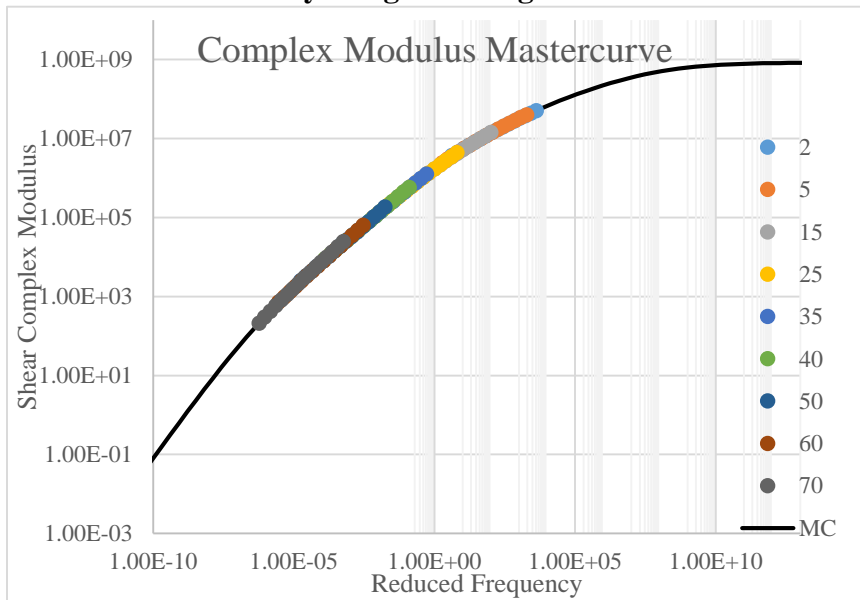
Laboratory Long-Term Aged Mixture – Extracted & Recovered from Bespoke Chamber: BC15-NoH₂O



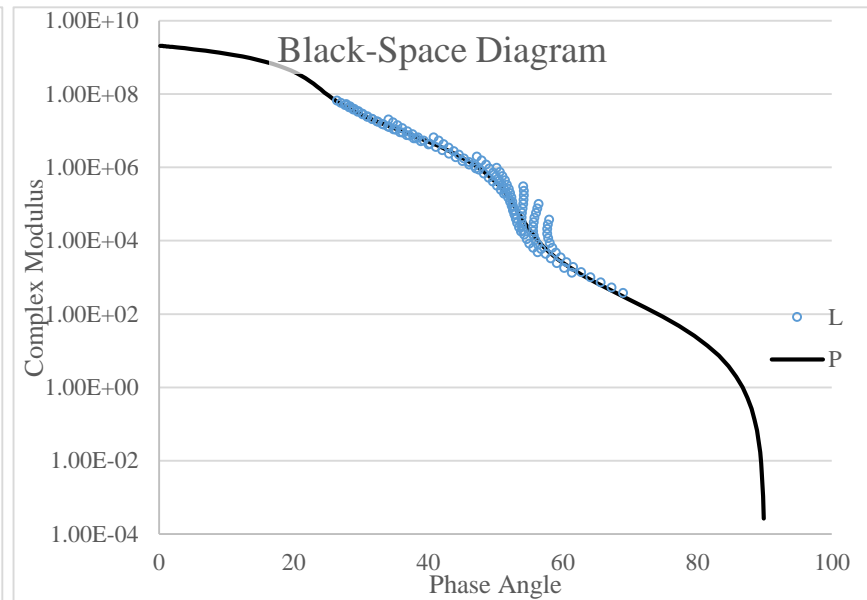
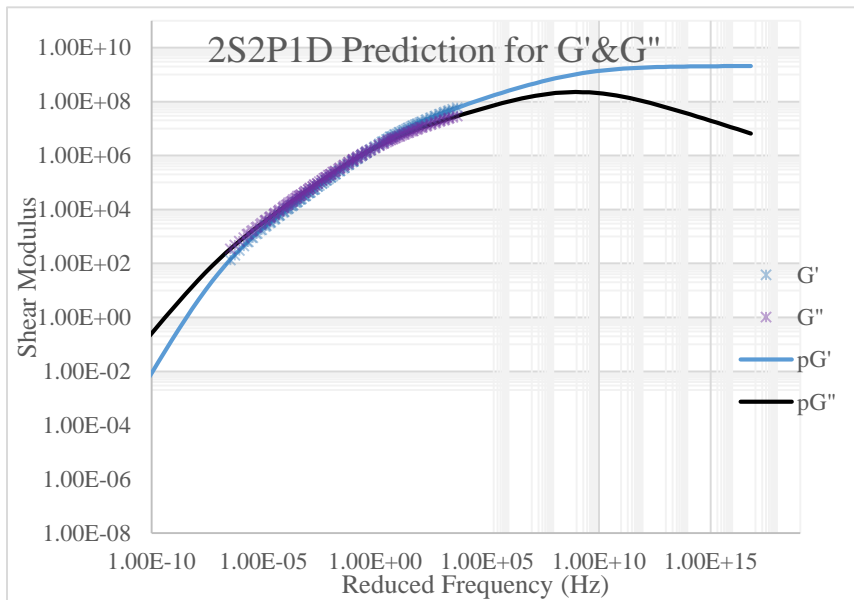
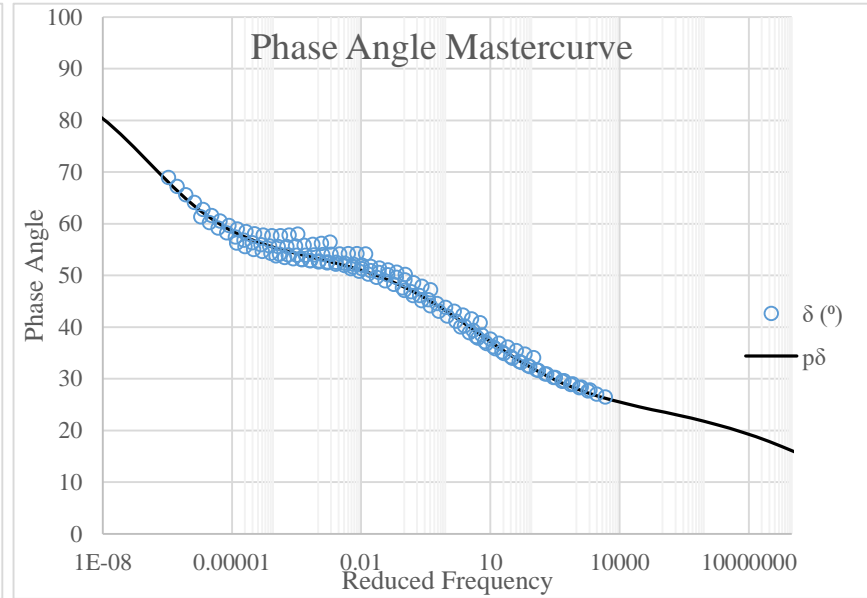
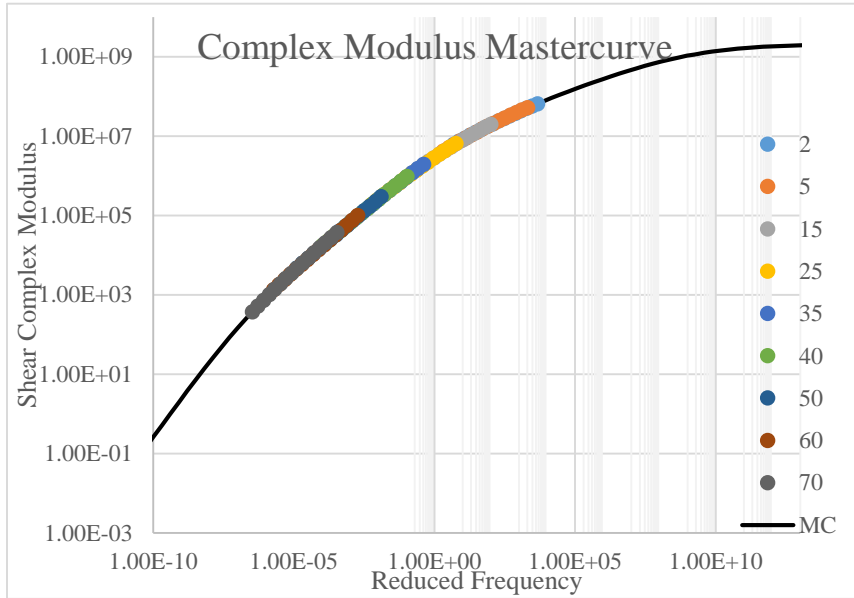
Laboratory Long-Term Aged Mixture – Extracted & Recovered from Bespoke Chamber: BC20-H₂O



Laboratory Long-Term Aged Mixture – Extracted & Recovered from Bespoke Chamber: BC20-NoH₂O



Extended PAV Conditioned Binder – RTFOT + Double PAV



APPENDIX D: MSCR TEST REPORTS

MSCR-Test (AASHTO T350-14) - Final Report

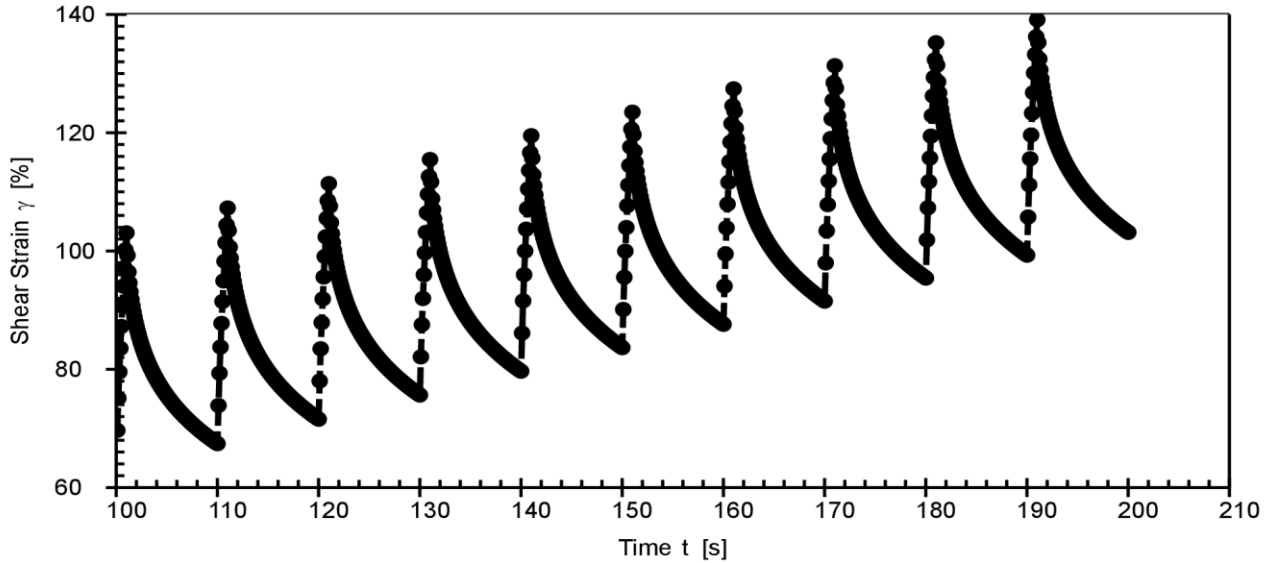
Project name: 2018-05-03_MSCR (V2)

Date, Time: 2018-05-03 4:45:50 PM
Test name: 2018-05-03_MSCR_0.1/3.2kPa
Operator: user
Sample: YASHAR
Batch no.: MTO2
Description: VIRGIN
Configuration: Anton Paar SmartPave 102 SN82314644
PP25/PE SN52739

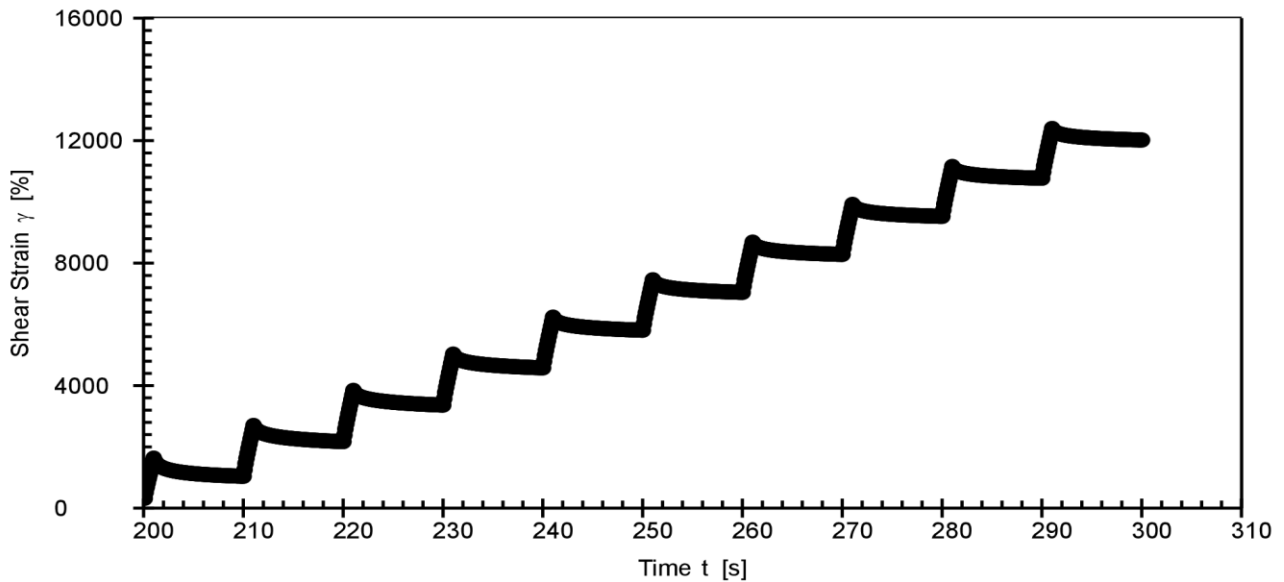
P-PTD200+H-PTD120 SN82331818-82284206



MSCR 0.1kPa (conditioning cycles are not shown)



MSCR 3.2kPa



Responsible Employee:

Signature:

MSCR-Test (AASHTO T350-14) - Final Report

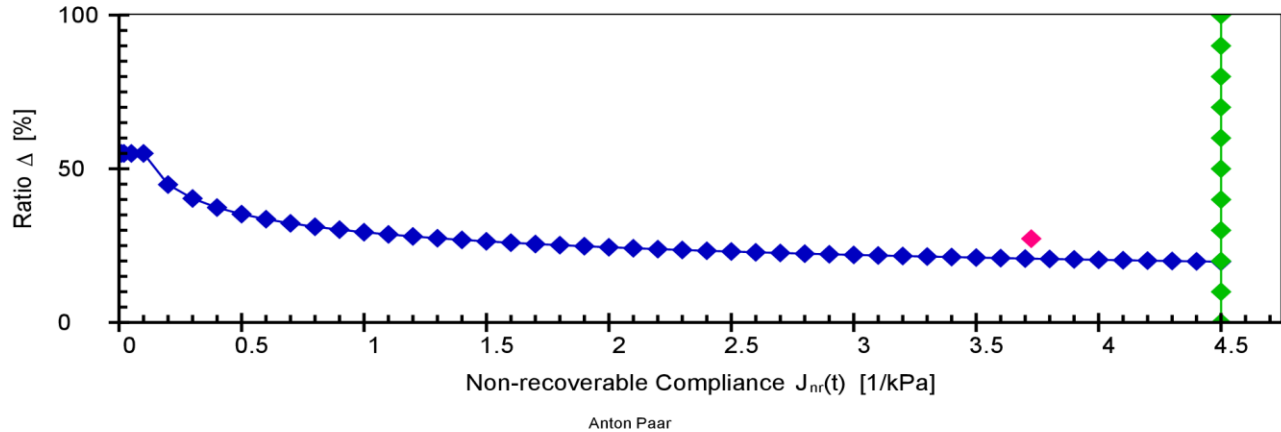
Project name: 2018-05-03_MSCR (V2)



Date, Time: 2018-05-03 4:45:50 PM
 Test name: 2018-05-03_MSCR_0.1/3.2kPa
 Operator: user
 Sample: YASHAR
 Batch no.: MTO2
 Description: VIRGIN
 Configuration: Anton Paar SmartPave 102 SN82314644
 PP25/PE SN52739

P-PTD200+H-PTD120 SN82331818-82284206

Jnr vs. % recovery (at 3.2 kPa)



Asphalt MSCR

Application version: Anton Paar RheoCompass™, V1.20.471-Release
 Licensed for: University of Waterloo - CPATT, License no. Rh17H7681, Version no. 1.20.0.0
 Project: 2018-05-03_MSCR (V2)
 Input data: 2018-05-03_MSCR_0.1/3.2kPa, <Last measuring result>, From interval 1, Point 1
 Result data: Asphalt MSCR Analysis

PARAMETERS:
 Load level mode: User-defined load levels (not according to norm)
 Number of intervals to skip: 0
 Calculation mode: Calculation according to ASTM D7405 - 15 and AASHTO M 332-14

Level 1
 Load: 0.1 kPa
 Conditioning cycles: 10
 Analyzed cycles: 10
 Creep phase duration: 1 s
 Recovery phase duration: 9 s

Level 2
 Load: 3.2 kPa
 Conditioning cycles: 0
 Analyzed cycles: 10
 Creep phase duration: 1 s
 Recovery phase duration: 9 s

Show parameter settings: On
 Show result table: Detailed (according to norm)
 Show classification: On

RESULTS:
 Sample name: -
 Test date: 4:30:20 PM
 Test temperature: 64.00 °C

Load level 0.1 kPa (average load: 0.1 kPa)

Cycle	Load [kPa]	$\bar{\epsilon}_0$ [%]	$\bar{\epsilon}_c$ [%]	$\bar{\epsilon}_1$ [%]	$\bar{\epsilon}_r$ [%]	$\bar{\epsilon}_{10}$ [%]	R _N [%]	J _{nr} (0.1, N) [1/kPa]
1	0.1	63.20	103.07	39.87	67.42	4.22	89.42	0.4218
2	0.1	67.42	107.27	39.85	71.56	4.14	89.61	0.4142

Responsible Employee:

Signature:

MSCR-Test (AASHTO T350-14) - Final Report

Project name: 2018-05-03_MSCR (V2)



Date, Time: 2018-05-03 4:45:50 PM
 Test name: 2018-05-03_MSCR_0.1/3.2kPa
 Operator: user
 Sample: YASHAR
 Batch no.: MTO2
 Description: VIRGIN
 Configuration: Anton Paar SmartPave 102 SN82314644

	PP25/PE SN52739						P-PTD200+H-PTD120 SN82331818-82284206		
3	0.1	71.56	111.41	39.85	75.64	4.08	89.76	0.4081	
4	0.1	75.64	115.48	39.84	79.67	4.03	89.90	0.4025	
5	0.1	79.67	119.50	39.83	83.65	3.99	90.00	0.3985	
6	0.1	83.65	123.48	39.83	87.60	3.95	90.08	0.3950	
7	0.1	87.60	127.43	39.82	91.52	3.92	90.16	0.3920	
8	0.1	91.52	131.34	39.82	95.42	3.90	90.21	0.3899	
9	0.1	95.42	135.22	39.80	99.29	3.87	90.27	0.3873	
10	0.1	99.29	139.11	39.81	103.15	3.86	90.32	0.3855	
							R _{0.1} = 89.97	J _{nr(0.1)} = 0.3995	

Load level 3.2 kPa (average load: 3.2 kPa)

Cycle	Load [kPa]	ϵ_0 [%]	ϵ_c [%]	ϵ_l [%]	ϵ_r [%]	ϵ_{10} [%]	R _N [%]	J _{nr(3.2, N)} [1/kPa]
1	3.2	103.15	1633.58	1530.43	1040.19	937.04	38.77	2.9282
2	3.2	1040.19	2701.86	1661.67	2171.39	1131.21	31.92	3.5350
3	3.2	2171.39	3846.20	1674.81	3364.93	1193.54	28.74	3.7298
4	3.2	3364.93	5030.32	1665.39	4580.64	1215.71	27.00	3.7991
5	3.2	4580.64	6237.71	1657.08	5809.62	1228.99	25.83	3.8406
6	3.2	5809.62	7459.10	1649.48	7045.89	1236.27	25.05	3.8633
7	3.2	7045.89	8687.66	1641.76	8285.34	1239.44	24.51	3.8733
8	3.2	8285.34	9920.86	1635.52	9527.61	1242.28	24.04	3.8821
9	3.2	9527.61	11158.04	1630.42	10772.60	1244.99	23.64	3.8906
10	3.2	10772.60	12400.12	1627.52	12023.16	1250.55	23.16	3.9080
							R _{3.2} = 27.27	J _{nr(3.2)} = 3.7250

Average percent recovery

Load level 0.1 kPa R_{0.1} = 89.97 %
 Load level 3.2 kPa R_{3.2} = 27.27 %

Percent difference of recovery

Load levels 0.1 kPa and 3.2 kPa R_{diff} = 69.69 %

Average non-recoverable creep compliance

Load level 0.1 kPa J_{nr(0.1)} = 0.3995 1/kPa
 Load level 3.2 kPa J_{nr(3.2)} = 3.7250 1/kPa

Percent difference of non-recoverable creep compliance

Load levels 0.1 kPa and 3.2 kPa J_{nr_diff} = 832.49 %

Indication that the asphalt binder is modified with an acceptable elastomeric polymer

Load level 3.2 kPa above criterion (probably modified)

FAILED at 64.00 °C according to AASHTO M 332-14.

Responsible Employee:

Signature:

MSCR-Test (AASHTO T350-14) - Final Report

Project name: 2018-05-02_MSCR (V2)

Date, Time: 2018-05-02 12:34:44 PM

Test name: 2018-05-02_MSCR_0.1/3.2kPa

Operator: user

Sample: YASHAR

Batch no.: MTO2

Description: EXTRACTED VIRGIN

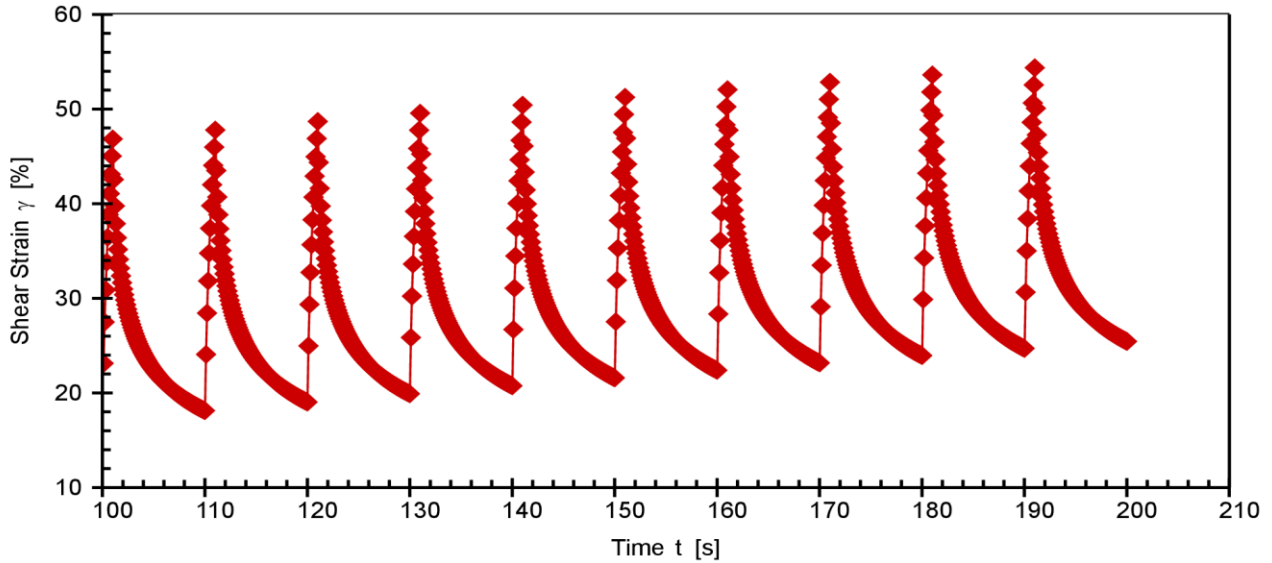
Configuration: Anton Paar SmartPave 102 SN82314644

PP25/PE SN52739

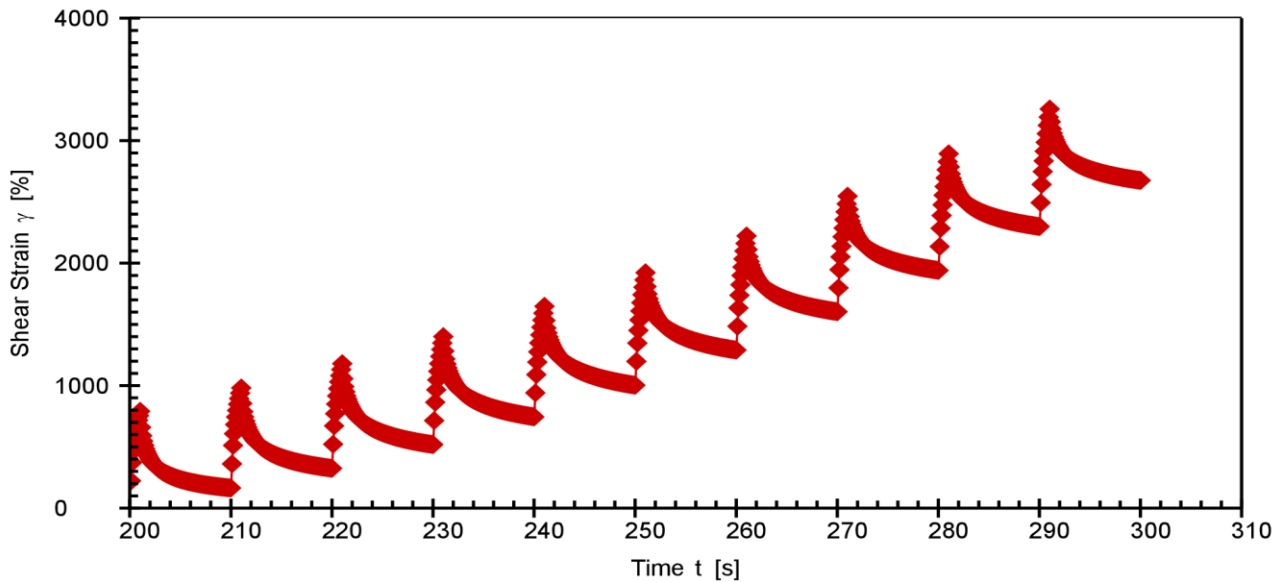
P-PTD200+H-PTD120 SN82331818-82284206



MSCR 0.1kPa (conditioning cycles are not shown)



MSCR 3.2kPa



Responsible Employee:

Signature:

MSCR-Test (AASHTO T350-14) - Final Report

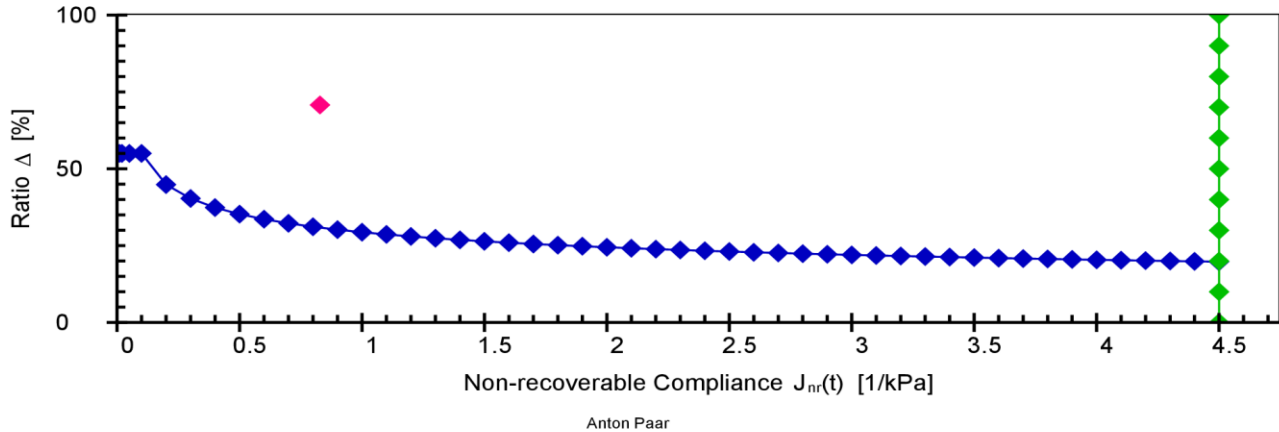
Project name: 2018-05-02_MSCR (V2)



Date, Time: 2018-05-02 12:34:44 PM
 Test name: 2018-05-02_MSCR_0.1/3.2kPa
 Operator: user
 Sample: YASHAR
 Batch no.: MTO2
 Description: EXTRACTED VIRGIN
 Configuration: Anton Paar SmartPave 102 SN82314644
 PP25/PE SN52739

P-PTD200+H-PTD120 SN82331818-82284206

J_{nr} vs. % recovery (at 3.2 kPa)



Asphalt MSCR

Application version: Anton Paar RheoCompass™, V1.20.471-Release
 Licensed for: University of Waterloo - CPATT, License no. Rh17H7681, Version no. 1.20.0.0
 Project: 2018-05-02_MSCR (V2)
 Input data: 2018-05-02_MSCR_0.1/3.2kPa, <Last measuring result>, From interval 1, Point 1
 Result data: Asphalt MSCR Analysis

PARAMETERS:
 Load level mode: User-defined load levels (not according to norm)
 Number of intervals to skip: 0
 Calculation mode: Calculation according to ASTM D7405 - 15 and AASHTO M 332-14

Level 1
 Load: 0.1 kPa
 Conditioning cycles: 10
 Analyzed cycles: 10
 Creep phase duration: 1 s
 Recovery phase duration: 9 s

Level 2
 Load: 3.2 kPa
 Conditioning cycles: 0
 Analyzed cycles: 10
 Creep phase duration: 1 s
 Recovery phase duration: 9 s

Show parameter settings: On
 Show result table: Detailed (according to norm)
 Show classification: On

RESULTS:
 Sample name: -
 Test date: 12:19:20 PM
 Test temperature: 64.00 °C

Load level 0.1 kPa (average load: 0.1 kPa)

Cycle	Load [kPa]	$\bar{\epsilon}_0$ [%]	$\bar{\epsilon}_c$ [%]	$\bar{\epsilon}_1$ [%]	$\bar{\epsilon}_r$ [%]	$\bar{\epsilon}_{10}$ [%]	R _N [%]	J _{nr} (0.1, N) [1/kPa]
1	0.1	17.18	46.84	29.66	18.13	0.95	96.81	0.0946
2	0.1	18.13	47.79	29.66	19.03	0.90	96.95	0.0905

Responsible Employee:

Signature:

MSCR-Test (AASHTO T350-14) - Final Report

Project name: 2018-05-02_MSCR (V2)



Date, Time: 2018-05-02 12:34:44 PM
 Test name: 2018-05-02_MSCR_0.1/3.2kPa
 Operator: user
 Sample: YASHAR
 Batch no.: MTO2
 Description: EXTRACTED VIRGIN
 Configuration: Anton Paar SmartPave 102 SN82314644

PP25/PE SN52739

P-PTD200+H-PTD120 SN82331818-82284206

3	0.1	19.03	48.69	29.66	19.91	0.88	97.03	0.0880
4	0.1	19.91	49.57	29.66	20.76	0.85	97.14	0.0847
5	0.1	20.76	50.42	29.66	21.59	0.83	97.21	0.0827
6	0.1	21.59	51.25	29.66	22.39	0.81	97.28	0.0807
7	0.1	22.39	52.05	29.66	23.18	0.78	97.35	0.0785
8	0.1	23.18	52.84	29.66	23.95	0.77	97.41	0.0770
9	0.1	23.95	53.62	29.67	24.70	0.75	97.46	0.0754
10	0.1	24.70	54.37	29.67	25.44	0.74	97.52	0.0737
R _{0.1} = 97.22 J _{nr} (0.1) = 0.0826								

Load level 3.2 kPa (average load: 3.2 kPa)

Cycle	Load [kPa]	ϵ_0 [%]	ϵ_c [%]	ϵ_l [%]	ϵ_r [%]	ϵ_{10} [%]	R _N [%]	J _{nr} (3.2, N) [1/kPa]
1	3.2	25.44	791.22	765.78	164.42	138.98	81.85	0.4343
2	3.2	164.42	981.10	816.68	325.12	160.70	80.32	0.5022
3	3.2	325.12	1179.20	854.08	518.91	193.79	77.31	0.6056
4	3.2	518.91	1400.45	881.54	745.51	226.60	74.29	0.7081
5	3.2	745.51	1647.87	902.36	1003.40	257.89	71.42	0.8059
6	3.2	1003.40	1921.95	918.55	1290.26	286.86	68.77	0.8965
7	3.2	1290.26	2222.54	932.27	1603.60	313.34	66.39	0.9792
8	3.2	1603.60	2547.09	943.49	1940.96	337.36	64.24	1.0543
9	3.2	1940.96	2892.82	951.86	2298.86	357.90	62.40	1.1184
10	3.2	2298.86	3258.53	959.67	2676.34	377.48	60.67	1.1796
R _{3.2} = 70.77 J _{nr} (3.2) = 0.8284								

Average percent recovery

Load level 0.1 kPa
 Load level 3.2 kPa

R_{0.1} = 97.22 %
 R_{3.2} = 70.77 %

Percent difference of recovery

Load levels 0.1 kPa and 3.2 kPa

R_{diff} = 27.21 %

Average non-recoverable creep compliance

Load level 0.1 kPa
 Load level 3.2 kPa

J_{nr}(0.1) = 0.0826 1/kPa
 J_{nr}(3.2) = 0.8284 1/kPa

Percent difference of non-recoverable creep compliance

Load levels 0.1 kPa and 3.2 kPa

J_{nr_diff} = 903.27 %

Indication that the asphalt binder is modified with an acceptable elastomeric polymer

Load level 3.2 kPa

above criterion (probably modified)

FAILED at 64.00 °C according to AASHTO M 332-14.

Responsible Employee:

Signature:

MSCR-Test (AASHTO T350-14) - Final Report

Project name: 2018-05-02_MSCR (V2)

Date, Time: 2018-05-02 1:27:02 PM

Test name: 2018-05-02_MSCR_0.1/3.2kPa

Operator: user

Sample: YASHAR

Batch no.: MTO2

Description: RTFOT

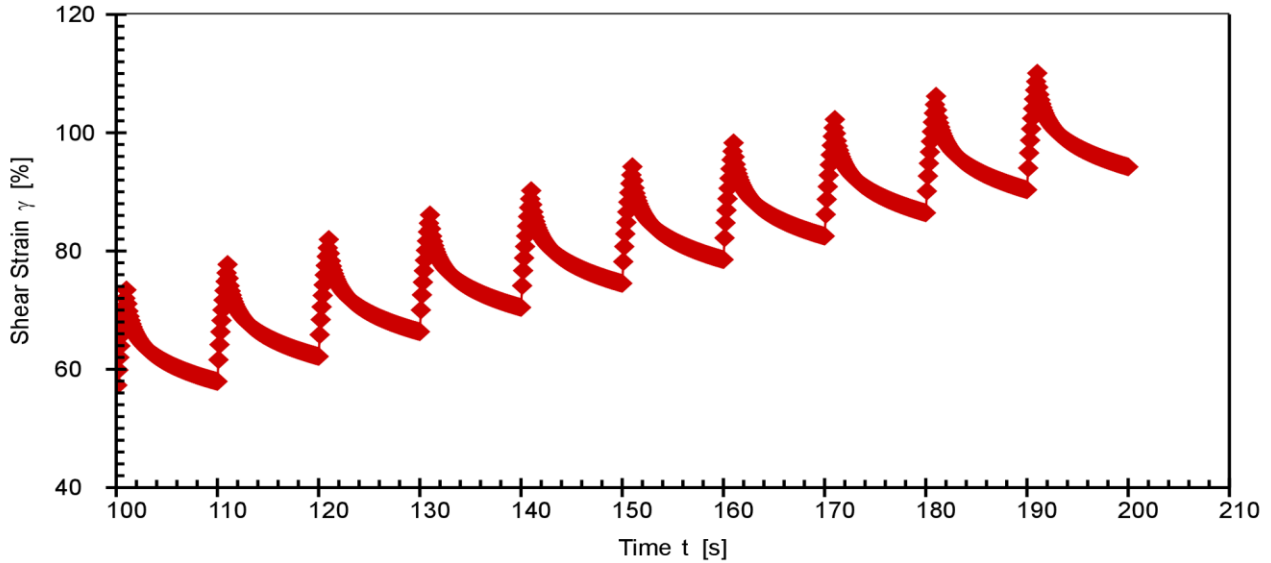
Configuration: Anton Paar SmartPave 102 SN82314644

PP25/PE SN52739

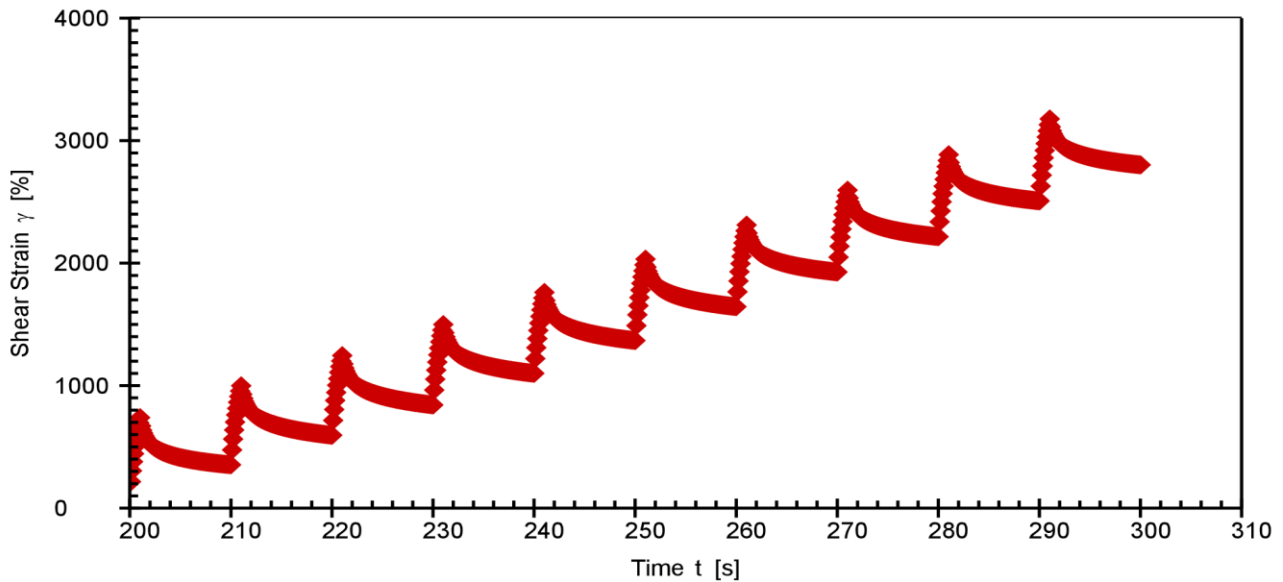
P-PTD200+H-PTD120 SN82331818-82284206



MSCR 0.1kPa (conditioning cycles are not shown)



MSCR 3.2kPa



Responsible Employee:

Signature:

MSCR-Test (AASHTO T350-14) - Final Report

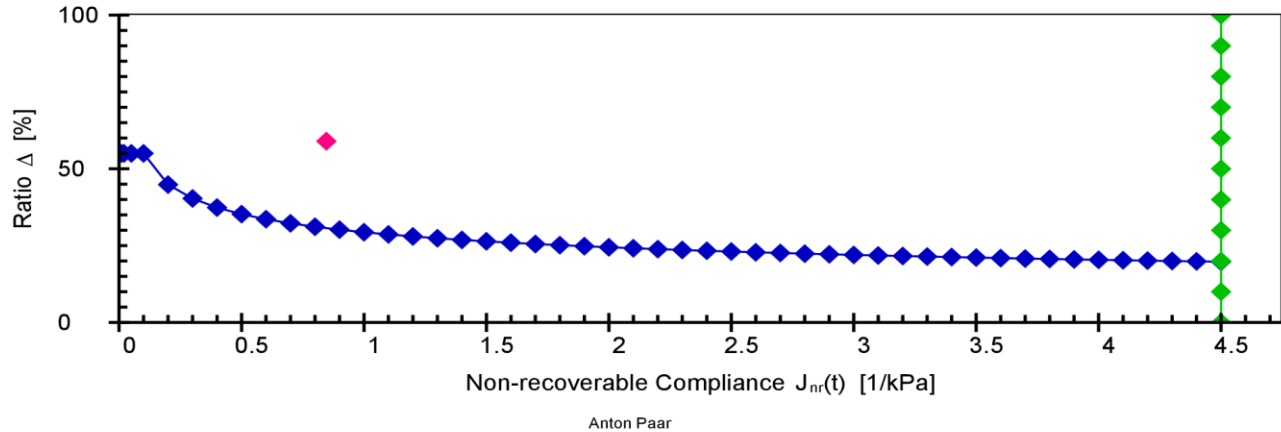
Project name: 2018-05-02_MSCR (V2)



Date, Time: 2018-05-02 1:27:02 PM
 Test name: 2018-05-02_MSCR_0.1/3.2kPa
 Operator: user
 Sample: YASHAR
 Batch no.: MTO2
 Description: RTFOT
 Configuration: Anton Paar SmartPave 102 SN82314644
 PP25/PE SN52739

P-PTD200+H-PTD120 SN82331818-82284206

J_{nr} vs. % recovery (at 3.2 kPa)



Asphalt MSCR

Application version: Anton Paar RheoCompass™, V1.20.471-Release
 Licensed for: University of Waterloo - CPATT, License no. Rh17H7681, Version no. 1.20.0.0
 Project: 2018-05-02_MSCR (V2)
 Input data: 2018-05-02_MSCR_0.1/3.2kPa, <Last measuring result>, From interval 1, Point 1
 Result data: Asphalt MSCR Analysis

PARAMETERS:
 Load level mode: User-defined load levels (not according to norm)
 Number of intervals to skip: 0
 Calculation mode: Calculation according to ASTM D7405 - 15 and AASHTO M 332-14

Level 1
 Load: 0.1 kPa
 Conditioning cycles: 10
 Analyzed cycles: 10
 Creep phase duration: 1 s
 Recovery phase duration: 9 s

Level 2
 Load: 3.2 kPa
 Conditioning cycles: 0
 Analyzed cycles: 10
 Creep phase duration: 1 s
 Recovery phase duration: 9 s

Show parameter settings: On
 Show result table: Detailed (according to norm)
 Show classification: On

RESULTS:
 Sample name: -
 Test date: 1:11:42 PM
 Test temperature: 64.00 °C

Load level 0.1 kPa (average load: 0.1 kPa)

Cycle	Load [kPa]	$\bar{\epsilon}_0$ [%]	$\bar{\epsilon}_c$ [%]	$\bar{\epsilon}_1$ [%]	$\bar{\epsilon}_r$ [%]	$\bar{\epsilon}_{10}$ [%]	R _N [%]	J _{nr} (0.1, N) [1/kPa]
1	0.1	53.64	73.43	19.80	57.95	4.31	78.23	0.4310
2	0.1	57.95	77.72	19.78	62.18	4.23	78.60	0.4233

Responsible Employee:

Signature:

MSCR-Test (AASHTO T350-14) - Final Report

Project name: 2018-05-02_MSCR (V2)



Date, Time: 2018-05-02 1:27:02 PM
 Test name: 2018-05-02_MSCR_0.1/3.2kPa
 Operator: user
 Sample: YASHAR
 Batch no.: MTO2
 Description: RTFOT
 Configuration: Anton Paar SmartPave 102 SN82314644

PP25/PE SN52739

P-PTD200+H-PTD120 SN82331818-82284206

3	0.1	62.18	81.95	19.77	66.35	4.17	78.91	0.4171
4	0.1	66.35	86.11	19.76	70.46	4.11	79.19	0.4112
5	0.1	70.46	90.22	19.76	74.52	4.06	79.43	0.4063
6	0.1	74.52	94.27	19.75	78.54	4.02	79.65	0.4018
7	0.1	78.54	98.28	19.74	82.52	3.97	79.87	0.3975
8	0.1	82.52	102.25	19.73	86.45	3.94	80.05	0.3936
9	0.1	86.45	106.18	19.73	90.36	3.90	80.22	0.3902
10	0.1	90.36	110.07	19.72	94.22	3.87	80.38	0.3869
R _{0.1} = 79.45 J _{nr} (0.1) = 0.4059								

Load level 3.2 kPa

(average load: 3.2 kPa)

Cycle	Load [kPa]	ϵ_0 [%]	ϵ_c [%]	ϵ_l [%]	ϵ_r [%]	ϵ_{10} [%]	R _N [%]	J _{nr} (3.2, N) [1/kPa]
1	3.2	94.22	739.79	645.57	353.82	259.60	59.79	0.8112
2	3.2	353.82	998.82	644.99	594.93	241.11	62.62	0.7535
3	3.2	594.93	1245.70	650.77	842.45	247.52	61.97	0.7735
4	3.2	842.45	1498.96	656.51	1100.25	257.79	60.73	0.8056
5	3.2	1100.25	1761.43	661.18	1368.18	267.93	59.48	0.8373
6	3.2	1368.18	2032.73	664.55	1644.69	276.51	58.39	0.8641
7	3.2	1644.69	2311.45	666.76	1927.69	283.00	57.56	0.8844
8	3.2	1927.69	2596.49	668.80	2216.07	288.38	56.88	0.9012
9	3.2	2216.07	2885.55	669.49	2507.98	291.91	56.40	0.9122
10	3.2	2507.98	3177.49	669.51	2802.89	294.91	55.95	0.9216
R _{3.2} = 58.98 J _{nr} (3.2) = 0.8465								

Average percent recovery

Load level 0.1 kPa
 Load level 3.2 kPa

R_{0.1} = 79.45 %
 R_{3.2} = 58.98 %

Percent difference of recovery

Load levels 0.1 kPa and 3.2 kPa

R_{diff} = 25.77 %

Average non-recoverable creep compliance

Load level 0.1 kPa
 Load level 3.2 kPa

J_{nr}(0.1) = 0.4059 1/kPa
 J_{nr}(3.2) = 0.8465 1/kPa

Percent difference of non-recoverable creep compliance

Load levels 0.1 kPa and 3.2 kPa

J_{nr_diff} = 108.54 %

Indication that the asphalt binder is modified with an acceptable elastomeric polymer

Load level 3.2 kPa

above criterion (probably modified)

FAILED at 64.00 °C according to AASHTO M 332-14.

Responsible Employee:

Signature:

MSCR-Test (AASHTO T350-14) - Final Report

Project name: 2018-05-02_MSCR (V2)

Date, Time: 2018-05-02 1:01:03 PM

Test name: 2018-05-02_MSCR_0.1/3.2kPa

Operator: user

Sample: YASHAR

Batch no.: MTO2

Description: LOOSE MIX

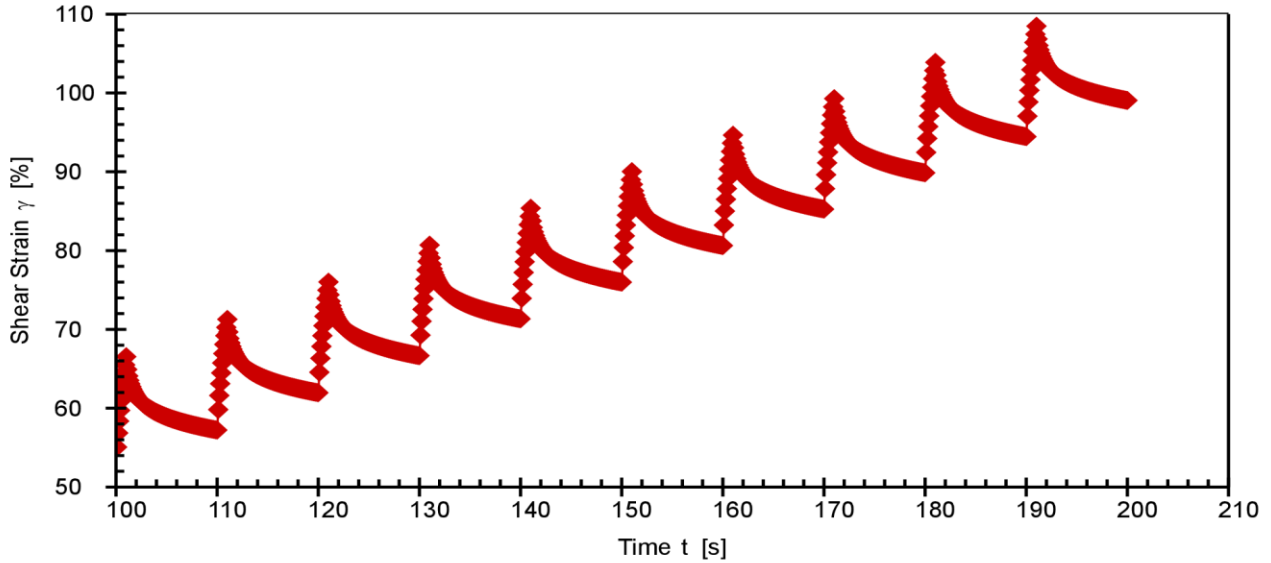
Configuration: Anton Paar SmartPave 102 SN82314644

PP25/PE SN52739

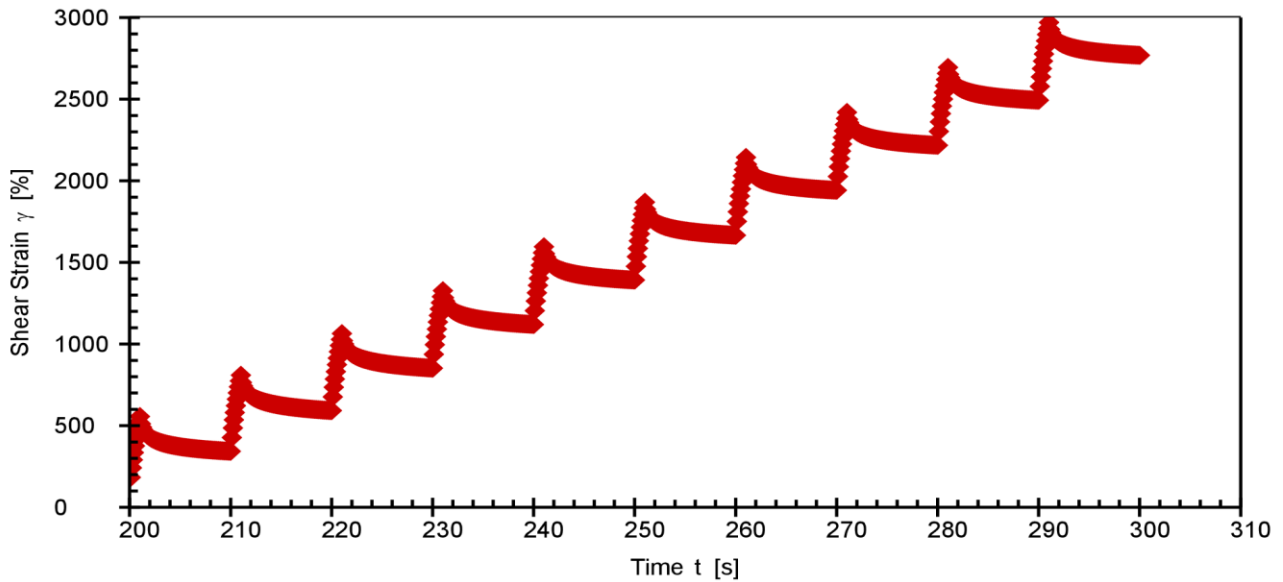
P-PTD200+H-PTD120 SN82331818-82284206



MSCR 0.1kPa (conditioning cycles are not shown)



MSCR 3.2kPa



Responsible Employee:

Signature:

MSCR-Test (AASHTO T350-14) - Final Report

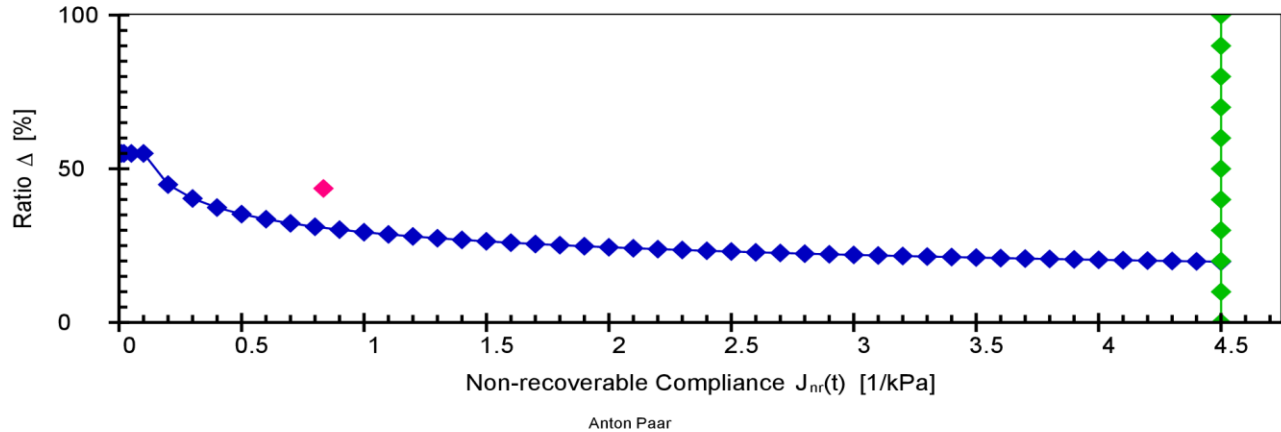
Project name: 2018-05-02_MSCR (V2)



Date, Time: 2018-05-02 1:01:03 PM
 Test name: 2018-05-02_MSCR_0.1/3.2kPa
 Operator: user
 Sample: YASHAR
 Batch no.: MTO2
 Description: LOOSE MIX
 Configuration: Anton Paar SmartPave 102 SN82314644
 PP25/PE SN52739

P-PTD200+H-PTD120 SN82331818-82284206

Jnr vs. % recovery (at 3.2 kPa)



Asphalt MSCR

Application version: Anton Paar RheoCompass™, V1.20.471-Release
 Licensed for: University of Waterloo - CPATT, License no. Rh17H7681, Version no. 1.20.0.0
 Project: 2018-05-02_MSCR (V2)
 Input data: 2018-05-02_MSCR_0.1/3.2kPa, <Last measuring result>, From interval 1, Point 1
 Result data: Asphalt MSCR Analysis

PARAMETERS:
 Load level mode: User-defined load levels (not according to norm)
 Number of intervals to skip: 0
 Calculation mode: Calculation according to ASTM D7405 - 15 and AASHTO M 332-14

Level 1
 Load: 0.1 kPa
 Conditioning cycles: 10
 Analyzed cycles: 10
 Creep phase duration: 1 s
 Recovery phase duration: 9 s

Level 2
 Load: 3.2 kPa
 Conditioning cycles: 0
 Analyzed cycles: 10
 Creep phase duration: 1 s
 Recovery phase duration: 9 s

Show parameter settings: On
 Show result table: Detailed (according to norm)
 Show classification: On

RESULTS:
 Sample name: -
 Test date: 12:45:39 PM
 Test temperature: 64.00 °C

Load level 0.1 kPa (average load: 0.1 kPa)

Cycle	Load [kPa]	$\bar{\epsilon}_0$ [%]	$\bar{\epsilon}_c$ [%]	$\bar{\epsilon}_1$ [%]	$\bar{\epsilon}_r$ [%]	$\bar{\epsilon}_{10}$ [%]	R _N [%]	J _{nr} (0.1, N) [1/kPa]
1	0.1	52.47	66.54	14.07	57.23	4.76	66.17	0.4759
2	0.1	57.23	71.29	14.06	61.96	4.73	66.35	0.4731

Responsible Employee:

Signature:

MSCR-Test (AASHTO T350-14) - Final Report

Project name: 2018-05-02_MSCR (V2)



Date, Time: 2018-05-02 1:01:03 PM
 Test name: 2018-05-02_MSCR_0.1/3.2kPa
 Operator: user
 Sample: YASHAR
 Batch no.: MTO2
 Description: LOOSE MIX
 Configuration: Anton Paar SmartPave 102 SN82314644

PP25/PE SN52739

P-PTD200+H-PTD120 SN82331818-82284206

3	0.1	61.96	76.01	14.05	66.66	4.70	66.55	0.4700
4	0.1	66.66	80.71	14.04	71.34	4.68	66.69	0.4678
5	0.1	71.34	85.38	14.04	76.00	4.66	66.82	0.4658
6	0.1	76.00	90.03	14.03	80.64	4.64	66.93	0.4640
7	0.1	80.64	94.66	14.02	85.26	4.62	67.01	0.4625
8	0.1	85.26	99.29	14.02	89.87	4.61	67.15	0.4605
9	0.1	89.87	103.89	14.02	94.47	4.60	67.22	0.4596
10	0.1	94.47	108.48	14.02	99.05	4.59	67.28	0.4587
R _{0.1} = 66.82								J _{nr(0.1)} = 0.4658

Load level 3.2 kPa

(average load: 3.2 kPa)

Cycle	Load [kPa]	ϵ_0 [%]	ϵ_c [%]	ϵ_l [%]	ϵ_r [%]	ϵ_{10} [%]	R _N [%]	J _{nr(3.2, N)} [1/kPa]
1	3.2	99.05	556.39	457.33	343.12	244.07	46.63	0.7627
2	3.2	343.12	809.26	466.14	592.08	248.96	46.59	0.7780
3	3.2	592.08	1064.40	472.32	852.35	260.28	44.89	0.8134
4	3.2	852.35	1327.28	474.93	1120.00	267.64	43.65	0.8364
5	3.2	1120.00	1596.49	476.50	1392.05	272.05	42.91	0.8502
6	3.2	1392.05	1869.40	477.35	1666.62	274.57	42.48	0.8580
7	3.2	1666.62	2144.00	477.38	1942.12	275.51	42.29	0.8610
8	3.2	1942.12	2419.39	477.26	2217.77	275.65	42.24	0.8614
9	3.2	2217.77	2695.12	477.35	2493.56	275.79	42.22	0.8619
10	3.2	2493.56	2970.45	476.88	2769.31	275.75	42.18	0.8617
R _{3.2} = 43.61								J _{nr(3.2)} = 0.8345

Average percent recovery

Load level 0.1 kPa

R_{0.1} = 66.82 %

Load level 3.2 kPa

R_{3.2} = 43.61 %

Percent difference of recovery

Load levels 0.1 kPa and 3.2 kPa

R_{diff} = 34.73 %

Average non-recoverable creep compliance

Load level 0.1 kPa

J_{nr(0.1)} = 0.4658 1/kPa

Load level 3.2 kPa

J_{nr(3.2)} = 0.8345 1/kPa

Percent difference of non-recoverable creep compliance

Load levels 0.1 kPa and 3.2 kPa

J_{nr_diff} = 79.15 %

Indication that the asphalt binder is modified with an acceptable elastomeric polymer

Load level 3.2 kPa

above criterion (probably modified)

FAILED at 64.00 °C according to AASHTO M 332-14.

Responsible Employee:

Signature:

MSCR-Test (AASHTO T350-14) - Final Report

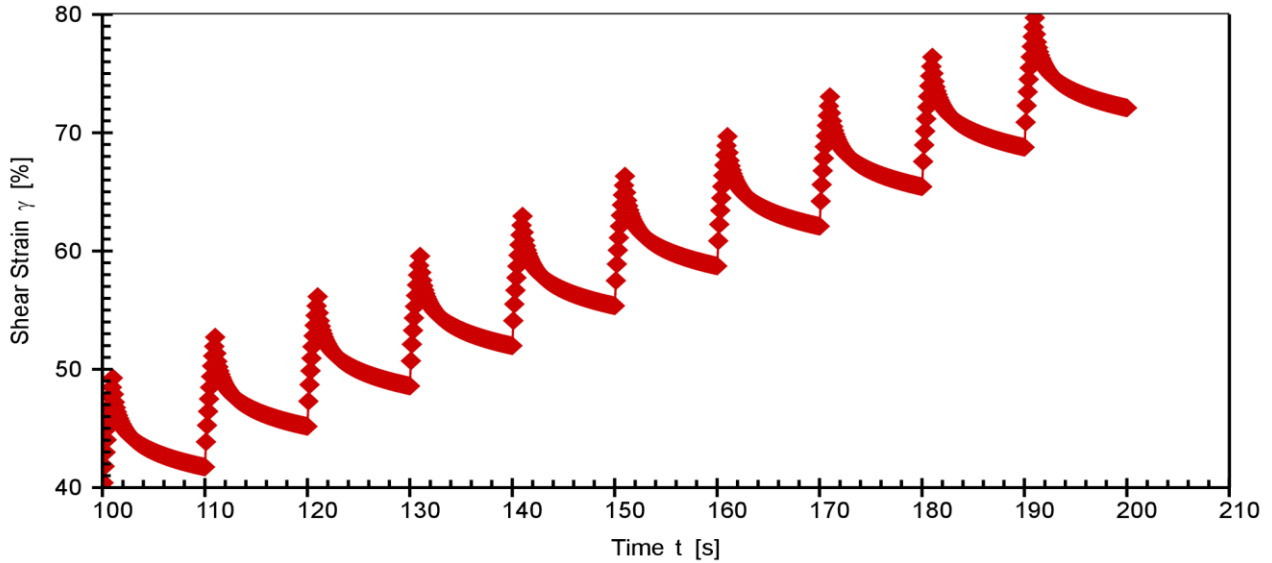
Project name: 2018-05-02_MSCR (V2)

Date, Time: 2018-05-02 12:07:21 PM
Test name: 2018-05-02_MSCR_0.1/3.2kPa
Operator: user
Sample: YASHAR
Batch no.: MTO2
Description: COMPACTED
Configuration: Anton Paar SmartPave 102 SN82314644
PP25/PE SN52739

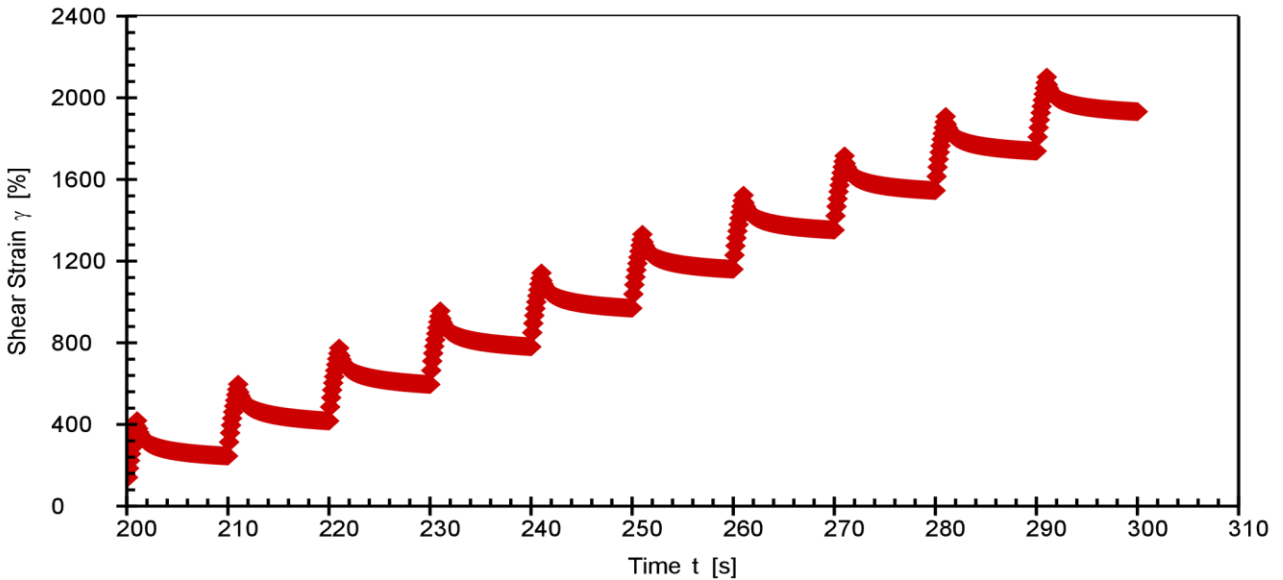
P-PTD200+H-PTD120 SN82331818-82284206



MSCR 0.1kPa (conditioning cycles are not shown)



MSCR 3.2kPa



Responsible Employee:

Signature:

MSCR-Test (AASHTO T350-14) - Final Report

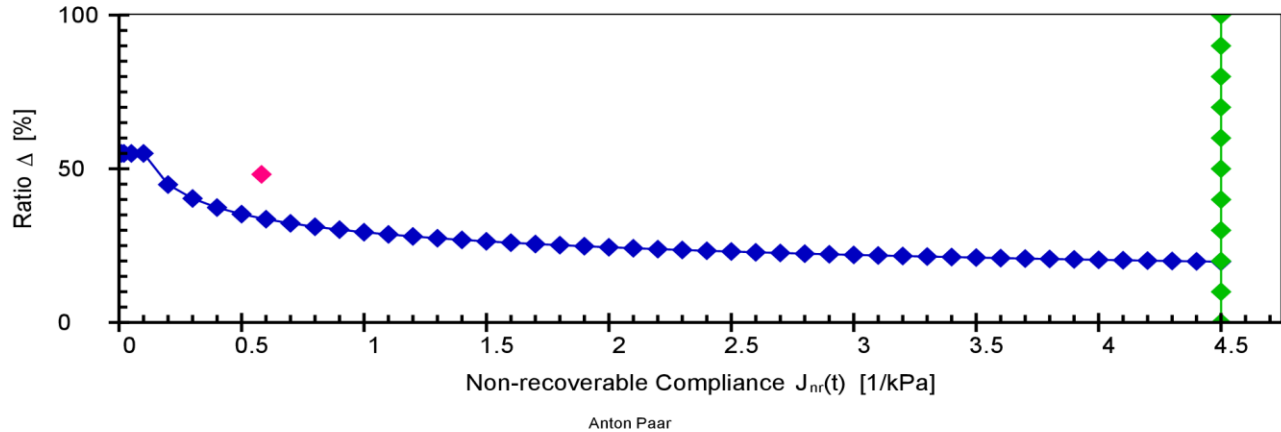
Project name: 2018-05-02_MSCR (V2)



Date, Time: 2018-05-02 12:07:21 PM
 Test name: 2018-05-02_MSCR_0.1/3.2kPa
 Operator: user
 Sample: YASHAR
 Batch no.: MTO2
 Description: COMPACTED
 Configuration: Anton Paar SmartPave 102 SN82314644
 PP25/PE SN52739

P-PTD200+H-PTD120 SN82331818-82284206

J_{nr} vs. % recovery (at 3.2 kPa)



Asphalt MSCR

Application version: Anton Paar RheoCompass™, V1.20.471-Release
 Licensed for: University of Waterloo - CPATT, License no. Rh17H7681, Version no. 1.20.0.0
 Project: 2018-05-02_MSCR (V2)
 Input data: 2018-05-02_MSCR_0.1/3.2kPa, <Last measuring result>, From interval 1, Point 1
 Result data: Asphalt MSCR Analysis

PARAMETERS:
 Load level mode: User-defined load levels (not according to norm)
 Number of intervals to skip: 0
 Calculation mode: Calculation according to ASTM D7405 - 15 and AASHTO M 332-14

Level 1
 Load: 0.1 kPa
 Conditioning cycles: 10
 Analyzed cycles: 10
 Creep phase duration: 1 s
 Recovery phase duration: 9 s

Level 2
 Load: 3.2 kPa
 Conditioning cycles: 0
 Analyzed cycles: 10
 Creep phase duration: 1 s
 Recovery phase duration: 9 s

Show parameter settings: On
 Show result table: Detailed (according to norm)
 Show classification: On

RESULTS:
 Sample name: -
 Test date: 11:51:42 AM
 Test temperature: 64.00 °C

Load level 0.1 kPa (average load: 0.1 kPa)

Cycle	Load [kPa]	$\bar{\epsilon}_0$ [%]	$\bar{\epsilon}_c$ [%]	$\bar{\epsilon}_1$ [%]	$\bar{\epsilon}_r$ [%]	$\bar{\epsilon}_{10}$ [%]	R _N [%]	J _{nr} (0.1, N) [1/kPa]
1	0.1	38.28	49.27	10.99	41.73	3.46	68.55	0.3456
2	0.1	41.73	52.72	10.98	45.17	3.44	68.70	0.3438

Responsible Employee:

Signature:

MSCR-Test (AASHTO T350-14) - Final Report

Project name: 2018-05-02_MSCR (V2)



Date, Time: 2018-05-02 12:07:21 PM
 Test name: 2018-05-02_MSCR_0.1/3.2kPa
 Operator: user
 Sample: YASHAR
 Batch no.: MTO2
 Description: COMPACTED
 Configuration: Anton Paar SmartPave 102 SN82314644

PP25/PE SN52739

P-PTD200+H-PTD120 SN82331818-82284206

3	0.1	45.17	56.15	10.97	48.59	3.41	68.90	0.3413
4	0.1	48.59	59.57	10.98	51.99	3.40	69.03	0.3401
5	0.1	51.99	62.95	10.96	55.37	3.38	69.15	0.3382
6	0.1	55.37	66.33	10.96	58.73	3.37	69.30	0.3366
7	0.1	58.73	69.70	10.96	62.09	3.36	69.37	0.3357
8	0.1	62.09	73.05	10.95	65.44	3.35	69.47	0.3345
9	0.1	65.44	76.39	10.95	68.77	3.33	69.58	0.3332
10	0.1	68.77	79.72	10.95	72.10	3.33	69.61	0.3327
							R _{0.1} = 69.17	J _{nr(0.1)} = 0.3382

Load level 3.2 kPa

(average load: 3.2 kPa)

Cycle	Load [kPa]	ϵ_0 [%]	ϵ_c [%]	ϵ_l [%]	ϵ_r [%]	ϵ_{10} [%]	R _N [%]	J _{nr(3.2, N)} [1/kPa]
1	3.2	72.10	418.62	346.52	245.54	173.45	49.95	0.5420
2	3.2	245.54	597.18	351.63	417.08	171.54	51.22	0.5361
3	3.2	417.08	774.29	357.21	596.06	178.98	49.90	0.5593
4	3.2	596.06	956.08	360.02	780.90	184.85	48.66	0.5776
5	3.2	780.90	1142.23	361.33	969.55	188.64	47.79	0.5895
6	3.2	969.55	1331.50	361.95	1160.43	190.89	47.26	0.5965
7	3.2	1160.43	1523.04	362.61	1352.80	192.37	46.95	0.6012
8	3.2	1352.80	1715.65	362.85	1545.94	193.14	46.77	0.6036
9	3.2	1545.94	1908.60	362.66	1739.15	193.21	46.72	0.6038
10	3.2	1739.15	2101.63	362.48	1932.55	193.40	46.65	0.6044
							R _{3.2} = 48.19	J _{nr(3.2)} = 0.5814

Average percent recovery

Load level 0.1 kPa

R_{0.1} = 69.17 %

Load level 3.2 kPa

R_{3.2} = 48.19 %

Percent difference of recovery

Load levels 0.1 kPa and 3.2 kPa

R_{diff} = 30.33 %

Average non-recoverable creep compliance

Load level 0.1 kPa

J_{nr(0.1)} = 0.3382 1/kPa

Load level 3.2 kPa

J_{nr(3.2)} = 0.5814 1/kPa

Percent difference of non-recoverable creep compliance

Load levels 0.1 kPa and 3.2 kPa

J_{nr_diff} = 71.92 %

Indication that the asphalt binder is modified with an acceptable elastomeric polymer

Load level 3.2 kPa

above criterion (probably modified)

PASSED Very Heavy Traffic "V" grade at 64.00 °C according to AASHTO M 332-14.

Responsible Employee:

Signature:

MSCR-Test (AASHTO T350-14) - Final Report

Project name: 2018-05-25_MSCR (V2)

Date, Time: 2018-05-25 2:19:59 PM

Test name: 2018-05-25_MSCR_0.1/3.2kPa

Operator: user

Sample: 64-28 RTFO + PAV

Batch no.: MTO2

Description: SUNNY

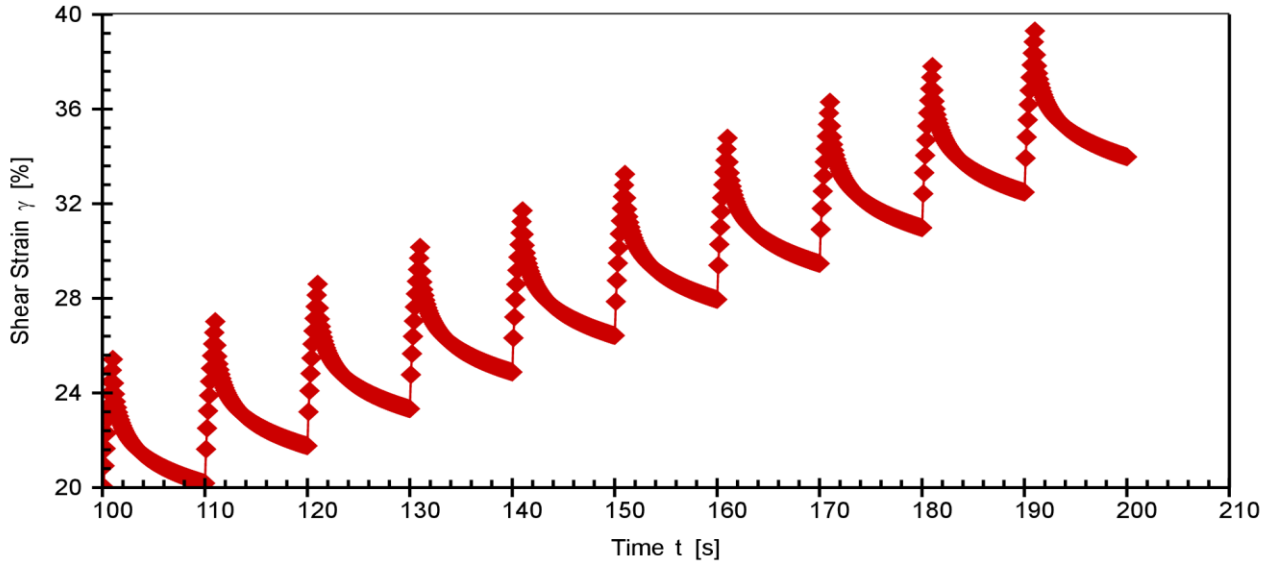
Configuration: Anton Paar SmartPave 102 SN82314644

PP25/PE SN52739

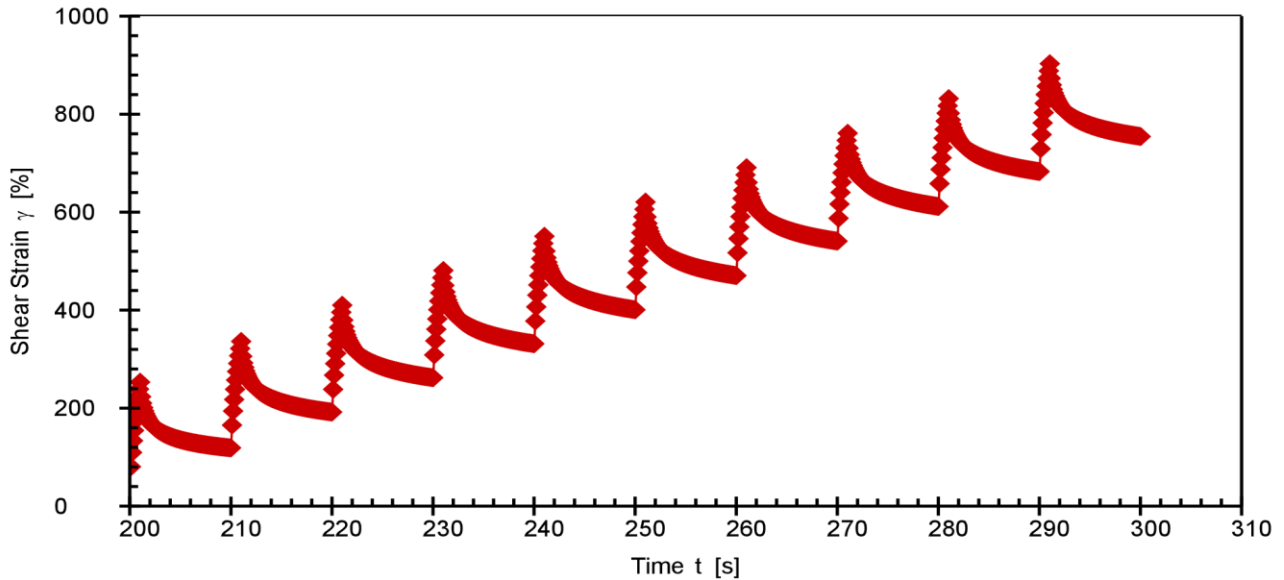
P-PTD200+H-PTD120 SN82331818-82284206



MSCR 0.1kPa (conditioning cycles are not shown)



MSCR 3.2kPa



Responsible Employee:

Signature:

MSCR-Test (AASHTO T350-14) - Final Report

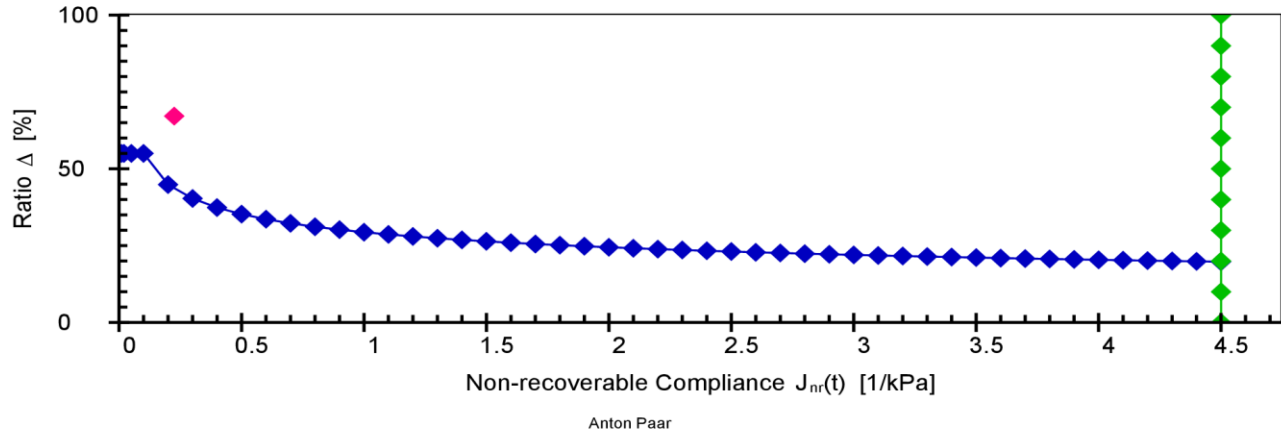
Project name: 2018-05-25_MSCR (V2)



Date, Time: 2018-05-25 2:19:59 PM
 Test name: 2018-05-25_MSCR_0.1/3.2kPa
 Operator: user
 Sample: 64-28 RTFO + PAV
 Batch no.: MTO2
 Description: SUNNY
 Configuration: Anton Paar SmartPave 102 SN82314644
 PP25/PE SN52739

P-PTD200+H-PTD120 SN82331818-82284206

J_{nr} vs. % recovery (at 3.2 kPa)



Asphalt MSCR

Application version: Anton Paar RheoCompass™, V1.20.471-Release
 Licensed for: University of Waterloo - CPATT, License no. Rh17H7681, Version no. 1.20.0.0
 Project: 2018-05-25_MSCR (V2)
 Input data: 2018-05-25_MSCR_0.1/3.2kPa, <Last measuring result>, From interval 1, Point 1
 Result data: Asphalt MSCR Analysis

PARAMETERS:
 Load level mode: User-defined load levels (not according to norm)
 Number of intervals to skip: 0
 Calculation mode: Calculation according to ASTM D7405 - 15 and AASHTO M 332-14

Level 1
 Load: 0.1 kPa
 Conditioning cycles: 10
 Analyzed cycles: 10
 Creep phase duration: 1 s
 Recovery phase duration: 9 s
 Level 2
 Load: 3.2 kPa
 Conditioning cycles: 0
 Analyzed cycles: 10
 Creep phase duration: 1 s
 Recovery phase duration: 9 s
 Show parameter settings: On
 Show result table: Detailed (according to norm)
 Show classification: On

RESULTS:
 Sample name: -
 Test date: 2:02:33 PM
 Test temperature: 64.00 °C

Load level 0.1 kPa (average load: 0.1 kPa)

Cycle	Load [kPa]	$\bar{\epsilon}_0$ [%]	$\bar{\epsilon}_c$ [%]	$\bar{\epsilon}_1$ [%]	$\bar{\epsilon}_r$ [%]	$\bar{\epsilon}_{10}$ [%]	R _N [%]	J _{nr} (0.1, N) [1/kPa]
1	0.1	18.59	25.42	6.84	20.18	1.60	76.63	0.1598
2	0.1	20.18	27.02	6.83	21.76	1.58	76.90	0.1578

Responsible Employee:	Signature:
-----------------------	------------

MSCR-Test (AASHTO T350-14) - Final Report

Project name: 2018-05-25_MSCR (V2)



Date, Time: 2018-05-25 2:19:59 PM
 Test name: 2018-05-25_MSCR_0.1/3.2kPa
 Operator: user
 Sample: 64-28 RTFO + PAV
 Batch no.: MTO2
 Description: SUNNY
 Configuration: Anton Paar SmartPave 102 SN82314644

PP25/PE SN52739

P-PTD200+H-PTD120 SN82331818-82284206

Cycle	Load [kPa]	ϵ_0 [%]	ϵ_c [%]	ϵ_l [%]	ϵ_r [%]	ϵ_{10} [%]	R_N [%]	J_nr
3	0.1	21.76	28.60	6.84	23.33	1.57	77.09	0.1566
4	0.1	23.33	30.16	6.83	24.88	1.55	77.25	0.1554
5	0.1	24.88	31.71	6.83	26.42	1.54	77.42	0.1541
6	0.1	26.42	33.25	6.82	27.95	1.53	77.60	0.1529
7	0.1	27.95	34.78	6.82	29.47	1.52	77.74	0.1519
8	0.1	29.47	36.29	6.82	30.98	1.51	77.85	0.1511
9	0.1	30.98	37.80	6.82	32.49	1.50	77.94	0.1505
10	0.1	32.49	39.30	6.82	33.98	1.49	78.10	0.1493
							R_0.1 = 77.45	J_nr(0.1) = 0.1539

Load level 3.2 kPa (average load: 3.2 kPa)

Cycle	Load [kPa]	ϵ_0 [%]	ϵ_c [%]	ϵ_l [%]	ϵ_r [%]	ϵ_{10} [%]	R_N [%]	J_nr(3.2, N) [1/kPa]
1	3.2	33.98	253.25	219.27	118.86	84.88	61.29	0.2653
2	3.2	118.86	336.16	217.30	192.00	73.14	66.34	0.2286
3	3.2	192.00	410.02	218.02	262.09	70.08	67.85	0.2190
4	3.2	262.09	480.95	218.86	331.43	69.34	68.32	0.2167
5	3.2	331.43	550.88	219.46	400.83	69.41	68.37	0.2169
6	3.2	400.83	620.77	219.93	470.62	69.79	68.27	0.2181
7	3.2	470.62	690.79	220.17	540.89	70.27	68.08	0.2196
8	3.2	540.89	761.16	220.27	611.66	70.77	67.87	0.2211
9	3.2	611.66	831.92	220.26	682.87	71.21	67.67	0.2225
10	3.2	682.87	903.15	220.29	754.82	71.95	67.34	0.2249
							R_3.2 = 67.14	J_nr(3.2) = 0.2253

Average percent recovery

Load level 0.1 kPa R_0.1 = 77.45 %
 Load level 3.2 kPa R_3.2 = 67.14 %

Percent difference of recovery

Load levels 0.1 kPa and 3.2 kPa R_diff = 13.31 %

Average non-recoverable creep compliance

Load level 0.1 kPa J_nr(0.1) = 0.1539 1/kPa
 Load level 3.2 kPa J_nr(3.2) = 0.2253 1/kPa

Percent difference of non-recoverable creep compliance

Load levels 0.1 kPa and 3.2 kPa J_nr_diff = 46.33 %

Indication that the asphalt binder is modified with an acceptable elastomeric polymer

Load level 3.2 kPa above criterion (probably modified)

PASSED Extremely Heavy Traffic "E" grade at 64.00 °C according to AASHTO M 332-14.

Responsible Employee:

Signature:

MSCR-Test (AASHTO T350-14) - Final Report

Project name: 2018-05-02_MSCR (V2)

Date, Time: 2018-05-02 1:54:44 PM

Test name: 2018-05-02_MSCR_0.1/3.2kPa

Operator: user

Sample: YASHAR

Batch no.: MTO2

Description: R30

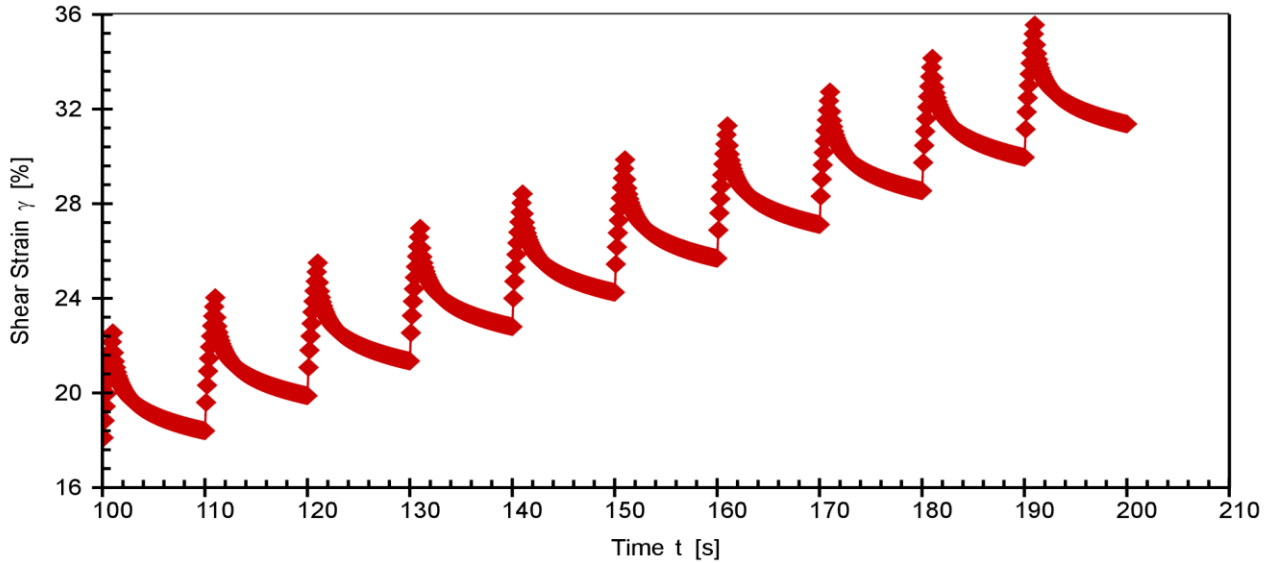
Configuration: Anton Paar SmartPave 102 SN82314644

PP25/PE SN52739

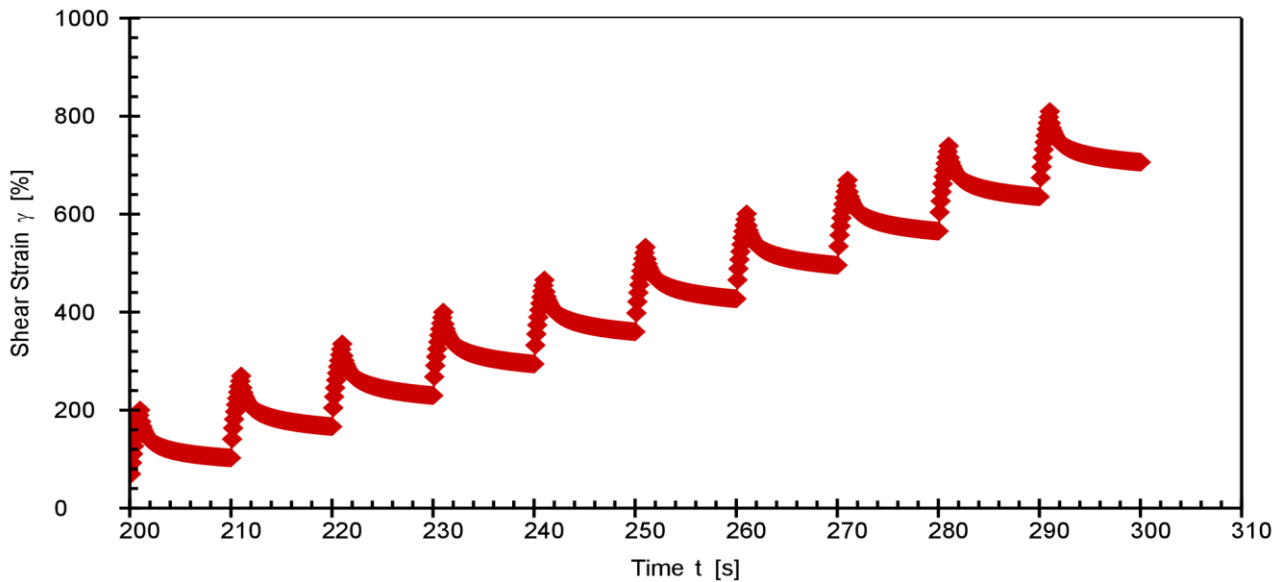
P-PTD200+H-PTD120 SN82331818-82284206



MSCR 0.1kPa (conditioning cycles are not shown)



MSCR 3.2kPa



Responsible Employee:

Signature:

MSCR-Test (AASHTO T350-14) - Final Report

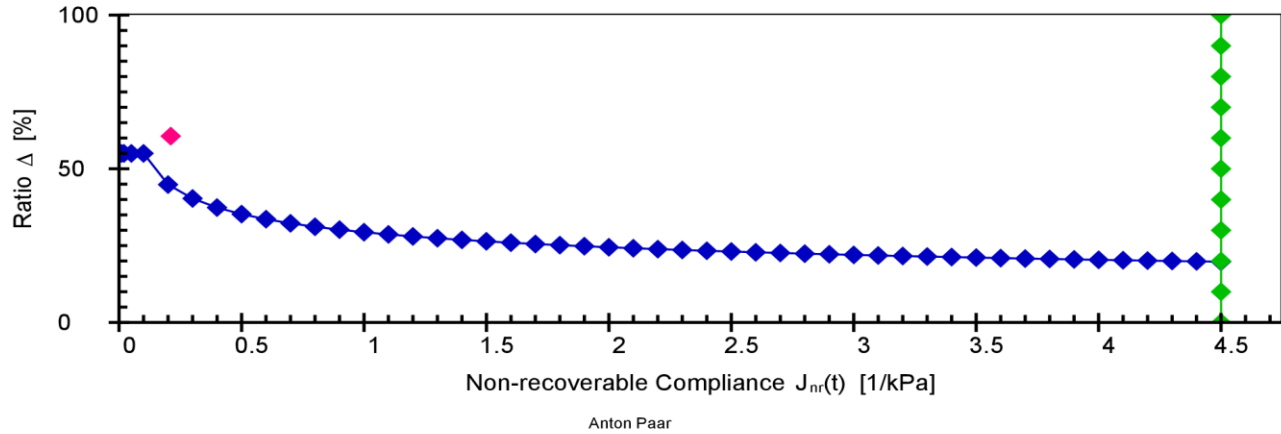
Project name: 2018-05-02_MSCR (V2)



Date, Time: 2018-05-02 1:54:44 PM
 Test name: 2018-05-02_MSCR_0.1/3.2kPa
 Operator: user
 Sample: YASHAR
 Batch no.: MTO2
 Description: R30
 Configuration: Anton Paar SmartPave 102 SN82314644
 PP25/PE SN52739

P-PTD200+H-PTD120 SN82331818-82284206

J_{nr} vs. % recovery (at 3.2 kPa)



Asphalt MSCR

Application version: Anton Paar RheoCompass™, V1.20.471-Release
 Licensed for: University of Waterloo - CPATT, License no. Rh17H7681, Version no. 1.20.0.0
 Project: 2018-05-02_MSCR (V2)
 Input data: 2018-05-02_MSCR_0.1/3.2kPa, <Last measuring result>, From interval 1, Point 1
 Result data: Asphalt MSCR Analysis

PARAMETERS:
 Load level mode: User-defined load levels (not according to norm)
 Number of intervals to skip: 0
 Calculation mode: Calculation according to ASTM D7405 - 15 and AASHTO M 332-14

Level 1
 Load: 0.1 kPa
 Conditioning cycles: 10
 Analyzed cycles: 10
 Creep phase duration: 1 s
 Recovery phase duration: 9 s

Level 2
 Load: 3.2 kPa
 Conditioning cycles: 0
 Analyzed cycles: 10
 Creep phase duration: 1 s
 Recovery phase duration: 9 s

Show parameter settings: On
 Show result table: Detailed (according to norm)
 Show classification: On

RESULTS:
 Sample name: -
 Test date: 1:39:22 PM
 Test temperature: 64.00 °C

Load level 0.1 kPa (average load: 0.1 kPa)

Cycle	Load [kPa]	$\bar{\epsilon}_0$ [%]	$\bar{\epsilon}_c$ [%]	$\bar{\epsilon}_1$ [%]	$\bar{\epsilon}_r$ [%]	$\bar{\epsilon}_{10}$ [%]	R _N [%]	J _{nr} (0.1, N) [1/kPa]
1	0.1	16.91	22.54	5.64	18.40	1.49	73.49	0.1494
2	0.1	18.40	24.03	5.63	19.88	1.48	73.68	0.1482

Responsible Employee:

Signature:

MSCR-Test (AASHTO T350-14) - Final Report

Project name: 2018-05-02_MSCR (V2)



Date, Time: 2018-05-02 1:54:44 PM
 Test name: 2018-05-02_MSCR_0.1/3.2kPa
 Operator: user
 Sample: YASHAR
 Batch no.: MTO2
 Description: R30

Configuration: Anton Paar SmartPave 102 SN82314644

PP25/PE SN52739

P-PTD200+H-PTD120 SN82331818-82284206

3	0.1	19.88	25.50	5.62	21.35	1.46	73.96	0.1463
4	0.1	21.35	26.96	5.62	22.80	1.46	74.10	0.1455
5	0.1	22.80	28.42	5.62	24.25	1.45	74.18	0.1451
6	0.1	24.25	29.86	5.61	25.69	1.44	74.40	0.1437
7	0.1	25.69	31.30	5.61	27.12	1.43	74.52	0.1429
8	0.1	27.12	32.73	5.61	28.54	1.43	74.57	0.1426
9	0.1	28.54	34.15	5.60	29.96	1.41	74.77	0.1414
10	0.1	29.96	35.56	5.60	31.37	1.41	74.84	0.1409
R _{0.1} = 74.25 J _{nr} (0.1) = 0.1446								

Load level 3.2 kPa

(average load: 3.2 kPa)

Cycle	Load [kPa]	ϵ_0 [%]	ϵ_c [%]	ϵ_1 [%]	ϵ_r [%]	ϵ_{10} [%]	R _N [%]	J _{nr} (3.2, N) [1/kPa]
1	3.2	31.37	200.23	168.87	102.62	71.25	57.81	0.2227
2	3.2	102.62	269.83	167.21	166.50	63.89	61.79	0.1997
3	3.2	166.50	335.06	168.56	229.76	63.26	62.47	0.1977
4	3.2	229.76	399.96	170.19	294.12	64.36	62.18	0.2011
5	3.2	294.12	465.70	171.58	359.98	65.86	61.62	0.2058
6	3.2	359.98	532.59	172.61	427.30	67.32	61.00	0.2104
7	3.2	427.30	600.61	173.31	495.81	68.51	60.47	0.2141
8	3.2	495.81	669.61	173.80	565.31	69.50	60.01	0.2172
9	3.2	565.31	739.30	173.98	635.49	70.18	59.66	0.2193
10	3.2	635.49	809.56	174.07	706.31	70.82	59.31	0.2213
R _{3.2} = 60.63 J _{nr} (3.2) = 0.2109								

Average percent recovery

Load level 0.1 kPa
 Load level 3.2 kPa

R_{0.1} = 74.25 %
 R_{3.2} = 60.63 %

Percent difference of recovery

Load levels 0.1 kPa and 3.2 kPa

R_{diff} = 18.34 %

Average non-recoverable creep compliance

Load level 0.1 kPa
 Load level 3.2 kPa

J_{nr}(0.1) = 0.1446 1/kPa
 J_{nr}(3.2) = 0.2109 1/kPa

Percent difference of non-recoverable creep compliance

Load levels 0.1 kPa and 3.2 kPa

J_{nr_diff} = 45.85 %

Indication that the asphalt binder is modified with an acceptable elastomeric polymer

Load level 3.2 kPa above criterion (probably modified)

PASSED Extremely Heavy Traffic "E" grade at 64.00 °C according to AASHTO M 332-14.

Responsible Employee:

Signature:

MSCR-Test (AASHTO T350-14) - Final Report

Project name: 2018-05-02_MSCR (V2)

Date, Time: 2018-05-02 2:26:18 PM

Test name: 2018-05-02_MSCR_0.1/3.2kPa

Operator: user

Sample: YASHAR

Batch no.: MTO2

Description: COCO

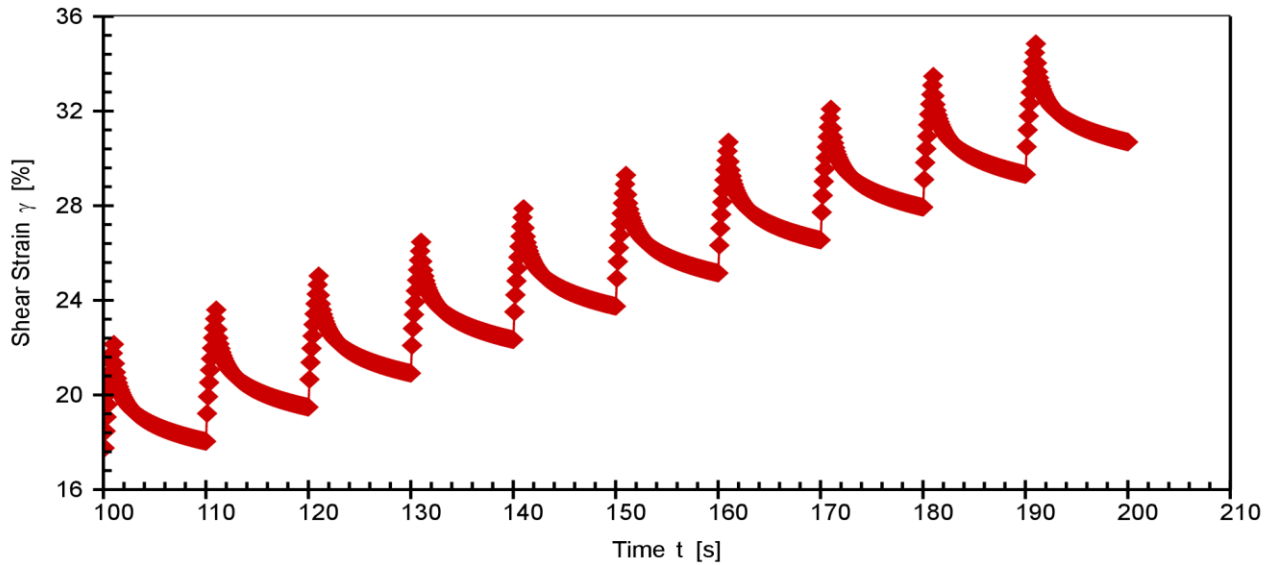
Configuration: Anton Paar SmartPave 102 SN82314644

PP25/PE SN52739

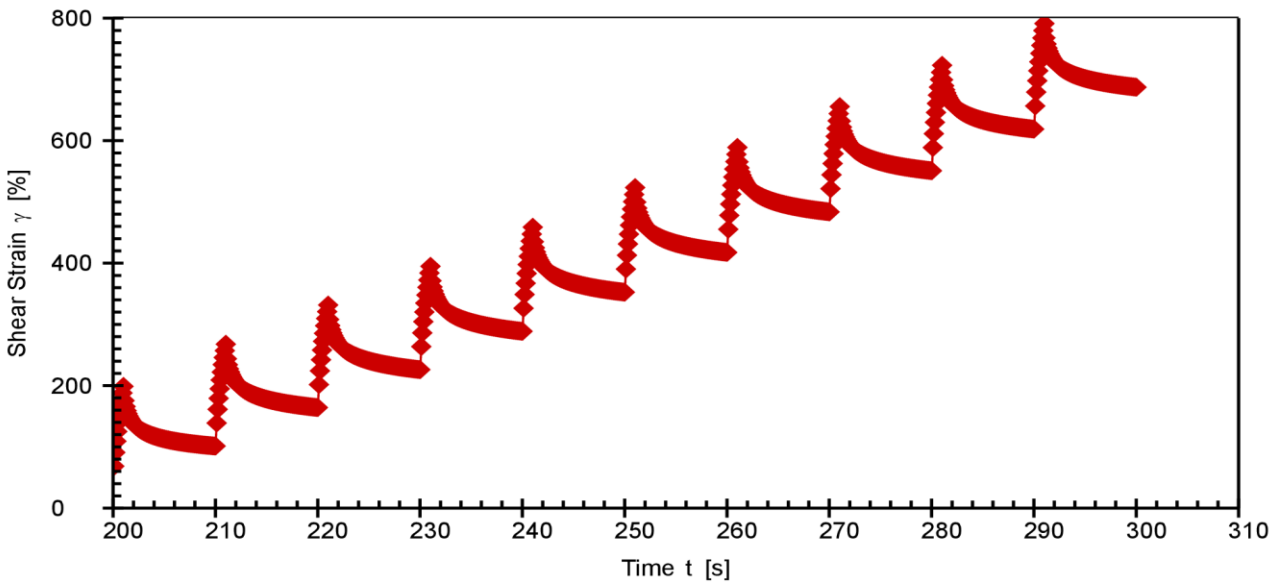
P-PTD200+H-PTD120 SN82331818-82284206



MSCR 0.1kPa (conditioning cycles are not shown)



MSCR 3.2kPa



Responsible Employee:

Signature:

MSCR-Test (AASHTO T350-14) - Final Report

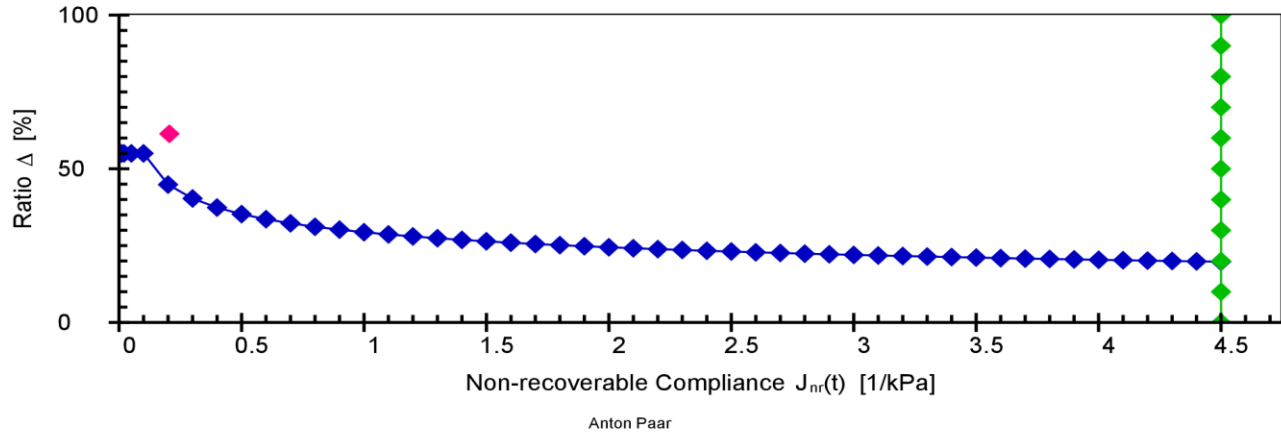
Project name: 2018-05-02_MSCR (V2)



Date, Time: 2018-05-02 2:26:18 PM
 Test name: 2018-05-02_MSCR_0.1/3.2kPa
 Operator: user
 Sample: YASHAR
 Batch no.: MTO2
 Description: COCO
 Configuration: Anton Paar SmartPave 102 SN82314644
 PP25/PE SN52739

P-PTD200+H-PTD120 SN82331818-82284206

Jnr vs. % recovery (at 3.2 kPa)



Asphalt MSCR

Application version: Anton Paar RheoCompass™, V1.20.471-Release
 Licensed for: University of Waterloo - CPATT, License no. Rh17H7681, Version no. 1.20.0.0
 Project: 2018-05-02_MSCR (V2)
 Input data: 2018-05-02_MSCR_0.1/3.2kPa, <Last measuring result>, From interval 1, Point 1
 Result data: Asphalt MSCR Analysis

PARAMETERS:
 Load level mode: User-defined load levels (not according to norm)
 Number of intervals to skip: 0
 Calculation mode: Calculation according to ASTM D7405 - 15 and AASHTO M 332-14

Level 1
 Load: 0.1 kPa
 Conditioning cycles: 10
 Analyzed cycles: 10
 Creep phase duration: 1 s
 Recovery phase duration: 9 s
 Level 2
 Load: 3.2 kPa
 Conditioning cycles: 0
 Analyzed cycles: 10
 Creep phase duration: 1 s
 Recovery phase duration: 9 s
 Show parameter settings: On
 Show result table: Detailed (according to norm)
 Show classification: On

RESULTS:
 Sample name: -
 Test date: 2:10:55 PM
 Test temperature: 64.00 °C

Load level 0.1 kPa (average load: 0.1 kPa)

Cycle	Load [kPa]	$\bar{\epsilon}_0$ [%]	$\bar{\epsilon}_c$ [%]	$\bar{\epsilon}_1$ [%]	$\bar{\epsilon}_r$ [%]	$\bar{\epsilon}_{10}$ [%]	R _N [%]	J _{nr} (0.1, N) [1/kPa]
1	0.1	16.58	22.14	5.56	18.04	1.45	73.84	0.1454
2	0.1	18.04	23.60	5.56	19.48	1.44	74.02	0.1444

Responsible Employee:

Signature:

MSCR-Test (AASHTO T350-14) - Final Report

Project name: 2018-05-02_MSCR (V2)



Date, Time: 2018-05-02 2:26:18 PM
 Test name: 2018-05-02_MSCR_0.1/3.2kPa
 Operator: user
 Sample: YASHAR
 Batch no.: MTO2
 Description: COCO

Configuration: Anton Paar SmartPave 102 SN82314644
 PP25/PE SN52739

P-PTD200+H-PTD120 SN82331818-82284206

Cycle	Load [kPa]	ϵ_0 [%]	ϵ_c [%]	ϵ_l [%]	ϵ_r [%]	ϵ_{10} [%]	R_N [%]	J_nr(0.1) [1/kPa]
3	0.1	19.48	25.04	5.56	20.92	1.44	74.16	0.1436
4	0.1	20.92	26.46	5.55	22.34	1.42	74.41	0.1419
5	0.1	22.34	27.88	5.54	23.75	1.41	74.55	0.1411
6	0.1	23.75	29.29	5.54	25.15	1.40	74.67	0.1405
7	0.1	25.15	30.69	5.54	26.55	1.39	74.83	0.1394
8	0.1	26.55	32.08	5.54	27.93	1.39	74.96	0.1387
9	0.1	27.93	33.47	5.54	29.32	1.38	74.98	0.1385
10	0.1	29.32	34.85	5.53	30.69	1.37	75.17	0.1373
							R_0.1 = 74.56	J_nr(0.1) = 0.1411

Load level 3.2 kPa (average load: 3.2 kPa)

Cycle	Load [kPa]	ϵ_0 [%]	ϵ_c [%]	ϵ_l [%]	ϵ_r [%]	ϵ_{10} [%]	R_N [%]	J_nr(3.2, N) [1/kPa]
1	3.2	30.69	198.88	168.19	101.32	70.63	58.01	0.2207
2	3.2	101.32	267.75	166.43	164.24	62.92	62.19	0.1966
3	3.2	164.24	331.73	167.49	226.12	61.87	63.06	0.1934
4	3.2	226.12	394.95	168.83	288.72	62.60	62.92	0.1956
5	3.2	288.72	458.69	169.97	352.55	63.83	62.45	0.1995
6	3.2	352.55	523.36	170.81	417.63	65.08	61.90	0.2034
7	3.2	417.63	589.01	171.38	483.81	66.18	61.39	0.2068
8	3.2	483.81	655.64	171.84	550.95	67.14	60.93	0.2098
9	3.2	550.95	723.10	172.16	618.83	67.88	60.57	0.2121
10	3.2	618.83	791.26	172.43	687.53	68.70	60.16	0.2147
							R_3.2 = 61.36	J_nr(3.2) = 0.2053

Average percent recovery

Load level 0.1 kPa R_0.1 = 74.56 %
 Load level 3.2 kPa R_3.2 = 61.36 %

Percent difference of recovery

Load levels 0.1 kPa and 3.2 kPa R_diff = 17.71 %

Average non-recoverable creep compliance

Load level 0.1 kPa J_nr(0.1) = 0.1411 1/kPa
 Load level 3.2 kPa J_nr(3.2) = 0.2053 1/kPa

Percent difference of non-recoverable creep compliance

Load levels 0.1 kPa and 3.2 kPa J_nr_diff = 45.49 %

Indication that the asphalt binder is modified with an acceptable elastomeric polymer

Load level 3.2 kPa above criterion (probably modified)

PASSED Extremely Heavy Traffic "E" grade at 64.00 °C according to AASHTO M 332-14.

Responsible Employee:

Signature:

MSCR-Test (AASHTO T350-14) - Final Report

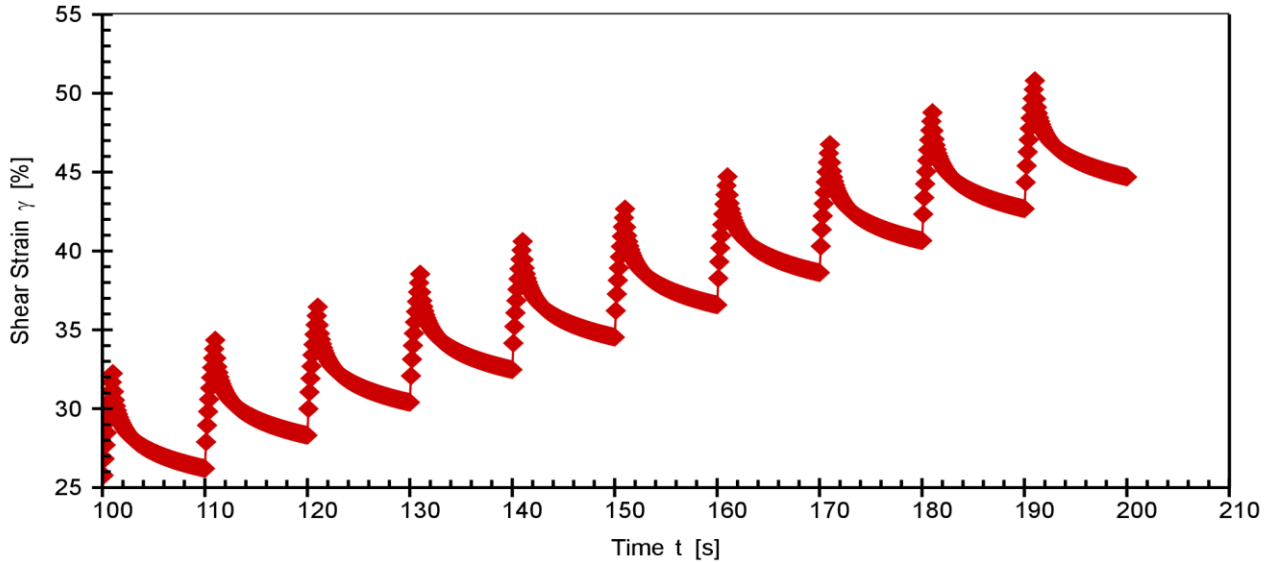
Project name: 2018-07-23_MSCR (V2)

Date, Time: 2018-07-23 12:14:53 PM
Test name: 2018-07-23_MSCR_0.1/3.2kPa
Operator: user
Sample: Sunny
Batch no.: MTO2
Description: BC5-H2O
Configuration: Anton Paar SmartPave 102 SN82314644
PP25/PE SN52739

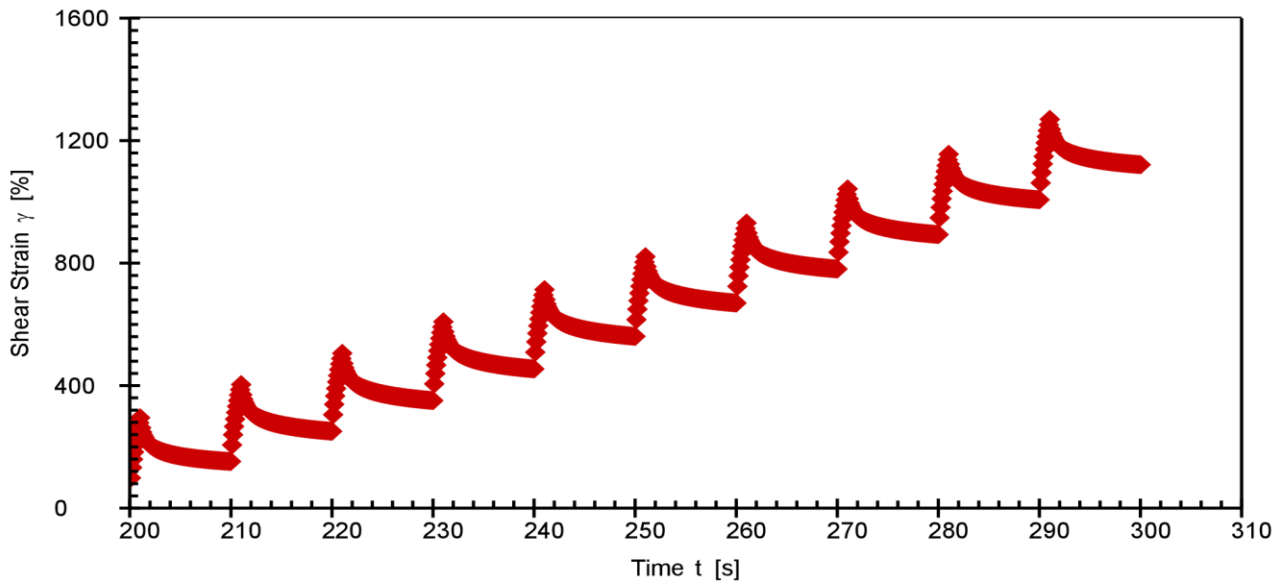
P-PTD200+H-PTD120 SN82331818-82284206



MSCR 0.1kPa (conditioning cycles are not shown)



MSCR 3.2kPa



Responsible Employee:

Signature:

MSCR-Test (AASHTO T350-14) - Final Report

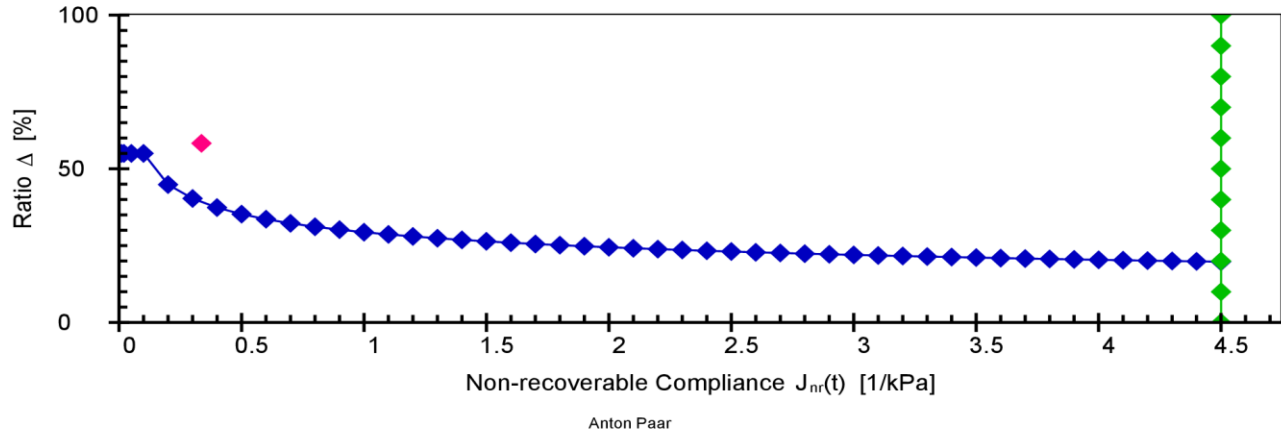
Project name: 2018-07-23_MSCR (V2)



Date, Time: 2018-07-23 12:14:53 PM
 Test name: 2018-07-23_MSCR_0.1/3.2kPa
 Operator: user
 Sample: Sunny
 Batch no.: MTO2
 Description: BC5-H2O
 Configuration: Anton Paar SmartPave 102 SN82314644
 PP25/PE SN52739

P-PTD200+H-PTD120 SN82331818-82284206

J_{nr} vs. % recovery (at 3.2 kPa)



Asphalt MSCR

Application version: Anton Paar RheoCompass™, V1.20.471-Release
 Licensed for: University of Waterloo - CPATT, License no. Rh17H7681, Version no. 1.20.0.0
 Project: 2018-07-23_MSCR (V2)
 Input data: 2018-07-23_MSCR_0.1/3.2kPa, <Last measuring result>, From interval 1, Point 1
 Result data: Asphalt MSCR Analysis

PARAMETERS:
 Load level mode: User-defined load levels (not according to norm)
 Number of intervals to skip: 0
 Calculation mode: Calculation according to ASTM D7405 - 15 and AASHTO M 332-14

Level 1
 Load: 0.1 kPa
 Conditioning cycles: 10
 Analyzed cycles: 10
 Creep phase duration: 1 s
 Recovery phase duration: 9 s

Level 2
 Load: 3.2 kPa
 Conditioning cycles: 0
 Analyzed cycles: 10
 Creep phase duration: 1 s
 Recovery phase duration: 9 s

Show parameter settings: On
 Show result table: Detailed (according to norm)
 Show classification: On

RESULTS:
 Sample name: -
 Test date: 11:56:36 AM
 Test temperature: 64.00 °C

Load level 0.1 kPa (average load: 0.1 kPa)

Cycle	Load [kPa]	$\bar{\epsilon}_0$ [%]	$\bar{\epsilon}_c$ [%]	$\bar{\epsilon}_1$ [%]	$\bar{\epsilon}_r$ [%]	$\bar{\epsilon}_{10}$ [%]	R _N [%]	J _{nr} (0.1, N) [1/kPa]
1	0.1	24.09	32.23	8.14	26.21	2.12	73.96	0.2121
2	0.1	26.21	34.35	8.14	28.31	2.10	74.17	0.2103

Responsible Employee:

Signature:

MSCR-Test (AASHTO T350-14) - Final Report

Project name: 2018-07-23_MSCR (V2)



Date, Time: 2018-07-23 12:14:53 PM
 Test name: 2018-07-23_MSCR_0.1/3.2kPa
 Operator: user
 Sample: Sunny
 Batch no.: MTO2
 Description: BC5-H2O
 Configuration: Anton Paar SmartPave 102 SN82314644

PP25/PE SN52739

P-PTD200+H-PTD120 SN82331818-82284206

Cycle	Load [kPa]	ϵ_0 [%]	ϵ_c [%]	ϵ_l [%]	ϵ_r [%]	ϵ_{10} [%]	R_N [%]	J_nr (1/kPa)
3	0.1	28.31	36.45	8.14	30.40	2.09	74.35	0.2088
4	0.1	30.40	38.54	8.14	32.48	2.07	74.53	0.2073
5	0.1	32.48	40.61	8.14	34.54	2.06	74.67	0.2061
6	0.1	34.54	42.67	8.13	36.59	2.05	74.80	0.2050
7	0.1	36.59	44.72	8.13	38.63	2.04	74.92	0.2040
8	0.1	38.63	46.76	8.13	40.66	2.03	75.03	0.2030
9	0.1	40.66	48.78	8.13	42.68	2.02	75.13	0.2021
10	0.1	42.68	50.80	8.13	44.69	2.01	75.22	0.2014
							R_0.1 = 74.68	J_nr(0.1) = 0.2060

Load level 3.2 kPa (average load: 3.2 kPa)

Cycle	Load [kPa]	ϵ_0 [%]	ϵ_c [%]	ϵ_l [%]	ϵ_r [%]	ϵ_{10} [%]	R_N [%]	J_nr (3.2, N) [1/kPa]
1	3.2	44.69	295.17	250.48	152.27	107.58	57.05	0.3362
2	3.2	152.27	403.43	251.16	251.01	98.73	60.69	0.3085
3	3.2	251.01	505.70	254.69	351.22	100.21	60.65	0.3132
4	3.2	351.22	608.64	257.42	454.55	103.33	59.86	0.3229
5	3.2	454.55	713.74	259.19	560.91	106.36	58.96	0.3324
6	3.2	560.91	821.35	260.44	669.88	108.97	58.16	0.3405
7	3.2	669.88	931.20	261.32	780.92	111.04	57.51	0.3470
8	3.2	780.92	1042.80	261.88	893.48	112.56	57.02	0.3517
9	3.2	893.48	1155.74	262.26	1007.09	113.62	56.68	0.3551
10	3.2	1007.09	1269.82	262.73	1121.81	114.71	56.34	0.3585
							R_3.2 = 58.29	J_nr(3.2) = 0.3366

Average percent recovery

Load level 0.1 kPa R_0.1 = 74.68 %
 Load level 3.2 kPa R_3.2 = 58.29 %

Percent difference of recovery

Load levels 0.1 kPa and 3.2 kPa R_diff = 21.94 %

Average non-recoverable creep compliance

Load level 0.1 kPa J_nr(0.1) = 0.2060 1/kPa
 Load level 3.2 kPa J_nr(3.2) = 0.3366 1/kPa

Percent difference of non-recoverable creep compliance

Load levels 0.1 kPa and 3.2 kPa J_nr_diff = 63.39 %

Indication that the asphalt binder is modified with an acceptable elastomeric polymer above criterion (probably modified)
 Load level 3.2 kPa

PASSED Extremely Heavy Traffic "E" grade at 64.00 °C according to AASHTO M 332-14.

Responsible Employee:	Signature:
-----------------------	------------

MSCR-Test (AASHTO T350-14) - Final Report

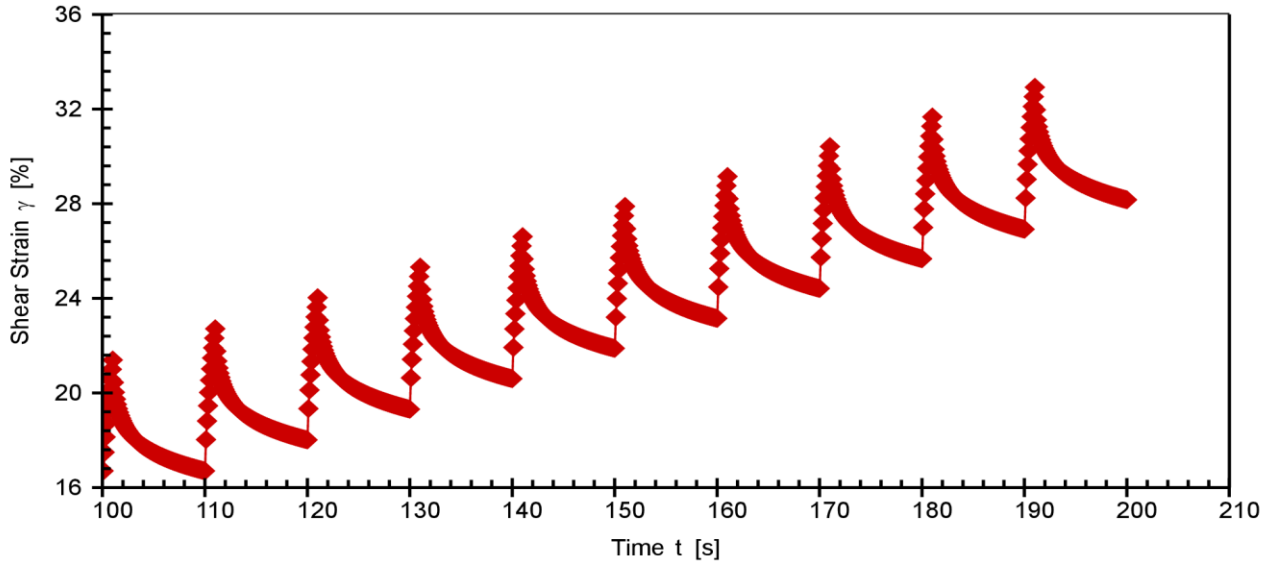
Project name: 2018-07-24_MSCR (V2)

Date, Time: 2018-07-24 1:08:23 PM
Test name: 2018-07-24_MSCR_0.1/3.2kPa
Operator: user
Sample: Sunny
Batch no.: MTO2
Description: BC5-NoH2O
Configuration: Anton Paar SmartPave 102 SN82314644
PP25/PE SN52739

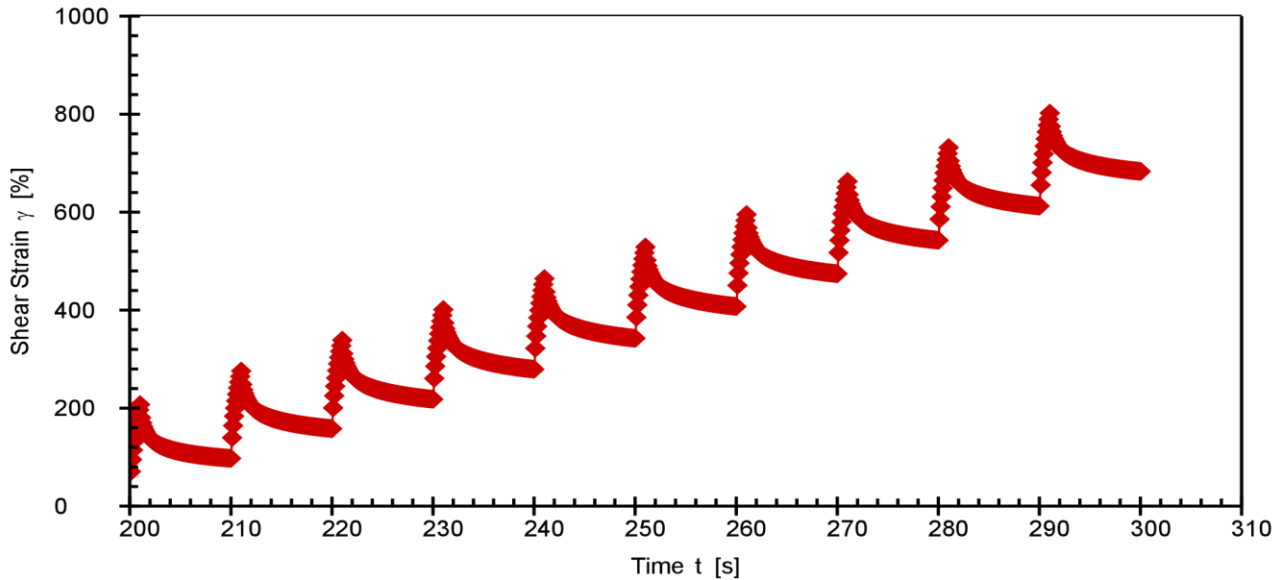
P-PTD200+H-PTD120 SN82331818-82284206



MSCR 0.1kPa (conditioning cycles are not shown)



MSCR 3.2kPa



Responsible Employee:

Signature:

MSCR-Test (AASHTO T350-14) - Final Report

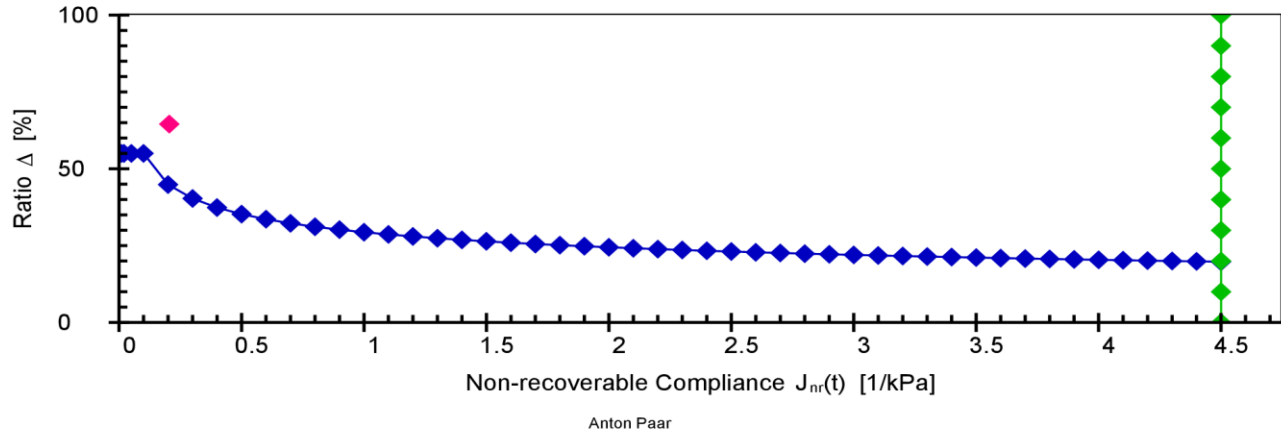
Project name: 2018-07-24_MSCR (V2)



Date, Time: 2018-07-24 1:08:23 PM
 Test name: 2018-07-24_MSCR_0.1/3.2kPa
 Operator: user
 Sample: Sunny
 Batch no.: MTO2
 Description: BC5-NoH2O
 Configuration: Anton Paar SmartPave 102 SN82314644
 PP25/PE SN52739

P-PTD200+H-PTD120 SN82331818-82284206

Jnr vs. % recovery (at 3.2 kPa)



Asphalt MSCR

Application version: Anton Paar RheoCompass™, V1.20.471-Release
 Licensed for: University of Waterloo - CPATT, License no. Rh17H7681, Version no. 1.20.0.0
 Project: 2018-07-24_MSCR (V2)
 Input data: 2018-07-24_MSCR_0.1/3.2kPa, <Last measuring result>, From interval 1, Point 1
 Result data: Asphalt MSCR Analysis

PARAMETERS:

Load level mode: User-defined load levels (not according to norm)
 Number of intervals to skip: 0
 Calculation mode: Calculation according to ASTM D7405 - 15 and AASHTO M 332-14

Level 1

Load: 0.1 kPa
 Conditioning cycles: 10
 Analyzed cycles: 10
 Creep phase duration: 1 s
 Recovery phase duration: 9 s

Level 2

Load: 3.2 kPa
 Conditioning cycles: 0
 Analyzed cycles: 10
 Creep phase duration: 1 s
 Recovery phase duration: 9 s

Show parameter settings: On

Show result table: Detailed (according to norm)

Show classification: On

RESULTS:

Sample name: -
 Test date: 12:51:24 PM
 Test temperature: 64.00 °C

Load level 0.1 kPa (average load: 0.1 kPa)

Cycle	Load [kPa]	$\bar{\epsilon}_0$ [%]	$\bar{\epsilon}_c$ [%]	$\bar{\epsilon}_1$ [%]	$\bar{\epsilon}_r$ [%]	$\bar{\epsilon}_{10}$ [%]	R _N [%]	J _{nr} (0.1, N) [1/kPa]
1	0.1	15.38	21.39	6.01	16.70	1.32	78.01	0.1322
2	0.1	16.70	22.71	6.01	18.02	1.31	78.19	0.1311

Responsible Employee:

Signature:

MSCR-Test (AASHTO T350-14) - Final Report

Project name: 2018-07-24_MSCR (V2)



Date, Time: 2018-07-24 1:08:23 PM
 Test name: 2018-07-24_MSCR_0.1/3.2kPa
 Operator: user
 Sample: Sunny
 Batch no.: MTO2
 Description: BC5-NoH2O
 Configuration: Anton Paar SmartPave 102 SN82314644

PP25/PE SN52739

P-PTD200+H-PTD120 SN82331818-82284206

3	0.1	18.02	24.03	6.01	19.31	1.30	78.41	0.1298
4	0.1	19.31	25.32	6.01	20.60	1.29	78.56	0.1288
5	0.1	20.60	26.61	6.01	21.88	1.28	78.69	0.1280
6	0.1	21.88	27.89	6.01	23.15	1.27	78.85	0.1270
7	0.1	23.15	29.15	6.00	24.42	1.26	78.95	0.1263
8	0.1	24.42	30.42	6.00	25.67	1.26	79.07	0.1255
9	0.1	25.67	31.67	6.00	26.92	1.25	79.20	0.1247
10	0.1	26.92	32.92	6.00	28.16	1.25	79.26	0.1245
R _{0.1} = 78.72								J _{nr(0.1)} = 0.1278

Load level 3.2 kPa

(average load: 3.2 kPa)

Cycle	Load [kPa]	ϵ_0 [%]	ϵ_c [%]	ϵ_l [%]	ϵ_r [%]	ϵ_{10} [%]	R _N [%]	J _{nr(3.2, N)} [1/kPa]
1	3.2	28.16	207.25	179.08	97.51	69.35	61.28	0.2167
2	3.2	97.51	275.69	178.18	158.21	60.70	65.93	0.1897
3	3.2	158.21	338.74	180.54	218.16	59.95	66.79	0.1873
4	3.2	218.16	401.12	182.96	279.41	61.26	66.52	0.1914
5	3.2	279.41	464.35	184.94	342.53	63.12	65.87	0.1973
6	3.2	342.53	529.00	186.47	407.58	65.05	65.12	0.2033
7	3.2	407.58	595.20	187.62	474.40	66.81	64.39	0.2088
8	3.2	474.40	662.90	188.51	542.75	68.35	63.74	0.2136
9	3.2	542.75	731.97	189.22	612.42	69.67	63.18	0.2177
10	3.2	612.42	802.24	189.82	683.39	70.97	62.61	0.2218
R _{3.2} = 64.54								J _{nr(3.2)} = 0.2048

Average percent recovery

Load level 0.1 kPa
 Load level 3.2 kPa

R_{0.1} = 78.72 %
 R_{3.2} = 64.54 %

Percent difference of recovery

Load levels 0.1 kPa and 3.2 kPa

R_{diff} = 18.01 %

Average non-recoverable creep compliance

Load level 0.1 kPa
 Load level 3.2 kPa

J_{nr(0.1)} = 0.1278 1/kPa
 J_{nr(3.2)} = 0.2048 1/kPa

Percent difference of non-recoverable creep compliance

Load levels 0.1 kPa and 3.2 kPa

J_{nr_diff} = 60.21 %

Indication that the asphalt binder is modified with an acceptable elastomeric polymer

Load level 3.2 kPa

above criterion (probably modified)

PASSED Extremely Heavy Traffic "E" grade at 64.00 °C according to AASHTO M 332-14.

Responsible Employee:

Signature:

MSCR-Test (AASHTO T350-14) - Final Report

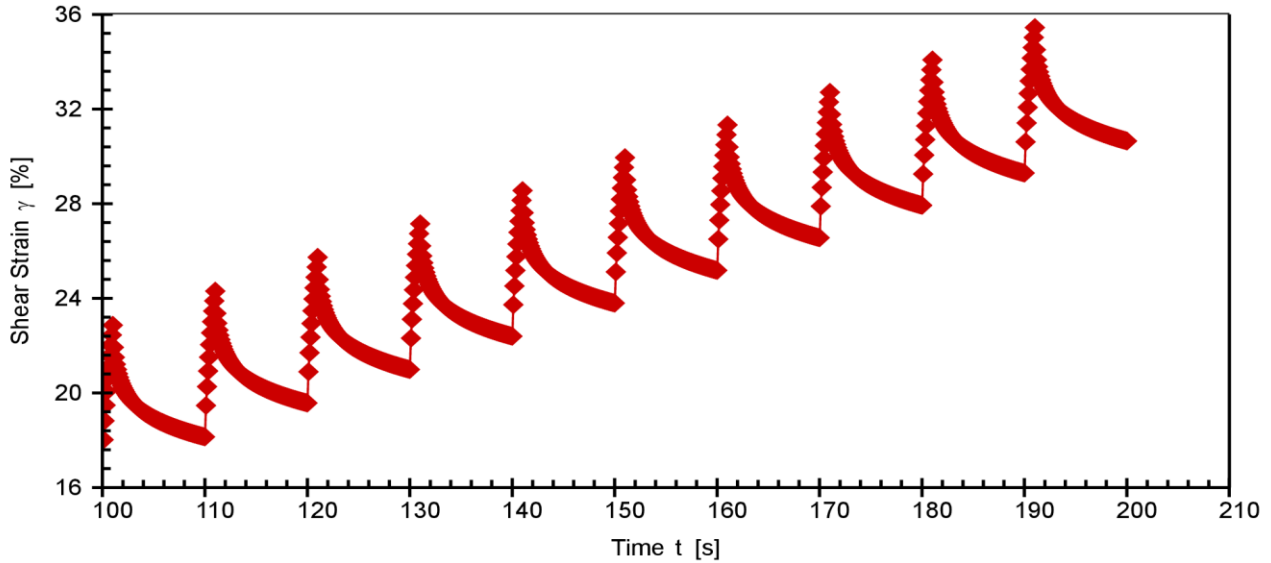
Project name: 2018-07-25_MSCR (V2)

Date, Time: 2018-07-25 12:04:56 PM
Test name: 2018-07-25_MSCR_0.1/3.2kPa
Operator: user
Sample: Sunny
Batch no.: MTO2
Description: BC10-H2O
Configuration: Anton Paar SmartPave 102 SN82314644
PP25/PE SN52739

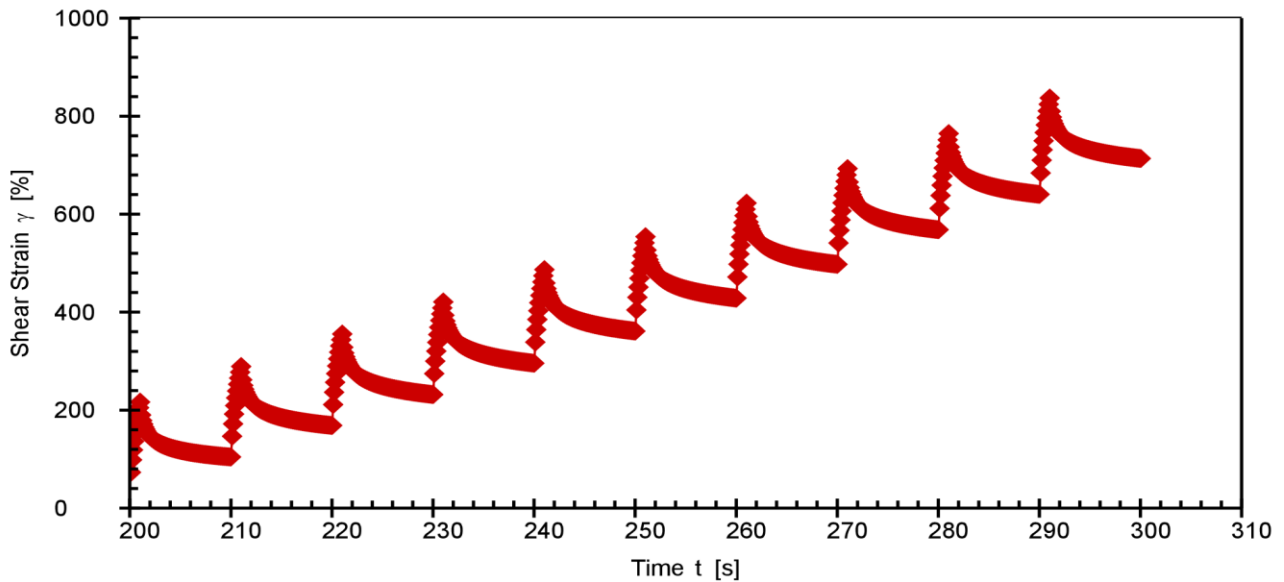
P-PTD200+H-PTD120 SN82331818-82284206



MSCR 0.1kPa (conditioning cycles are not shown)



MSCR 3.2kPa



Responsible Employee:

Signature:

MSCR-Test (AASHTO T350-14) - Final Report

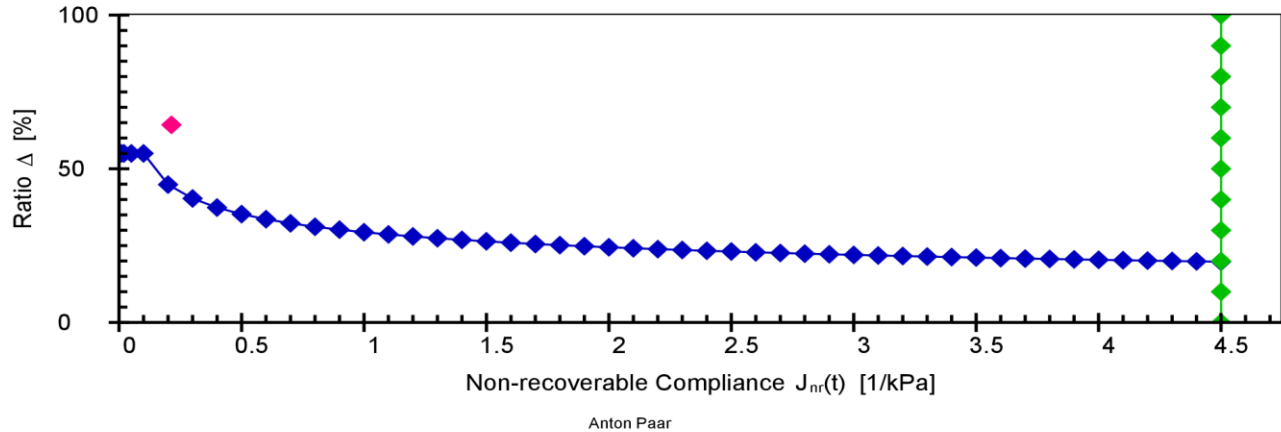
Project name: 2018-07-25_MSCR (V2)



Date, Time: 2018-07-25 12:04:56 PM
 Test name: 2018-07-25_MSCR_0.1/3.2kPa
 Operator: user
 Sample: Sunny
 Batch no.: MTO2
 Description: BC10-H2O
 Configuration: Anton Paar SmartPave 102 SN82314644
 PP25/PE SN52739

P-PTD200+H-PTD120 SN82331818-82284206

Jnr vs. % recovery (at 3.2 kPa)



Asphalt MSCR

Application version: Anton Paar RheoCompass™, V1.20.471-Release
 Licensed for: University of Waterloo - CPATT, License no. Rh17H7681, Version no. 1.20.0.0
 Project: 2018-07-25_MSCR (V2)
 Input data: 2018-07-25_MSCR_0.1/3.2kPa, <Last measuring result>, From interval 1, Point 1
 Result data: Asphalt MSCR Analysis

PARAMETERS:
 Load level mode: User-defined load levels (not according to norm)
 Number of intervals to skip: 0
 Calculation mode: Calculation according to ASTM D7405 - 15 and AASHTO M 332-14

Level 1
 Load: 0.1 kPa
 Conditioning cycles: 10
 Analyzed cycles: 10
 Creep phase duration: 1 s
 Recovery phase duration: 9 s
 Level 2
 Load: 3.2 kPa
 Conditioning cycles: 0
 Analyzed cycles: 10
 Creep phase duration: 1 s
 Recovery phase duration: 9 s
 Show parameter settings: On
 Show result table: Detailed (according to norm)
 Show classification: On

RESULTS:
 Sample name: -
 Test date: 11:47:53 AM
 Test temperature: 64.00 °C

Load level 0.1 kPa (average load: 0.1 kPa)

Cycle	Load [kPa]	$\bar{\epsilon}_0$ [%]	$\bar{\epsilon}_c$ [%]	$\bar{\epsilon}_1$ [%]	$\bar{\epsilon}_r$ [%]	$\bar{\epsilon}_{10}$ [%]	R _N [%]	J _{nr} (0.1, N) [1/kPa]
1	0.1	16.70	22.86	6.17	18.14	1.45	76.56	0.1445
2	0.1	18.14	24.30	6.16	19.57	1.43	76.77	0.1432

Responsible Employee:

Signature:

MSCR-Test (AASHTO T350-14) - Final Report

Project name: 2018-07-25_MSCR (V2)



Date, Time: 2018-07-25 12:04:56 PM
 Test name: 2018-07-25_MSCR_0.1/3.2kPa
 Operator: user
 Sample: Sunny
 Batch no.: MTO2
 Description: BC10-H2O
 Configuration: Anton Paar SmartPave 102 SN82314644

PP25/PE SN52739

P-PTD200+H-PTD120 SN82331818-82284206

Cycle	Load [kPa]	ϵ_0 [%]	ϵ_c [%]	ϵ_l [%]	ϵ_r [%]	ϵ_{10} [%]	R_N [%]	J_nr(0.1) [1/kPa]
3	0.1	19.57	25.73	6.16	20.99	1.42	77.01	0.1416
4	0.1	20.99	27.15	6.16	22.40	1.41	77.16	0.1406
5	0.1	22.40	28.56	6.16	23.80	1.40	77.29	0.1399
6	0.1	23.80	29.95	6.15	25.18	1.39	77.48	0.1385
7	0.1	25.18	31.33	6.15	26.56	1.38	77.59	0.1378
8	0.1	26.56	32.71	6.15	27.93	1.37	77.70	0.1371
9	0.1	27.93	34.08	6.15	29.29	1.36	77.83	0.1363
10	0.1	29.29	35.44	6.15	30.65	1.36	77.92	0.1358
							R_0.1 = 77.33	J_nr(0.1) = 0.1395

Load level 3.2 kPa (average load: 3.2 kPa)

Cycle	Load [kPa]	ϵ_0 [%]	ϵ_c [%]	ϵ_l [%]	ϵ_r [%]	ϵ_{10} [%]	R_N [%]	J_nr(3.2, N) [1/kPa]
1	3.2	30.65	216.66	186.01	104.35	73.70	60.38	0.2303
2	3.2	104.35	289.13	184.78	168.73	64.38	65.16	0.2012
3	3.2	168.73	355.51	186.78	231.81	63.08	66.23	0.1971
4	3.2	231.81	420.82	189.01	295.76	63.95	66.16	0.1999
5	3.2	295.76	486.75	190.99	361.29	65.53	65.69	0.2048
6	3.2	361.29	553.98	192.69	428.59	67.29	65.08	0.2103
7	3.2	428.59	622.74	194.16	497.64	69.05	64.44	0.2158
8	3.2	497.64	693.00	195.36	568.32	70.68	63.82	0.2209
9	3.2	568.32	764.55	196.23	640.42	72.10	63.26	0.2253
10	3.2	640.42	837.10	196.67	713.87	73.45	62.66	0.2295
							R_3.2 = 64.29	J_nr(3.2) = 0.2135

Average percent recovery

Load level 0.1 kPa R_0.1 = 77.33 %
 Load level 3.2 kPa R_3.2 = 64.29 %

Percent difference of recovery

Load levels 0.1 kPa and 3.2 kPa R_diff = 16.87 %

Average non-recoverable creep compliance

Load level 0.1 kPa J_nr(0.1) = 0.1395 1/kPa
 Load level 3.2 kPa J_nr(3.2) = 0.2135 1/kPa

Percent difference of non-recoverable creep compliance

Load levels 0.1 kPa and 3.2 kPa J_nr_diff = 53.01 %

Indication that the asphalt binder is modified with an acceptable elastomeric polymer above criterion (probably modified)
 Load level 3.2 kPa

PASSED Extremely Heavy Traffic "E" grade at 64.00 °C according to AASHTO M 332-14.

Responsible Employee:

Signature:

MSCR-Test (AASHTO T350-14) - Final Report

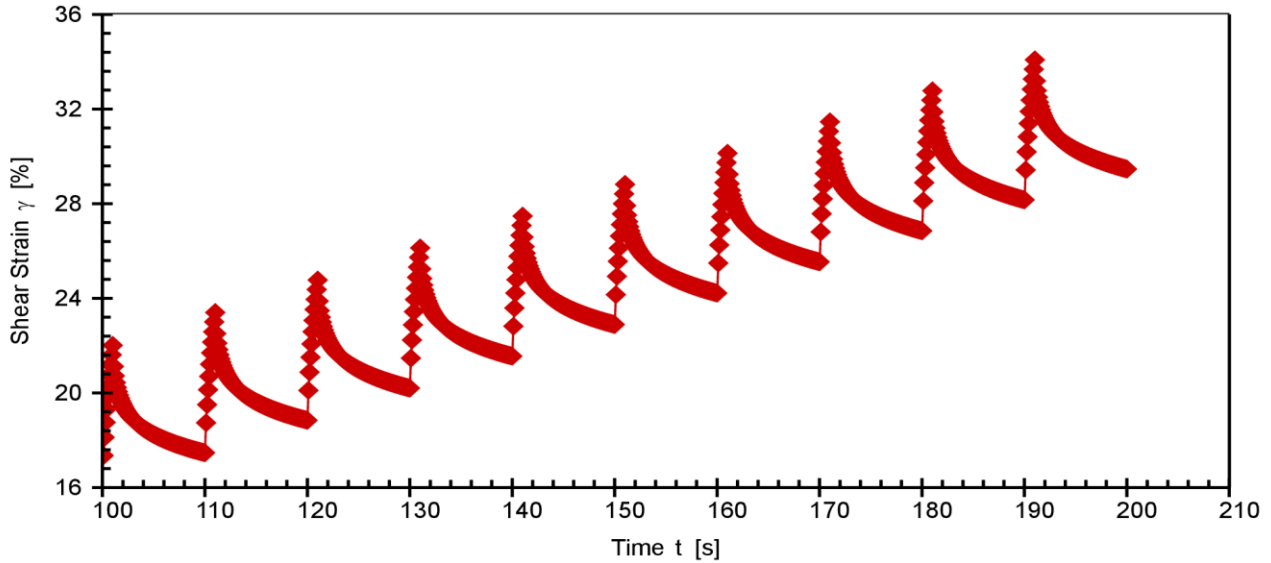
Project name: 2018-07-26_MSCR (V2)

Date, Time: 2018-07-26 4:30:50 PM
Test name: 2018-07-26_MSCR_0.1/3.2kPa
Operator: user
Sample: Sunny
Batch no.: MTO2
Description: BC10-NoH2O
Configuration: Anton Paar SmartPave 102 SN82314644
PP25/PE SN52739

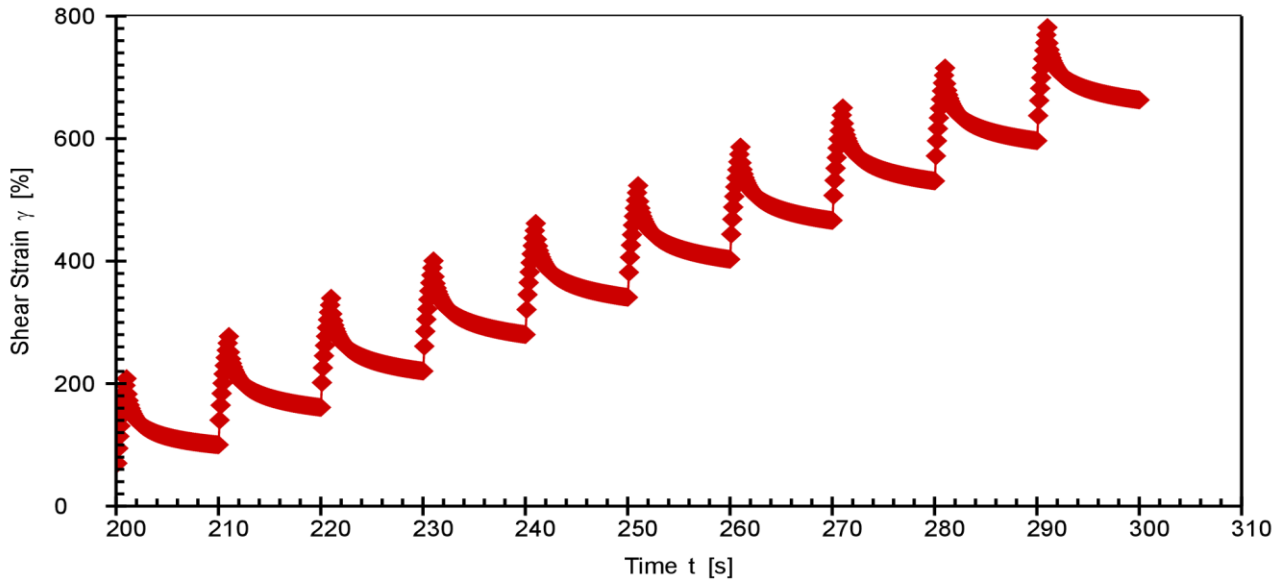
P-PTD200+H-PTD120 SN82331818-82284206



MSCR 0.1kPa (conditioning cycles are not shown)



MSCR 3.2kPa



Responsible Employee:

Signature:

MSCR-Test (AASHTO T350-14) - Final Report

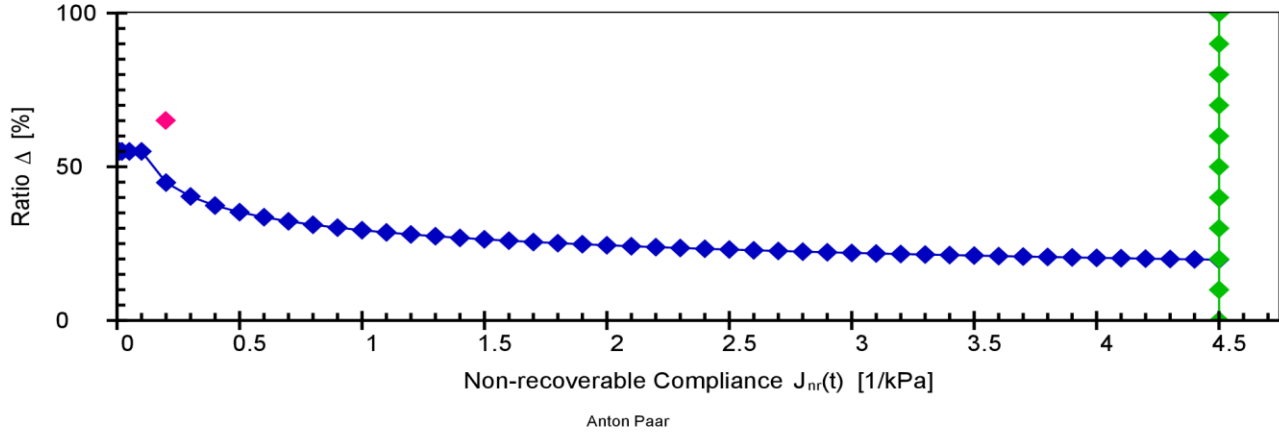
Project name: 2018-07-26_MSCR (V2)



Date, Time: 2018-07-26 4:30:50 PM
 Test name: 2018-07-26_MSCR_0.1/3.2kPa
 Operator: user
 Sample: Sunny
 Batch no.: MTO2
 Description: BC10-NoH2O
 Configuration: Anton Paar SmartPave 102 SN82314644
 PP25/PE SN52739

P-PTD200+H-PTD120 SN82331818-82284206

Jnr vs. % recovery (at 3.2 kPa)



Asphalt MSCR

Application version: Anton Paar RheoCompass™, V1.20.471-Release
 Licensed for: University of Waterloo - CPATT, License no. Rh17H7681, Version no. 1.20.0.0
 Project: 2018-07-26_MSCR (V2)
 Input data: 2018-07-26_MSCR_0.1/3.2kPa, <Last measuring result>, From interval 1, Point 1
 Result data: Asphalt MSCR Analysis

PARAMETERS:
 Load level mode: User-defined load levels (not according to norm)
 Number of intervals to skip: 0
 Calculation mode: Calculation according to ASTM D7405 - 15 and AASHTO M 332-14

Level 1
 Load: 0.1 kPa
 Conditioning cycles: 10
 Analyzed cycles: 10
 Creep phase duration: 1 s
 Recovery phase duration: 9 s

Level 2
 Load: 3.2 kPa
 Conditioning cycles: 0
 Analyzed cycles: 10
 Creep phase duration: 1 s
 Recovery phase duration: 9 s

Show parameter settings: On
 Show result table: Detailed (according to norm)
 Show classification: On

RESULTS:
 Sample name: -
 Test date: 4:13:51 PM
 Test temperature: 64.00 °C

Load level 0.1 kPa (average load: 0.1 kPa)

Cycle	Load [kPa]	$\bar{\epsilon}_0$ [%]	$\bar{\epsilon}_c$ [%]	$\bar{\epsilon}_1$ [%]	$\bar{\epsilon}_r$ [%]	$\bar{\epsilon}_{10}$ [%]	R _N [%]	J _{nr} (0.1, N) [1/kPa]
1	0.1	16.09	22.01	5.93	17.47	1.39	76.62	0.1385
2	0.1	17.47	23.40	5.93	18.84	1.37	76.84	0.1374

Responsible Employee:

Signature:

MSCR-Test (AASHTO T350-14) - Final Report

Project name: 2018-07-26_MSCR (V2)



Date, Time: 2018-07-26 4:30:50 PM
 Test name: 2018-07-26_MSCR_0.1/3.2kPa
 Operator: user
 Sample: Sunny
 Batch no.: MTO2
 Description: BC10-NoH2O
 Configuration: Anton Paar SmartPave 102 SN82314644

PP25/PE SN52739

P-PTD200+H-PTD120 SN82331818-82284206

Cycle	Load [kPa]	ϵ_0 [%]	ϵ_c [%]	ϵ_l [%]	ϵ_r [%]	ϵ_{10} [%]	R_N [%]	J_nr(N) [1/kPa]
3	0.1	18.84	24.77	5.93	20.20	1.36	77.09	0.1358
4	0.1	20.20	26.13	5.93	21.55	1.35	77.21	0.1351
5	0.1	21.55	27.48	5.92	22.89	1.34	77.39	0.1340
6	0.1	22.89	28.82	5.92	24.22	1.33	77.59	0.1327
7	0.1	24.22	30.14	5.91	25.54	1.32	77.67	0.1321
8	0.1	25.54	31.46	5.92	26.85	1.31	77.82	0.1313
9	0.1	26.85	32.77	5.92	28.16	1.31	77.94	0.1305
10	0.1	28.16	34.08	5.92	29.46	1.30	77.98	0.1304
							R_0.1 = 77.42	J_nr(0.1) = 0.1338

Load level 3.2 kPa (average load: 3.2 kPa)

Cycle	Load [kPa]	ϵ_0 [%]	ϵ_c [%]	ϵ_l [%]	ϵ_r [%]	ϵ_{10} [%]	R_N [%]	J_nr(3.2, N) [1/kPa]
1	3.2	29.46	208.36	178.90	100.10	70.64	60.51	0.2207
2	3.2	100.10	277.19	177.08	161.19	61.09	65.50	0.1909
3	3.2	161.19	339.65	178.46	220.50	59.31	66.77	0.1853
4	3.2	220.50	400.55	180.05	280.17	59.67	66.86	0.1865
5	3.2	280.17	461.63	181.46	340.95	60.78	66.51	0.1899
6	3.2	340.95	523.47	182.52	403.03	62.08	65.99	0.1940
7	3.2	403.03	586.37	183.35	466.39	63.36	65.44	0.1980
8	3.2	466.39	650.40	184.01	530.97	64.58	64.90	0.2018
9	3.2	530.97	715.52	184.55	596.63	65.66	64.42	0.2052
10	3.2	596.63	781.62	184.99	663.46	66.83	63.87	0.2088
							R_3.2 = 65.08	J_nr(3.2) = 0.1981

Average percent recovery

Load level 0.1 kPa R_0.1 = 77.42 %
 Load level 3.2 kPa R_3.2 = 65.08 %

Percent difference of recovery

Load levels 0.1 kPa and 3.2 kPa R_diff = 15.94 %

Average non-recoverable creep compliance

Load level 0.1 kPa J_nr(0.1) = 0.1338 1/kPa
 Load level 3.2 kPa J_nr(3.2) = 0.1981 1/kPa

Percent difference of non-recoverable creep compliance

Load levels 0.1 kPa and 3.2 kPa J_nr_diff = 48.09 %

Indication that the asphalt binder is modified with an acceptable elastomeric polymer

Load level 3.2 kPa above criterion (probably modified)

PASSED Extremely Heavy Traffic "E" grade at 64.00 °C according to AASHTO M 332-14.

Responsible Employee:

Signature:

MSCR-Test (AASHTO T350-14) - Final Report

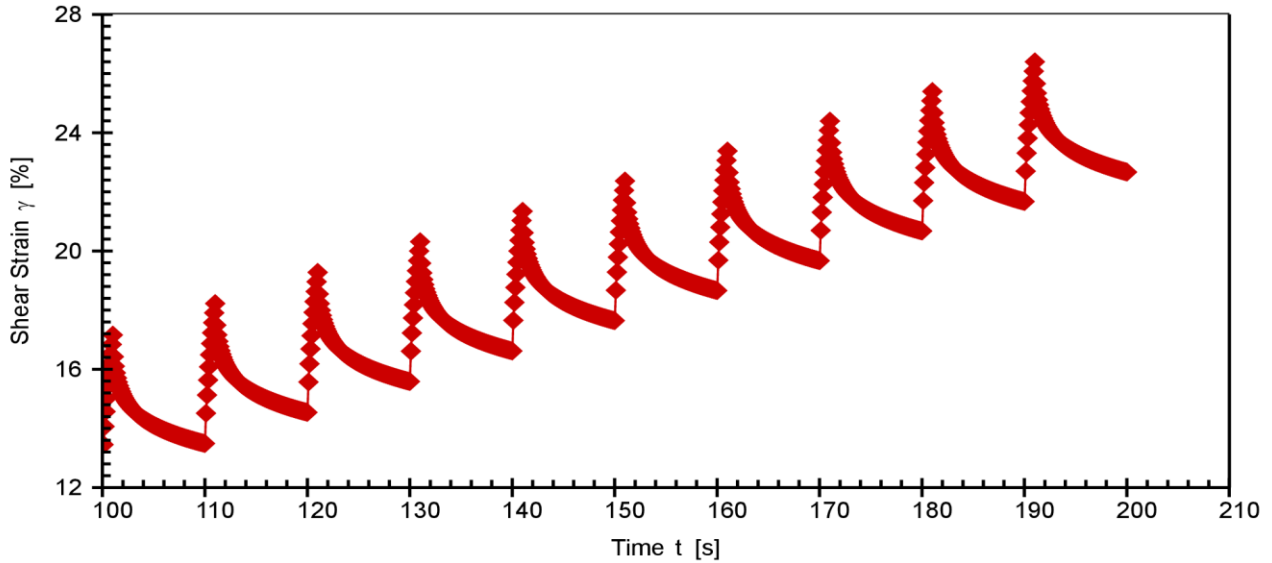
Project name: 2018-07-28_MSCR (V2)

Date, Time: 2018-07-28 2:06:58 PM
Test name: 2018-07-28_MSCR_0.1/3.2kPa
Operator: user
Sample: Sunny
Batch no.: MTO2
Description: BC15-H2O
Configuration: Anton Paar SmartPave 102 SN82314644
PP25/PE SN52739

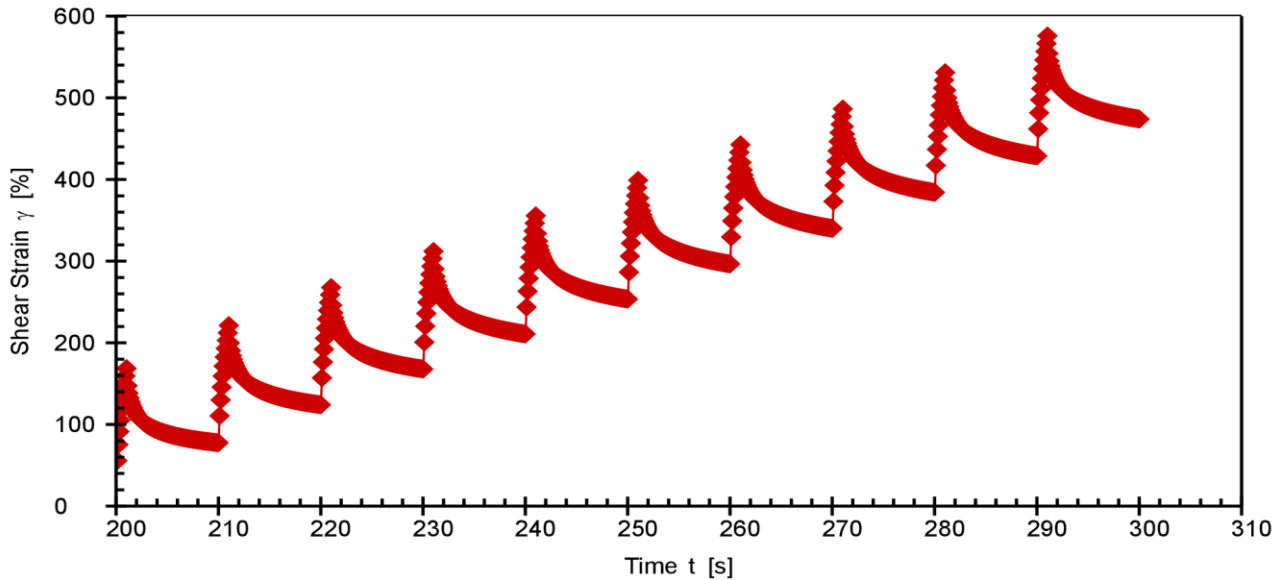
P-PTD200+H-PTD120 SN82331818-82284206



MSCR 0.1kPa (conditioning cycles are not shown)



MSCR 3.2kPa



Responsible Employee:

Signature:

MSCR-Test (AASHTO T350-14) - Final Report

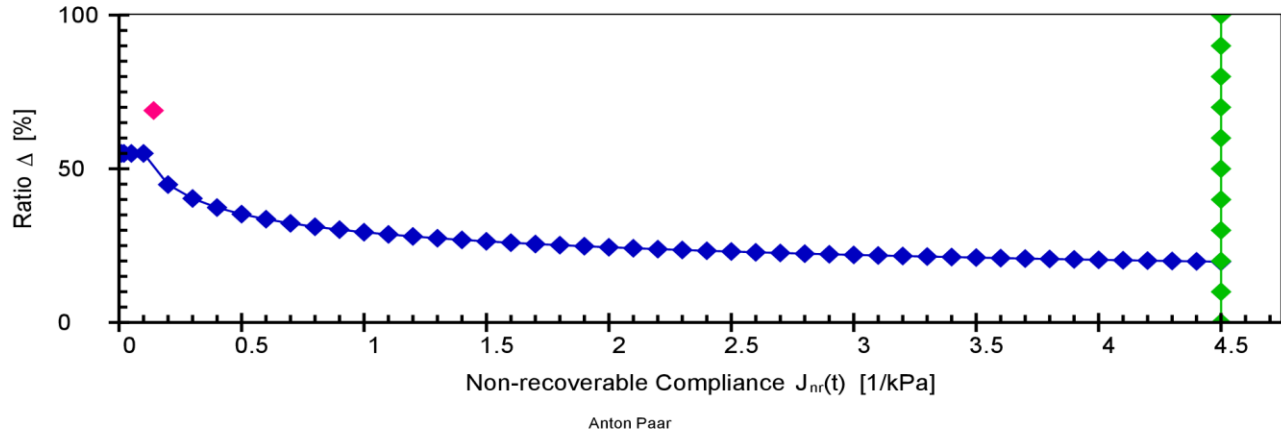
Project name: 2018-07-28_MSCR (V2)



Date, Time: 2018-07-28 2:06:58 PM
 Test name: 2018-07-28_MSCR_0.1/3.2kPa
 Operator: user
 Sample: Sunny
 Batch no.: MTO2
 Description: BC15-H2O
 Configuration: Anton Paar SmartPave 102 SN82314644
 PP25/PE SN52739

P-PTD200+H-PTD120 SN82331818-82284206

Jnr vs. % recovery (at 3.2 kPa)



Asphalt MSCR

Application version: Anton Paar RheoCompass™, V1.20.471-Release
 Licensed for: University of Waterloo - CPATT, License no. Rh17H7681, Version no. 1.20.0.0
 Project: 2018-07-28_MSCR (V2)
 Input data: 2018-07-28_MSCR_0.1/3.2kPa, <Last measuring result>, From interval 1, Point 1
 Result data: Asphalt MSCR Analysis

PARAMETERS:

Load level mode: User-defined load levels (not according to norm)
 Number of intervals to skip: 0
 Calculation mode: Calculation according to ASTM D7405 - 15 and AASHTO M 332-14

Level 1

Load: 0.1 kPa
 Conditioning cycles: 10
 Analyzed cycles: 10
 Creep phase duration: 1 s
 Recovery phase duration: 9 s

Level 2

Load: 3.2 kPa
 Conditioning cycles: 0
 Analyzed cycles: 10
 Creep phase duration: 1 s
 Recovery phase duration: 9 s

Show parameter settings: On

Show result table: Detailed (according to norm)

Show classification: On

RESULTS:

Sample name: -
 Test date: 1:51:26 PM
 Test temperature: 64.00 °C

Load level 0.1 kPa (average load: 0.1 kPa)

Cycle	Load [kPa]	$\bar{\epsilon}_0$ [%]	$\bar{\epsilon}_c$ [%]	$\bar{\epsilon}_1$ [%]	$\bar{\epsilon}_r$ [%]	$\bar{\epsilon}_{10}$ [%]	R _N [%]	$J_{nr}(0.1, N)$ [1/kPa]
1	0.1	12.42	17.16	4.73	13.49	1.06	77.51	0.1064
2	0.1	13.49	18.22	4.73	14.54	1.05	77.75	0.1054

Responsible Employee:

Signature:

MSCR-Test (AASHTO T350-14) - Final Report

Project name: 2018-07-28_MSCR (V2)



Date, Time: 2018-07-28 2:06:58 PM
 Test name: 2018-07-28_MSCR_0.1/3.2kPa
 Operator: user
 Sample: Sunny
 Batch no.: MTO2
 Description: BC15-H2O
 Configuration: Anton Paar SmartPave 102 SN82314644

PP25/PE SN52739

P-PTD200+H-PTD120 SN82331818-82284206

3	0.1	14.54	19.28	4.73	15.59	1.04	77.97	0.1043
4	0.1	15.59	20.32	4.73	16.62	1.03	78.12	0.1035
5	0.1	16.62	21.35	4.72	17.64	1.02	78.33	0.1024
6	0.1	17.64	22.37	4.72	18.66	1.02	78.46	0.1017
7	0.1	18.66	23.38	4.72	19.67	1.01	78.61	0.1010
8	0.1	19.67	24.39	4.72	20.68	1.00	78.73	0.1005
9	0.1	20.68	25.40	4.72	21.67	1.00	78.85	0.0998
10	0.1	21.67	26.40	4.73	22.67	0.99	78.95	0.0995
R _{0.1} = 78.33								J _{nr(0.1)} = 0.1024

Load level 3.2 kPa

(average load: 3.2 kPa)

Cycle	Load [kPa]	ϵ_0 [%]	ϵ_c [%]	ϵ_l [%]	ϵ_r [%]	ϵ_{10} [%]	R _N [%]	J _{nr(3.2, N)} [1/kPa]
1	3.2	22.67	168.57	145.90	77.62	54.95	62.34	0.1717
2	3.2	77.62	221.22	143.60	124.14	46.52	67.61	0.1454
3	3.2	124.14	267.78	143.64	167.89	43.76	69.54	0.1367
4	3.2	167.89	312.10	144.21	210.75	42.86	70.28	0.1339
5	3.2	210.75	355.62	144.86	253.52	42.77	70.47	0.1337
6	3.2	253.52	398.98	145.46	296.59	43.06	70.39	0.1346
7	3.2	296.59	442.56	145.97	340.12	43.53	70.18	0.1360
8	3.2	340.12	486.53	146.41	384.19	44.07	69.90	0.1377
9	3.2	384.19	530.95	146.76	428.84	44.64	69.58	0.1395
10	3.2	428.84	575.89	147.05	474.24	45.40	69.13	0.1419
R _{3.2} = 68.94								J _{nr(3.2)} = 0.1411

Average percent recovery

Load level 0.1 kPa
 Load level 3.2 kPa

R_{0.1} = 78.33 %
 R_{3.2} = 68.94 %

Percent difference of recovery

Load levels 0.1 kPa and 3.2 kPa

R_{diff} = 11.98 %

Average non-recoverable creep compliance

Load level 0.1 kPa
 Load level 3.2 kPa

J_{nr(0.1)} = 0.1024 1/kPa
 J_{nr(3.2)} = 0.1411 1/kPa

Percent difference of non-recoverable creep compliance

Load levels 0.1 kPa and 3.2 kPa

J_{nr_diff} = 37.75 %

Indication that the asphalt binder is modified with an acceptable elastomeric polymer

Load level 3.2 kPa above criterion (probably modified)

PASSED Extremely Heavy Traffic "E" grade at 64.00 °C according to AASHTO M 332-14.

Responsible Employee:

Signature:

MSCR-Test (AASHTO T350-14) - Final Report

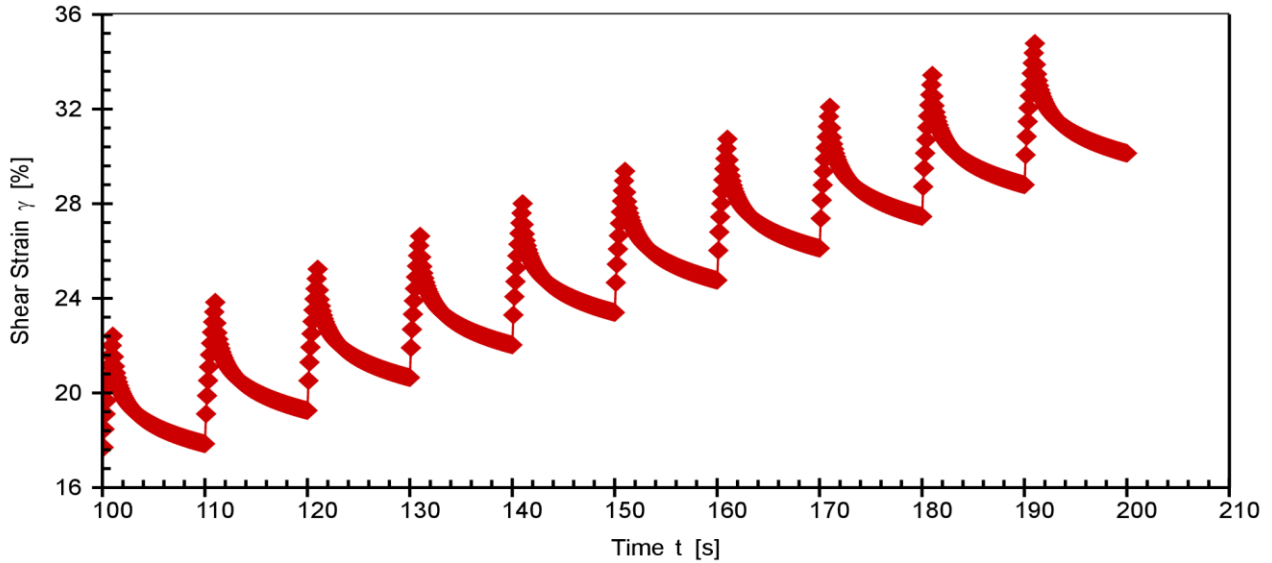
Project name: 2018-08-03_MSCR (V2)

Date, Time: 2018-08-03 11:33:53 AM
Test name: 2018-08-03_MSCR_0.1/3.2kPa
Operator: user
Sample: Sunny
Batch no.: MTO2
Description: BC15-NoH2O
Configuration: Anton Paar SmartPave 102 SN82314644
PP25/PE SN52739

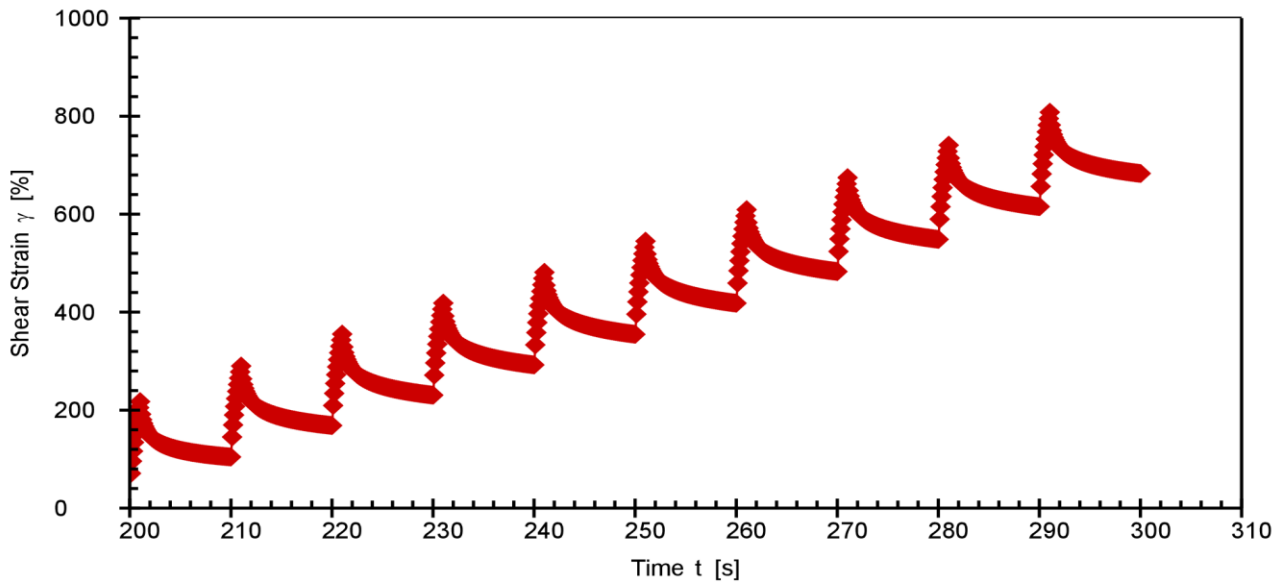
P-PTD200+H-PTD120 SN82331818-82284206



MSCR 0.1kPa (conditioning cycles are not shown)



MSCR 3.2kPa



Responsible Employee:

Signature:

MSCR-Test (AASHTO T350-14) - Final Report

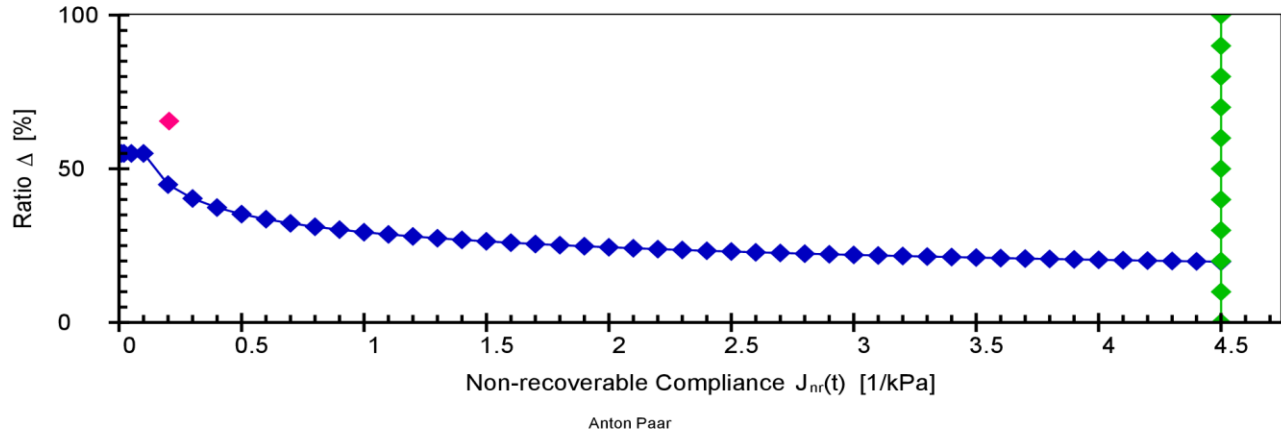
Project name: 2018-08-03_MSCR (V2)



Date, Time: 2018-08-03 11:33:53 AM
 Test name: 2018-08-03_MSCR_0.1/3.2kPa
 Operator: user
 Sample: Sunny
 Batch no.: MTO2
 Description: BC15-NoH2O
 Configuration: Anton Paar SmartPave 102 SN82314644
 PP25/PE SN52739

P-PTD200+H-PTD120 SN82331818-82284206

Jnr vs. % recovery (at 3.2 kPa)



Asphalt MSCR

Application version: Anton Paar RheoCompass™, V1.20.471-Release
 Licensed for: University of Waterloo - CPATT, License no. Rh17H7681, Version no. 1.20.0.0
 Project: 2018-08-03_MSCR (V2)
 Input data: 2018-08-03_MSCR_0.1/3.2kPa, <Last measuring result>, From interval 1, Point 1
 Result data: Asphalt MSCR Analysis

PARAMETERS:
 Load level mode: User-defined load levels (not according to norm)
 Number of intervals to skip: 0
 Calculation mode: Calculation according to ASTM D7405 - 15 and AASHTO M 332-14

Level 1
 Load: 0.1 kPa
 Conditioning cycles: 10
 Analyzed cycles: 10
 Creep phase duration: 1 s
 Recovery phase duration: 9 s

Level 2
 Load: 3.2 kPa
 Conditioning cycles: 0
 Analyzed cycles: 10
 Creep phase duration: 1 s
 Recovery phase duration: 9 s

Show parameter settings: On
 Show result table: Detailed (according to norm)
 Show classification: On

RESULTS:
 Sample name: -
 Test date: 11:17:31 AM
 Test temperature: 64.00 °C

Load level 0.1 kPa (average load: 0.1 kPa)

Cycle	Load [kPa]	$\bar{\epsilon}_0$ [%]	$\bar{\epsilon}_c$ [%]	$\bar{\epsilon}_1$ [%]	$\bar{\epsilon}_r$ [%]	$\bar{\epsilon}_{10}$ [%]	R _N [%]	J _{nr} (0.1, N) [1/kPa]
1	0.1	16.43	22.41	5.98	17.85	1.42	76.27	0.1420
2	0.1	17.85	23.83	5.98	19.26	1.41	76.50	0.1406

Responsible Employee:

Signature:

MSCR-Test (AASHTO T350-14) - Final Report

Project name: 2018-08-03_MSCR (V2)



Date, Time: 2018-08-03 11:33:53 AM
 Test name: 2018-08-03_MSCR_0.1/3.2kPa
 Operator: user
 Sample: Sunny
 Batch no.: MTO2
 Description: BC15-NoH2O
 Configuration: Anton Paar SmartPave 102 SN82314644

PP25/PE SN52739

P-PTD200+H-PTD120 SN82331818-82284206

3	0.1	19.26	25.24	5.98	20.65	1.39	76.73	0.1392
4	0.1	20.65	26.63	5.98	22.03	1.38	76.90	0.1382
5	0.1	22.03	28.01	5.98	23.40	1.37	77.04	0.1372
6	0.1	23.40	29.38	5.97	24.76	1.36	77.24	0.1360
7	0.1	24.76	30.73	5.97	26.12	1.35	77.35	0.1353
8	0.1	26.12	32.09	5.97	27.46	1.35	77.47	0.1345
9	0.1	27.46	33.43	5.97	28.80	1.34	77.60	0.1338
10	0.1	28.80	34.77	5.98	30.13	1.33	77.71	0.1332
R _{0.1} = 77.08 J _{nr} (0.1) = 0.1370								

Load level 3.2 kPa (average load: 3.2 kPa)

Cycle	Load [kPa]	ϵ_0 [%]	ϵ_c [%]	ϵ_l [%]	ϵ_r [%]	ϵ_{10} [%]	R _N [%]	J _{nr} (3.2, N) [1/kPa]
1	3.2	30.13	217.34	187.21	104.41	74.28	60.32	0.2321
2	3.2	104.41	289.97	185.56	168.68	64.27	65.36	0.2008
3	3.2	168.68	355.21	186.53	230.60	61.92	66.81	0.1935
4	3.2	230.60	418.39	187.79	292.36	61.76	67.11	0.1930
5	3.2	292.36	481.34	188.98	354.81	62.45	66.96	0.1951
6	3.2	354.81	544.86	190.05	418.29	63.49	66.60	0.1984
7	3.2	418.29	609.25	190.95	482.90	64.61	66.17	0.2019
8	3.2	482.90	674.61	191.71	548.62	65.72	65.72	0.2054
9	3.2	548.62	740.89	192.27	615.36	66.74	65.29	0.2086
10	3.2	615.36	808.05	192.69	683.22	67.86	64.78	0.2121
R _{3.2} = 65.51 J _{nr} (3.2) = 0.2041								

Average percent recovery

Load level 0.1 kPa
 Load level 3.2 kPa

R_{0.1} = 77.08 %
 R_{3.2} = 65.51 %

Percent difference of recovery

Load levels 0.1 kPa and 3.2 kPa

R_{diff} = 15.01 %

Average non-recoverable creep compliance

Load level 0.1 kPa
 Load level 3.2 kPa

J_{nr}(0.1) = 0.1370 1/kPa
 J_{nr}(3.2) = 0.2041 1/kPa

Percent difference of non-recoverable creep compliance

Load levels 0.1 kPa and 3.2 kPa

J_{nr_diff} = 48.97 %

Indication that the asphalt binder is modified with an acceptable elastomeric polymer

Load level 3.2 kPa

above criterion (probably modified)

PASSED Extremely Heavy Traffic "E" grade at 64.00 °C according to AASHTO M 332-14.

Responsible Employee:

Signature:

MSCR-Test (AASHTO T350-14) - Final Report

Project name: 2018-08-03_MSCR (V2)

Date, Time: 2018-08-03 7:18:47 PM

Test name: 2018-08-03_MSCR_0.1/3.2kPa

Operator: user

Sample: Sunny

Batch no.: MTO2

Description: BC20-H2O

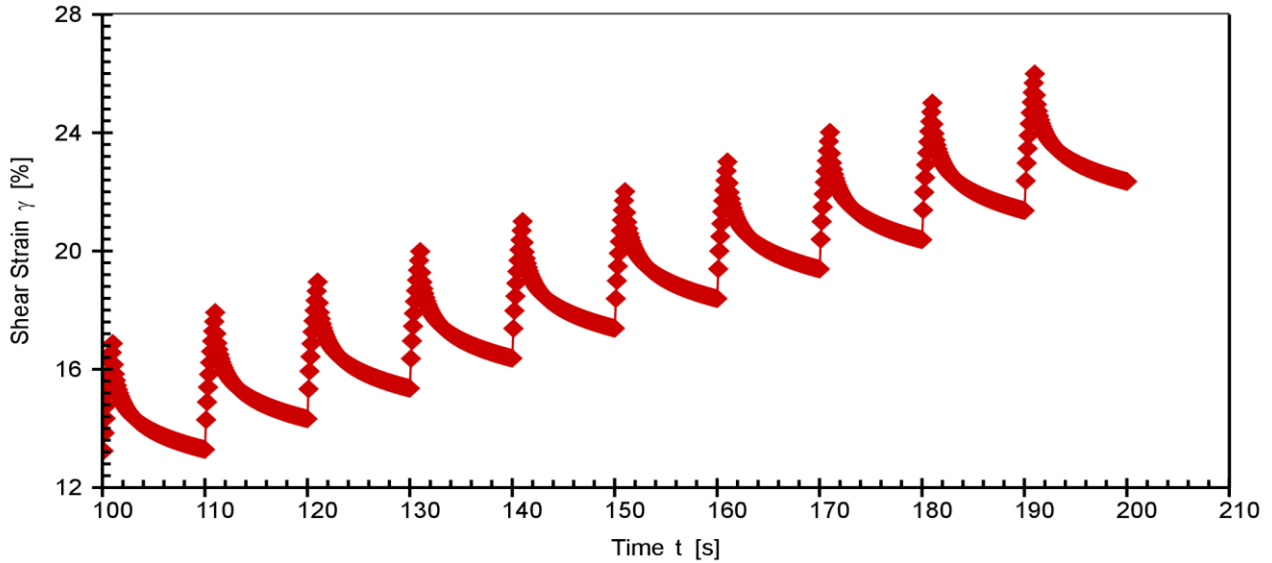
Configuration: Anton Paar SmartPave 102 SN82314644

PP25/PE SN52739

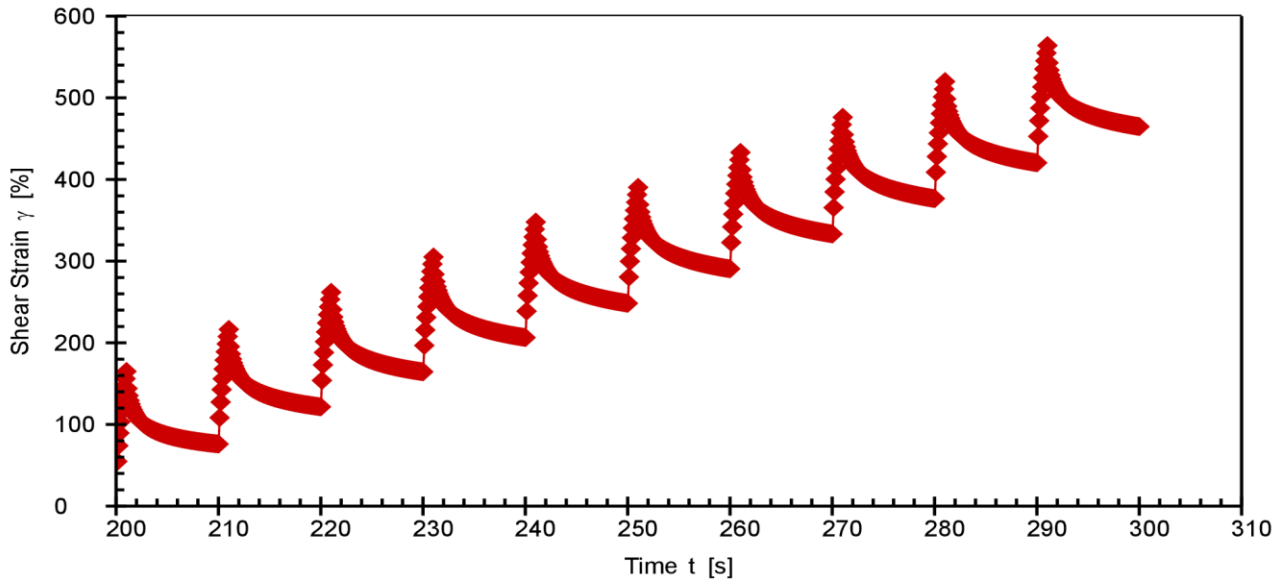
P-PTD200+H-PTD120 SN82331818-82284206



MSCR 0.1kPa (conditioning cycles are not shown)



MSCR 3.2kPa



Responsible Employee:

Signature:

MSCR-Test (AASHTO T350-14) - Final Report

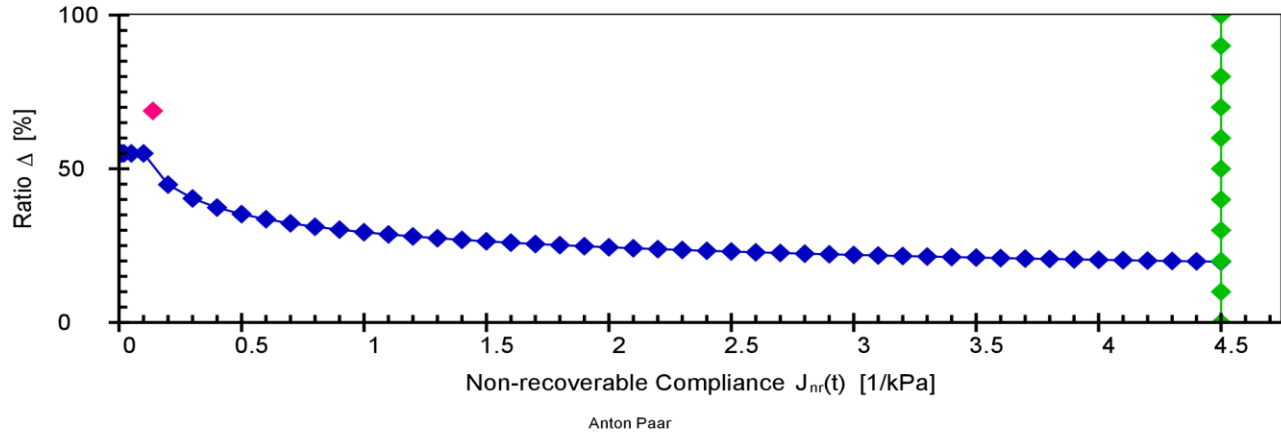
Project name: 2018-08-03_MSCR (V2)



Date, Time: 2018-08-03 7:18:47 PM
 Test name: 2018-08-03_MSCR_0.1/3.2kPa
 Operator: user
 Sample: Sunny
 Batch no.: MTO2
 Description: BC20-H2O
 Configuration: Anton Paar SmartPave 102 SN82314644
 PP25/PE SN52739

P-PTD200+H-PTD120 SN82331818-82284206

Jnr vs. % recovery (at 3.2 kPa)



Asphalt MSCR

Application version: Anton Paar RheoCompass™, V1.20.471-Release
 Licensed for: University of Waterloo - CPATT, License no. Rh17H7681, Version no. 1.20.0.0
 Project: 2018-08-03_MSCR (V2)
 Input data: 2018-08-03_MSCR_0.1/3.2kPa, <Last measuring result>, From interval 1, Point 1
 Result data: Asphalt MSCR Analysis

PARAMETERS:
 Load level mode: User-defined load levels (not according to norm)
 Number of intervals to skip: 0
 Calculation mode: Calculation according to ASTM D7405 - 15 and AASHTO M 332-14

Level 1
 Load: 0.1 kPa
 Conditioning cycles: 10
 Analyzed cycles: 10
 Creep phase duration: 1 s
 Recovery phase duration: 9 s

Level 2
 Load: 3.2 kPa
 Conditioning cycles: 0
 Analyzed cycles: 10
 Creep phase duration: 1 s
 Recovery phase duration: 9 s

Show parameter settings: On
 Show result table: Detailed (according to norm)
 Show classification: On

RESULTS:
 Sample name: -
 Test date: 7:01:48 PM
 Test temperature: 64.00 °C

Load level 0.1 kPa (average load: 0.1 kPa)

Cycle	Load [kPa]	$\bar{\epsilon}_0$ [%]	$\bar{\epsilon}_c$ [%]	$\bar{\epsilon}_1$ [%]	$\bar{\epsilon}_r$ [%]	$\bar{\epsilon}_{10}$ [%]	R _N [%]	J _{nr} (0.1, N) [1/kPa]
1	0.1	12.23	16.87	4.64	13.29	1.05	77.30	0.1053
2	0.1	13.29	17.92	4.64	14.32	1.04	77.64	0.1037

Responsible Employee:

Signature:

MSCR-Test (AASHTO T350-14) - Final Report

Project name: 2018-08-03_MSCR (V2)



Date, Time: 2018-08-03 7:18:47 PM
 Test name: 2018-08-03_MSCR_0.1/3.2kPa
 Operator: user
 Sample: Sunny
 Batch no.: MTO2
 Description: BC20-H2O
 Configuration: Anton Paar SmartPave 102 SN82314644

PP25/PE SN52739

P-PTD200+H-PTD120 SN82331818-82284206

3	0.1	14.32	18.96	4.63	15.36	1.03	77.74	0.1031
4	0.1	15.36	19.99	4.63	16.37	1.02	78.03	0.1017
5	0.1	16.37	21.00	4.63	17.39	1.01	78.12	0.1013
6	0.1	17.39	22.02	4.63	18.39	1.00	78.32	0.1004
7	0.1	18.39	23.02	4.63	19.39	1.00	78.40	0.1000
8	0.1	19.39	24.02	4.63	20.38	0.99	78.58	0.0991
9	0.1	20.38	25.01	4.63	21.37	0.99	78.64	0.0989
10	0.1	21.37	25.99	4.63	22.35	0.98	78.77	0.0982
R _{0.1} = 78.16								J _{nr(0.1)} = 0.1012

Load level 3.2 kPa

(average load: 3.2 kPa)

Cycle	Load [kPa]	ϵ_0 [%]	ϵ_c [%]	ϵ_l [%]	ϵ_r [%]	ϵ_{10} [%]	R _N [%]	J _{nr(3.2, N)} [1/kPa]
1	3.2	22.35	164.96	142.61	76.11	53.76	62.30	0.1680
2	3.2	76.11	216.41	140.29	121.64	45.52	67.55	0.1423
3	3.2	121.64	261.92	140.28	164.48	42.84	69.46	0.1339
4	3.2	164.48	305.28	140.80	206.46	41.98	70.18	0.1312
5	3.2	206.46	347.88	141.42	248.38	41.91	70.36	0.1310
6	3.2	248.38	390.38	142.01	290.59	42.22	70.27	0.1319
7	3.2	290.59	433.15	142.55	333.31	42.71	70.04	0.1335
8	3.2	333.31	476.28	142.97	376.56	43.25	69.75	0.1352
9	3.2	376.56	519.94	143.38	420.42	43.86	69.41	0.1371
10	3.2	420.42	564.07	143.65	465.02	44.60	68.95	0.1394
R _{3.2} = 68.83								J _{nr(3.2)} = 0.1383

Average percent recovery

Load level 0.1 kPa
 Load level 3.2 kPa

R_{0.1} = 78.16 %
 R_{3.2} = 68.83 %

Percent difference of recovery

Load levels 0.1 kPa and 3.2 kPa

R_{diff} = 11.94 %

Average non-recoverable creep compliance

Load level 0.1 kPa
 Load level 3.2 kPa

J_{nr(0.1)} = 0.1012 1/kPa
 J_{nr(3.2)} = 0.1383 1/kPa

Percent difference of non-recoverable creep compliance

Load levels 0.1 kPa and 3.2 kPa

J_{nr_diff} = 36.74 %

Indication that the asphalt binder is modified with an acceptable elastomeric polymer

Load level 3.2 kPa

above criterion (probably modified)

PASSED Extremely Heavy Traffic "E" grade at 64.00 °C according to AASHTO M 332-14.

Responsible Employee:

Signature:

MSCR-Test (AASHTO T350-14) - Final Report

Project name: 2018-08-04_MSCR (V2)

Date, Time: 2018-08-04 5:07:34 PM

Test name: 2018-08-04_MSCR_0.1/3.2kPa

Operator: user

Sample: Sunny

Batch no.: MTO2

Description: BC20-NoH2O

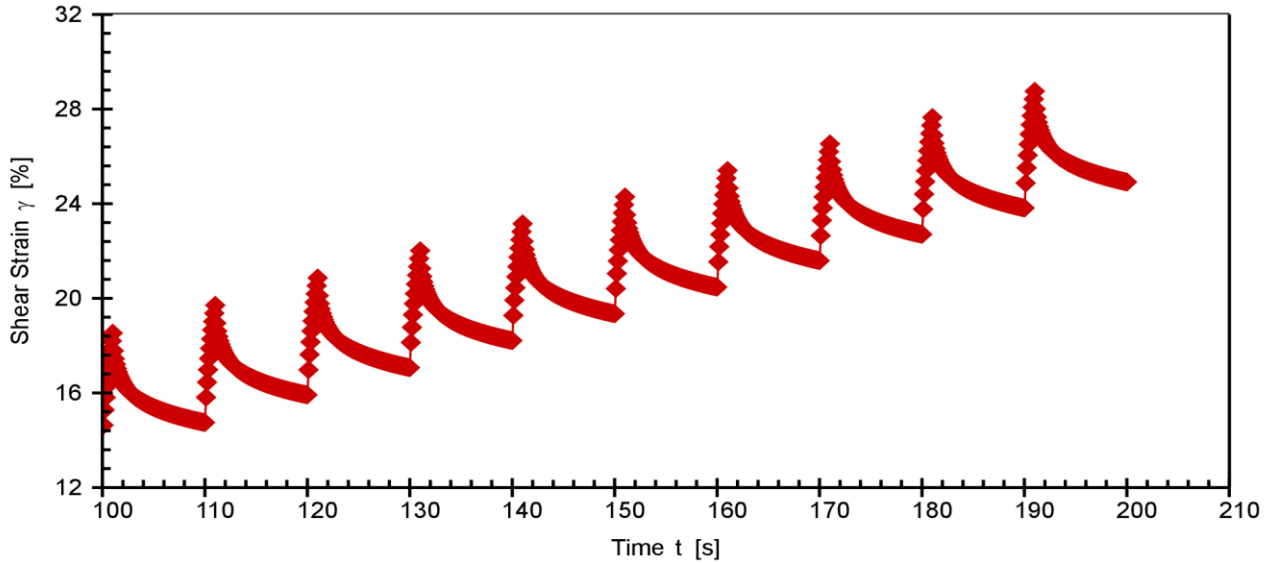
Configuration: Anton Paar SmartPave 102 SN82314644

PP25/PE SN52739

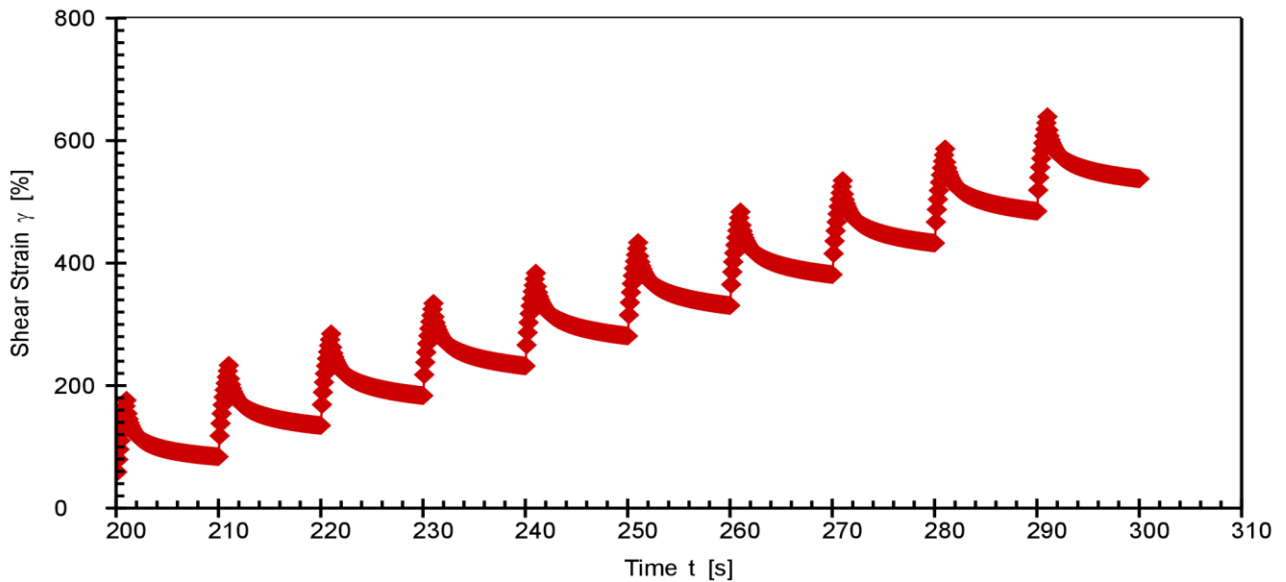
P-PTD200+H-PTD120 SN82331818-82284206



MSCR 0.1kPa (conditioning cycles are not shown)



MSCR 3.2kPa



Responsible Employee:

Signature:

MSCR-Test (AASHTO T350-14) - Final Report

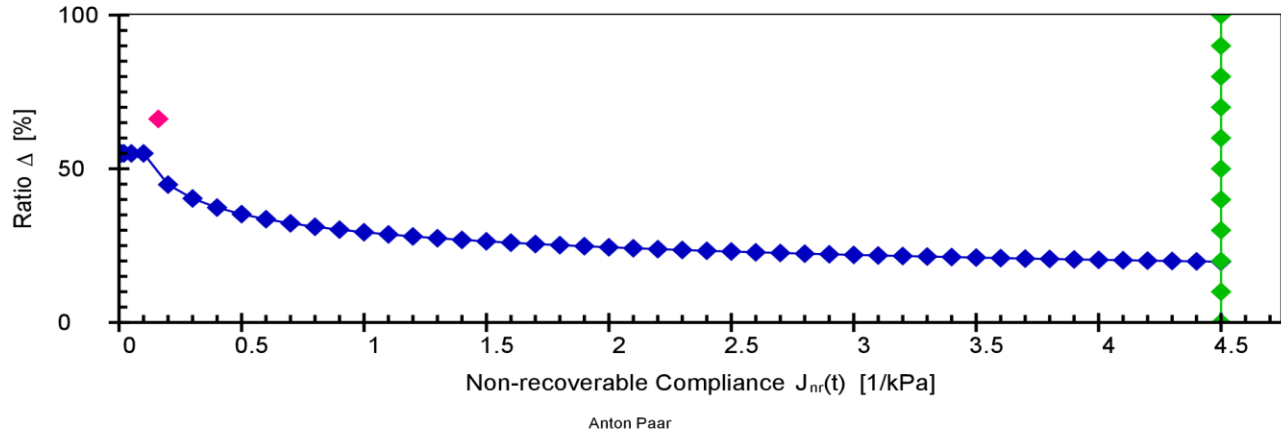
Project name: 2018-08-04_MSCR (V2)



Date, Time: 2018-08-04 5:07:34 PM
 Test name: 2018-08-04_MSCR_0.1/3.2kPa
 Operator: user
 Sample: Sunny
 Batch no.: MTO2
 Description: BC20-NoH2O
 Configuration: Anton Paar SmartPave 102 SN82314644
 PP25/PE SN52739

P-PTD200+H-PTD120 SN82331818-82284206

J_{nr} vs. % recovery (at 3.2 kPa)



Asphalt MSCR

Application version: Anton Paar RheoCompass™, V1.20.471-Release
 Licensed for: University of Waterloo - CPATT, License no. Rh17H7681, Version no. 1.20.0.0
 Project: 2018-08-04_MSCR (V2)
 Input data: 2018-08-04_MSCR_0.1/3.2kPa, <Last measuring result>, From interval 1, Point 1
 Result data: Asphalt MSCR Analysis

PARAMETERS:
 Load level mode: User-defined load levels (not according to norm)
 Number of intervals to skip: 0
 Calculation mode: Calculation according to ASTM D7405 - 15 and AASHTO M 332-14

Level 1
 Load: 0.1 kPa
 Conditioning cycles: 10
 Analyzed cycles: 10
 Creep phase duration: 1 s
 Recovery phase duration: 9 s
 Level 2
 Load: 3.2 kPa
 Conditioning cycles: 0
 Analyzed cycles: 10
 Creep phase duration: 1 s
 Recovery phase duration: 9 s
 Show parameter settings: On
 Show result table: Detailed (according to norm)
 Show classification: On

RESULTS:
 Sample name: -
 Test date: 4:51:03 PM
 Test temperature: 64.00 °C

Load level 0.1 kPa (average load: 0.1 kPa)

Cycle	Load [kPa]	$\bar{\epsilon}_0$ [%]	$\bar{\epsilon}_c$ [%]	$\bar{\epsilon}_1$ [%]	$\bar{\epsilon}_r$ [%]	$\bar{\epsilon}_{10}$ [%]	R _N [%]	J _{nr} (0.1, N) [1/kPa]
1	0.1	13.58	18.53	4.95	14.75	1.17	76.33	0.1172
2	0.1	14.75	19.70	4.96	15.92	1.17	76.45	0.1167

Responsible Employee:	Signature:
-----------------------	------------

MSCR-Test (AASHTO T350-14) - Final Report

Project name: 2018-08-04_MSCR (V2)



Date, Time: 2018-08-04 5:07:34 PM
 Test name: 2018-08-04_MSCR_0.1/3.2kPa
 Operator: user
 Sample: Sunny
 Batch no.: MTO2
 Description: BC20-NoH2O
 Configuration: Anton Paar SmartPave 102 SN82314644

PP25/PE SN52739

P-PTD200+H-PTD120 SN82331818-82284206

Cycle	Load [kPa]	ϵ_0 [%]	ϵ_c [%]	ϵ_l [%]	ϵ_r [%]	ϵ_{10} [%]	R_N [%]	J_nr
3	0.1	15.92	20.86	4.95	17.07	1.15	76.72	0.1152
4	0.1	17.07	22.02	4.95	18.21	1.15	76.86	0.1145
5	0.1	18.21	23.15	4.94	19.35	1.13	77.05	0.1134
6	0.1	19.35	24.29	4.94	20.47	1.13	77.22	0.1126
7	0.1	20.47	25.41	4.93	21.59	1.12	77.31	0.1120
8	0.1	21.59	26.53	4.94	22.70	1.11	77.49	0.1112
9	0.1	22.70	27.64	4.94	23.82	1.11	77.50	0.1112
10	0.1	23.82	28.75	4.94	24.92	1.10	77.72	0.1100
							R_0.1 = 77.06	J_nr(0.1) = 0.1134

Load level 3.2 kPa (average load: 3.2 kPa)

Cycle	Load [kPa]	ϵ_0 [%]	ϵ_c [%]	ϵ_l [%]	ϵ_r [%]	ϵ_{10} [%]	R_N [%]	J_nr(3.2, N) [1/kPa]
1	3.2	24.92	176.18	151.26	84.07	59.15	60.89	0.1849
2	3.2	84.07	233.27	149.20	135.01	50.94	65.86	0.1592
3	3.2	135.01	284.69	149.68	183.75	48.75	67.43	0.1523
4	3.2	183.75	334.41	150.65	232.23	48.47	67.83	0.1515
5	3.2	232.23	383.82	151.60	281.16	48.93	67.72	0.1529
6	3.2	281.16	433.58	152.43	330.86	49.70	67.39	0.1553
7	3.2	330.86	483.91	153.05	381.41	50.55	66.97	0.1580
8	3.2	381.41	534.95	153.53	432.78	51.37	66.54	0.1605
9	3.2	432.78	586.69	153.91	484.92	52.14	66.13	0.1629
10	3.2	484.92	639.13	154.21	537.94	53.03	65.62	0.1657
							R_3.2 = 66.24	J_nr(3.2) = 0.1603

Average percent recovery

Load level 0.1 kPa R_0.1 = 77.06 %
 Load level 3.2 kPa R_3.2 = 66.24 %

Percent difference of recovery

Load levels 0.1 kPa and 3.2 kPa R_diff = 14.05 %

Average non-recoverable creep compliance

Load level 0.1 kPa J_nr(0.1) = 0.1134 1/kPa
 Load level 3.2 kPa J_nr(3.2) = 0.1603 1/kPa

Percent difference of non-recoverable creep compliance

Load levels 0.1 kPa and 3.2 kPa J_nr_diff = 41.39 %

Indication that the asphalt binder is modified with an acceptable elastomeric polymer above criterion (probably modified)
 Load level 3.2 kPa

PASSED Extremely Heavy Traffic "E" grade at 64.00 °C according to AASHTO M 332-14.

Responsible Employee:

Signature:

MSCR-Test (AASHTO T350-14) - Final Report

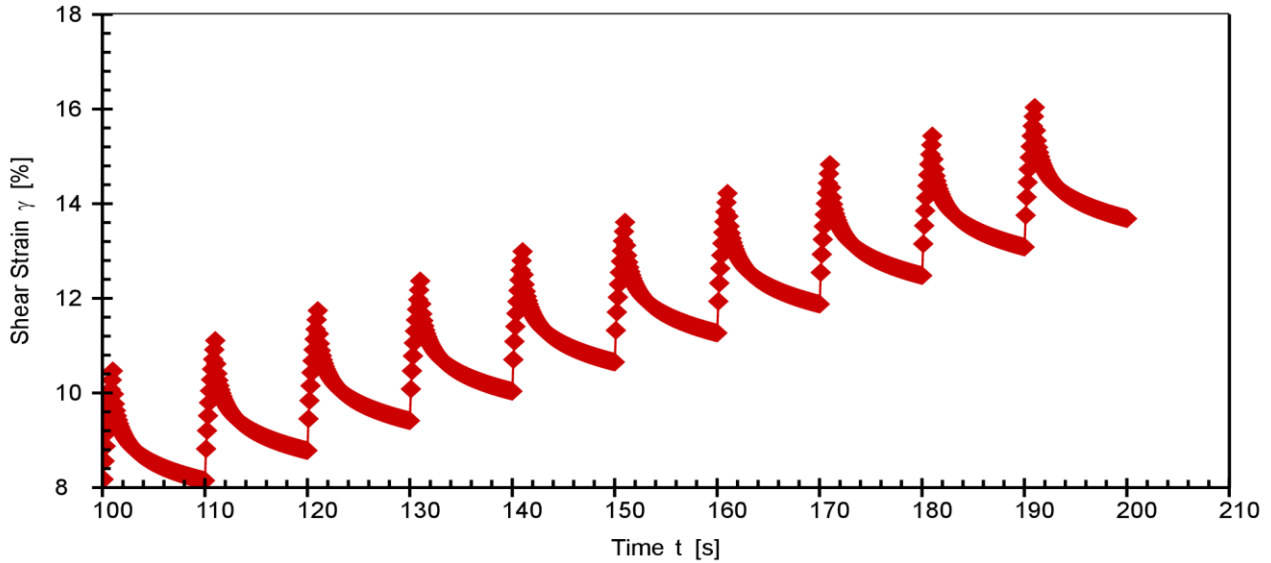
Project name: 2018-05-25_MSCR (V2)

Date, Time: 2018-05-25 4:10:55 PM
Test name: 2018-05-25_MSCR_0.1/3.2kPa
Operator: user
Sample: 64-28 RTFO + DOUBLE PAV
Batch no.: MTO2
Description: SUNNY
Configuration: Anton Paar SmartPave 102 SN82314644
PP25/PE SN52739

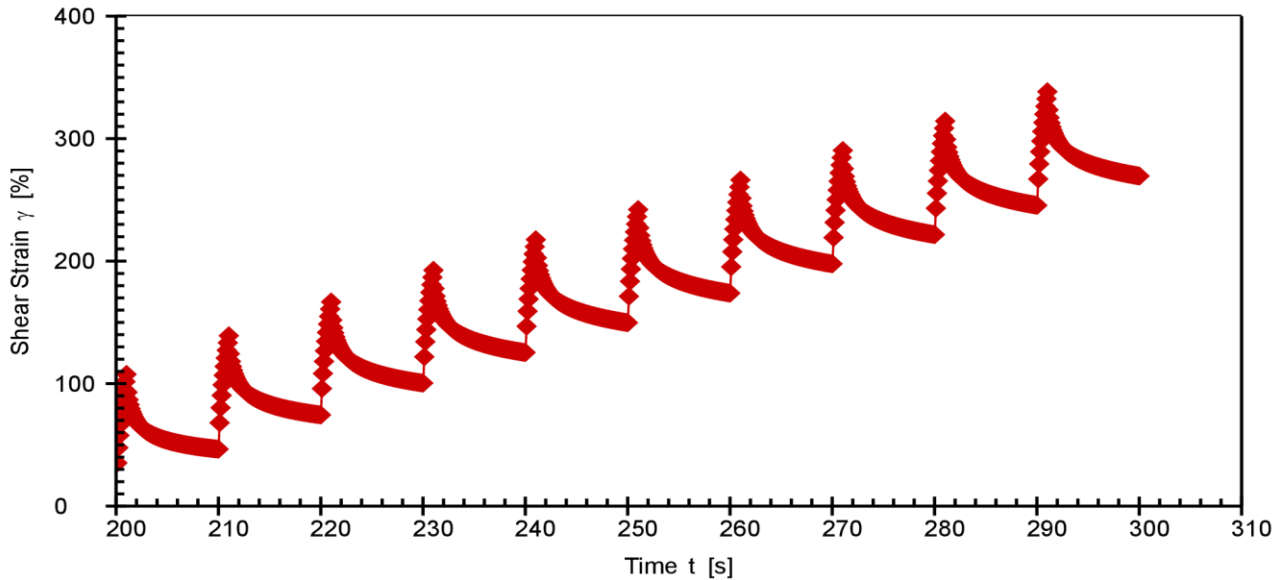
P-PTD200+H-PTD120 SN82331818-82284206



MSCR 0.1kPa (conditioning cycles are not shown)



MSCR 3.2kPa



Responsible Employee:

Signature:

MSCR-Test (AASHTO T350-14) - Final Report

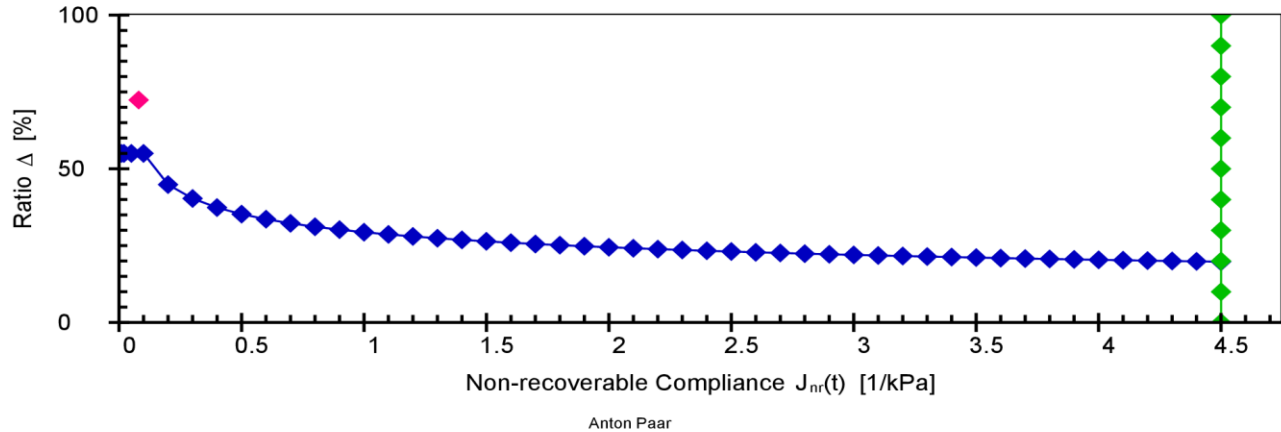
Project name: 2018-05-25_MSCR (V2)



Date, Time: 2018-05-25 4:10:55 PM
 Test name: 2018-05-25_MSCR_0.1/3.2kPa
 Operator: user
 Sample: 64-28 RTFO + DOUBLE PAV
 Batch no.: MTO2
 Description: SUNNY
 Configuration: Anton Paar SmartPave 102 SN82314644
 PP25/PE SN52739

P-PTD200+H-PTD120 SN82331818-82284206

J_{nr} vs. % recovery (at 3.2 kPa)



Asphalt MSCR

Application version: Anton Paar RheoCompass™, V1.20.471-Release
 Licensed for: University of Waterloo - CPATT, License no. Rh17H7681, Version no. 1.20.0.0
 Project: 2018-05-25_MSCR (V2)
 Input data: 2018-05-25_MSCR_0.1/3.2kPa, <Last measuring result>, From interval 1, Point 1
 Result data: Asphalt MSCR Analysis

PARAMETERS:
 Load level mode: User-defined load levels (not according to norm)
 Number of intervals to skip: 0
 Calculation mode: Calculation according to ASTM D7405 - 15 and AASHTO M 332-14

Level 1
 Load: 0.1 kPa
 Conditioning cycles: 10
 Analyzed cycles: 10
 Creep phase duration: 1 s
 Recovery phase duration: 9 s
 Level 2
 Load: 3.2 kPa
 Conditioning cycles: 0
 Analyzed cycles: 10
 Creep phase duration: 1 s
 Recovery phase duration: 9 s
 Show parameter settings: On
 Show result table: Detailed (according to norm)
 Show classification: On

RESULTS:
 Sample name: -
 Test date: 3:53:18 PM
 Test temperature: 64.00 °C

Load level 0.1 kPa (average load: 0.1 kPa)

Cycle	Load [kPa]	ϵ_0 [%]	ϵ_c [%]	ϵ_1 [%]	ϵ_r [%]	ϵ_{10} [%]	R _N [%]	J _{nr} (0.1, N) [1/kPa]
1	0.1	7.51	10.47	2.96	8.15	0.64	78.33	0.0641
2	0.1	8.15	11.11	2.96	8.78	0.63	78.57	0.0634

Responsible Employee:	Signature:
-----------------------	------------

MSCR-Test (AASHTO T350-14) - Final Report

Project name: 2018-05-25_MSCR (V2)



Date, Time: 2018-05-25 4:10:55 PM
 Test name: 2018-05-25_MSCR_0.1/3.2kPa
 Operator: user
 Sample: 64-28 RTFO + DOUBLE PAV
 Batch no.: MTO2
 Description: SUNNY
 Configuration: Anton Paar SmartPave 102 SN82314644

PP25/PE SN52739

P-PTD200+H-PTD120 SN82331818-82284206

Cycle	Load [kPa]	ϵ_0 [%]	ϵ_c [%]	ϵ_1 [%]	ϵ_r [%]	ϵ_{10} [%]	R_N [%]	J_nr (1/kPa)
3	0.1	8.78	11.74	2.96	9.41	0.63	78.69	0.0630
4	0.1	9.41	12.37	2.96	10.04	0.62	78.94	0.0622
5	0.1	10.04	12.99	2.95	10.65	0.62	79.11	0.0617
6	0.1	10.65	13.61	2.96	11.27	0.61	79.20	0.0615
7	0.1	11.27	14.22	2.95	11.88	0.61	79.33	0.0610
8	0.1	11.88	14.83	2.95	12.48	0.60	79.52	0.0604
9	0.1	12.48	15.43	2.95	13.08	0.60	79.59	0.0602
10	0.1	13.08	16.04	2.95	13.68	0.60	79.65	0.0601
							R_0.1 = 79.09	J_nr(0.1) = 0.0618

Load level 3.2 kPa

(average load: 3.2 kPa)

Cycle	Load [kPa]	ϵ_0 [%]	ϵ_c [%]	ϵ_1 [%]	ϵ_r [%]	ϵ_{10} [%]	R_N [%]	J_nr (3.2, N) [1/kPa]
1	3.2	13.68	107.57	93.89	46.51	32.82	65.04	0.1026
2	3.2	46.51	139.12	92.62	74.47	27.96	69.81	0.0874
3	3.2	74.47	166.69	92.22	100.44	25.97	71.84	0.0812
4	3.2	100.44	192.60	92.16	125.38	24.94	72.93	0.0779
5	3.2	125.38	217.61	92.23	149.77	24.39	73.55	0.0762
6	3.2	149.77	242.11	92.34	173.86	24.09	73.92	0.0753
7	3.2	173.86	266.31	92.45	197.78	23.93	74.12	0.0748
8	3.2	197.78	290.37	92.59	221.67	23.88	74.21	0.0746
9	3.2	221.67	314.38	92.71	245.56	23.89	74.23	0.0747
10	3.2	245.56	338.35	92.79	269.64	24.08	74.05	0.0752
							R_3.2 = 72.37	J_nr(3.2) = 0.0800

Average percent recovery

Load level 0.1 kPa
 Load level 3.2 kPa

R_0.1 = 79.09 %
 R_3.2 = 72.37 %

Percent difference of recovery

Load levels 0.1 kPa and 3.2 kPa

R_diff = 8.50 %

Average non-recoverable creep compliance

Load level 0.1 kPa
 Load level 3.2 kPa

J_nr(0.1) = 0.0618 1/kPa
 J_nr(3.2) = 0.0800 1/kPa

Percent difference of non-recoverable creep compliance

Load levels 0.1 kPa and 3.2 kPa

J_nr_diff = 29.47 %

Indication that the asphalt binder is modified with an acceptable elastomeric polymer

Load level 3.2 kPa above criterion (probably modified)

PASSED Extremely Heavy Traffic "E" grade at 64.00 °C according to AASHTO M 332-14.

Responsible Employee:

Signature:

APPENDIX E: LAS TEST REPORTS

LAS-Test (AASHTO TP101-14) - Report

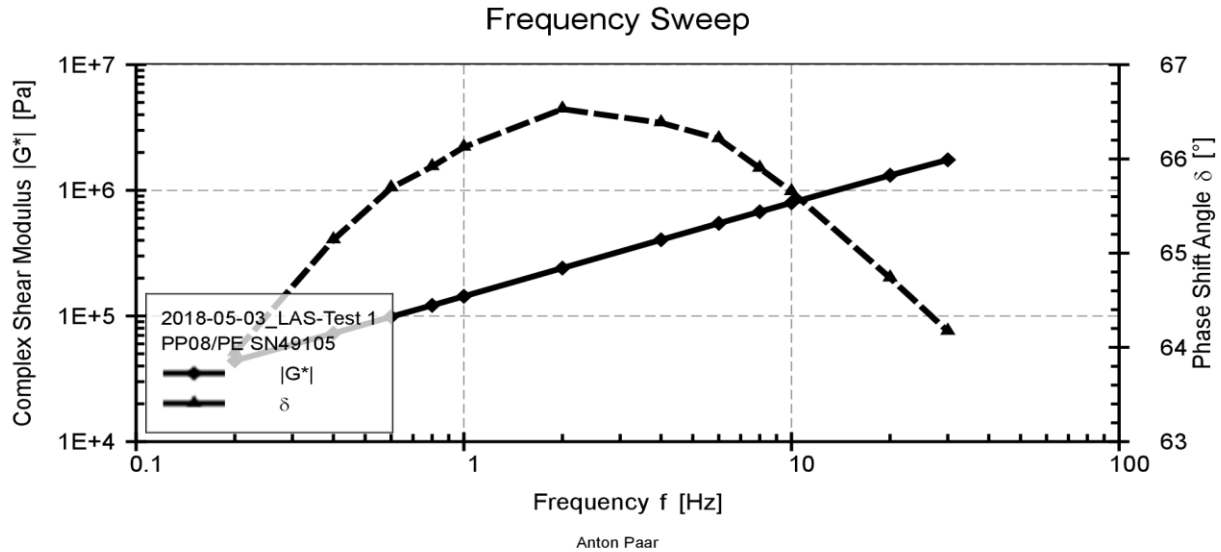
Project name: 2018-05-03_LAS-Test (V2)

Date, Time: 2018-05-03 4:17:28 PM
 Test name: 2018-05-03_LAS-Test 1
 Operator: user
 Sample: VIRGIN
 Batch no.: MTO2
 Description: YASHAR



Configuration: Anton Paar SmartPave 102 SN82314644
 PP08/PE SN49105

P-PTD200+H-PTD120 SN82331818-82284206



2018-05-03_LAS-Test 1, Frequency Sweep_22 °C, Interval 1

Frequency f [Hz]	Complex Shear Modulus G* [Pa]	Phase Shift Angle δ [°]	Storage Modulus G' [Pa]
0.20	44038.92	63.95	19343.1
0.40	72785.68	65.14	30596.69
0.60	98599.81	65.69	40586.51
0.80	121528	65.92	49588.14
1.00	143438.8	66.13	58054.87
2.00	240616.6	66.53	95833.9
4.00	403992	66.38	161844.4
6.00	546475.1	66.21	220404
8.00	676023.9	65.90	276020.9
10.00	797045.2	65.65	328588.3
20.00	1317219	64.74	562146.6
30.00	1750071	64.17	762479

Responsible Employee:

Signature:

LAS-Test (AASHTO TP101-14) - Report

Project name: 2018-05-03_LAS-Test (V2)



Date, Time: 2018-05-03 4:17:28 PM

Test name: 2018-05-03_LAS-Test 1

Operator: user

Sample: VIRGIN

Batch no.: MTO2

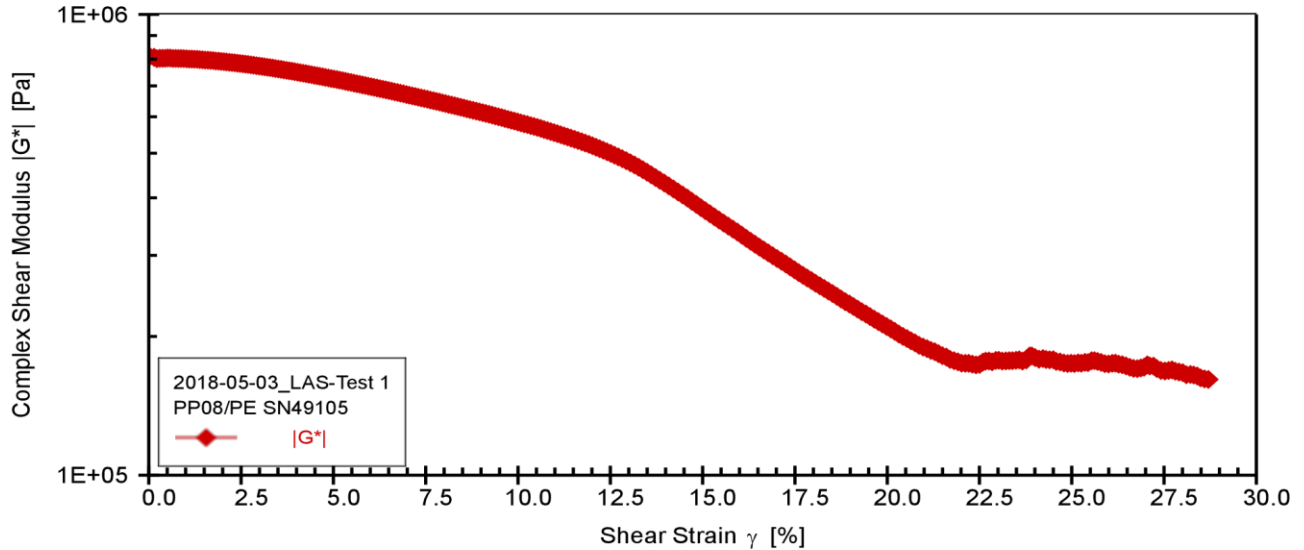
Description: YASHAR

Configuration: Anton Paar SmartPave 102 SN82314644

PP08/PE SN49105

P-PTD200+H-PTD120 SN82331818-82284206

Linear Amplitude Sweep



Anton Paar

2018-05-03_LAS-Test 1, LAS-Test_22 °C, Interval 1

Complex Shear Modulus G* [Pa]	Shear Stress τ [Pa]	Shear Strain γ [%]	Time t [s]	Phase Shift Angle δ [°]
810320.1	192.9809	0.02	1.00	66.33
807297.7	1178.976	0.15	2.00	65.69
801739.2	1765.96	0.22	3.00	65.30
803521.2	2357.531	0.29	4.00	65.52
803515.3	2934.294	0.37	5.00	65.55
803422.4	3515.131	0.44	6.00	65.60
804627.3	4102.17	0.51	7.00	65.58
804274.1	4683.071	0.58	8.00	65.57
802922.6	5258.249	0.65	9.00	65.59
803086.3	5842.608	0.73	10.00	65.59
802462	6418.186	0.80	11.00	65.63
802531.5	7000.364	0.87	12.00	65.62
801982.8	7578.261	0.94	13.00	65.62
801075.1	8152.548	1.02	14.00	65.63
800420.6	8726.266	1.09	15.00	65.66
800225.2	9302.905	1.16	16.00	65.68
799754.3	9877.272	1.24	17.00	65.68

Responsible Employee:

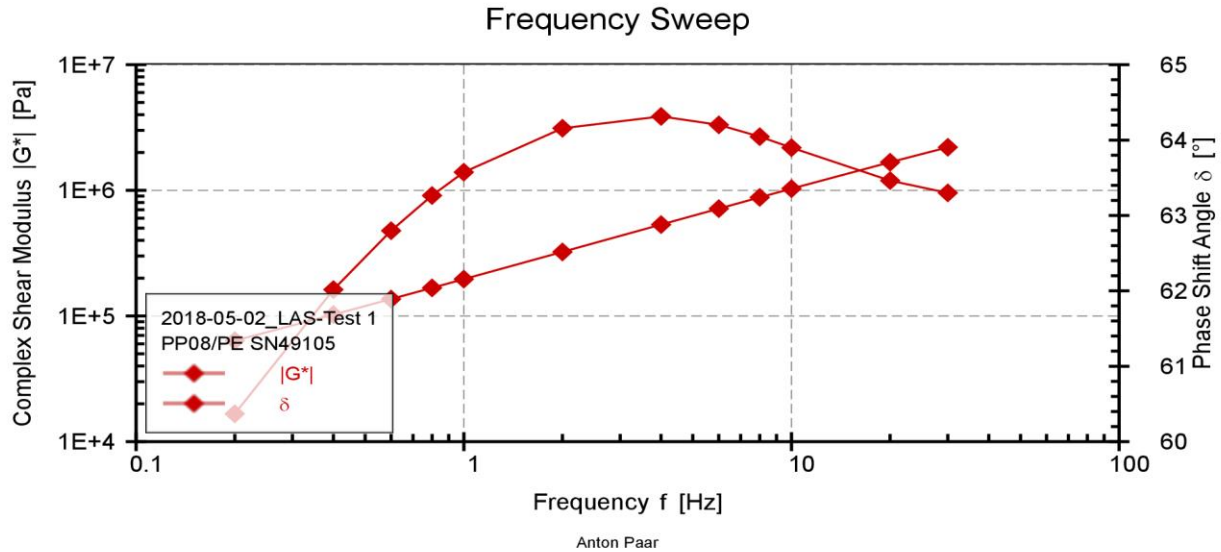
Signature:

LAS-Test (AASHTO TP101-14) - Report

Project name: 2018-05-02_LAS-Test (V2)

Date, Time: 2018-05-02 4:36:14 PM
 Test name: 2018-05-02_LAS-Test 1
 Operator: user
 Sample: EXTRACTED VIRGIN
 Batch no.: MTO2
 Description: YASHAR
 Configuration: Anton Paar SmartPave 102 SN82314644
 PP08/PE SN49105

P-PTD200+H-PTD120 SN82331818-82284206



2018-05-02_LAS-Test 1, Frequency Sweep_22 °C, Interval 1

Frequency f [Hz]	Complex Shear Modulus G* [Pa]	Phase Shift Angle δ [°]	Storage Modulus G' [Pa]
0.20	63611.61	60.37	31451.36
0.40	102589.6	62.02	48137.41
0.60	136502.7	62.80	62398.92
0.80	167444.4	63.27	75327.15
1.00	196465.7	63.57	87434.19
2.00	323676.7	64.16	141095.1
4.00	534081.7	64.31	231487.8
6.00	715290.4	64.20	311288.8
8.00	879297.6	64.05	384821.2
10.00	1031119	63.90	453630
20.00	1674611	63.46	748194.4
30.00	2201813	63.30	989342.2

Responsible Employee:

Signature:

LAS-Test (AASHTO TP101-14) - Report

Project name: 2018-05-02_LAS-Test (V2)



Date, Time: 2018-05-02 4:36:14 PM

Test name: 2018-05-02_LAS-Test 1

Operator: user

Sample: EXTRACTED VIRGIN

Batch no.: MTO2

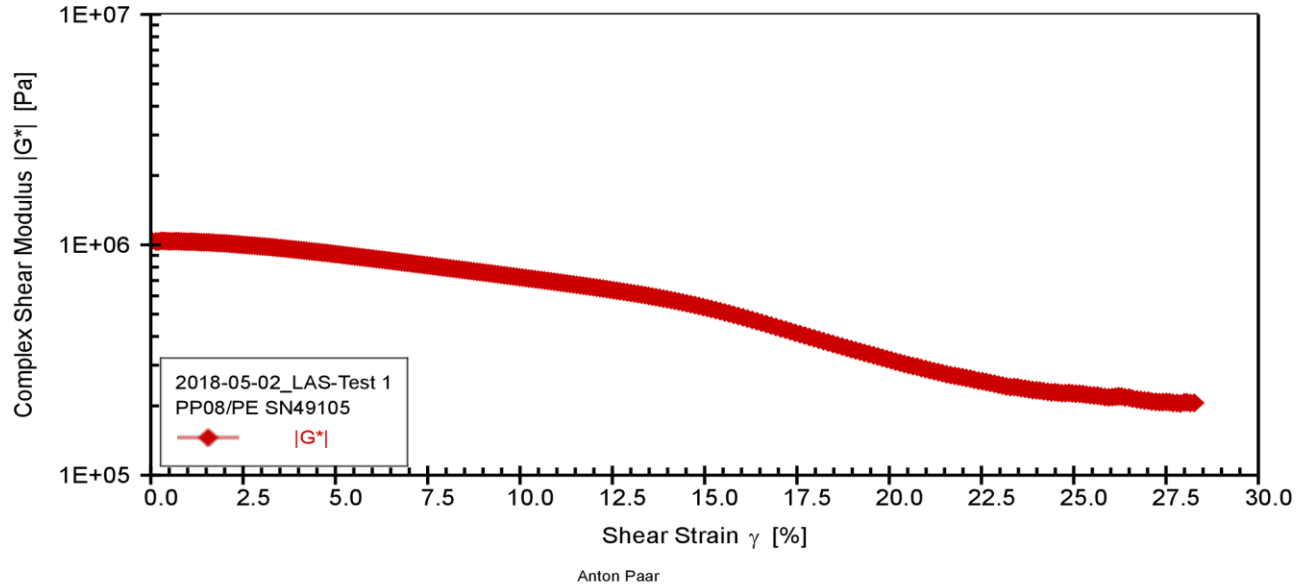
Description: YASHAR

Configuration: Anton Paar SmartPave 102 SN82314644

PP08/PE SN49105

P-PTD200+H-PTD120 SN82331818-82284206

Linear Amplitude Sweep



2018-05-02_LAS-Test 1, LAS-Test_22 °C, Interval 1

Complex Shear Modulus G* [Pa]	Shear Stress τ [Pa]	Shear Strain γ [%]	Time t [s]	Phase Shift Angle δ [°]
1039323	240.9721	0.02	1.00	63.61
1034763	1448.724	0.14	2.00	63.46
1034350	2162.022	0.21	3.00	63.66
1040086	2880.102	0.28	4.00	63.70
1040761	3595.315	0.35	5.00	63.60
1038965	4308.598	0.41	6.00	63.58
1036078	5011.963	0.48	7.00	63.60
1034880	5717.424	0.55	8.00	63.65
1036268	6428.674	0.62	9.00	63.75
1037111	7137.532	0.69	10.00	63.74
1035973	7843.823	0.76	11.00	63.71
1034893	8551.909	0.83	12.00	63.71
1033775	9253.24	0.90	13.00	63.74
1031833	9940.055	0.96	14.00	63.80
1031168	10633.94	1.03	15.00	63.85
1032635	11350.94	1.10	16.00	63.84
1031662	12049.9	1.17	17.00	63.83

Responsible Employee:

Signature:

LAS-Test (AASHTO TP101-14) - Report

Project name: 2018-05-02_LAS-Test (V2)



Date, Time: 2018-05-02 5:20:13 PM

Test name: 2018-05-02_LAS-Test

Operator: user

Sample: RTFOT

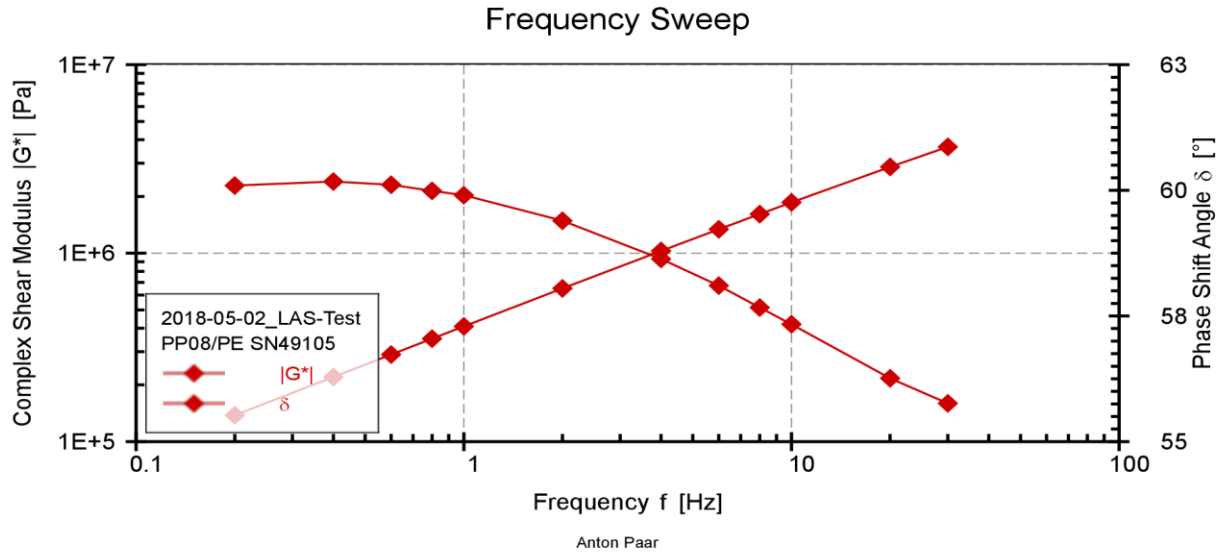
Batch no.: MTO2

Description: YASHAR

Configuration: Anton Paar SmartPave 102 SN82314644

PP08/PE SN49105

P-PTD200+H-PTD120 SN82331818-82284206



2018-05-02_LAS-Test, Frequency Sweep_22 °C, Interval 1

Frequency f [Hz]	Complex Shear Modulus G* [Pa]	Phase Shift Angle δ [°]	Storage Modulus G' [Pa]
0.20	138003.1	60.10	68800.74
0.40	220403.3	60.18	109616.6
0.60	289695.2	60.11	144361.7
0.80	351766.2	59.99	175936.4
1.00	408816	59.90	205001.2
2.00	649889.7	59.40	330856.5
4.00	1027525	58.63	534820.3
6.00	1338641	58.10	707307.5
8.00	1611590	57.67	861893.6
10.00	1859807	57.33	1003815
20.00	2869029	56.26	1593547
30.00	3665712	55.76	2062517

Responsible Employee:

Signature:

LAS-Test (AASHTO TP101-14) - Report

Project name: 2018-05-02_LAS-Test (V2)



Date, Time: 2018-05-02 5:20:13 PM

Test name: 2018-05-02_LAS-Test

Operator: user

Sample: RTFOT

Batch no.: MTO2

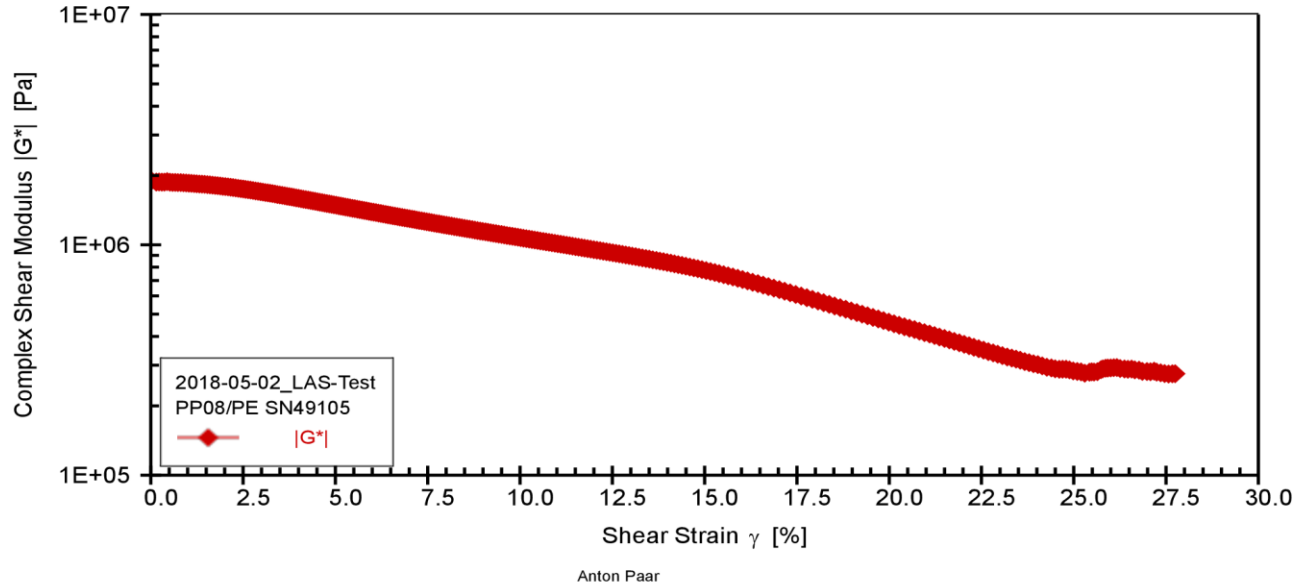
Description: YASHAR

Configuration: Anton Paar SmartPave 102 SN82314644

PP08/PE SN49105

P-PTD200+H-PTD120 SN82331818-82284206

Linear Amplitude Sweep



2018-05-02_LAS-Test, LAS-Test_22 °C, Interval 1

Complex Shear Modulus G* [Pa]	Shear Stress τ [Pa]	Shear Strain γ [%]	Time t [s]	Phase Shift Angle δ [°]
1896944	364.4784	0.02	1.00	57.49
1873696	2809.853	0.15	2.00	57.19
1874017	4180.189	0.22	3.00	57.19
1871145	5558.471	0.30	4.00	57.14
1871922	6935.667	0.37	5.00	57.17
1880697	8320.449	0.44	6.00	57.23
1869226	9692.458	0.52	7.00	57.21
1865586	11028.14	0.59	8.00	57.22
1864543	12379.06	0.66	9.00	57.23
1863051	13735.52	0.74	10.00	57.25
1862064	15088.69	0.81	11.00	57.27
1858812	16429.72	0.88	12.00	57.29
1855697	17757.83	0.96	13.00	57.29
1852444	19075.16	1.03	14.00	57.34
1849250	20373.56	1.10	15.00	57.39
1844451	21649.6	1.17	16.00	57.45
1840962	22913.01	1.24	17.00	57.50

Responsible Employee:

Signature:

LAS-Test (AASHTO TP101-14) - Report

Project name: 2018-05-02_LAS-Test (V2)



Date, Time: 2018-05-02 3:08:33 PM

Test name: 2018-05-02_LAS-Test

Operator: user

Sample: LOOSE MIX

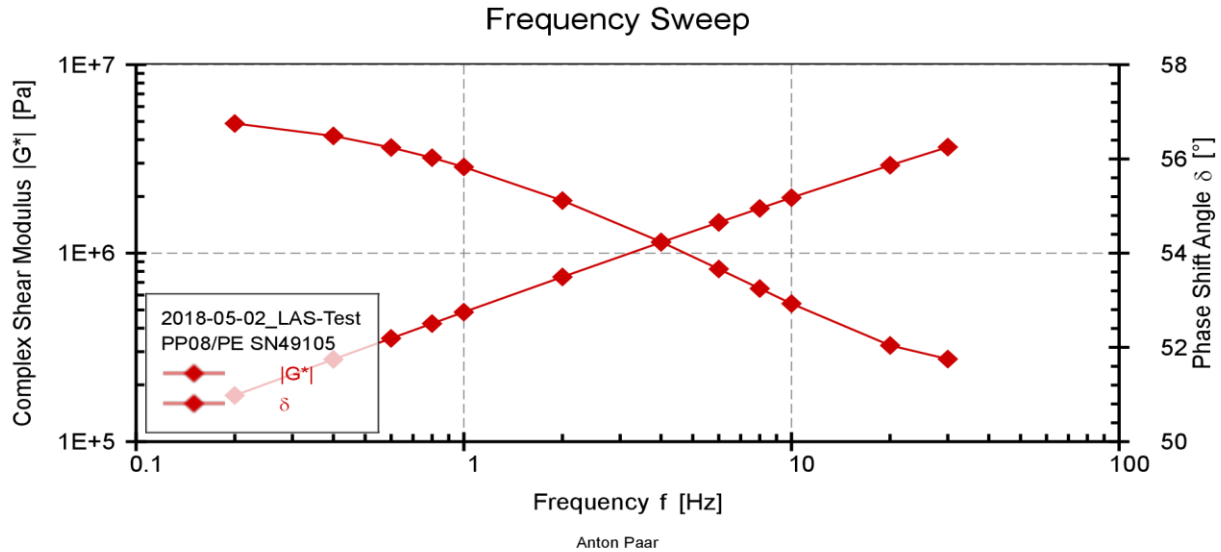
Batch no.: MTO2

Description: YASHAR

Configuration: Anton Paar SmartPave 102 SN82314644

PP08/PE SN49105

P-PTD200+H-PTD120 SN82331818-82284206



2018-05-02_LAS-Test, Frequency Sweep_22 °C, Interval 1

Frequency f [Hz]	Complex Shear Modulus G* [Pa]	Phase Shift Angle δ [°]	Storage Modulus G' [Pa]
0.20	175901	56.75	96437.49
0.40	273312.4	56.49	150897.5
0.60	353087.7	56.24	196205.8
0.80	423160.6	56.03	236468.6
1.00	486774.5	55.83	273401.1
2.00	747916.1	55.12	427734.1
4.00	1142057	54.24	667407.7
6.00	1456838	53.66	863214
8.00	1728232	53.25	1034035
10.00	1970486	52.93	1187814
20.00	2927955	52.04	1800935
30.00	3653914	51.75	2261976

Responsible Employee:

Signature:

LAS-Test (AASHTO TP101-14) - Report

Project name: 2018-05-02_LAS-Test (V2)



Date, Time: 2018-05-02 3:08:33 PM

Test name: 2018-05-02_LAS-Test

Operator: user

Sample: LOOSE MIX

Batch no.: MTO2

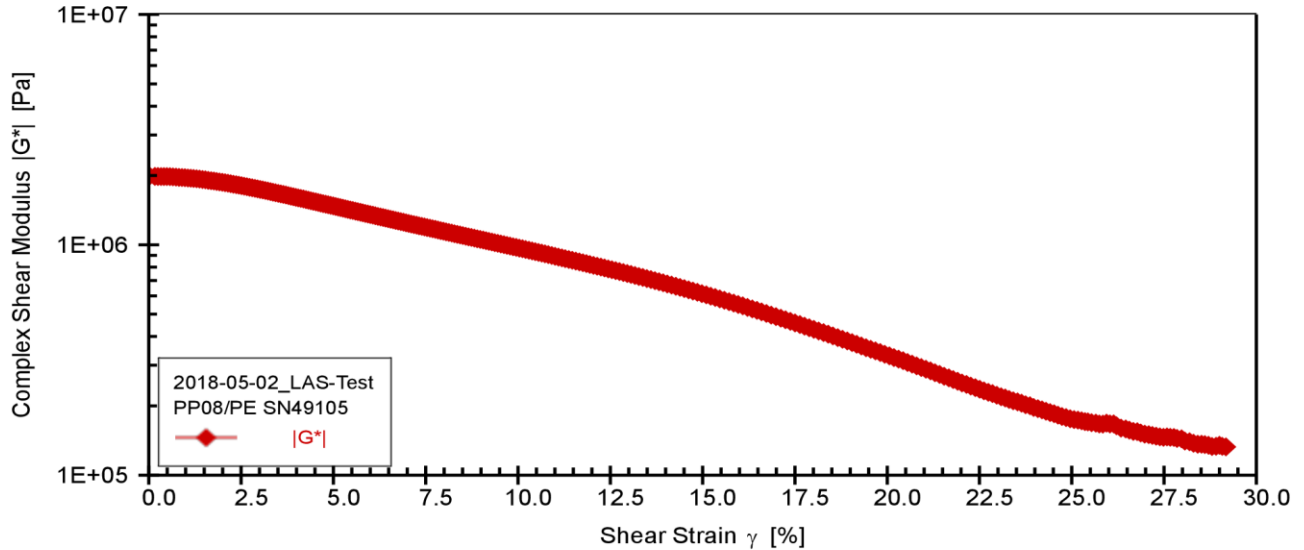
Description: YASHAR

Configuration: Anton Paar SmartPave 102 SN82314644

PP08/PE SN49105

P-PTD200+H-PTD120 SN82331818-82284206

Linear Amplitude Sweep



Anton Paar

2018-05-02_LAS-Test, LAS-Test_22 °C, Interval 1

Complex Shear Modulus G* [Pa]	Shear Stress τ [Pa]	Shear Strain γ [%]	Time t [s]	Phase Shift Angle δ [°]
1989079	392.831	0.02	1.00	53.03
1982079	3294.162	0.17	2.00	52.66
1979856	4915.034	0.25	3.00	52.83
1978456	6506.894	0.33	4.00	52.92
1978025	8106.889	0.41	5.00	52.91
1978183	9724.959	0.49	6.00	52.86
1977125	11344.05	0.57	7.00	52.86
1973542	12935.6	0.66	8.00	52.90
1968010	14497.21	0.74	9.00	52.94
1963380	16042.32	0.82	10.00	52.99
1959603	17583.07	0.90	11.00	53.03
1955580	19115.6	0.98	12.00	53.09
1950151	20623.8	1.06	13.00	53.15
1945200	22112.64	1.14	14.00	53.21
1941426	23607.31	1.22	15.00	53.25
1935416	25082.66	1.30	16.00	53.31
1929873	26525.51	1.37	17.00	53.37

Responsible Employee:

Signature:

LAS-Test (AASHTO TP101-14) - Report

Project name: 2018-05-03_LAS-Test (V2)



Date, Time: 2018-05-03 1:53:24 PM

Test name: 2018-05-03_LAS-Test

Operator: user

Sample: COMPACTED

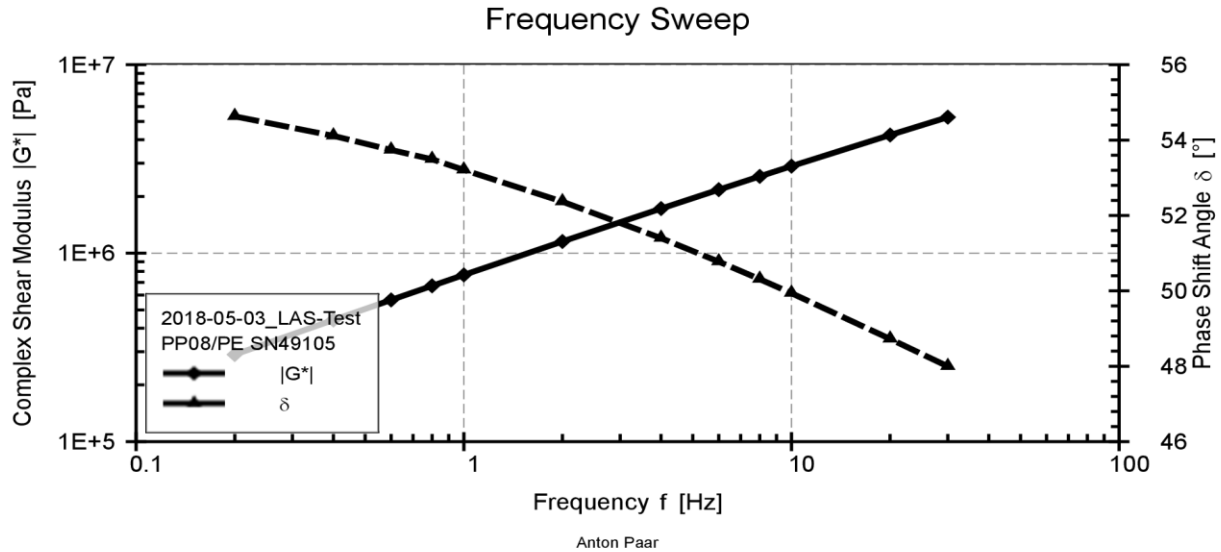
Batch no.: MTO2

Description: YASHAR

Configuration: Anton Paar SmartPave 102 SN82314644

PP08/PE SN49105

P-PTD200+H-PTD120 SN82331818-82284206



2018-05-03_LAS-Test, Frequency Sweep_22 °C, Interval 1

Frequency f [Hz]	Complex Shear Modulus G* [Pa]	Phase Shift Angle δ [°]	Storage Modulus G' [Pa]
0.20	289648	54.63	167666.2
0.40	442103.7	54.11	259155.6
0.60	564605.9	53.74	333948.2
0.80	670928	53.49	399165.9
1.00	766552.9	53.21	459079.4
2.00	1153743	52.37	704484.2
4.00	1724156	51.40	1075714
6.00	2172677	50.77	1373942
8.00	2555659	50.31	1632136
10.00	2895951	49.94	1863882
20.00	4237454	48.72	2795409
30.00	5266350	48.00	3524093

Responsible Employee:

Signature:

LAS-Test (AASHTO TP101-14) - Report

Project name: 2018-05-03_LAS-Test (V2)



Date, Time: 2018-05-03 1:53:24 PM

Test name: 2018-05-03_LAS-Test

Operator: user

Sample: COMPACTED

Batch no.: MTO2

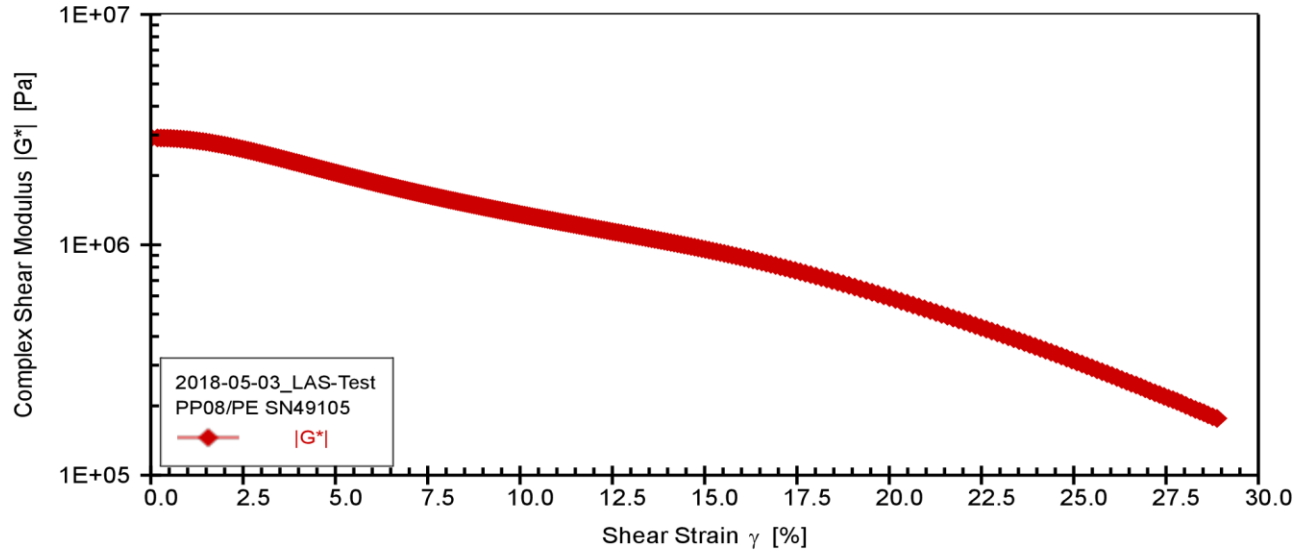
Description: YASHAR

Configuration: Anton Paar SmartPave 102 SN82314644

PP08/PE SN49105

P-PTD200+H-PTD120 SN82331818-82284206

Linear Amplitude Sweep



Anton Paar

2018-05-03_LAS-Test, LAS-Test_22 °C, Interval 1

Complex Shear Modulus G* [Pa]	Shear Stress τ [Pa]	Shear Strain γ [%]	Time t [s]	Phase Shift Angle δ [°]
2913393	435.0992	0.01	1.00	49.82
2911523	5285.997	0.18	2.00	49.82
2909208	7876.317	0.27	3.00	49.86
2908417	10457.93	0.36	4.00	49.90
2904092	13035.79	0.45	5.00	49.92
2900722	15594.4	0.54	6.00	49.95
2894746	18139.96	0.63	7.00	50.00
2889818	20656.67	0.71	8.00	50.06
2881665	23156.28	0.80	9.00	50.12
2874513	25620.39	0.89	10.00	50.17
2865608	28064.52	0.98	11.00	50.24
2857155	30472.27	1.07	12.00	50.30
2844542	32837.55	1.15	13.00	50.41
2833455	35138.72	1.24	14.00	50.49
2822172	37429.42	1.33	15.00	50.58
2809828	39684.39	1.41	16.00	50.66
2796665	41892.48	1.50	17.00	50.75

Responsible Employee:

Signature:

LAS-Test (AASHTO TP101-14) - Report

Project name: 2018-06-05_LAS-Test (V2)



Date, Time: 2018-06-05 10:09:55 AM

Test name: 2018-06-05_LAS-Test

Operator: user

Sample: 64-28 RTFO + PAV @ 22

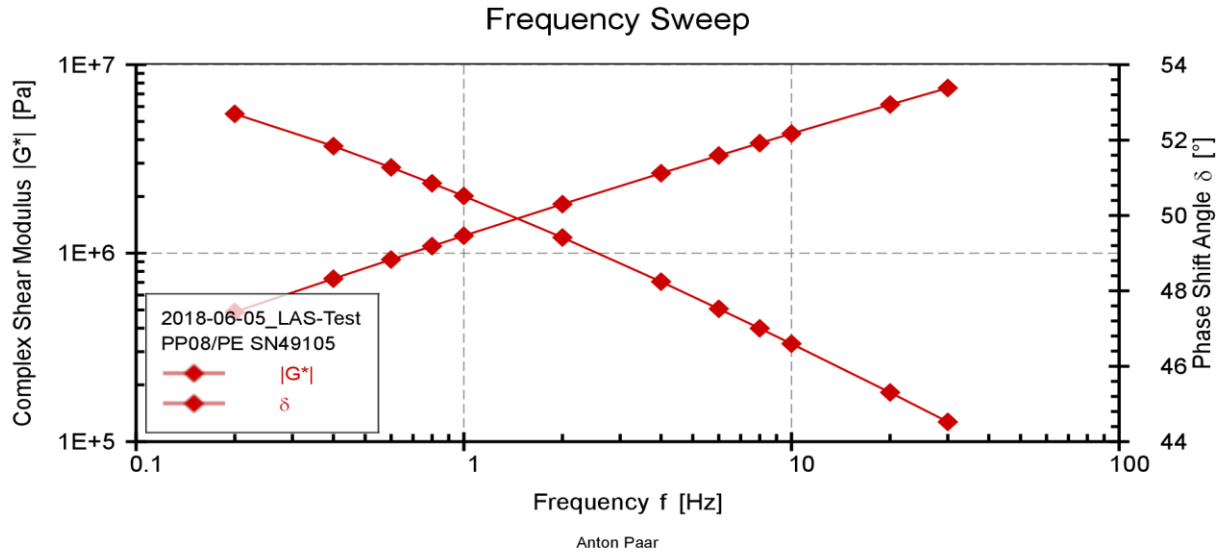
Batch no.: MTO2

Description: Sunny

Configuration: Anton Paar SmartPave 102 SN82314644

PP08/PE SN49105

P-PTD200+H-PTD120 SN82331818-82284206



2018-06-05_LAS-Test, Frequency Sweep_22 °C, Interval 1

Frequency f [Hz]	Complex Shear Modulus G* [Pa]	Phase Shift Angle δ [°]	Storage Modulus G' [Pa]
0.20	487539	52.70	295474.9
0.40	731998.8	51.84	452265.5
0.60	924737.4	51.27	578507
0.80	1089875	50.85	688041.5
1.00	1237038	50.52	786574.3
2.00	1820566	49.42	1184395
4.00	2654874	48.24	1768080
6.00	3296135	47.52	2225858
8.00	3835540	47.01	2615585
10.00	4309253	46.60	2961002
20.00	6144370	45.30	4321672
30.00	7527127	44.52	5366612

Responsible Employee:

Signature:

LAS-Test (AASHTO TP101-14) - Report

Project name: 2018-06-05_LAS-Test (V2)



Date, Time: 2018-06-05 10:09:55 AM

Test name: 2018-06-05_LAS-Test

Operator: user

Sample: 64-28 RTFO + PAV @ 22

Batch no.: MTO2

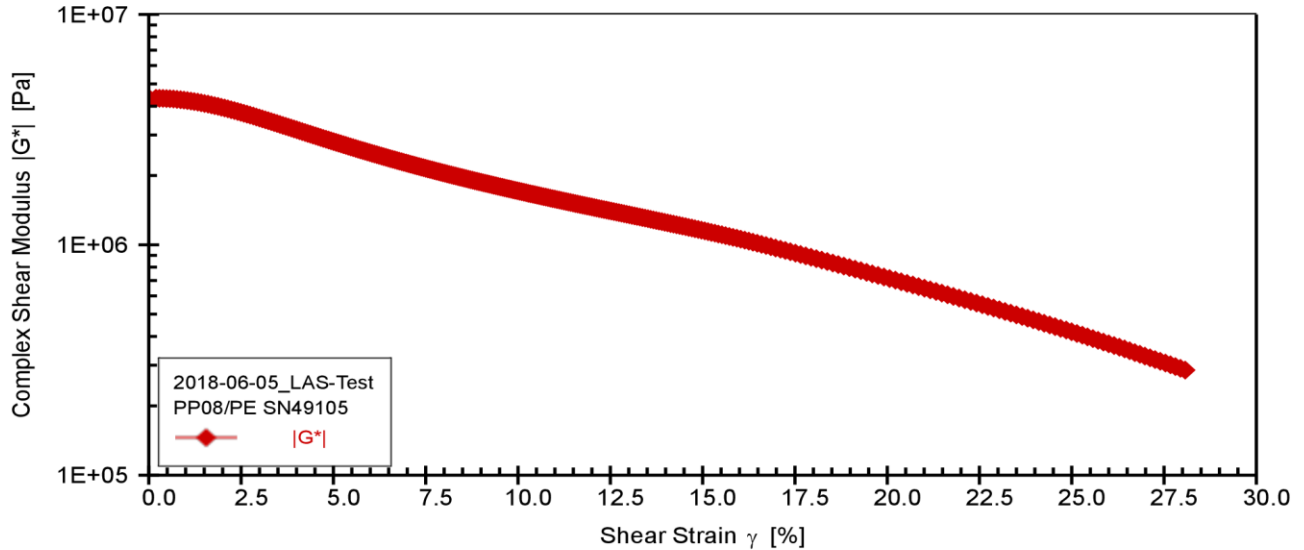
Description: Sunny

Configuration: Anton Paar SmartPave 102 SN82314644

PP08/PE SN49105

P-PTD200+H-PTD120 SN82331818-82284206

Linear Amplitude Sweep



Anton Paar

2018-06-05_LAS-Test, LAS-Test_22 °C, Interval 1

Complex Shear Modulus G* [Pa]	Shear Stress τ [Pa]	Shear Strain γ [%]	Time t [s]	Phase Shift Angle δ [°]
4317526	446.9221	0.01	1.00	46.50
4325616	8356.407	0.19	2.00	46.48
4326696	12482.15	0.29	3.00	46.51
4322292	16591.33	0.38	4.00	46.53
4317075	20675.97	0.48	5.00	46.57
4307658	24736.72	0.57	6.00	46.62
4296608	28746.25	0.67	7.00	46.72
4280910	32713.97	0.76	8.00	46.80
4265936	36616.38	0.86	9.00	46.88
4248829	40479.83	0.95	10.00	46.98
4230151	44278.41	1.05	11.00	47.08
4209118	48013.99	1.14	12.00	47.19
4186525	51667.49	1.23	13.00	47.31
4162382	55242.51	1.33	14.00	47.44
4136471	58732.97	1.42	15.00	47.57
4108999	62135.95	1.51	16.00	47.71
4081052	65449.72	1.60	17.00	47.85

Responsible Employee:

Signature:

LAS-Test (AASHTO TP101-14) - Report

Project name: 2018-05-02_LAS-Test (V2)



Date, Time: 2018-05-02 3:56:51 PM

Test name: 2018-05-02_LAS-Test

Operator: user

Sample: R30

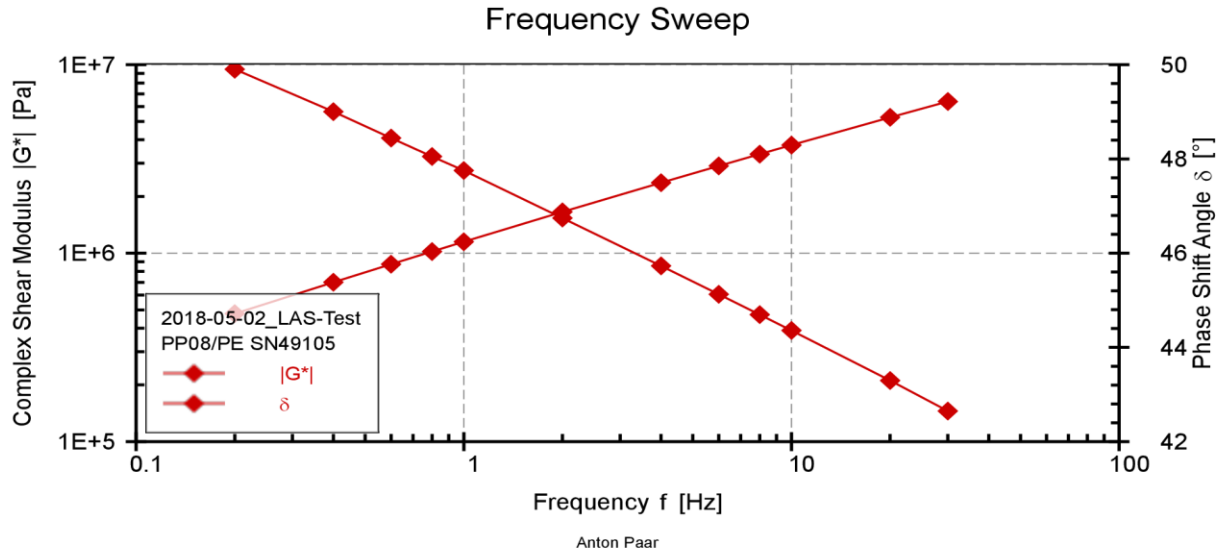
Batch no.: MTO2

Description: YASHAR

Configuration: Anton Paar SmartPave 102 SN82314644

PP08/PE SN49105

P-PTD200+H-PTD120 SN82331818-82284206



2018-05-02_LAS-Test, Frequency Sweep_22 °C, Interval 1

Frequency f [Hz]	Complex Shear Modulus G* [Pa]	Phase Shift Angle δ [°]	Storage Modulus G' [Pa]
0.20	477404.5	49.90	307480.9
0.40	700751.7	49.00	459697.7
0.60	873842.2	48.44	579669.1
0.80	1020274	48.05	682013.7
1.00	1149972	47.75	773130.1
2.00	1655860	46.74	1134681
4.00	2365825	45.73	1651446
6.00	2903530	45.13	2048560
8.00	3353934	44.70	2384165
10.00	3746881	44.36	2678933
20.00	5254120	43.30	3823992
30.00	6379292	42.65	4691994

Responsible Employee:

Signature:

LAS-Test (AASHTO TP101-14) - Report

Project name: 2018-05-02_LAS-Test (V2)



Date, Time: 2018-05-02 3:56:51 PM

Test name: 2018-05-02_LAS-Test

Operator: user

Sample: R30

Batch no.: MTO2

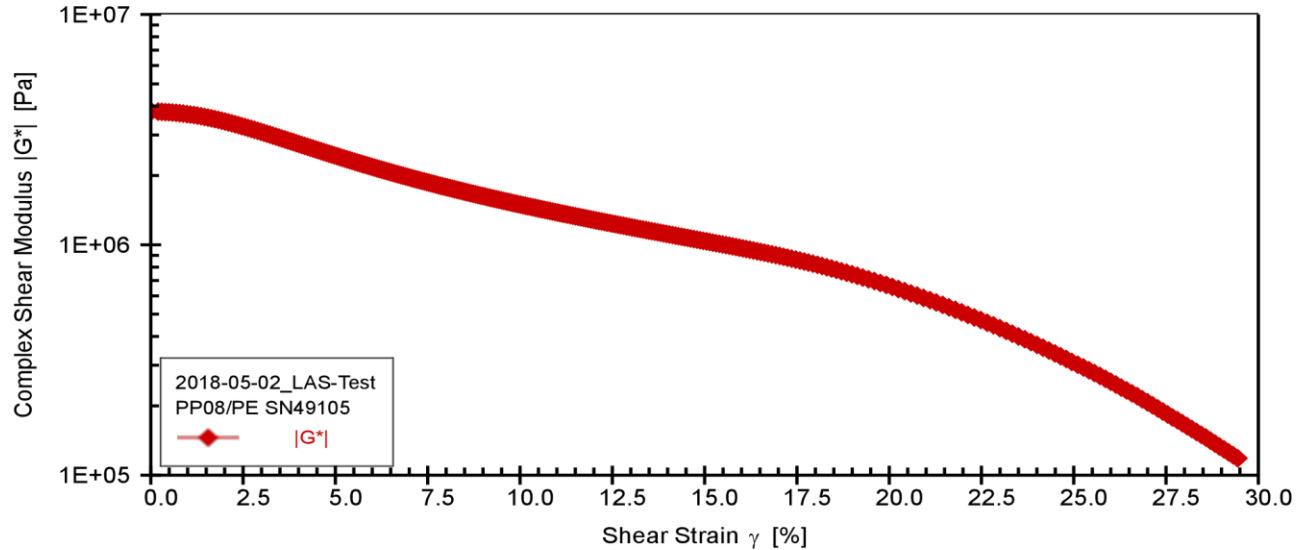
Description: YASHAR

Configuration: Anton Paar SmartPave 102 SN82314644

PP08/PE SN49105

P-PTD200+H-PTD120 SN82331818-82284206

Linear Amplitude Sweep



Anton Paar

2018-05-02_LAS-Test, LAS-Test_22 °C, Interval 1

Complex Shear Modulus G* [Pa]	Shear Stress τ [Pa]	Shear Strain γ [%]	Time t [s]	Phase Shift Angle δ [°]
3798514	460.1052	0.01	1.00	44.50
3787023	7515.63	0.20	2.00	44.36
3778988	11191.73	0.30	3.00	44.40
3769888	14845.74	0.39	4.00	44.43
3764255	18475.99	0.49	5.00	44.47
3755127	22097.08	0.59	6.00	44.53
3742032	25674.14	0.69	7.00	44.60
3727638	29197.15	0.78	8.00	44.67
3713377	32672.01	0.88	9.00	44.76
3695384	36110.71	0.98	10.00	44.83
3677934	39477.88	1.07	11.00	44.92
3658910	42792.07	1.17	12.00	45.03
3638310	46035.14	1.27	13.00	45.15
3615178	49202.62	1.36	14.00	45.28
3591410	52276.27	1.46	15.00	45.42
3567335	55279.48	1.55	16.00	45.56
3541928	58217.68	1.64	17.00	45.69

Responsible Employee:

Signature:

LAS-Test (AASHTO TP101-14) - Report

Project name: 2018-06-01_LAS-Test (V2)

Date, Time: 2018-06-01 12:19:07 PM

Test name: 2018-06-01_LAS-Test

Operator: user

Sample: COCO @ 22oC

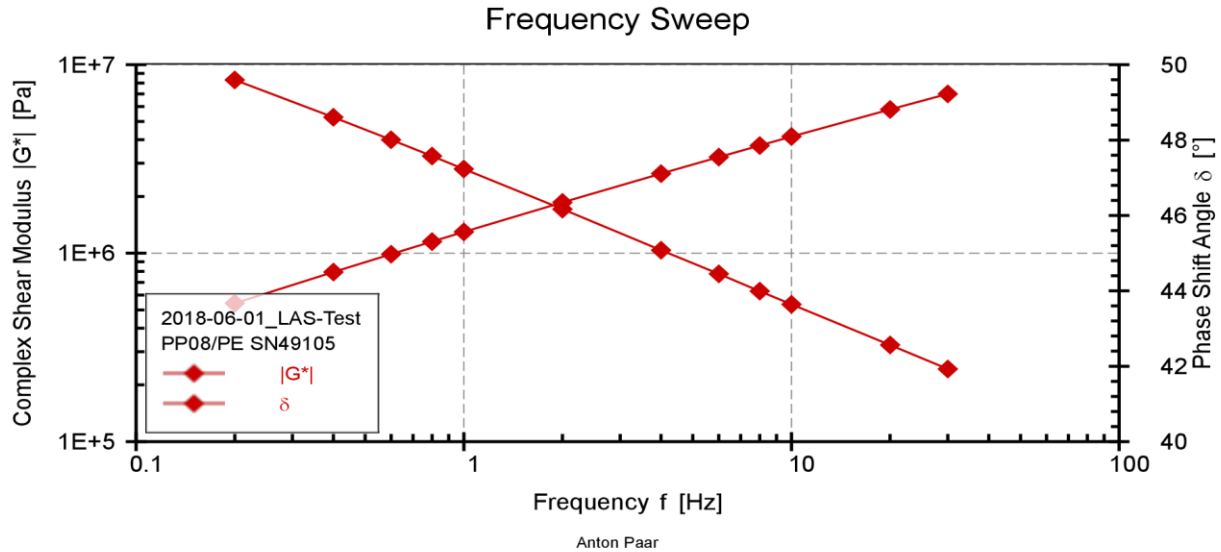
Batch no.: MTO2

Description: SUNNY

Configuration: Anton Paar SmartPave 102 SN82314644

PP08/PE SN49105

P-PTD200+H-PTD120 SN82331818-82284206



2018-06-01_LAS-Test, Frequency Sweep_22 °C, Interval 1

Frequency f [Hz]	Complex Shear Modulus G* [Pa]	Phase Shift Angle δ [°]	Storage Modulus G' [Pa]
0.20	542214	49.60	351448.3
0.40	794046.5	48.61	525046.7
0.60	987919.3	48.01	660923.3
0.80	1152026	47.58	777163.5
1.00	1296656	47.23	880455.8
2.00	1858973	46.17	1287390
4.00	2643054	45.08	1866354
6.00	3234156	44.45	2308718
8.00	3725819	43.99	2680504
10.00	4154755	43.64	3006630
20.00	5789034	42.56	4263790
30.00	7003001	41.93	5210216

Responsible Employee:

Signature:

LAS-Test (AASHTO TP101-14) - Report

Project name: 2018-06-01_LAS-Test (V2)



Date, Time: 2018-06-01 12:19:07 PM

Test name: 2018-06-01_LAS-Test

Operator: user

Sample: COCO @ 22oC

Batch no.: MTO2

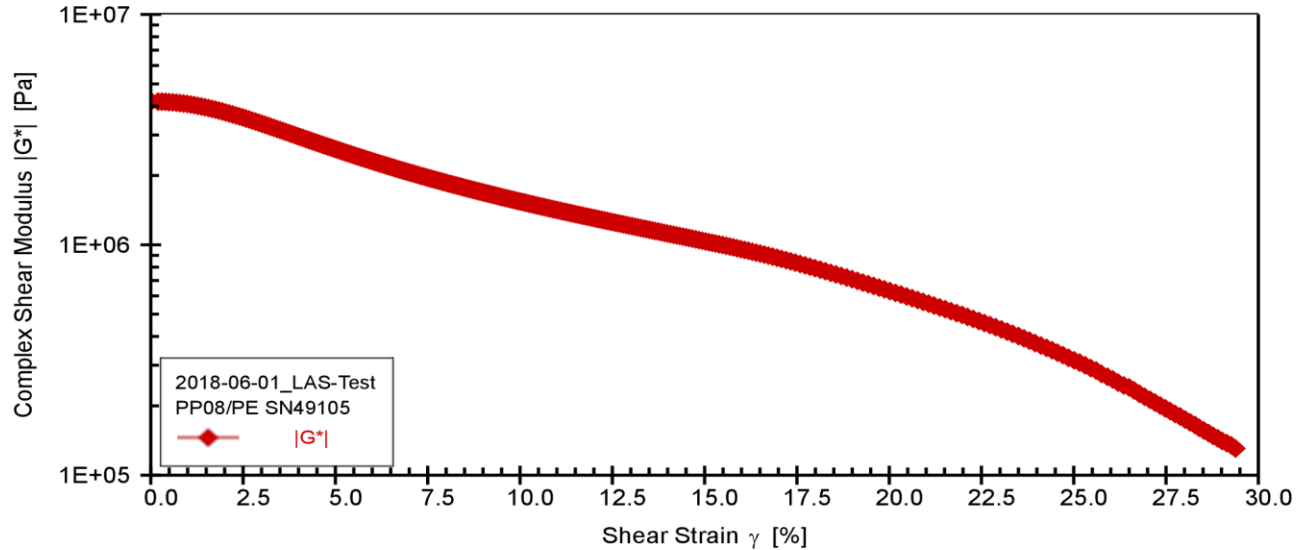
Description: SUNNY

Configuration: Anton Paar SmartPave 102 SN82314644

PP08/PE SN49105

P-PTD200+H-PTD120 SN82331818-82284206

Linear Amplitude Sweep



Anton Paar

2018-06-01_LAS-Test, LAS-Test_22 °C, Interval 1

Complex Shear Modulus G* [Pa]	Shear Stress τ [Pa]	Shear Strain γ [%]	Time t [s]	Phase Shift Angle δ [°]
4194861	457.7889	0.01	1.00	43.69
4185345	8373.161	0.20	2.00	43.62
4181914	12472.33	0.30	3.00	43.62
4174070	16564.89	0.40	4.00	43.65
4166040	20624.54	0.50	5.00	43.69
4154563	24656.09	0.59	6.00	43.77
4141340	28641.2	0.69	7.00	43.83
4124778	32577.78	0.79	8.00	43.93
4107068	36446.73	0.89	9.00	44.03
4086272	40256.08	0.99	10.00	44.14
4064299	43985.31	1.08	11.00	44.26
4039659	47641.56	1.18	12.00	44.39
4013492	51206.31	1.28	13.00	44.53
3985683	54686.02	1.37	14.00	44.67
3956159	58070.46	1.47	15.00	44.83
3925520	61355.14	1.56	16.00	44.98
3893376	64542.67	1.66	17.00	45.15

Responsible Employee:

Signature:

LAS-Test (AASHTO TP101-14) - Report

Project name: 2018-07-20_LAS-Test (V2)



Date, Time: 2018-07-20 4:15:13 PM

Test name: 2018-07-20_LAS-Test

Operator: user

Sample: BC5-H2O

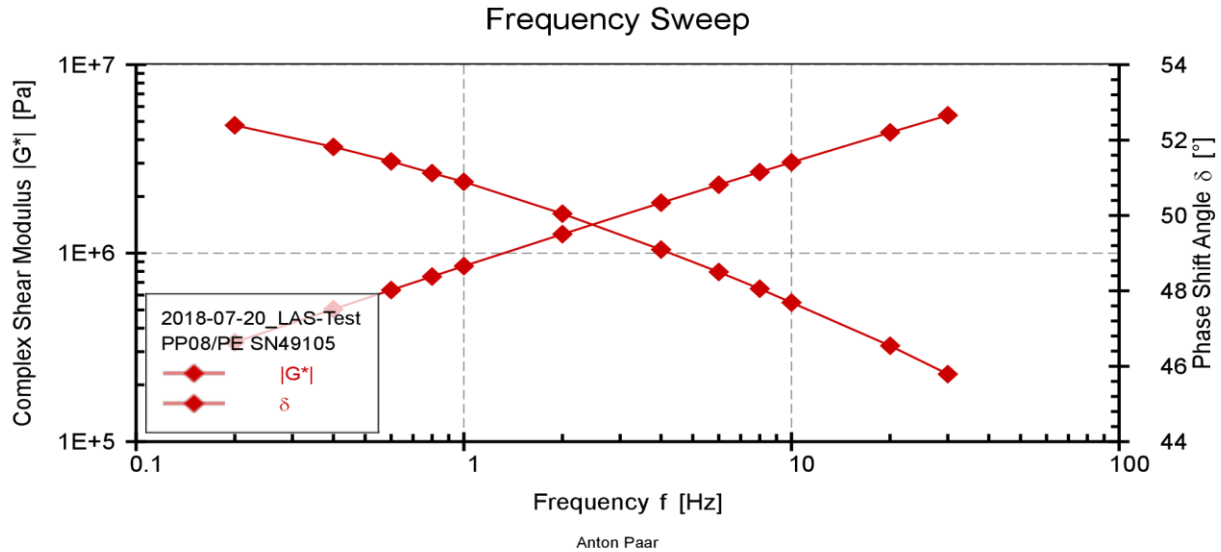
Batch no.: MTO2

Description: Sunny

Configuration: Anton Paar SmartPave 102 SN82314644

PP08/PE SN49105

P-PTD200+H-PTD120 SN82331818-82284206



2018-07-20_LAS-Test, Frequency Sweep_22 °C, Interval 1

Frequency f [Hz]	Complex Shear Modulus G* [Pa]	Phase Shift Angle δ [°]	Storage Modulus G' [Pa]
0.20	336640.1	52.39	205434.4
0.40	504597.8	51.82	311909.9
0.60	637434	51.44	397371.9
0.80	751546	51.12	471691.4
1.00	853867.9	50.89	538581.7
2.00	1261466	50.05	810063.9
4.00	1850516	49.09	1211757
6.00	2307263	48.50	1528839
8.00	2694360	48.06	1800936
10.00	3035686	47.69	2043415
20.00	4371264	46.54	3006626
30.00	5389761	45.79	3758192

Responsible Employee:

Signature:

LAS-Test (AASHTO TP101-14) - Report

Project name: 2018-07-20_LAS-Test (V2)



Date, Time: 2018-07-20 4:15:13 PM

Test name: 2018-07-20_LAS-Test

Operator: user

Sample: BC5-H2O

Batch no.: MTO2

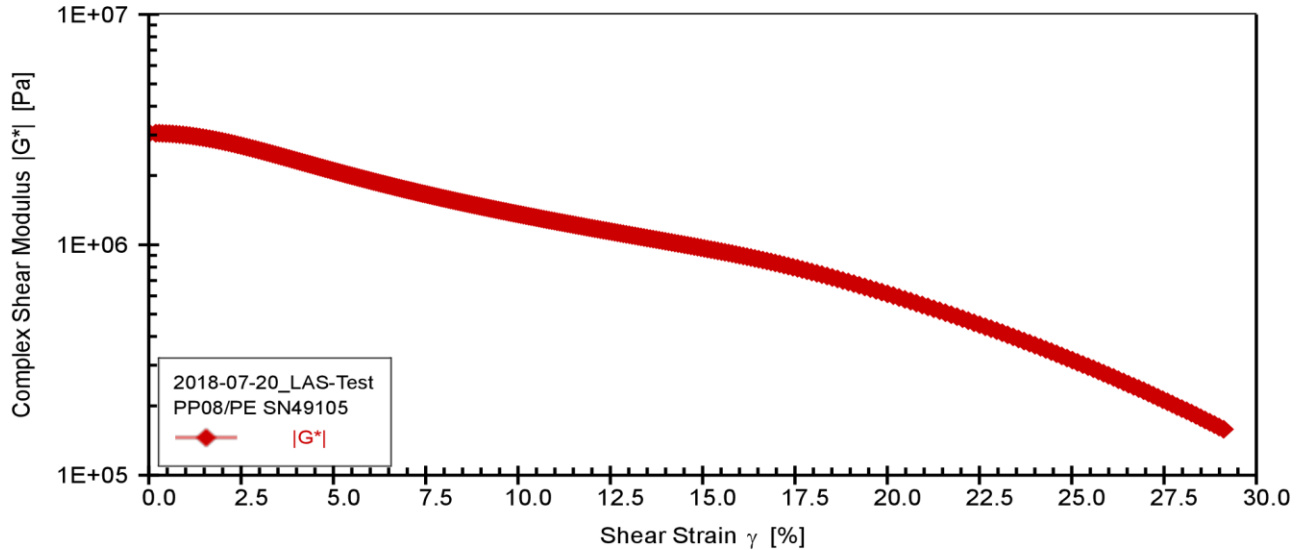
Description: Sunny

Configuration: Anton Paar SmartPave 102 SN82314644

PP08/PE SN49105

P-PTD200+H-PTD120 SN82331818-82284206

Linear Amplitude Sweep



Anton Paar

2018-07-20_LAS-Test, LAS-Test_22 °C, Interval 1

Complex Shear Modulus G* [Pa]	Shear Stress τ [Pa]	Shear Strain γ [%]	Time t [s]	Phase Shift Angle δ [°]
3052080	447.5617	0.01	1.00	47.57
3050735	5754.271	0.19	2.00	47.72
3052134	8570.762	0.28	3.00	47.74
3046436	11392.61	0.37	4.00	47.74
3041657	14186.83	0.47	5.00	47.77
3036171	16966.87	0.56	6.00	47.82
3029252	19725.3	0.65	7.00	47.86
3020613	22455.79	0.74	8.00	47.91
3012186	25152.87	0.84	9.00	47.98
3002442	27822.95	0.93	10.00	48.05
2991512	30451.73	1.02	11.00	48.13
2979497	33040.9	1.11	12.00	48.20
2964435	35560.25	1.20	13.00	48.34
2951042	38019.11	1.29	14.00	48.44
2936412	40462.8	1.38	15.00	48.54
2921024	42851.87	1.47	16.00	48.65
2904910	45186.55	1.56	17.00	48.76

Responsible Employee:

Signature:

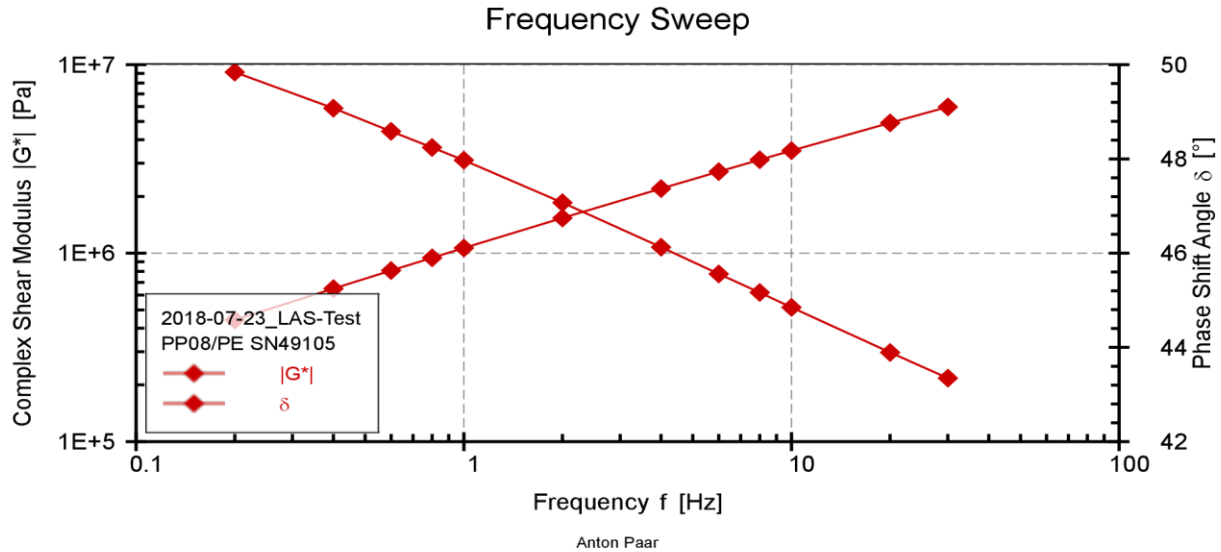
LAS-Test (AASHTO TP101-14) - Report

Project name: 2018-07-23_LAS-Test (V2)

Date, Time: 2018-07-23 5:39:08 PM
 Test name: 2018-07-23_LAS-Test
 Operator: user
 Sample: BC5-NoH2O
 Batch no.: MTO2
 Description: SUNNY



Configuration: Anton Paar SmartPave 102 SN82314644
 PP08/PE SN49105 P-PTD200+H-PTD120 SN82331818-82284206



2018-07-23_LAS-Test, Frequency Sweep_22 °C, Interval 1

Frequency f [Hz]	Complex Shear Modulus G* [Pa]	Phase Shift Angle δ [°]	Storage Modulus G' [Pa]
0.20	441782.4	49.84	284903.6
0.40	648410	49.08	424737.8
0.60	808722.7	48.59	534970.9
0.80	944645.9	48.24	629101.4
1.00	1065092	47.97	713052.4
2.00	1537307	47.07	1047008
4.00	2201721	46.13	1525908
6.00	2707460	45.56	1895669
8.00	3130226	45.16	2207029
10.00	3499430	44.85	2480944
20.00	4916608	43.89	3543093
30.00	5970564	43.35	4341804

Responsible Employee:

Signature:

LAS-Test (AASHTO TP101-14) - Report

Project name: 2018-07-23_LAS-Test (V2)



Date, Time: 2018-07-23 5:39:08 PM

Test name: 2018-07-23_LAS-Test

Operator: user

Sample: BC5-NoH2O

Batch no.: MTO2

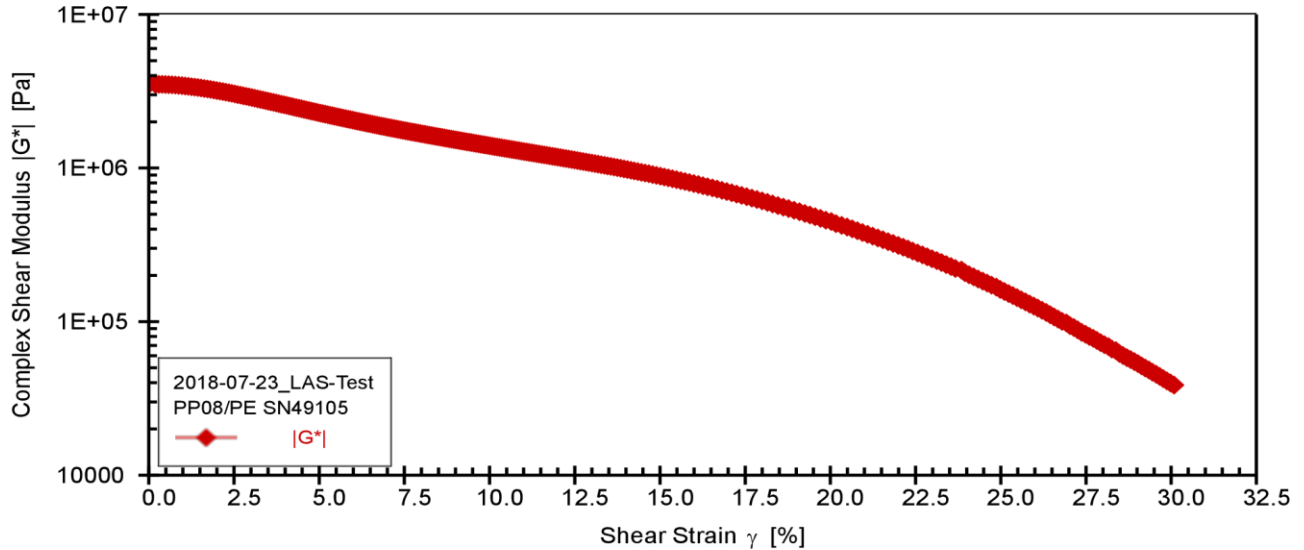
Description: SUNNY

Configuration: Anton Paar SmartPave 102 SN82314644

PP08/PE SN49105

P-PTD200+H-PTD120 SN82331818-82284206

Linear Amplitude Sweep



Anton Paar

2018-07-23_LAS-Test, LAS-Test_22 °C, Interval 1

Complex Shear Modulus G* [Pa]	Shear Stress τ [Pa]	Shear Strain γ [%]	Time t [s]	Phase Shift Angle δ [°]
3527369	459.229	0.01	1.00	44.59
3514605	6960.254	0.20	2.00	44.80
3511466	10337.91	0.29	3.00	44.81
3507547	13731.72	0.39	4.00	44.83
3500975	17104.2	0.49	5.00	44.89
3492203	20445.31	0.59	6.00	44.95
3482276	23752.51	0.68	7.00	45.02
3470998	27022.46	0.78	8.00	45.10
3457229	30244.65	0.87	9.00	45.19
3441681	33413.17	0.97	10.00	45.29
3423224	36501.94	1.07	11.00	45.45
3405736	39522.67	1.16	12.00	45.56
3385870	42512.85	1.26	13.00	45.68
3365637	45424.1	1.35	14.00	45.81
3344257	48271.25	1.44	15.00	45.94
3322049	51044.4	1.54	16.00	46.08
3298620	53746.42	1.63	17.00	46.23

Responsible Employee:

Signature:

LAS-Test (AASHTO TP101-14) - Report

Project name: 2018-07-24_LAS-Test (V2)

Date, Time: 2018-07-24 5:49:27 PM

Test name: 2018-07-24_LAS-Test

Operator: user

Sample: BC10-H2O

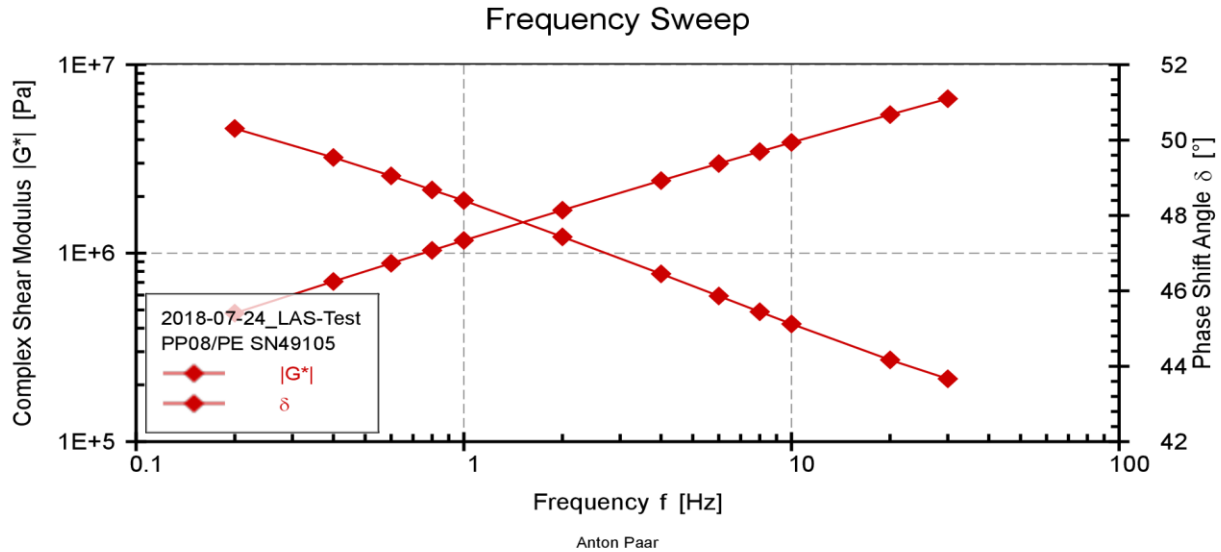
Batch no.: MTO2

Description: Sunny

Configuration: Anton Paar SmartPave 102 SN82314644

PP08/PE SN49105

P-PTD200+H-PTD120 SN82331818-82284206



2018-07-24_LAS-Test, Frequency Sweep_22 °C, Interval 1

Frequency f [Hz]	Complex Shear Modulus G* [Pa]	Phase Shift Angle δ [°]	Storage Modulus G' [Pa]
0.20	480449	50.31	306844.2
0.40	707902.4	49.54	459390.4
0.60	884323.7	49.05	579562.8
0.80	1034695	48.68	683203.1
1.00	1168047	48.40	775512.5
2.00	1690935	47.43	1143855
4.00	2427879	46.45	1672706
6.00	2989387	45.86	2081690
8.00	3458364	45.45	2426328
10.00	3868253	45.12	2729398
20.00	5438887	44.17	3901399
30.00	6601947	43.67	4775717

Responsible Employee:

Signature:

LAS-Test (AASHTO TP101-14) - Report

Project name: 2018-07-24_LAS-Test (V2)



Date, Time: 2018-07-24 5:49:27 PM

Test name: 2018-07-24_LAS-Test

Operator: user

Sample: BC10-H2O

Batch no.: MTO2

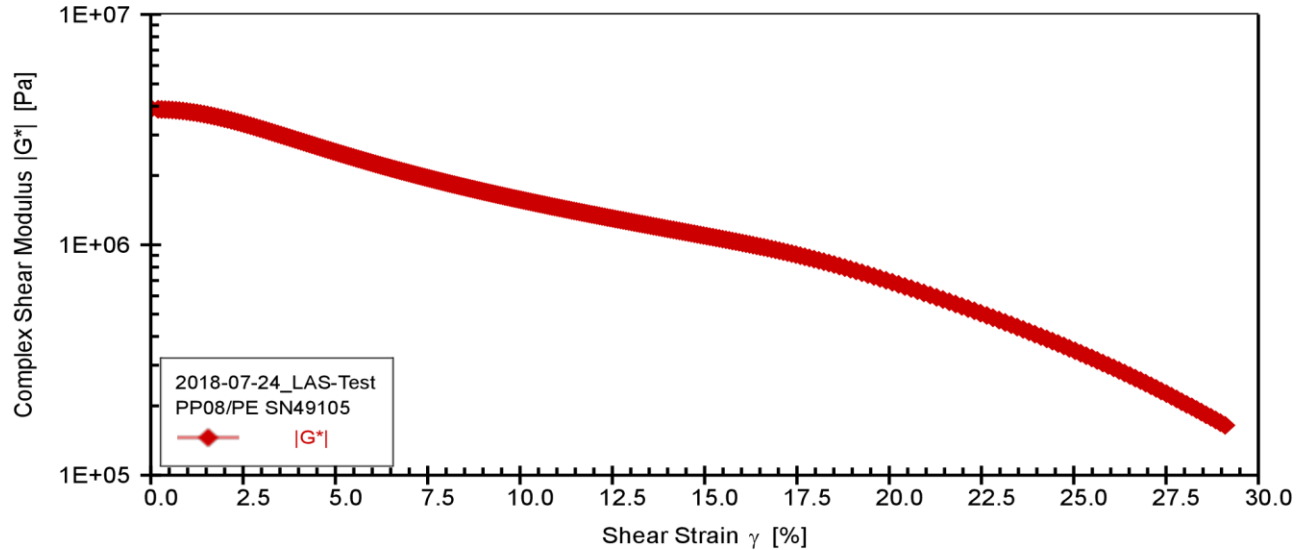
Description: Sunny

Configuration: Anton Paar SmartPave 102 SN82314644

PP08/PE SN49105

P-PTD200+H-PTD120 SN82331818-82284206

Linear Amplitude Sweep



Anton Paar

2018-07-24_LAS-Test, LAS-Test_22 °C, Interval 1

Complex Shear Modulus G* [Pa]	Shear Stress τ [Pa]	Shear Strain γ [%]	Time t [s]	Phase Shift Angle δ [°]
3898545	455.371	0.01	1.00	45.07
3877336	7651.646	0.20	2.00	45.06
3870265	11362.84	0.29	3.00	45.07
3865419	15081.36	0.39	4.00	45.09
3858179	18786.51	0.49	5.00	45.14
3849385	22462.48	0.58	6.00	45.18
3838463	26106.93	0.68	7.00	45.24
3826466	29707.23	0.78	8.00	45.32
3811930	33262.71	0.87	9.00	45.40
3793983	36761.15	0.97	10.00	45.48
3776810	40189.27	1.06	11.00	45.58
3758102	43568.87	1.16	12.00	45.69
3737455	46882.13	1.25	13.00	45.80
3715378	50118.21	1.35	14.00	45.93
3691923	53271.14	1.44	15.00	46.07
3667181	56342.57	1.54	16.00	46.21
3641304	59332.23	1.63	17.00	46.35

Responsible Employee:

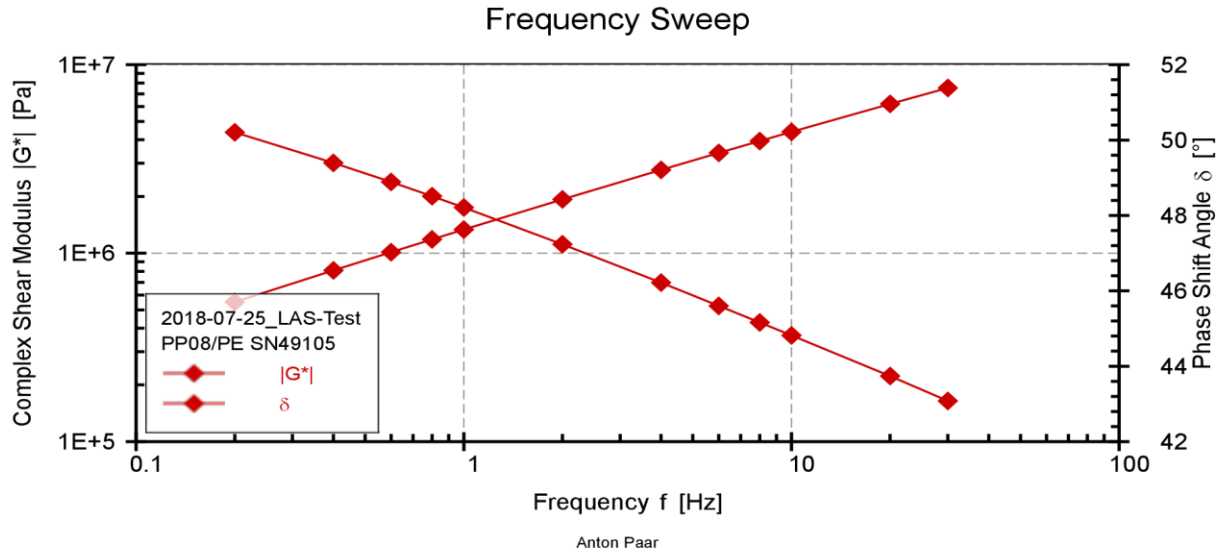
Signature:

LAS-Test (AASHTO TP101-14) - Report

Project name: 2018-07-25_LAS-Test (V2)

Date, Time: 2018-07-25 5:17:14 PM
 Test name: 2018-07-25_LAS-Test
 Operator: user
 Sample: BC10-NoH2O
 Batch no.: MTO2
 Description: Sunny
 Configuration: Anton Paar SmartPave 102 SN82314644
 PP08/PE SN49105

P-PTD200+H-PTD120 SN82331818-82284206



2018-07-25_LAS-Test, Frequency Sweep_22 °C, Interval 1

Frequency f [Hz]	Complex Shear Modulus G* [Pa]	Phase Shift Angle δ [°]	Storage Modulus G' [Pa]
0.20	550616.1	50.21	352405.1
0.40	810247.3	49.40	527335.8
0.60	1012046	48.89	665424.7
0.80	1183253	48.51	783863.5
1.00	1334587	48.21	889347
2.00	1929793	47.23	1310327
4.00	2766955	46.22	1914501
6.00	3404129	45.60	2381648
8.00	3936832	45.16	2775883
10.00	4402139	44.82	3122585
20.00	6192565	43.74	4474132
30.00	7529041	43.08	5499209

Responsible Employee:

Signature:

LAS-Test (AASHTO TP101-14) - Report

Project name: 2018-07-25_LAS-Test (V2)



Date, Time: 2018-07-25 5:17:14 PM

Test name: 2018-07-25_LAS-Test

Operator: user

Sample: BC10-NoH2O

Batch no.: MTO2

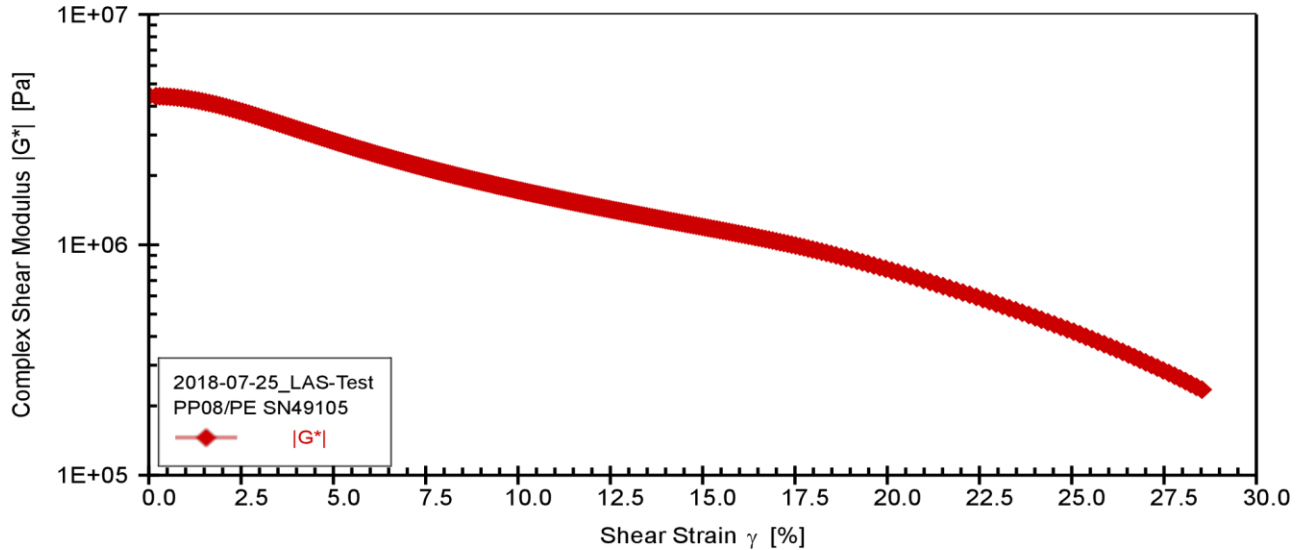
Description: Sunny

Configuration: Anton Paar SmartPave 102 SN82314644

PP08/PE SN49105

P-PTD200+H-PTD120 SN82331818-82284206

Linear Amplitude Sweep



Anton Paar

2018-07-25_LAS-Test, LAS-Test_22 °C, Interval 1

Complex Shear Modulus G* [Pa]	Shear Stress τ [Pa]	Shear Strain γ [%]	Time t [s]	Phase Shift Angle δ [°]
4433692	451.872	0.01	1.00	44.74
4415849	8736.398	0.20	2.00	44.75
4415145	12986.15	0.29	3.00	44.77
4410464	17255.05	0.39	4.00	44.82
4400519	21496.05	0.49	5.00	44.87
4390115	25693.68	0.59	6.00	44.93
4377468	29856.18	0.68	7.00	45.01
4359953	33954.25	0.78	8.00	45.15
4342173	37981.45	0.87	9.00	45.24
4322189	41965.44	0.97	10.00	45.34
4299737	45871.07	1.07	11.00	45.47
4276300	49696.67	1.16	12.00	45.60
4249450	53449.32	1.26	13.00	45.73
4221753	57099.18	1.35	14.00	45.86
4193029	60666.75	1.45	15.00	46.01
4162280	64146.33	1.54	16.00	46.15
4131106	67522.5	1.63	17.00	46.30

Responsible Employee:

Signature:

LAS-Test (AASHTO TP101-14) - Report

Project name: 2018-07-27_LAS-Test (V2)



Date, Time: 2018-07-27 12:01:36 PM

Test name: 2018-07-27_LAS-Test

Operator: user

Sample: BC15-H2O

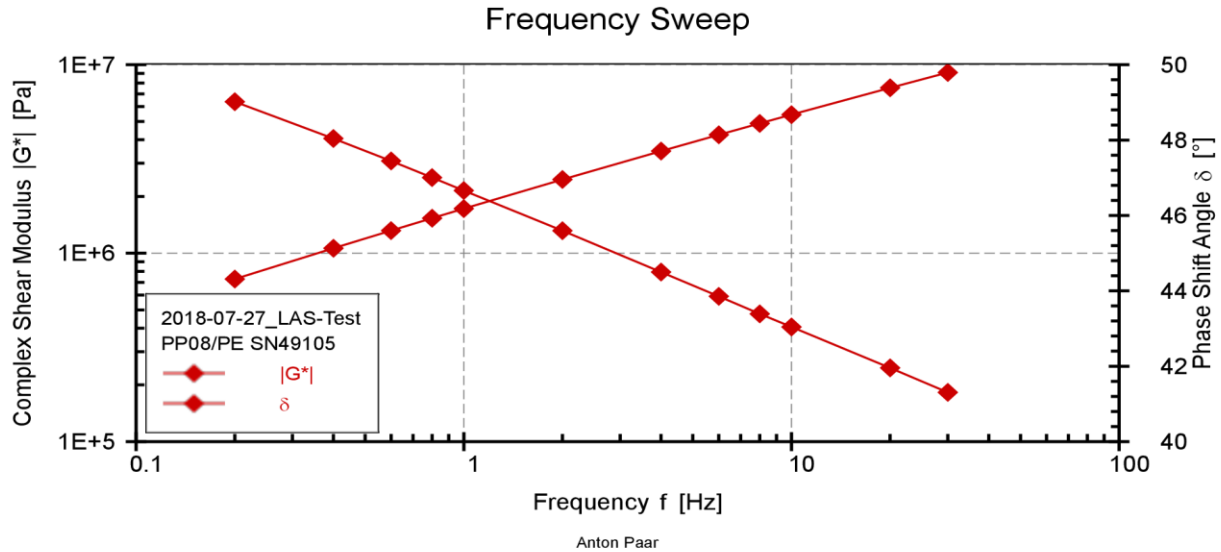
Batch no.: MTO2

Description: Sunny

Configuration: Anton Paar SmartPave 102 SN82314644

PP08/PE SN49105

P-PTD200+H-PTD120 SN82331818-82284206



2018-07-27_LAS-Test, Frequency Sweep_22 °C, Interval 1

Frequency f [Hz]	Complex Shear Modulus G* [Pa]	Phase Shift Angle δ [°]	Storage Modulus G' [Pa]
0.20	728706.6	49.02	477898.5
0.40	1061749	48.04	709880
0.60	1317731	47.45	891144.1
0.80	1532963	47.01	1045350
1.00	1722792	46.66	1182380
2.00	2459215	45.60	1720721
4.00	3479818	44.50	2482069
6.00	4246628	43.85	3062256
8.00	4881922	43.39	3547631
10.00	5435489	43.04	3972431
20.00	7537885	41.96	5605629
30.00	9091622	41.31	6829610

Responsible Employee:

Signature:

LAS-Test (AASHTO TP101-14) - Report

Project name: 2018-07-27_LAS-Test (V2)



Date, Time: 2018-07-27 12:01:36 PM

Test name: 2018-07-27_LAS-Test

Operator: user

Sample: BC15-H2O

Batch no.: MTO2

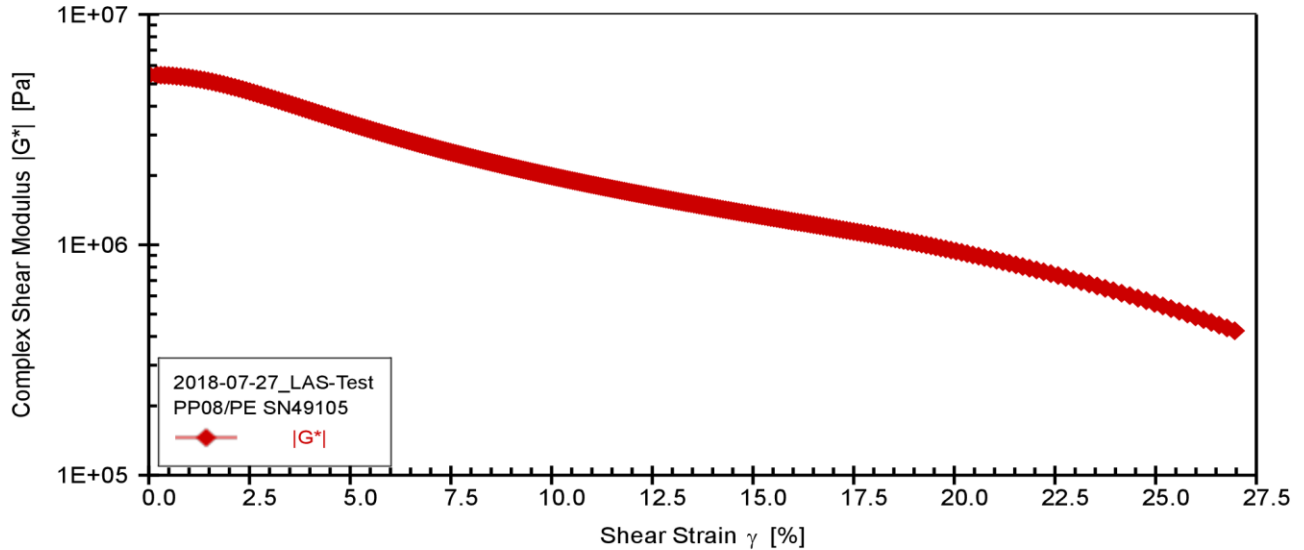
Description: Sunny

Configuration: Anton Paar SmartPave 102 SN82314644

PP08/PE SN49105

P-PTD200+H-PTD120 SN82331818-82284206

Linear Amplitude Sweep



Anton Paar

2018-07-27_LAS-Test, LAS-Test_22 °C, Interval 1

Complex Shear Modulus G* [Pa]	Shear Stress τ [Pa]	Shear Strain γ [%]	Time t [s]	Phase Shift Angle δ [°]
5469799	447.6722	0.01	1.00	42.91
5459543	10941.85	0.20	2.00	42.96
5454003	16288.87	0.30	3.00	43.00
5445990	21626.65	0.40	4.00	43.05
5433405	26937.26	0.50	5.00	43.10
5413199	32199.67	0.59	6.00	43.15
5394104	37378.02	0.69	7.00	43.25
5372771	42509.12	0.79	8.00	43.34
5348361	47569.78	0.89	9.00	43.44
5321477	52548.46	0.99	10.00	43.55
5291311	57435.58	1.09	11.00	43.68
5257774	62215.28	1.18	12.00	43.82
5222453	66875.2	1.28	13.00	43.97
5184762	71424.53	1.38	14.00	44.13
5145237	75856.51	1.47	15.00	44.29
5103445	80166.98	1.57	16.00	44.45
5060439	84344.21	1.67	17.00	44.63

Responsible Employee:

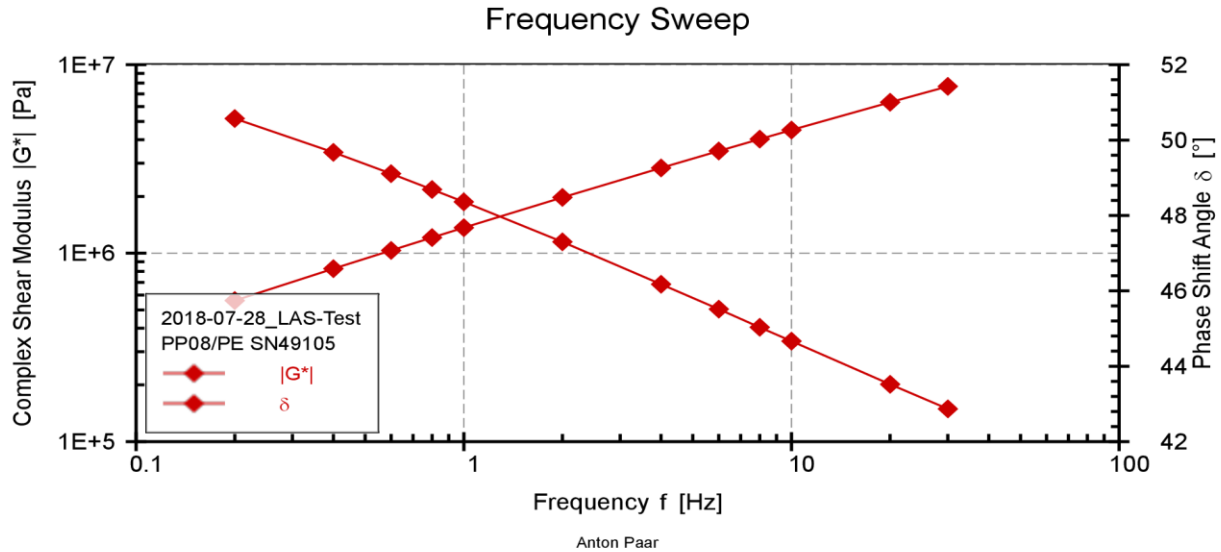
Signature:

LAS-Test (AASHTO TP101-14) - Report

Project name: 2018-07-28_LAS-Test (V2)

Date, Time: 2018-07-28 5:13:19 PM
 Test name: 2018-07-28_LAS-Test
 Operator: user
 Sample: BC15-NoH2O
 Batch no.: MTO2
 Description: Sunny
 Configuration: Anton Paar SmartPave 102 SN82314644
 PP08/PE SN49105

P-PTD200+H-PTD120 SN82331818-82284206



2018-07-28_LAS-Test, Frequency Sweep_22 °C, Interval 1

Frequency f [Hz]	Complex Shear Modulus G* [Pa]	Phase Shift Angle δ [°]	Storage Modulus G' [Pa]
0.20	560430.5	50.57	355936.6
0.40	827026.3	49.68	535179.6
0.60	1034010	49.11	676872.1
0.80	1210119	48.69	798842.9
1.00	1365591	48.36	907337.4
2.00	1975914	47.30	1340009
4.00	2833933	46.18	1962343
6.00	3484839	45.51	2441920
8.00	4027800	45.03	2846461
10.00	4502298	44.67	3202093
20.00	6320254	43.52	4582938
30.00	7672456	42.87	5623240

Responsible Employee:

Signature:

LAS-Test (AASHTO TP101-14) - Report

Project name: 2018-07-28_LAS-Test (V2)



Date, Time: 2018-07-28 5:13:19 PM

Test name: 2018-07-28_LAS-Test

Operator: user

Sample: BC15-NoH2O

Batch no.: MTO2

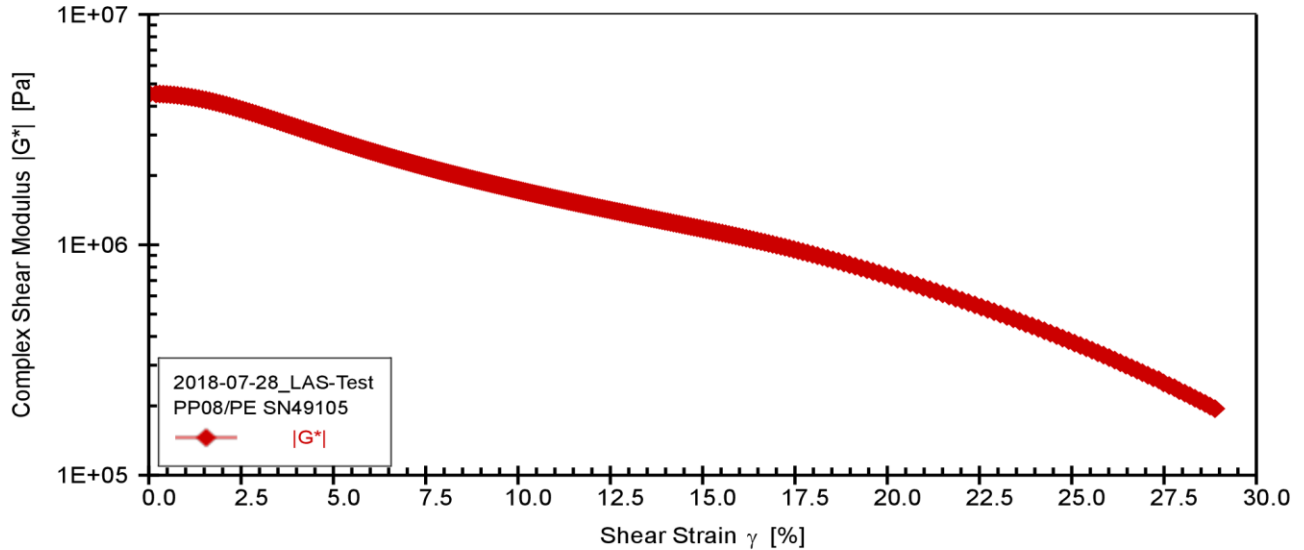
Description: Sunny

Configuration: Anton Paar SmartPave 102 SN82314644

PP08/PE SN49105

P-PTD200+H-PTD120 SN82331818-82284206

Linear Amplitude Sweep



Anton Paar

2018-07-28_LAS-Test, LAS-Test_22 °C, Interval 1

Complex Shear Modulus G* [Pa]	Shear Stress τ [Pa]	Shear Strain γ [%]	Time t [s]	Phase Shift Angle δ [°]
4520509	451.026	0.01	1.00	44.56
4520658	8924.907	0.20	2.00	44.65
4516398	13306.67	0.29	3.00	44.65
4509176	17670.56	0.39	4.00	44.70
4499467	22006.74	0.49	5.00	44.74
4487741	26307.8	0.59	6.00	44.79
4473272	30564.8	0.68	7.00	44.87
4456074	34761.44	0.78	8.00	44.96
4436920	38897.58	0.88	9.00	45.06
4415897	42969.89	0.97	10.00	45.16
4393090	46971.18	1.07	11.00	45.28
4368826	50895.05	1.16	12.00	45.40
4342217	54739.4	1.26	13.00	45.53
4314026	58488.22	1.36	14.00	45.67
4283851	62142.43	1.45	15.00	45.82
4252355	65695.2	1.54	16.00	45.97
4219592	69149.93	1.64	17.00	46.13

Responsible Employee:

Signature:

LAS-Test (AASHTO TP101-14) - Report

Project name: 2018-08-03_LAS-Test (V2)



Date, Time: 2018-08-03 3:50:27 PM

Test name: 2018-08-03_LAS-Test

Operator: user

Sample: BC20-H2O

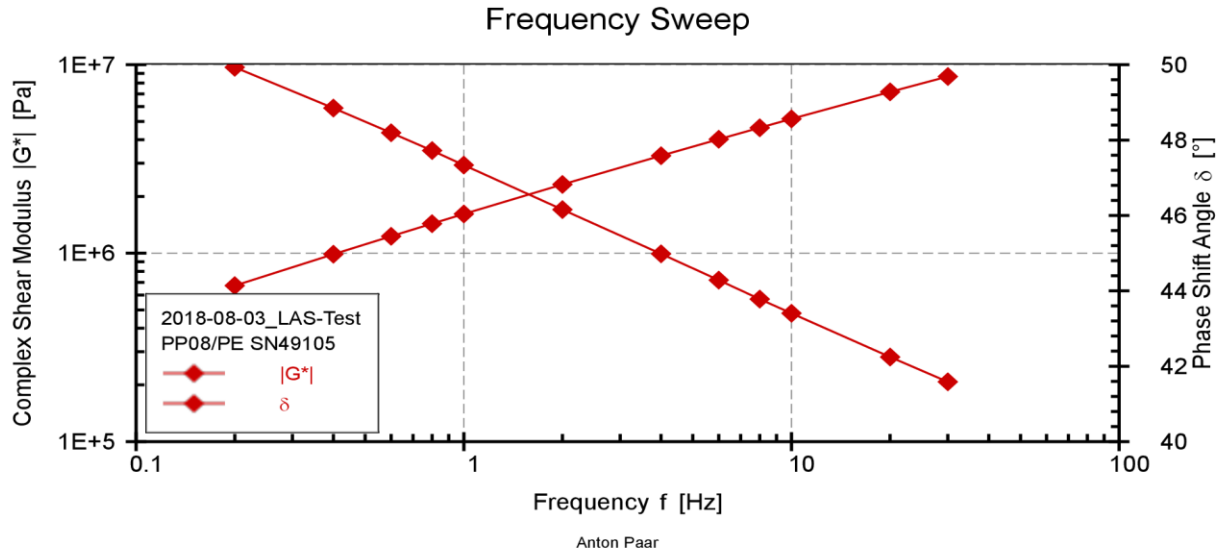
Batch no.: MTO2

Description: Sunny

Configuration: Anton Paar SmartPave 102 SN82314644

PP08/PE SN49105

P-PTD200+H-PTD120 SN82331818-82284206



2018-08-03_LAS-Test, Frequency Sweep_22 °C, Interval 1

Frequency f [Hz]	Complex Shear Modulus G* [Pa]	Phase Shift Angle δ [°]	Storage Modulus G' [Pa]
0.20	672541.9	49.93	432913.7
0.40	986991.6	48.85	649487.8
0.60	1229453	48.19	819558.1
0.80	1434151	47.72	964769.5
1.00	1614115	47.34	1093838
2.00	2315452	46.16	1603896
4.00	3289722	44.98	2326928
6.00	4022695	44.28	2879785
8.00	4630842	43.78	3343385
10.00	5160217	43.40	3748994
20.00	7173096	42.25	5310016
30.00	8659554	41.59	6477003

Responsible Employee:

Signature:

LAS-Test (AASHTO TP101-14) - Report

Project name: 2018-08-03_LAS-Test (V2)



Date, Time: 2018-08-03 3:50:27 PM

Test name: 2018-08-03_LAS-Test

Operator: user

Sample: BC20-H2O

Batch no.: MTO2

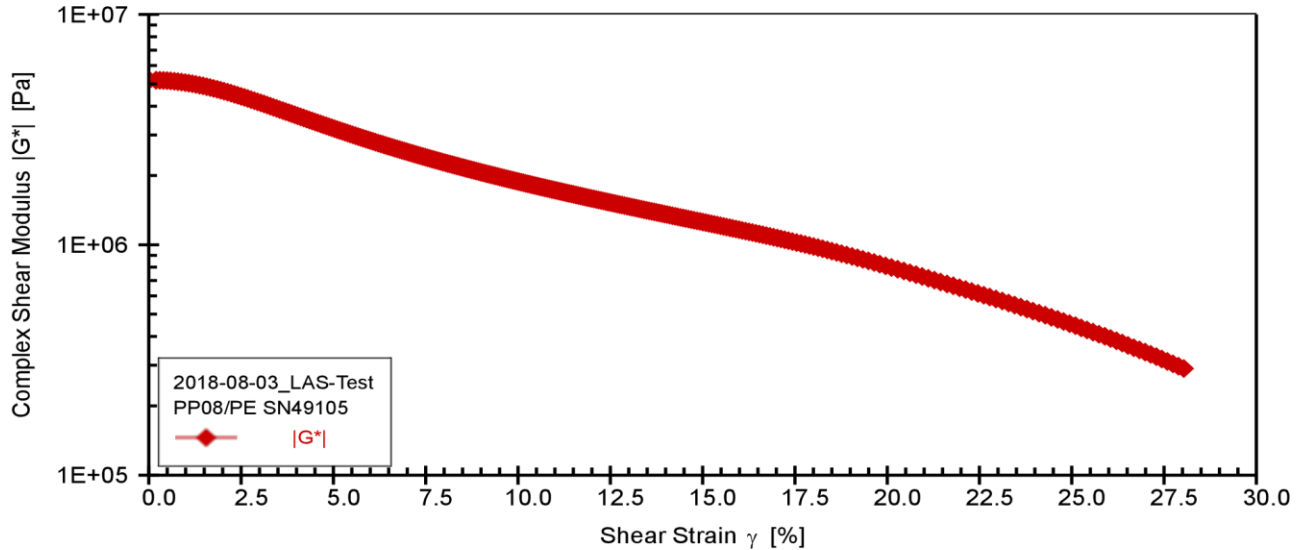
Description: Sunny

Configuration: Anton Paar SmartPave 102 SN82314644

PP08/PE SN49105

P-PTD200+H-PTD120 SN82331818-82284206

Linear Amplitude Sweep



Anton Paar

2018-08-03_LAS-Test, LAS-Test_22 °C, Interval 1

Complex Shear Modulus G* [Pa]	Shear Stress τ [Pa]	Shear Strain γ [%]	Time t [s]	Phase Shift Angle δ [°]
5187995	449.7606	0.01	1.00	43.22
5183481	10363.55	0.20	2.00	43.30
5180131	15437.93	0.30	3.00	43.33
5174445	20505.49	0.40	4.00	43.37
5163556	25545.99	0.49	5.00	43.43
5148857	30536.89	0.59	6.00	43.50
5128237	35471.86	0.69	7.00	43.58
5108984	40327.85	0.79	8.00	43.67
5086419	45139.03	0.89	9.00	43.76
5060541	49865.44	0.99	10.00	43.88
5032982	54499.58	1.08	11.00	44.00
5002755	59044.07	1.18	12.00	44.13
4970622	63485.87	1.28	13.00	44.27
4935486	67820.16	1.37	14.00	44.42
4897825	72027.99	1.47	15.00	44.59
4858643	76114.63	1.57	16.00	44.75
4818009	80083.07	1.66	17.00	44.92

Responsible Employee:

Signature:

LAS-Test (AASHTO TP101-14) - Report

Project name: 2018-08-04_LAS-Test (V2)



Date, Time: 2018-08-04 2:06:59 PM

Test name: 2018-08-04_LAS-Test

Operator: user

Sample: BC20-NoH2O

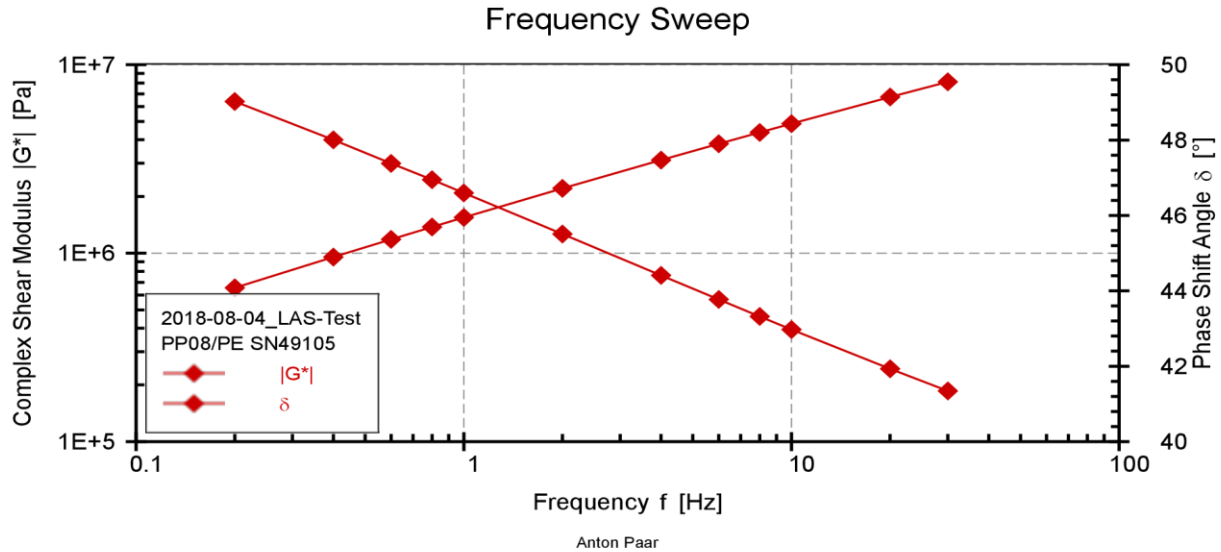
Batch no.: MTO2

Description: Sunny

Configuration: Anton Paar SmartPave 102 SN82314644

PP08/PE SN49105

P-PTD200+H-PTD120 SN82331818-82284206



2018-08-04_LAS-Test, Frequency Sweep_22 °C, Interval 1

Frequency f [Hz]	Complex Shear Modulus G* [Pa]	Phase Shift Angle δ [°]	Storage Modulus G' [Pa]
0.20	654906.5	49.03	429441.6
0.40	954011.9	48.01	638270.1
0.60	1183483	47.38	801347.9
0.80	1376838	46.95	939869
1.00	1547366	46.60	1063202
2.00	2206985	45.51	1546659
4.00	3120123	44.41	2228848
6.00	3805542	43.77	2747958
8.00	4373103	43.32	3181592
10.00	4866430	42.97	3560566
20.00	6738928	41.93	5013401
30.00	8110685	41.34	6089074

Responsible Employee:

Signature:

LAS-Test (AASHTO TP101-14) - Report

Project name: 2018-08-04_LAS-Test (V2)

Date, Time: 2018-08-04 2:06:59 PM

Test name: 2018-08-04_LAS-Test

Operator: user

Sample: BC20-NoH2O

Batch no.: MTO2

Description: Sunny

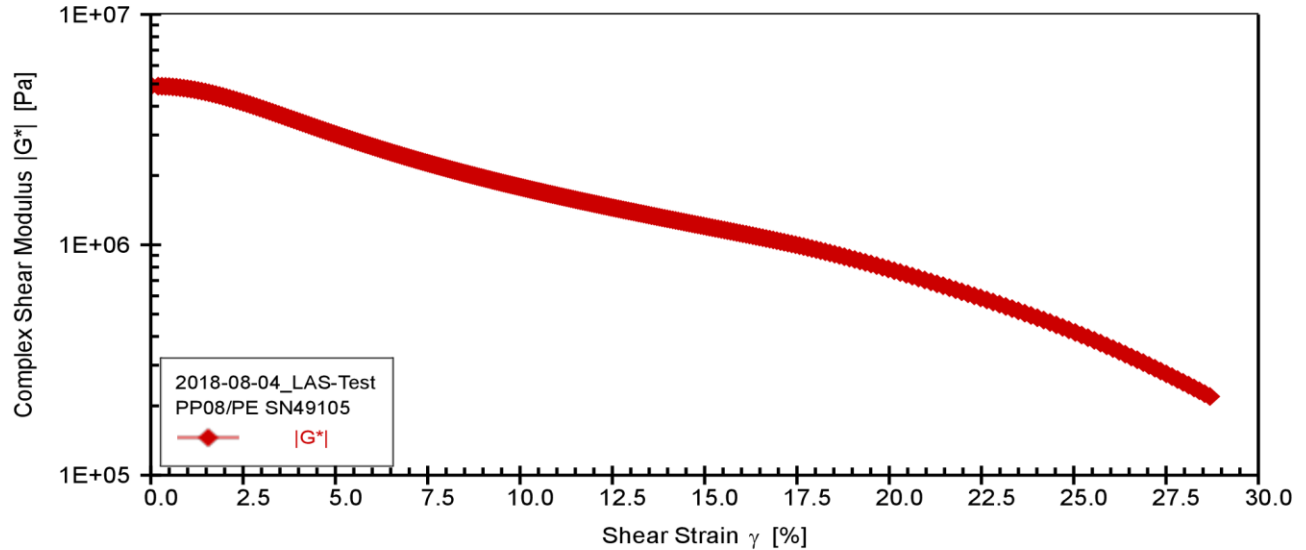
Configuration: Anton Paar SmartPave 102 SN82314644

PP08/PE SN49105

P-PTD200+H-PTD120 SN82331818-82284206



Linear Amplitude Sweep



Anton Paar

2018-08-04_LAS-Test, LAS-Test_22 °C, Interval 1

Complex Shear Modulus G* [Pa]	Shear Stress τ [Pa]	Shear Strain γ [%]	Time t [s]	Phase Shift Angle δ [°]
4902351	453.6504	0.01	1.00	42.82
4886827	9835.798	0.20	2.00	42.90
4882694	14625.06	0.30	3.00	42.93
4875103	19419.4	0.40	4.00	42.98
4865044	24183.22	0.50	5.00	43.03
4849765	28908.04	0.60	6.00	43.10
4832188	33569.09	0.69	7.00	43.19
4811785	38171.71	0.79	8.00	43.28
4789501	42704.75	0.89	9.00	43.38
4764185	47163.59	0.99	10.00	43.50
4737803	51537.76	1.09	11.00	43.61
4708747	55830.43	1.19	12.00	43.74
4677174	60016.58	1.28	13.00	43.89
4644446	64097.54	1.38	14.00	44.03
4608228	68073.72	1.48	15.00	44.20
4571145	71917.53	1.57	16.00	44.36
4532987	75658.38	1.67	17.00	44.53

Responsible Employee:

Signature:

LAS-Test (AASHTO TP101-14) - Report

Project name: 2018-06-05_LAS-Test (V2)



Date, Time: 2018-06-05 11:04:25 AM

Test name: 2018-06-05_LAS-Test

Operator: user

Sample: 64-28 RTFO + 2PAV @ 22

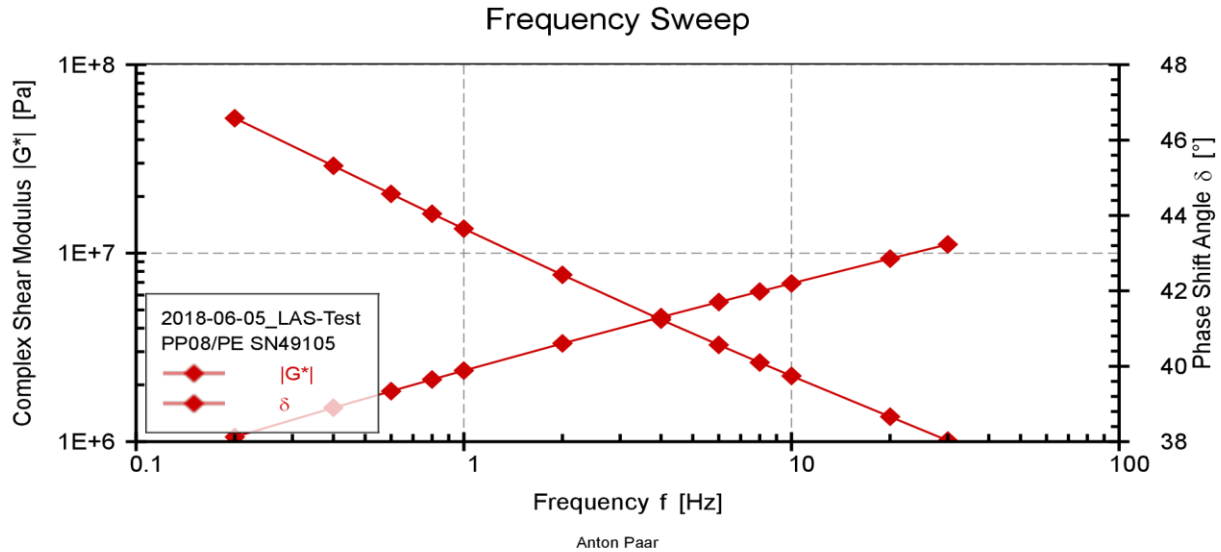
Batch no.: MTO2

Description: SUNNY

Configuration: Anton Paar SmartPave 102 SN82314644

PP08/PE SN49105

P-PTD200+H-PTD120 SN82331818-82284206



2018-06-05_LAS-Test, Frequency Sweep_22 °C, Interval 1

Frequency f [Hz]	Complex Shear Modulus G* [Pa]	Phase Shift Angle δ [°]	Storage Modulus G' [Pa]
0.20	1058699	46.58	727673.3
0.40	1512183	45.32	1063336
0.60	1852476	44.57	1319631
0.80	2135750	44.05	1535114
1.00	2381701	43.65	1723359
2.00	3317892	42.42	2449184
4.00	4577675	41.24	3442409
6.00	5503376	40.57	4180619
8.00	6260563	40.10	4788810
10.00	6913190	39.74	5315720
20.00	9353444	38.66	7303803
30.00	11125700	38.03	8763809

Responsible Employee:

Signature:

LAS-Test (AASHTO TP101-14) - Report

Project name: 2018-06-05_LAS-Test (V2)



Date, Time: 2018-06-05 11:04:25 AM

Test name: 2018-06-05_LAS-Test

Operator: user

Sample: 64-28 RTFO + 2PAV @ 22

Batch no.: MTO2

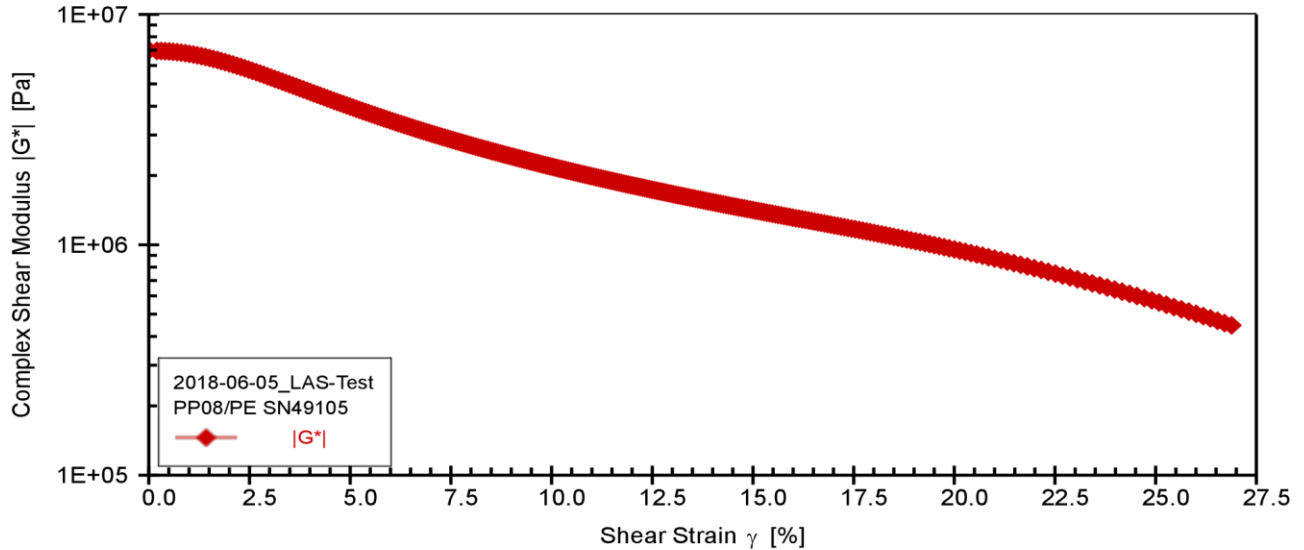
Description: SUNNY

Configuration: Anton Paar SmartPave 102 SN82314644

PP08/PE SN49105

P-PTD200+H-PTD120 SN82331818-82284206

Linear Amplitude Sweep



Anton Paar

2018-06-05_LAS-Test, LAS-Test_22 °C, Interval 1

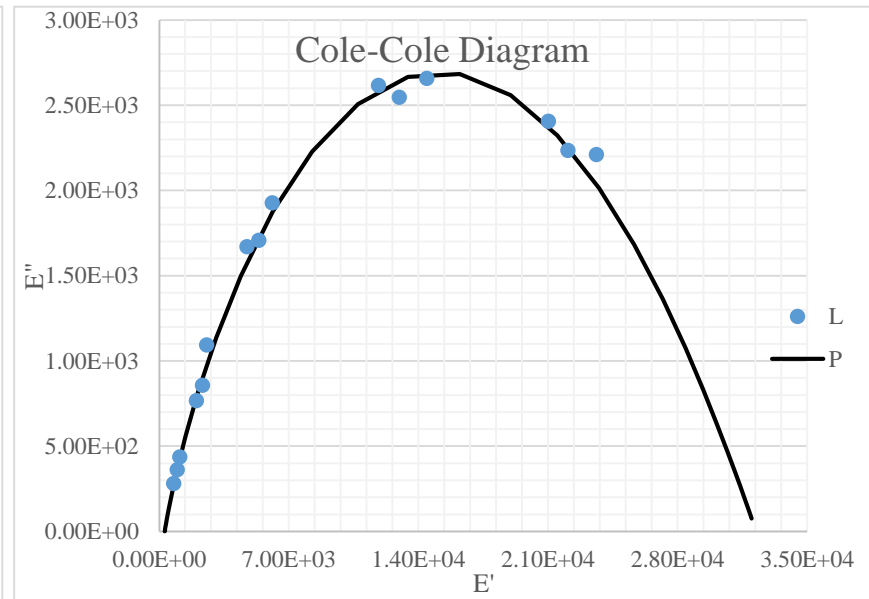
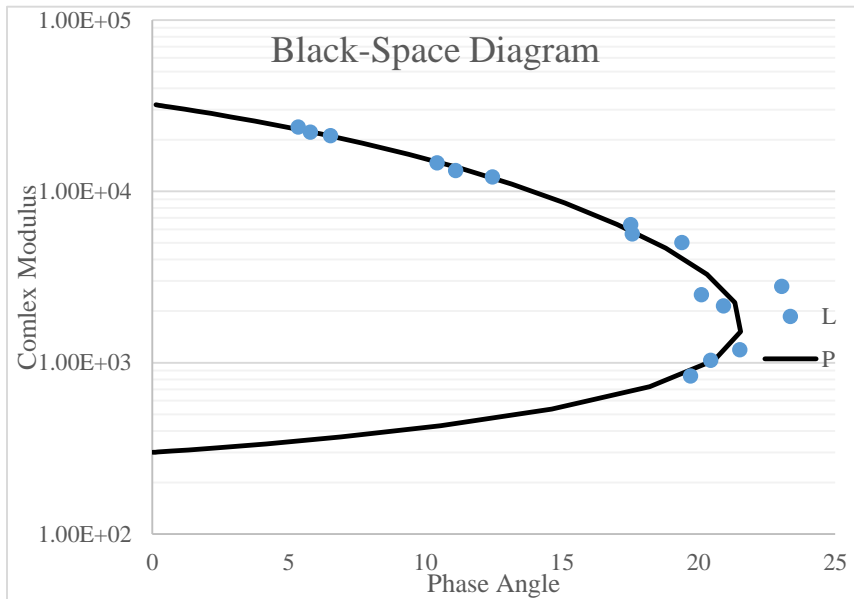
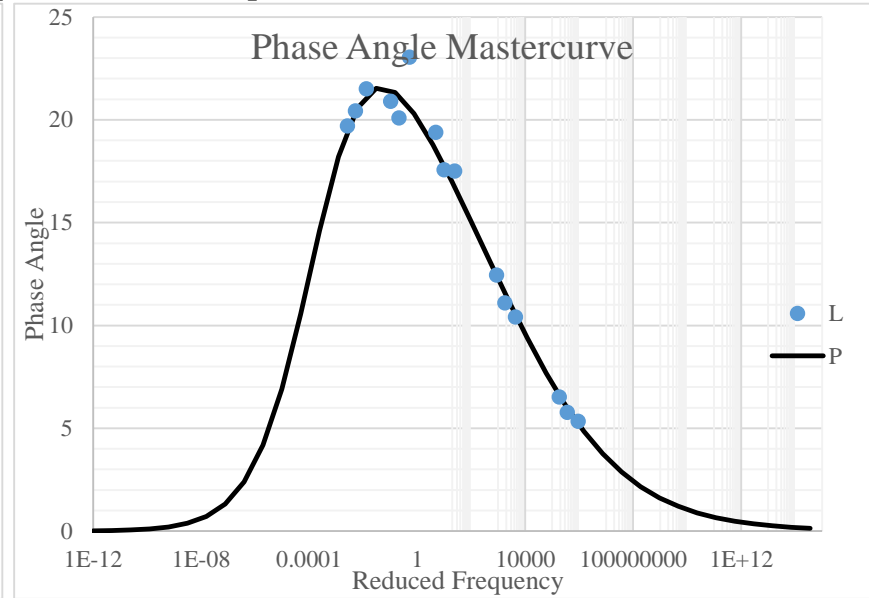
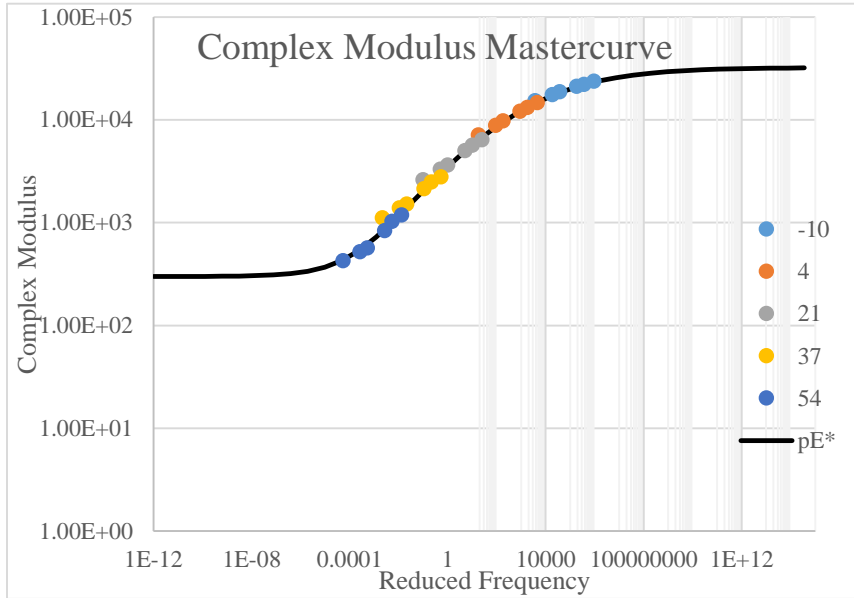
Complex Shear Modulus G* [Pa]	Shear Stress τ [Pa]	Shear Strain γ [%]	Time t [s]	Phase Shift Angle δ [°]
6994117	443.4593	0.01	1.00	40.21
6952850	14186.89	0.20	2.00	39.69
6942779	21096.31	0.30	3.00	39.73
6930297	28004.42	0.40	4.00	39.78
6912699	34865.31	0.50	5.00	39.85
6887914	41663.24	0.60	6.00	39.95
6859289	48367.84	0.71	7.00	40.06
6829665	54986.46	0.81	8.00	40.15
6792326	61520.96	0.91	9.00	40.27
6750141	67901.75	1.01	10.00	40.43
6703406	74140.35	1.11	11.00	40.59
6654016	80227.24	1.21	12.00	40.75
6598361	86165.06	1.31	13.00	40.94
6540253	91902.44	1.41	14.00	41.14
6478076	97469.57	1.50	15.00	41.35
6413786	102841.7	1.60	16.00	41.56
6348212	108040.5	1.70	17.00	41.77

Responsible Employee:

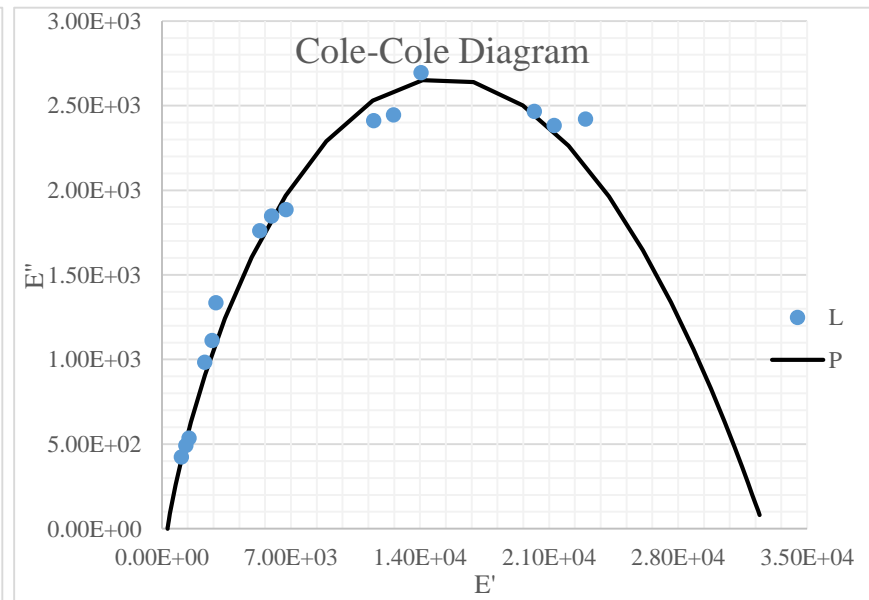
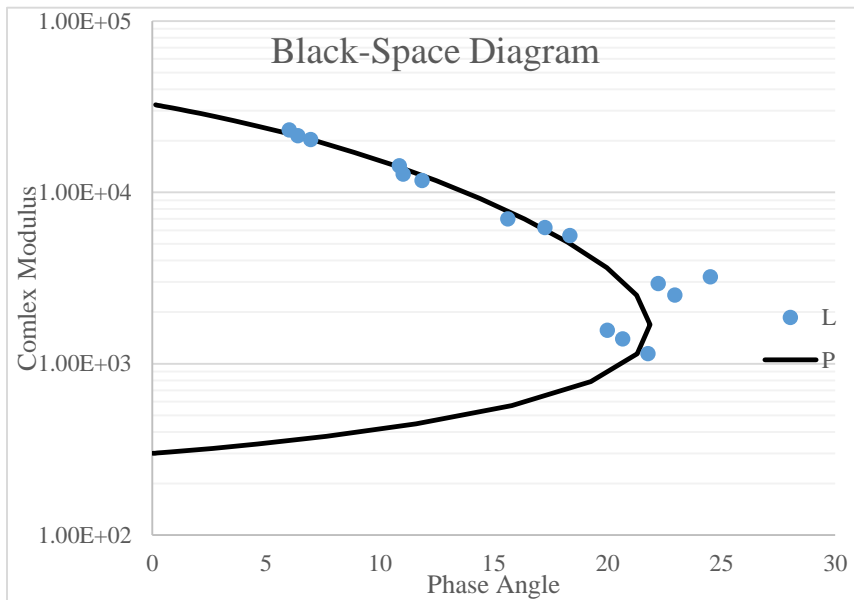
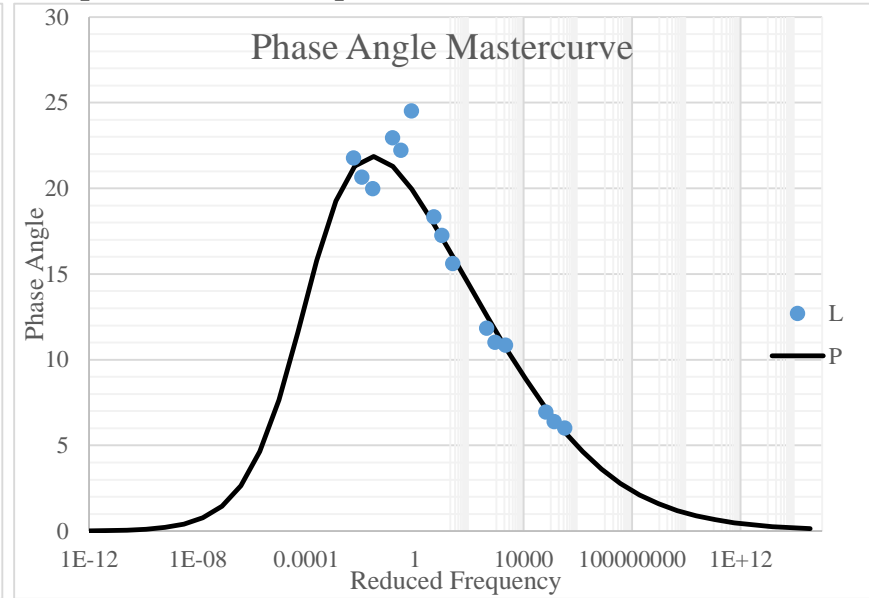
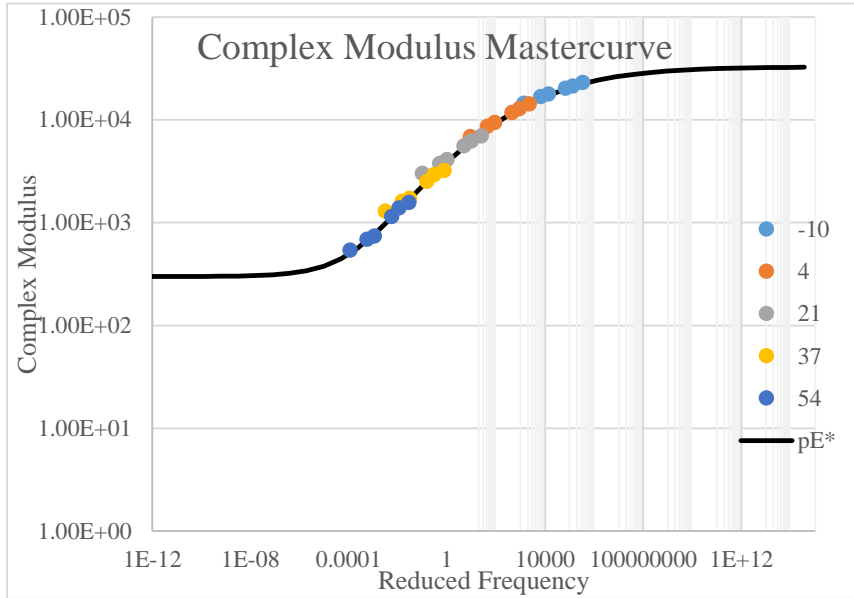
Signature:

**APPENDIX F: RHEOLOGICAL ANALYSIS – ASPHALT
MIXTURE**

Unconditioned Complex Modulus Samples



AASHTO R30 Conditioned Complex Modulus Samples



Atlas Weatherometer Conditioned Complex Modulus Samples

